Circulating tumor DNA measurements to refine cancer treatment

Tolmeijer, S.H.

2023, Dissertation

Circulating tumor DNA measurements

to refine cancer treatment

SOFIE H. TOLMEIJER

The work in this thesis was carried out within the Radboudumc Graduate School, at the department of Medical Oncology of the Radboud university medical center in Nijmegen, the Netherlands.

ISBN
978-94-93315-95-2

Cover design
Sebastiaan Krijnen

Lay-out
Guus Gijben | Proefschrift-aio.nl

Printing
Proefschrift-aio.nl

Circulating tumor DNA measurements to refine cancer treatment

Proefschrift ter verkrijging van de graad van doctor
aan de Radboud Universiteit Nijmegen
op gezag van de rector magnificus prof. dr. J.H.J.M. van Krieken,
volgens besluit van het college voor promoties
in het openbaar te verdedigen op

donderdag 26 oktober 2023
om 10.30 uur precies

door

Sofie Henriëtte Tolmeijer
geboren op 15 oktober 1995
te ‘s-Hertogenbosch

Promotoren:
Dr. N. Mehra
Prof. dr. M.J.L. Ligtenberg
Prof. dr. W.R. Gerritsen

Copromotor:
Dr. M.J. Geerlings-Wagemaker

Manuscriptcommissie:
Prof. dr. J.A. Witjes
Prof. dr. M. van den Heuvel
Dr. ir. W.W.J. de Leng (UMC Utrecht)

Table of contents

Chapter 1

General introduction and outline of the thesis

Cancer is one of the leading causes of death worldwide. Cancer treatment can highly impact quality of life and is a major economic burden on health services. More and more treatments are becoming available for cancer patients, including improved surgical and radiotherapeutic strategies mainly focused in a curative setting. However, increasingly systemic targeted therapy options are only beneficial for selected patient populations, and personalized medicine utilizing predictive biomarkers has evolved as a new paradigm in the care of cancer patients. The aim of personalized medicine is to tailor treatment for each patient with the goal to improve treatment outcomes and reduce adverse events. In order to provide a personalized treatment strategy per patient, biomarkers have become essential for therapy selection and treatment monitoring. One novel and promising biomarker for cancer management is circulating tumor DNA (ctDNA).

CtDNA is the fraction of cell-free DNA (cfDNA) that is derived from tumor cells. CfDNA can be found in different body fluids, including blood, urine and cerebrospinal fluid [1]. CfDNA is present in every individual due to apoptosis, necrosis and active secretion of DNA from cells [2, 3]. In the blood of healthy individuals, the majority of cfDNA is derived from white blood cells [4]. CfDNA is highly fragmented and the fragment size distribution corresponds to the length of DNA wrapped around a nucleosome, which is approximately 167 bp or multiples of that [2]. The size of ctDNA fragments are overall shorter compared to non-tumor derived cfDNA fragments [5-7]. The ctDNA quantity can vary depending on the tumor location and tumor burden of patients with increasing levels of ctDNA in more advanced disease stage [8-14]. As ctDNA molecules are derived from tumor cells, their genomic profile represents the genetic aberrations present in the tumor. Interestingly, the half-life of cfDNA and ctDNA in blood is short (~16 minutes to 2 hours) [15], enabling a real-time snapshot of the genomic profile of the tumor. Consequently, ctDNA analyses can be used for personalized medicine as it is a minimally-invasive alternative to tumor tissue testing for the molecular characterization of the tumor. The molecular analysis by ctDNA can be used for treatment selection (e.g. targeted therapy approaches) and the detection of resistance mechanisms by tumor evolution.

As the level of ctDNA is related to the tumor burden, another application of ctDNA measurements is for prognostication of cancer patients. In advanced solid tumor, high levels (>10%) of ctDNA are prognostic for patient outcomes independent of other prognostic clinical variables [16]. Treatment intensification could be considered for these patients to improve outcome. Additionally, detectable levels of ctDNA following curative intent surgery or radiotherapy can be relevant for the detection of minimal residual disease (MRD) or early cancer detection. Timely treatment interventions can be applied upon the detection of ctDNA in these settings, such as the administration of adjuvant therapy after surgery or radiotherapy for patients with ctDNA-based MRD [17, 18].

Finally, serial measurements of ctDNA can be used for disease and treatment monitoring throughout disease stages (Figure 1). While an increase in ctDNA or persistent ctDNA levels during treatment are associated with disease progression and lack of benefit to therapy, a decrease in ctDNA and ctDNA clearance are associated with durable treatment responses [19]. The ability to obtain real-time information on disease status and response to therapy may help to inform personalized treatment decisions, with timely treatment switches, treatment intensifications or treatment de-escalations to improve patient outcomes.

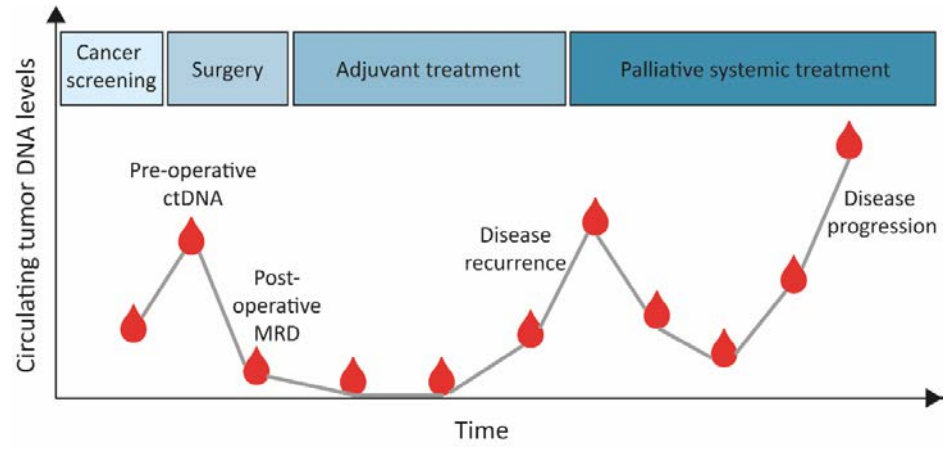

Figure 1: Serial circulating tumor DNA (ctDNA) measurements throughout disease stages. Abbreviation: MRD = minimal residual disease.

The detection of ctDNA can be performed by various techniques focusing on different characteristics of ctDNA. The most broadly used techniques for ctDNA assessments focus on the detection of genetic alterations which are present in the tumor enabling the detection of the ctDNA fraction within the total of cfDNA. Methods focusing on genomic alterations range from assays assessing single nucleotide changes (e.g. droplet digital PCR) to whole genome sequencing approaches [3]. The sensitivity and specificity of each assay is different, as well as the cost and complexity of the technique [3]. Alternatively, ctDNA can be detected by the analysis of cfDNA fragmentation patterns [5-7] or tumor and tissue specific methylation profiles [20, 21].

Besides differences in ctDNA detection techniques, also pre-analytical factors and biological factors highly impact ctDNA analysis. Firstly, adequate sample collection and sample handing is essential to prevent high molecular weight DNA to contaminate the cfDNA sample, with differences between the collection tube used for blood draws (e.g. EDTA tubes, cell-stabilizing tubes). This includes careful sample transportation [22], timely plasma processing [23] and the use of proper centrifuge protocols [24].

Secondly, although ctDNA can capture tumor heterogeneity, low abundance of ctDNA limits molecular analyses and requires advanced platforms for ctDNA detection [25]. Finally, ctDNA detection can be affected by the detection of other non-tumor derived alterations present in blood, including germline alterations and clonal hematopoietic variants [26-28]. Therefore, to ensure reliable and reproducible ctDNA testing it is important to optimize and standardize sample processing protocols and account for technical and biological factors that can affect ctDNA detection. Nevertheless, with optimalization and standardization of ctDNA tests reporting on ctDNA-based molecular profiles and ctDNA quantification, ctDNA measurements hold promise to improve patient management.

In this thesis, multiple applications of ctDNA testing are described in various clinical contexts. Firstly, the potential of ctDNA testing for molecular profiling in prostate cancer is explored. **Chapter 2** represents a comprehensive review and meta-analysis on the predictive value of cfDNA-based detection of androgen receptor (AR) copy number gain, a frequently described marker for treatment resistance in metastatic castration resistant prostate cancer (mCRPC).

Next, we performed serial ctDNA testing and investigated on-treatment changes in ctDNA levels in relation to the durability of treatment response. In **chapter 3**, we utilized a targeted sequencing approach to investigate early on-treatment ctDNA detection in relation to the response to standard of care AR pathway inhibitors in mCRPC patients. Similarly, in **chapter 4** we used targeted sequencing to investigate early on-treatment changes in ctDNA levels in relation to the responsiveness of immunotherapy in advanced urothelial cancer. In **chapter 5**, the changes in ctDNA levels during systemic treatment with BRAF/MEK inhibitors and immunotherapy were studied in relation to treatment outcomes in advanced melanoma patients. Additionally, ctDNA-based *BRAF* status testing was investigated as an alternative to tissue testing using droplet digital PCR.

The potential of ctDNA testing to detect MRD in resected stage III/IV melanoma patients is described in **chapter 6**. Moreover, the utility of serial ctDNA measurements for adjuvant therapy monitoring and recurrence prediction is described.

Finally, this thesis is concluded with a summary and general discussion of the results in **chapter 7**, including the future perspectives for ctDNA measurements in cancer management.

References

1. Tivey, A., et al., Circulating tumour DNA - looking beyond the blood. Nat Rev Clin Oncol, 2022. 19(9): p. 600-612.
2. Volckmar, A.L., et al., A field guide for cancer diagnostics using cell-free DNA: From principles to practice and clinical applications. Genes Chromosomes Cancer, 2018. 57(3): p. 123-139.
3. Wan, J.C.M., et al., Liquid biopsies come of age: towards implementation of circulating tumour DNA. Nat Rev Cancer, 2017. 17(4): p. 223-238.
4. Oberhofer, A., et al., Tracing the Origin of Cell-Free DNA Molecules through Tissue-Specific Epigenetic Signatures. Diagnostics (Basel), 2022. 12(8).
5. Mouliere, F., et al., Enhanced detection of circulating tumor DNA by fragment size analysis. Sci Transl Med, 2018. 10(466).
6. Chabon, J.J., et al., Integrating genomic features for non-invasive early lung cancer detection. Nature, 2020. 580(7802): p. 245-251.
7. Marass, F., et al., Fragment Size Analysis May Distinguish Clonal Hematopoiesis from Tumor-Derived Mutations in Cell-Free DNA. Clin Chem, 2020. 66(4): p. 616-618.
8. Fan, L., et al., Comparative Analysis of Genomic Alterations across Castration Sensitive and Castration Resistant Prostate Cancer via Circulating Tumor DNA Sequencing. J Urol, 2021. 205(2): p. 461-469.
9. Kohli, M., et al., Clinical and genomic insights into circulating tumor DNA-based alterations across the spectrum of metastatic hormone-sensitive and castrate-resistant prostate cancer. EBioMedicine, 2020. 54: p. 102728.
10. Vandekerkhove, G., et al., Circulating Tumor DNA Abundance and Potential Utility in De Novo Metastatic Prostate Cancer. Eur Urol, 2019. 75(4): p. 667-675.
11. Bando, H., et al., Effects of Metastatic Sites on Circulating Tumor DNA in Patients With Metastatic Colorectal Cancer. JCO Precis Oncol, 2022. 6: p. e2100535.
12. Zhang, E.W., et al., Association between circulating tumor DNA burden and disease burden in patients with ALK-positive lung cancer. Cancer, 2020. 126(20): p. 4473-4484.
13. Kirchweger, P., et al., Circulating tumor DNA correlates with tumor burden and predicts outcome in pancreatic cancer irrespective of tumor stage. Eur J Surg Oncol, 2022. 48(5): p. 1046-1053.
14. McEvoy, A.C., et al., Correlation between circulating tumour DNA and metabolic tumour burden in metastatic melanoma patients. BMC Cancer, 2018. 18(1): p. 726.
15. Khier, S. and L. Lohan, Kinetics of circulating cell-free DNA for biomedical applications: critical appraisal of the literature. Future Sci OA, 2018. 4(4): p. FSO295.
16. Reichert, Z.R., et al., Prognostic value of plasma circulating tumor DNA fraction across four common cancer types: a real-world outcomes study. Ann Oncol, 2023. 34(1): p. 111-120.

17. Kotani, D., et al., Molecular residual disease and efficacy of adjuvant chemotherapy in patients with colorectal cancer. Nat Med, 2023. 29(1): p. 127-134.
18. Tie, J., et al., Circulating Tumor DNA Analysis Guiding Adjuvant Therapy in Stage II Colon Cancer. N Engl J Med, 2022. 386(24): p. 2261-2272.
19. Sanz-Garcia, E., et al., Monitoring and adapting cancer treatment using circulating tumor DNA kinetics: Current research, opportunities, and challenges. Sci Adv, 2022. 8(4): p. eabi8618.
20. Shen, S.Y., et al., Sensitive tumour detection and classification using plasma cell-free DNA methylomes. Nature, 2018. 563(7732): p. 579-583.
21. Nassar, F.J., et al., Methylated circulating tumor DNA as a biomarker for colorectal cancer diagnosis, prognosis, and prediction. Clin Epigenetics, 2021. 13(1): p. 111.
22. Geerlings, M.J., et al., Effect of Pneumatic Tube System Transport on Cell-Free DNA. Clin Chem, 2021. 67(2): p. 434-435.
23. Risberg, B., et al., Effects of Collection and Processing Procedures on Plasma Circulating Cell-Free DNA from Cancer Patients. J Mol Diagn, 2018. 20(6): p. 883-892.
24. Sorber, L., et al., Circulating Cell-Free DNA and RNA Analysis as Liquid Biopsy: Optimal Centrifugation Protocol. Cancers (Basel), 2019. 11(4).
25. Russano, M., et al., Liquid biopsy and tumor heterogeneity in metastatic solid tumors: the potentiality of blood samples. J Exp Clin Cancer Res, 2020. 39(1): p. 95.
26. Jensen, K., et al., Association of Clonal Hematopoiesis in DNA Repair Genes With Prostate Cancer Plasma Cell-free DNA Testing Interference. JAMA Oncol, 2021. 7(1): p. 107-110.
27. Sena, J.A., et al., Unique Molecular Identifiers reveal a novel sequencing artefact with implications for RNA-Seq based gene expression analysis. Sci Rep, 2018. 8(1): p. 13121.
28. Abbosh, C., C. Swanton, and N.J. Birkbak, Clonal haematopoiesis: a source of biological noise in cell-free DNA analyses. Ann Oncol, 2019. 30(3): p. 358-359.

Chapter 2

A systematic review and meta-analysis on the predictive value of cell-free DNA-based androgen receptor copy number gain in patients with castration-resistant prostate cancer

Sofie H. Tolmeijer
Emmy Boerrigter
Jack A. Schalken
Maartje J. Geerlings
Inge M. van Oort
Nielka P. van Erp
Winald R. Gerritsen
Marjolijn J.L. Ligtenberg
Niven Mehra

JCO Precision Oncology 2020 Nov;4:714-729. doi: 10.1200/PO.20.00084.

Abstract

Purpose: It has been suggested that androgen receptor copy number gain (*AR* gain) detected in cell-free DNA (cfDNA) can predict treatment response to androgen receptor signaling inhibitors (ARSIs) in patients with castration-resistant prostate cancer (CRPC). But it is unclear whether cfDNA-based *AR* gain is a true resistance mechanism to ARSIs or mainly a reflection of the tumor burden. In this systematic review, we aim to summarize current literature and comment on the potential of cfDNA-based *AR* gain as a predictive biomarker to guide therapy choices.

Methods: A literature search was conducted in PubMed/Medline, Cochrane, Embase and Web of Science. Sixteen articles published before November 2019 were selected for the meta-analysis, representing over 1,000 patients. Using a random effects model, the progression-free survival (PFS) and overall survival (OS) were compared between patients with and without cfDNA-based *AR* gain treated with ARSIs or taxane chemotherapy.

Results: Upon ARSIs-treatment, the PFS (hazard ratio [HR] 2.33, 95% confidence interval [CI] 2.00-2.72; P < 0.0001) and the OS (HR 3.83, CI 3.11-4.70; P < 0.0001) were worse for patients with cfDNA-based *AR* gain, independent of the line and type of ARSIs. The OS and PFS in patients treated with first-line docetaxel or second/third-line cabazitaxel appeared unaffected by *AR* gain, despite a higher disease burden in *AR* gain patients. *AR* gain was associated with reduced response on later lines of docetaxel.

Conclusion: In patients with CRPC, cfDNA-based *AR* gain is associated with a worse outcome to ARSIs. The effect on taxane chemotherapy appears dependent on the type and line of treatment, although limited data is available. Future prospective studies are essential to assess the true potential of cfDNA-based *AR* gain as a minimally-invasive biomarker to guide therapy choice.

Introduction

Prostate cancer is the second most common cancer among men worldwide [1]. To suppress prostate cancer growth, patients often receive androgen deprivation therapy (ADT) in the form of surgical or chemical castration. ADT ablates androgen production by approximately 95%, leading to the suppression of androgen receptor (AR) signaling , which is essential for prostate cancer growth and survival. Although generally effective at first, in time the cancer transitions from a castration-sensitive to a castration-resistant state, commonly followed by an accelerating tumor growth.

In the castration-resistant state, AR signaling remains critical for disease progression [2]. Accordingly, potent second-generation AR signaling inhibitors (ARSIs) have been developed to further suppress AR signaling. These ARSIs include abiraterone [3], which suppresses androgen synthesis, and enzalutamide [4], which blocks the binding of androgens to the AR. Both abiraterone and enzalutamide have been shown to extend life expectancy in patients with castration-resistant prostate cancer (CRPC), but treatment resistance will develop in time [3-6].

Several resistance mechanisms have been described for ARSIs, many (in)directly linked to the restoration of AR signaling. A well-known example is the development of the ligand-independent splice variant AR-V7. The presence of AR-V7 in patients with CRPC is associated with a poor response to ARSIs [7, 8]. Though, still a subset of patients who express AR-V7 will still demonstrate clinical benefit when being treated with ARSIs [9, 10]. In addition to AR-V7 detection, *AR* copy number detection could provide valuable insights into AR signaling activity. An increase in *AR* copies in the tumor DNA, referred to as *AR* gain, is the most common AR-associated alteration in CRPC. *AR* gain can be detected in up to 70% of castration-resistant tumors [11-13], but in only 1% of hormone-sensitive prostate cancers [14]. *AR* gain results in an increased expression of the *AR* gene and is associated with a higher prevalence of ligand-independent splice variants of *AR*, such as AR-V7 [13, 15, 16]. The consequent enhanced AR signaling could overcome the inhibition by ARSIs and result in resistance to therapy.

Until recently, repetitive measuring of the *AR* copy number status was hampered by the difficulty of obtaining sequential and adequate tissue biopsies for genomic profiling [11]. Liquid biopsies provided a solution to this problem. Cell-free DNA (cfDNA) can be isolated from a liquid biopsy, which is partly derived from the tumor (circulating tumor DNA [ctDNA]) and contains the genomic aberrations present in tumor tissue such as *AR* gain. Because ctDNA can be released from metastases and the primary tumor, liquid biopsies grant the opportunity to noninvasively and longitudinally detect genomic

aberrations and their changes from hormone-sensitive prostate cancer to the varying stages of CRPC.

Since the discovery of cfDNA, several groups have investigated the potential of *AR* gain detection in cfDNA to predict response to ARSIs. Nevertheless, it is still unclear whether cfDNA-based *AR* gain is a true resistance mechanism to ARSIs or whether it mainly has prognostic value as a reflection of the tumor burden. For the first time (to our knowledge), we have synthesized the current literature on the relation between detection of *AR* gain in cfDNA and overall survival (OS) and progression-free survival (PFS) achieved by patients with CRPC who have been treated with ARSIs compared with taxane chemotherapy. By using a systematic approach and meta-analysis, we hope to gain more insight into the potential of cfDNA-based *AR* gain detection as a minimally invasive biomarker to guide treatment choices in patients with CRPC.

Methods

Search strategy

This systematic review and meta-analysis were performed according to the guidelines of the Preferred Reporting Items for Systematic Reviews and Meta-Analyses (PRISMA) statement [17], PROSTERO registration number CRD42019133188 [18]. The studies published up to November 27, 2019, were retrieved from PubMed/Medline, Embase, Cochrane, and Web of Science databases. We used three terms for our search: "castration-resistant prostate cancer" AND "cell-free DNA" AND "androgen receptor". The full literature search terms can be found in the PROSTERO registration. The reference sections of the publications we retrieved were searched for additional eligible studies.

Selection criteria

To determine which studies were eligible, two independent reviewers screened the titles, the abstracts, and the full texts of each publication being assessed for inclusion. Eligible studies reported the treatment response of patients with CRPC who received either chemotherapy or ARSIs and were stratified by the presence or absence of cfDNA-based *AR* copy number gain. Studies were excluded if (1) the Population, Intervention, Comparison, Outcome, Study (PICOS) criteria were not fulfilled (PROSTERO: CRD42019133188 [18]), (2) detection of *AR* copy number gain in a tumor biopsy and not in liquid biopsy was reported, (3) circulating RNA but not circulating DNA was analyzed, (4) the article focused on neuroendocrine prostate cancer, (5) epigenetic (methylation) profiles of cfDNA but not genetic profiles of cfDNA were studied, or (6) patients were preselected on the basis of an additional biomarker. Abstracts and reviews were not eligible for inclusion, but their references were assessed for potential

eligible primary studies. All studies published before 2011 were excluded, because ARSIs first became available for patients with CRPC in 2011 [3, 4].

Data collection

To assess the study characteristics for each publication, we abstracted the material used for detection, *AR* copy number detection method, and study design. For an overview of the patient characteristics, we abstracted the number of patients, type of treatment they received, line of treatment, median age, baseline prostate-specific antigen (PSA) levels, baseline alkaline phosphatase (ALK) levels, baseline lactate dehydrogenase (LDH) levels, and median follow-up time. In addition, we assessed the overlap in patient cohorts by examining the trial registration number, ethical committee number, and/or the period of study enrollment; all of this information combined is referred to as cohort identification. Only unique patient cohorts were included in the meta-analysis. For the association between *AR* gain and treatment outcome, the classifications described in the original articles were used. Only the results for the association between outcome and *AR* gain detection at the start of therapy were included.

Statistical methods

After data were collected, we performed the meta-analysis by using the R-package meta (R version 3.5.3, package version 4.9-5). The results of the univariable analysis per study were used in the meta-analysis. For all articles, the PFS was defined according to the Prostate Cancer Working Group criteria 2 or 3 [19]. If the hazard ratios (HRs) for the OS and PFS were not directly available in the main text or supplementary text of the article, but the graphs representing the data were available, authors were contacted for additional information or the data were extracted from the graphs using graphreader (www.graphreader.com). Subsequently, the survival analysis was performed using IMP SPSS Statistics 25.

For all meta-analyses, a random effects model was applied because we assumed that the true effect size could vary between the included studies as a result of varying previous lines of therapy, varying *AR* copy number detection methods, different *AR* gain cutoffs, and different ARSIs (enzalutamide or abiraterone) or chemotherapies (cabazitaxel or docetaxel). An overview of the data that were included in the meta-analysis can be found in Supplementary Table 1. Because the proportion of patients with *AR* gain can vary between treatment stages, the meta-analysis was stratified by line of treatment in a subgroup analysis.

Results

Study and patient characteristics

The search and selection process for all publications is illustrated in Figure 1. The search conducted on November 27, 2019, resulted in 1,533 publications. Of these 1,533 publications, 556 were excluded because of duplication, 122 were published before 2011 and were therefore excluded, 552 were excluded because the title did not satisfy the study criteria, and 207 were excluded after abstract screening. The remaining 65 nonprimary (abstracts or reviews) and 31 primary publications were screened for additional eligible studies in their reference lists, which resulted in 2 additional articles for full reading. In total, 33 primary articles were assessed on their full text, of which 13 articles were excluded from the meta-analysis because they did not provide sufficient information. The 20 remaining studies often described more than 1 patient cohort. On the basis of the ethical committee codes and inclusion periods, we excluded patient cohorts that potentially overlapped with previously described cohorts (Supplementary Table 2). The results of the remaining 23 unique patient cohorts were described in 16 different articles. Although only unique patient cohorts were included in the meta-analysis, a subset of articles were written by the same research groups, potentially introducing a bias. Altogether, the articles reported the effect of *AR* gain in 1,249 patients with CRPC treated with ARSIs and 424 treated with taxane chemotherapy. The study characteristics of these articles are summarized in Table 1 and the patient characteristics are described in Table 2. The patient characteristics in Table 2, were mostly comparable between the different cohorts with some exceptions, such as a relatively high median PSA level in the cohort treated with docetaxel described by Buelens *et al.* [20] and a relatively high median LDH level in the cohort treated with ARSIs described by De Laere *et al.* [21].

The *AR* copy number status was determined by using 3 main techniques: (1) small amplicon polymerase chain reaction (PCR)–based techniques (droplet digital PCR [ddPCR], digital PCR [dPCR], or quantitative PCR [qPCR]), (2) next-generation sequencing (NGS) approaches (whole-genome sequencing, targeted sequencing, or whole-exome sequencing), or (3) comparative genomic hybridization arrays (Table 1). The articles included in the meta-analysis described patients with CRPC who were treatment naïve or were at later lines of therapy. In line with previous literature [22], the proportion of *AR* gain was higher in the articles describing later lines of therapy (37.3%) compared with those that described treatment-naïve patients (21.4%, Supplementary Figure 1).

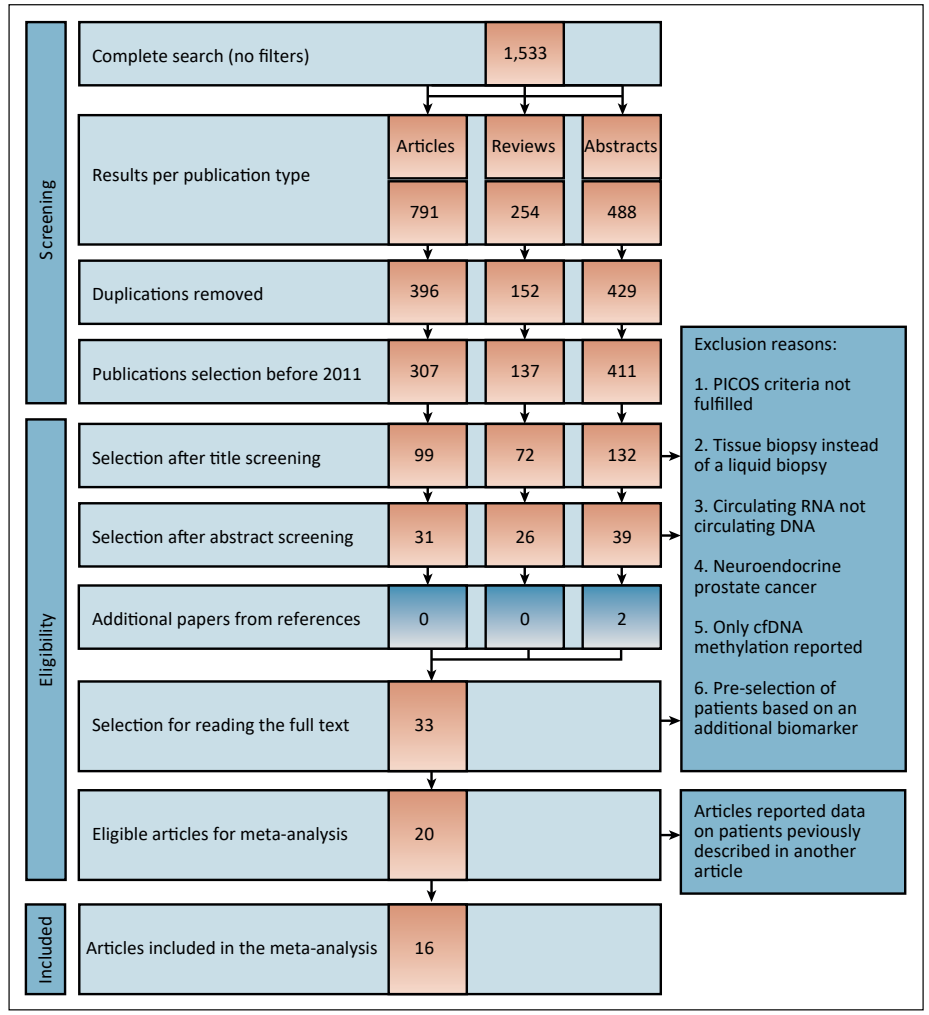

Figure 1: The study selection process according to the Preferred Reporting Items for Systematic Reviews and Meta-analysis (PRISMA). PICOS = Population, Intervention, Comparison, Outcome, Study design; cfDNA = cell-fee DNA.

cfDNA-Based *AR* Gain and Response to ARSIs and Chemotherapy

The effect of *AR* gain on PFS could be assessed in 1,184 patients treated with ARSIs [12, 20, 21, 23-31] and 408 patients treated with taxane chemotherapy [20, 32-34]. The effect of *AR* gain on OS could be assessed in 1,098 patients treated with ARSIs [20, 21, 23, 25-31, 34] and 421 patients treated with taxane chemotherapy [20, 32-34]. Because these therapies were given to patients with CRPC in first, second, and later lines, we assessed the effect of *AR* gain on the PFS and OS in relation to the line of therapy in a subgroup analysis.

Table 1: The study characteristics of the studies included in the meta-analyses.

Study	Year	Country	AR detection method	Material	Study design	Patients	Cohort identification	Treatment
Author [ref]						*n/n* with AR gain	Ethical, trial number or *collection period*	
Annala [23]	2018	Canada	WES, DTS	Plasma	RCT	201/67	NCT02125357	Abi , Enza
Azad [24]	2015	Canada	aCGH, DTS	Plasma	PS	39/14	*August 2013 – March 2014*	Enza
Buelens [20]	2017	Belgium	ddPCR	Serum	PS	15/5	B670201420716, B670201524204	Abi
						20/7		Enza
						22/9		Doce
Conteduca [26]	2017	Italy, UK	ddPCR	Plasma	RS	73/10	REC 04/Q0801/6	Abi, Enza
					RS	98/34	REC 2192/2013	Abi, Enza
Conteduca [33]	2018	Italy, UK	ddPCR	Plasma	RS	115/32	*May 2011 – January 2017*	Doce
					RS	48/18		
Conteduca [25]	2018	Italy, UK	ddPCR	Plasma	PS	59/11	REC 6798/2015	Abi, Enza
Conteduca [32]	2019	Italy, UK, Spain	ddPCR	Plasma	RS	155/65	NCT03381326	Caba
					RCT	71/30	NCT01308580	Caba
De Laere [21]	2018	Belgium, NL, Sweden	lpWGS, DTS	Plasma	PS	168*/54	B300201524217, NL53474.078.15, 2016/101-32	Abi, Enza
Hovelson [34]	2017	USA	(u)lpWGS	Plasma	RS	16/6		Abi, Enza
						13/4		Doce
Jayaram [27]	2019	UK, Italy, others	ddPCR, DTS	Plasma	RCT	133/22	NCT01867710	Abi
					SGA	94/?	NCT02288936	Enza
Kohli [28]	2018	USA	dPCR	Plasma	PS	70/19	*May 2013 – September 2015*	Abi
Salvi [29]	2015	Italy, UK	qPCR, dPCR	Serum	RS	53/16	*March 2011 – August 2012*	Abi
Salvi [30]	2016	Italy, UK	qPCR, dPCR	Serum	RS	59/21	*August 2012 – November 2015*	Enza
Sumiyoshi [46]	2019	Japan	dPCR, DTS	Plasma	PS	24/11	G1083	Enza
Torquato [31]	2019	USA	DTS	Plasma	PS	62/32	*September 2014 – April 2018*	Abi, Enza
Wyatt [12]	2016	Canada	aCGH, DTS	Plasma	PS	65*/19	*August 2013 – July 2015*	Enza

PS = Prospective Study, RS = Retrospective Study, RCT = Randomized Controlled Trail, SGA = Single group assignment, ((u)lp)WGS = ((ultra-)low pass) whole genome sequencing, WES = whole exome sequencing, (d)dPCR = (droplet) digital Polymerase Chain Reaction, qPCR = quantitative PCR, aCGH = array Comparative Genomic Hybridization, DTS = Deep Targeted Sequencing, Abi = Abiraterone, Enza = Enzalutamide, Doce = Docetaxel, Caba = Cabazitaxel. *Not all patients were tested for *AR* gain.

For patients treated with ARSIs, the PFS was worse for patients with *AR* gain than for patients who were *AR* neutral (HR, 2.33; 95% CI, 2.00 to 2.72; P < 0.0001; Figure 2A). The results were highly homogeneous (I^2 = 0%; P = 0.67), with no subgroup differences between the different lines of treatment (P = 0.27). Similarly, the OS was shorter for patients with an *AR* gain when they were treated with ARSIs (HR, 3.82; 95% CI, 3.11 to 4.70; Figure 3A). The results were again highly homogeneous (I^2 = 0%; P = 0.99) with no difference between the subgroups with different lines of treatment (P = 0.82). For both the PFS and OS data, the funnel plots with the accompanying trimfill plots showed limited to no evidence of publication bias (Supplementary Figure 2).

For patients treated with taxane chemotherapy, the effect of *AR* gain on the PFS and OS was dependent on the type of chemotherapy (docetaxel or cabazitaxel) and the line of treatment. No difference in PFS (HR, 1.28; 95% CI, 0.90 to 1.83; I^2 = 32%; Figure 2B) and OS (HR, 1.30; 95% CI, 0.94 to 1.79; I^2 = 0%; Figure 3B) could be detected between patients with *AR* gain and those who were *AR* neutral and who were treated with cabazitaxel or first-line docetaxel (only one study). In contrast, *AR* gain did seem to be associated with a shorter PFS (HR, 2.79; 95% CI, 1.59 to 4.89; I^2 = 0%; Figure 2B) and OS (HR, 3.58; 95% CI, 2.01 to 6.38; I^2 = 0%; Figure 3B) in patients treated with docetaxel in mostly higher lines of therapy.

Table 2: The baseline patient characteristics of the studies included in the meta-analyses.

Study	Patients**	Age (years)	PSA (ng/mL)	LDH (U/L)	ALK (U/L)	Treatment	Line	Median follow-up
Author [ref]	n	Median [range or IQR*]						Months [range or IQR*]
Annala [23]	201	75.3 [49.3-94.1]	36.1 [1.7-2817]	154.1 [60.5-2515.5]	102.1 [36.5-6022.8]	Abi, Enza	First	12.9 [0-32.1]
Azad [24]	39	72 [49-92]*		209 [174-316]*	144 [93-320]*	Enza	Second-eighth	- [0-13]
Buelens [20]	15	68 [63-77]*	46.1 [12.3-185]*			Abi	First-third	10.2
	20	70 [65.8-78.8]*	29.8 [13.7-94.5]*			Enza	First-third	10.6
	22	66.4 [63-69.3]*	140.9 [29.3-370.9]*			Doce	First-third	30.2
Conteduca [26]	73	73 [69-82]*	32 [10.2-81.4]*	- [77-915]	- [44-531]	Abi, Enza	First	[0.9-33]
	98	- [41-91]	- [1-3150]	- [78-968]	- [36-1040]	Abi, Enza	Second- third	[0.8-68]
Conteduca [33]	115	70 [65–75]	49.7 [14.4–143]			Doce	First	24 [18–36]*
	48					Doce	Second	-
Conteduca [25]	59	75 [72-91]	20.5 [1.48-4294]	179 [88-695]	110 [12-321]	Abi, Enza	First-higher	17.6 [1-49]
Conteduca [32]	155	70 [43-87]	80 [0.1-5000]			Caba	Second-third	24 [0.5-47]
	71					Caba	Second-third	-
De Laere [21]	168	76 [69.3-83.7]*	36.92 [13.5-144.9]*	335 [217-655.5]*	102 [73-160.5]*	Abi, Enza	First-third	12.4 [7-17.3]
Hovelson [34]	16					Abi, Enza	Second-fifth	12.5 [0.6-40.7]
	13					Doce	First-fifth	11.5 [0.6-35.4]
Jayaram [27]	133	70 [53-88]	50.75 [0.67-1537]	171.6 [85.8-881.4]	102.1 [23.9-1127.7]	Abi	First	46
	94	77 [57-95]	24.95 [1.99-4319]	163.8 [56.6-655.2]	90.7 [30.2-2200]	Enza	First	32
Kohli [28]	70	71.5 [39-91]	16.2 [8-38.9]*	187 [170-209]*		Abi	First	26.4 [17.5-31.7]*
Salvi [29]	53	74 [57-87]	33.1 [1-1501]	201 [48-999]	117 [35-1144]	Abi	Second-higher	- [0-21]
Salvi [30]	59	75 [43-91]	68.2 [0.6-4351]	204 [122-1808]	125 [32-6000]	Enza	Second-higher	- [0-21]
Sumiyoshi [46]	24					Enza	Second-higher	- [0-14.8]
Torquato [31]	62	71.5 [41-90]	19.3 [0.6-1966]			Abi, Enza	First-second	17.0 [1.1-41.9]
Wyatt [12]	65	74 [68-79]*		236 [190-330]*	130 [97-242]*	Enza	Second-higher	- [1-20]

*Interquartile range (IQR) reported instead of full range. **All patients had metastatic castration resistant prostate cancer patients (mCRPC), except in the paper of Sumiyoshi et al [46] and Buelens et al [20] who also included non-metastatic CRPC patients. Abi = Abiraterone, Enza = Enzalutamide , Doce = Docetaxel, Caba = Cabazitaxel.

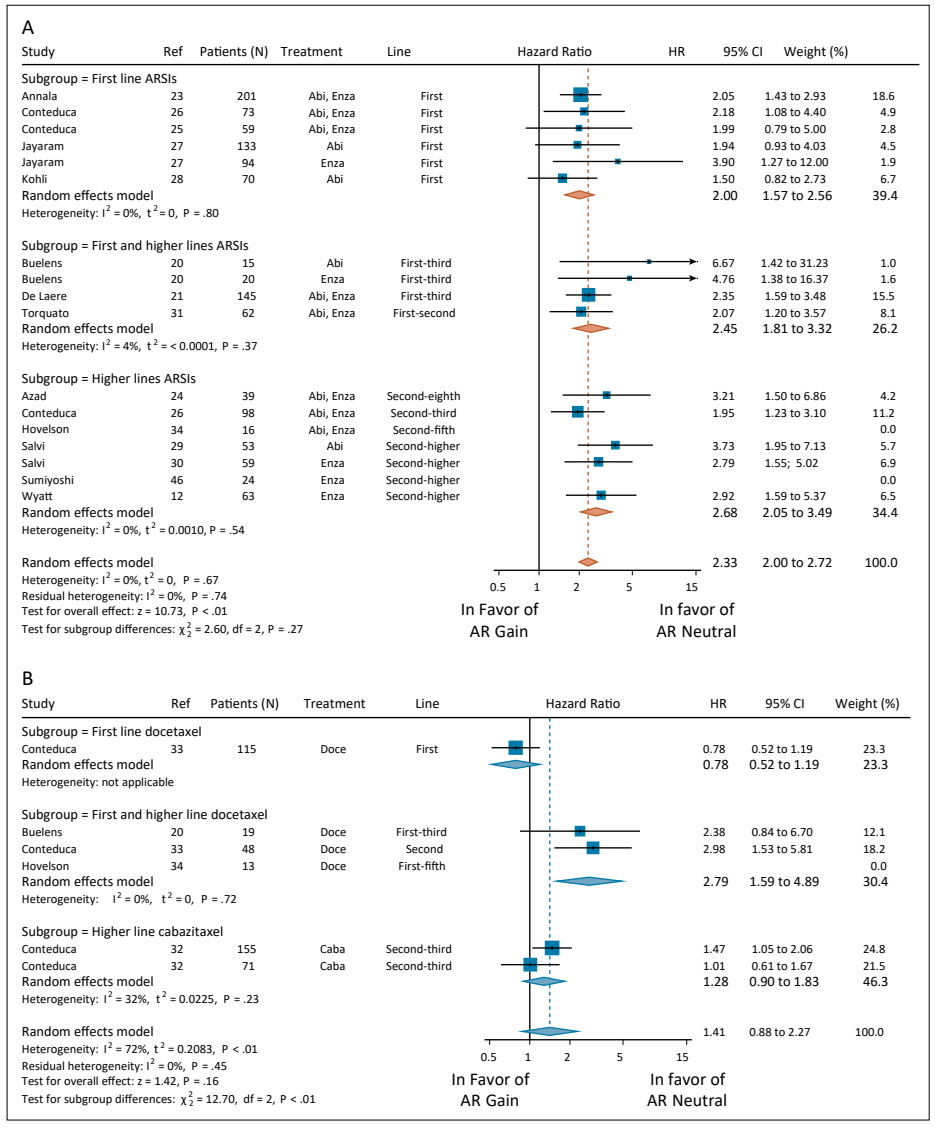

Figure 2: Forest-plot of the progression free survival (PFS) achieved with (**A**) androgen receptor signaling inhibitors (ARSIs) or (**B**) taxane chemotherapy in patient with castration resistant prostate cancer stratified by their cfDNA-based *AR* copy number status (*AR* gain or neutral). The bars indicate the mean ± 95% confidence interval. Abi = Abiraterone, Enza = Enzalutamide, Doce = Docetaxel, Caba = Cabazitaxel.

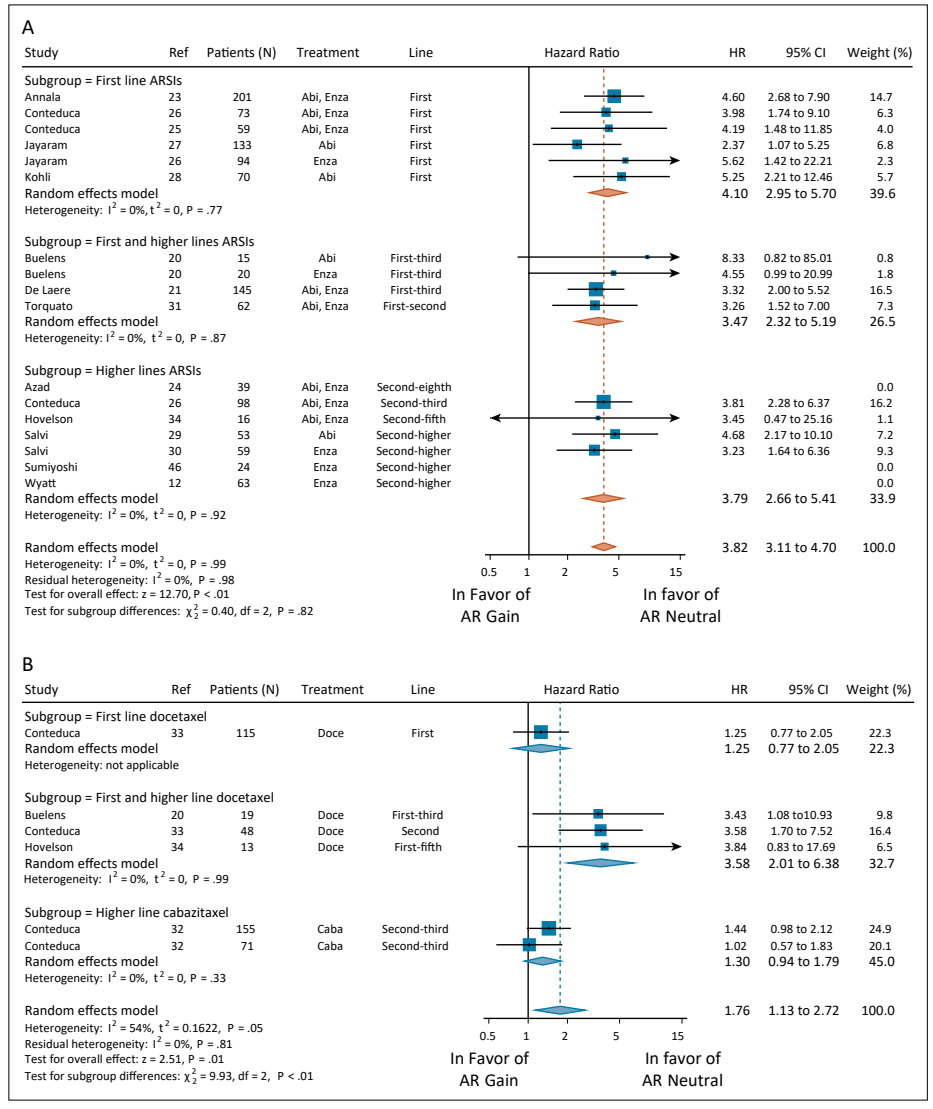

Figure 3: Forest-plot of the overall survival (OS) achieved with (**A**) androgen receptor signaling inhibitors (ARSIs) or (**B**) taxane chemotherapy in patient with castration resistant prostate cancer stratified by their cfDNA-based *AR* copy number status (*AR* gain or neutral). The bars indicate the mean ± 95% confidence interval. Abi = Abiraterone, Enza = Enzalutamide, Doce = Docetaxel, Caba = Cabazitaxel.

Discussion

AR signaling remains critical for prostate cancer development and growth in both the hormone-sensitive disease stage and the castration-resistant state. A strong suppression of *AR* signaling is achieved by ARSIs such as abiraterone or enzalutamide, but resistance to these inhibitors eventually occurs in all patients. Detecting resistance mechanisms at the start of treatment could help predict patients' responses to ARSIs. By using a systematic approach and meta-analysis, we investigated the potential of AR copy number gain detected in cfDNA to predict responses and patient outcome to ARSIs and taxane chemotherapy.

AR copy number gain is associated with an enhanced expression of AR and AR splice variants, which could lead to enhanced AR signaling and could overcome inhibition by ARSIs. In line with this hypothesis, our meta-analysis demonstrates that the PFS was 2.33 times shorter and the OS was 3.82 times shorter for *AR*-gain patients compared with *AR*-neutral patients treated with ARSIs (Figure 2A and 3A). The shorter PFS and OS associated with *AR* gain was highly consistent over different lines and types of ARSIs, even though *AR* gain was measured with different techniques. This suggests that cfDNA-based *AR* gain has a robust and fixed effect on the response to ARSIs. Our meta-analysis also showed that the proportion patients who are positive for *AR* gain increases in successive lines of therapy (Supplementary Figure 1). This is in line with previous reports demonstrating that from a spectrum of aberrations, only the proportion of cfDNA-based *AR* gain and *AR* structural variants increase in successive lines of therapy [22]. Consequently, the number of patients that derive limited benefit from ARSIs will proportionally expand when more patients are heavily pretreated.

A few articles describe that *AR* gain no longer seems to be of prognostic significance in patients treated with ARSIs when the analysis is corrected for ctDNA burden or other disease burden markers [21, 23, 31]. In general, the presence of cfDNA-based *AR* gain is associated with a higher disease burden [29, 30, 32, 33] and ctDNA purity [35]. As a consequence, it is difficult to distinguish the prognostic value of cfDNA-based *AR* gain as an indirect measure of the tumor burden and the possibly predictive value of cfDNA-based *AR* gain as a resistance mechanism to ARSIs. Nevertheless, our meta-analyses showed no difference in the prognosis between *AR*-gain and *AR*-neutral patients when they were treated with first-line docetaxel or higher lines of cabazitaxel. *AR*-gain patients treated with these chemotherapeutic agents did have higher tumor burden markers (e.g., LDH, PSA, ALK, or the prevalence of visceral, liver, and bone metastasis) compared with *AR*-neutral patients, which were prognostic for response to the chemotherapeutic agents [32, 33]. Consequently, tumor burden seems to be a robust prognostic biomarker, independent of treatment type, whereas cfDNA-based *AR* gain detection seems to have additional predictive characteristics, with dampened response specific to ARSIs.

AR gain is associated with a 3.8-fold higher prevalence [15] and a more than fourfold higher expression of AR-V7 [16], which could partly explain the inferior response of *AR*-gain patients to ARSIs. The meta-analysis of Li et al. [7] demonstrated that like *AR*-gain patients, AR-V7–positive patients have an inferior response to ARSIs. Nonetheless, in the PREMIERE trial (ClinicalTrials.gov identifier: NCT02288936), no relation was found between detection of AR-V7–positive circulating tumor cells (CTCs) and primary resistance to first-line enzalutamide [10], whereas cfDNA-based *AR* gain detection was strongly associated with an inferior response to enzalutamide [26, 27]. This implies that cfDNA-based *AR* gain detection has an additional predictive value for detection of AR-V7.

The detection of cfDNA-based *AR* gain as a putative predictive biomarker could possibly outperform AR-V7 mostly in the early treatment stages of CRPC, because in this stage, the proportion of patients who are positive for CTC-based AR-V7 is much lower (approximately 3% [36]) than the proportion of patients who are positive for cfDNA-based AR gain (approximately 21%, Supplementary Figure 1). In advanced CRPC, the proportion of AR-V7–positive patients expands up to 31% [36], which is similar to the proportion of *AR*-gain–positive patients at this stage of disease (approximately 37%, Supplementary Figure 1).

The presence of AR-V7 could also influence the response to docetaxel, because docetaxel can inhibit the microtubule-associated translocation of the full-length AR protein into the nucleus, but not the translocation of AR-V7 [37]. This was indeed supported by the results of Tagawa et al. [38], who showed that patients with AR-V7–positive CTCs demonstrated a poorer outcome to docetaxel compared with patients with AR-V7–negative CTCs. Considering that the proportion of AR-V7 patients is similar to the proportion of *AR*-gain patients in advanced treatment stages, but not in early treatment stages, the prognostic differences of *AR* gain in sequential lines of docetaxel treatment (Figs 2B and 3B) might be partially explained by the co-occurrence of AR-V7.

Interestingly, cabazitaxel is suggested to have a strong AR-independent working mechanism that induces [39] an AR-V7 status-independent response [40]. In line with this, our meta-analysis suggests that *AR* gain is not prognostic for the response to cabazitaxel in higher treatment lines while it is prognostic for docetaxel (Figs 2B and 3B). As a result, it could be hypothesized that patients with a cfDNA-based *AR* gain might benefit more from cabazitaxel (or first-line docetaxel) than from ARSIs, which was also suggested by Conteduca et al. who compared first-line docetaxel with first-line ARSIs and second-line cabazitaxel with second-line ARSIs in patients with CRPC

[32, 33]. Similarly, patients without *AR* gain could still benefit from ARSIs even with later lines of treatment (Supplementary Table 1).

Still, in some individual cases, the presence of cfDNA-based *AR* gain does not result in resistance to ARSIs [41]. These cases can potentially be explained by various alternative mechanisms of resistance, being AR dependent or AR independent. In the first place, the level of copy number gain can influence responsiveness or duration of response to ARSIs [23]. Annala et al. [23] described a poorer response to ARSIs in patients with a high *AR* gain (more than eight copies) compared with a low *AR* gain (two to eight copies). This implies that there is a dose effect in overcoming inhibition of the AR signaling by ARSIs. In addition to *AR* copy number levels, Viswanathan et al. [42] reported that many CRPC tumors carry a copy number gain in the *AR* enhancer. They showed that both the *AR* and *AR* enhancer copy number, measured in tumor tissue and blood-derived cfDNA, increase during treatment with ARSIs and result in a higher AR expression followed by ARSI resistance. Overall, this suggests that for prognostic purposes, reporting cfDNA-based *AR* gain could be optimized by identifying the optimal cutoff value for *AR* gain detection (as was suggested by Jayaram et al. [27]), should possibly include *AR* enhancer gain detection, and might need to be longitudinally assessed because of selected treatment pressure and tumor evolution.

This meta-analysis has some limitations. First, the analysis included a heterogeneous study population, various study designs, and various patient characteristics (Tables 1 and 2). Second, only a limited number of patients treated with taxane chemotherapy could be included in the analysis. Consequently, the estimates of the effect size could be less reliable and the results could be prone to a publication bias, especially because limited research groups have published the majority of articles composed of multiple cohorts. In addition, the differences in treatment regimens complicate direct comparison between the different chemotherapeutic agents. To truly distinguish whether both taxanes have differential mechanisms with regard to AR nuclear transport and signaling, it will be vital to await the results from ongoing translational research on ctDNA performed in FIRSTANA (ClinicalTrials.gov identifier: NCT01308567) [43], which compares first-line docetaxel and cabazitaxel, and PROSELICA (ClinicalTrials.gov identifier: NCT01308580) [44], which will provide insight into the response to cabazitaxel in relation to dose and different tumor genotypes after docetaxel treatment [32, 45]. Third, the *AR* detection methods with accompanying cutoffs for *AR* gain varied among the articles. The two techniques mainly used for *AR* detection were ddPCR and NGS (Table 1). If NGS was used, the ctDNA burden was often taken into account for the *AR* copy number estimations. This is not possible for ddPCR, which could potentially influence the classification between *AR*-gain and *AR*-neutral patients. These differences could not be directly addressed in the meta-analysis. Finally, this meta-analysis focuses on only 1 genomic alteration. Other genomic alterations, such as *TP53, RB1, PI3K*, or damage repair pathway defects, are also known to be prognostic and to affect the treatment response [21, 23, 31]. The possible enrichment of these alterations in *AR*-gain patients or the potential effect of these alterations on AR signaling could not be considered in this meta-analysis.

Despite these limitations, the results were highly homogeneous for all analyses that included a large number of patients, and the chance of publication bias was low (Supplementary Figure 2). The most relevant studies were selected by using a reproducible and comprehensive search. By carefully assessing the overlap between patient cohorts, we were able to include only unique patient results in the meta-analysis. In total, the effect of *AR* gain on response to treatment with ARSIs could be summarized for more than 1,000 patients. In addition, this study enabled a detailed description of all studies, including the patient baseline characteristics, study designs, and outcome measures, which will be available for future reference.

In conclusion, our meta-analysis revealed that detection of *AR* gain in the cfDNA of patients with CRPC provides a robust prognostic biomarker for the response to ARSIs, with a fixed effect of *AR* gain in different lines of ARSIs. Future prospective studies will be essential for assessing the outcomes of taxane chemotherapies among each other and compared with ARSIs in relation to *AR* status.

References

1. Wong, M.C., et al., Global Incidence and Mortality for Prostate Cancer: Analysis of Temporal Patterns and Trends in 36 Countries. Eur Urol, 2016. 70(5): p. 862-874.
2. Sharma, N.L., et al., The Androgen Receptor Induces a Distinct Transcriptional Program in Castration-Resistant Prostate Cancer in Man. Cancer Cell, 2013. 23(1): p. 35-47.
3. de Bono, J.S., et al., Abiraterone and increased survival in metastatic prostate cancer. N Engl J Med, 2011. 364(21): p. 1995-2005.
4. Scher, H.I., et al., Increased Survival with Enzalutamide in Prostate Cancer after Chemotherapy. New England Journal of Medicine, 2012. 367(13): p. 1187-1197.
5. Beer, T.M., et al., Enzalutamide in Metastatic Prostate Cancer before Chemotherapy. New England Journal of Medicine, 2014. 371(5): p. 424-433.
6. Ryan, C.J., et al., Abiraterone in Metastatic Prostate Cancer without Previous Chemotherapy. New England Journal of Medicine, 2013. 368(2): p. 138-148.
7. Li, H., et al., Prognostic Value of Androgen Receptor Splice Variant 7 in the Treatment of Castration-resistant Prostate Cancer with Next generation Androgen Receptor Signal Inhibition: A Systematic Review and Meta-analysis. Eur Urol Focus, 2018. 4(4): p. 529-539.
8. Armstrong, A.J., et al., Prospective Multicenter Validation of Androgen Receptor Splice Variant 7 and Hormone Therapy Resistance in High-Risk Castration-Resistant Prostate Cancer: The PROPHECY Study. J Clin Oncol, 2019. 37(13): p. 1120-1129.
9. Bernemann, C., et al., Expression of AR-V7 in Circulating Tumour Cells Does Not Preclude Response to Next Generation Androgen Deprivation Therapy in Patients with Castration Resistant Prostate Cancer. European Urology, 2017. 71(1): p. 1-3.
10. Grande, E., et al., Early responses to enzalutamide in AR-V7 positive first line metastatic castration-resistant prostate cancer (mCRPC). A prospective SOGUG clinical trial: The PREMIERE study. Annals of Oncology, 2016. 27(suppl_6).
11. Robinson, D., et al., Integrative Clinical Genomics of Advanced Prostate Cancer. Cell, 2015. 161(5): p. 1215-1228.
12. Wyatt, A.W., et al., Genomic Alterations in Cell-Free DNA and Enzalutamide Resistance in Castration-Resistant Prostate Cancer. Jama Oncology, 2016. 2(12): p. 1598-1606.
13. Quigley, D.A., et al., Genomic Hallmarks and Structural Variation in Metastatic Prostate Cancer. Cell, 2018. 175(3): p. 889.
14. Merson, S., et al., Focal amplification of the androgen receptor gene in hormone-naive human prostate cancer. British Journal of Cancer, 2014. 110(6): p. 1655-1662.
15. De Laere, B., et al., Comprehensive Profiling of the Androgen Receptor in Liquid Biopsies from Castration-resistant Prostate Cancer Reveals Novel Intra-AR Structural Variation and Splice Variant Expression Patterns. European Urology, 2017. 72(2): p. 192-200.
16. Djusberg, E., et al., High levels of the AR-V7 Splice Variant and Co-Amplification of the Golgi Protein Coding YIPF6 in AR Amplified Prostate Cancer Bone Metastases. Prostate, 2017. 77(6): p. 625-638.
17. Moher, D., et al., Preferred reporting items for systematic review and meta-analysis protocols (PRISMA-P) 2015 statement. Syst Rev, 2015. 4: p. 1.
18. Centre for Reviews and Dissemination, U.o.Y. PROSPERO. 2019 [cited 2019; Available from: https://www.crd.york.ac.uk/PROSPERO/.
19. Scher, H.I., et al., Trial Design and Objectives for Castration-Resistant Prostate Cancer: Updated Recommendations From the Prostate Cancer Clinical Trials Working Group 3. Journal of clinical oncology : official journal of the American Society of Clinical Oncology, 2016. 34(12): p. 1402-1418.
20. Buelens, S., et al., Prognostic and Therapeutic Implications of Circulating Androgen Receptor Gene Copy Number in Prostate Cancer Patients Using Droplet Digital Polymerase Chain Reaction. Clinical Genitourinary Cancer, 2018. 16(3): p. 197-+.
21. De Laere, B., et al., TP53 Outperforms Other Androgen Receptor Biomarkers to Predict Abiraterone or Enzalutamide Outcome in Metastatic Castration-Resistant Prostate Cancer. Clin Cancer Res, 2019. 25(6): p. 1766-1773.
22. Mayrhofer, M., et al., Cell-free DNA profiling of metastatic prostate cancer reveals microsatellite instability, structural rearrangements and clonal hematopoiesis. Genome Med, 2018. 10(1): p. 85.
23. Annala, M., et al., Circulating Tumor DNA Genomics Correlate with Resistance to Abiraterone and Enzalutamide in Prostate Cancer. Cancer Discov, 2018. 8(4): p. 444-457.
24. Azad, A.A., et al., Androgen Receptor Gene Aberrations in Circulating Cell-Free DNA: Biomarkers of Therapeutic Resistance in Castration-Resistant Prostate Cancer. Clin Cancer Res, 2015. 21(10): p. 2315-24.
25. Conteduca, V., et al., Plasma androgen receptor and serum chromogranin A in advanced prostate cancer. Scientific Reports, 2018. 8.
26. Conteduca, V., et al., Androgen receptor gene status in plasma DNA associates with worse outcome on enzalutamide or abiraterone for castration-resistant prostate cancer: a multi-institution correlative biomarker study. Annals of Oncology, 2017. 28(7): p. 1508-1516.
27. Jayaram, A., et al., Plasma Androgen Receptor Copy Number Status at Emergence of Metastatic Castration-Resistant Prostate Cancer: A Pooled Multicohort Analysis. JCO Precision Oncology, 2019(3): p. 1-13.
28. Kohli, M., et al., Prognostic association of plasma cell-free DNA-based androgen receptor amplification and circulating tumor cells in pre-chemotherapy metastatic castration-resistant prostate cancer patients. Prostate Cancer and Prostatic Diseases, 2018. 21(3): p. 411-418.

29. Salvi, S., et al., Circulating cell-free AR and CYP17A1 copy number variations may associate with outcome of metastatic castration-resistant prostate cancer patients treated with abiraterone. British Journal of Cancer, 2015. 112(10): p. 1717-1724.
30. Salvi, S., et al., Circulating AR copy number and outcome to enzalutamide in docetaxel-treated metastatic castration-resistant prostate cancer. Oncotarget, 2016. 7(25): p. 37839-37845.
31. Torquato, S., et al., Genetic Alterations Detected in Cell-Free DNA Are Associated With Enzalutamide and Abiraterone Resistance in Castration-Resistant Prostate Cancer. JCO Precis Oncol, 2019. 3.
32. Conteduca, V., et al., Plasma AR status and cabazitaxel in heavily treated metastatic castration-resistant prostate cancer. Eur J Cancer, 2019. 116: p. 158-168.
33. Conteduca, V., et al., Plasma Androgen Receptor and Docetaxel for Metastatic Castration-resistant Prostate Cancer. Eur Urol, 2019. 75(3): p. 368-373.
34. Hovelson, D.H., et al., Rapid, ultra low coverage copy number profiling of cell-free DNA as a precision oncology screening strategy. Oncotarget, 2017. 8(52): p. 89848-89866.
35. Romanel, A., et al., Plasma AR and abiraterone-resistant prostate cancer. Sci Transl Med, 2015. 7(312): p. 312re10.
36. Scher, H.I., D. Lu, and N.A. Schreiber, Association of AR-V7 on Circulating Tumor Cells as a Treatment-Specific Biomarker With Outcomes and Survival in Castration-Resistant Prostate Cancer" (vol 2, pg 1441, 2016). Jama Oncology, 2016. 2(11): p. 1511-1511.
37. Thadani-Mulero, M., et al., Androgen Receptor Splice Variants Determine Taxane Sensitivity in Prostate Cancer. Cancer Research, 2014. 74(8): p. 2270-2282.
38. Tagawa, S.T., et al., Expression of AR-V7 and ARv^{567es} in Circulating Tumor Cells Correlates with Outcomes to Taxane Therapy in Men with Metastatic Prostate Cancer Treated in TAXYNERGY. Clinical Cancer Research, 2019. 25(6): p. 1880-1888.
39. Al Nakouzi, N., et al., Cabazitaxel Remains Active in Patients Progressing After Docetaxel Followed by Novel Androgen Receptor Pathway Targeted Therapies. European Urology, 2015. 68(2): p. 228-235.
40. Onstenk, W., et al., Efficacy of Cabazitaxel in Castration-resistant Prostate Cancer Is Independent of the Presence of AR-V7 in Circulating Tumor Cells. European Urology, 2015. 68(6): p. 939-945.
41. Belic, J., et al., Genomic alterations in plasma DNA from patients with metastasized prostate cancer receiving abiraterone or enzalutamide. International Journal of Cancer, 2018. 143(5): p. 1236-1248.
42. Viswanathan, S.R., et al., Structural Alterations Driving Castration-Resistant Prostate Cancer Revealed by Linked-Read Genome Sequencing. Cell, 2018. 174(2): p. 433-+.
43. Oudard, S., et al., Cabazitaxel Versus Docetaxel As First-Line Therapy for Patients With Metastatic Castration-Resistant Prostate Cancer: A Randomized Phase III Trial—FIRSTANA. Journal of Clinical Oncology, 2017. 35(28): p. 3189-3197.
44. Eisenberger, M., et al., Phase III Study Comparing a Reduced Dose of Cabazitaxel (20 mg/m(2)) and the Currently Approved Dose (25 mg/m(2)) in Postdocetaxel Patients With Metastatic Castration-Resistant Prostate Cancer-PROSELICA. J Clin Oncol, 2017. 35(28): p. 3198-3206.
45. Sumanasuriya, S., et al., Cell-free DNA as a biomarker for taxane treatment in advanced prostate cancer. Journal of Clinical Oncology, 2019. 37(15_suppl): p. 5070-5070.
46. Sumiyoshi, T., et al., Clinical utility of androgen receptor gene aberrations in circulating cell-free DNA as a biomarker for treatment of castration-resistant prostate cancer. Scientific Reports, 2019. 9.
47. Conteduca, V., et al., Circulating androgen receptor combined with 18F-fluorocholine PET/CT metabolic activity and outcome to androgen receptor signalling-directed therapies in castration-resistant prostate cancer. Scientific Reports, 2017. 7.
48. Conteduca, V., et al., Multimodal approach to outcome prediction in metastatic castration-resistant prostate cancer by integrating functional imaging and plasma DNA analysis. JCO Precision Oncology, 2019. 3(no pagination).
49. Lolli, C., et al., Testosterone levels and androgen receptor copy number variations in castration-resistant prostate cancer treated with abiraterone or enzalutamide. Prostate, 2019. 79(11): p. 1211-1220.

Supplementary Data

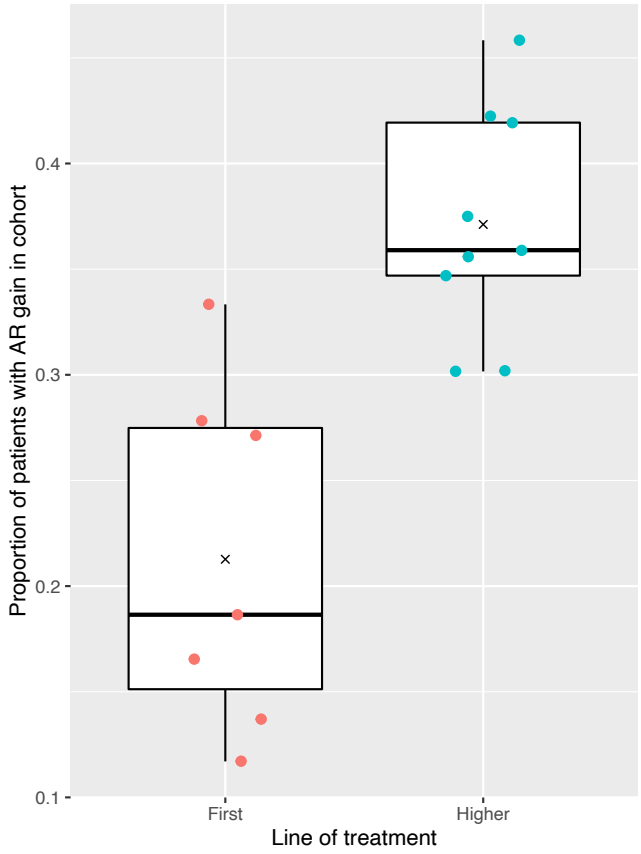

Supplementary Figure 1: The proportion of cfDNA-based *AR* gain positive patients with CRPC. The proportion patients with *AR* gain was assessed in treatment-naïve and later stages, extracted from evaluable data from published cohorts. The studies that described first- and higher lines of treatment in the same cohort were excluded from the analysis. The two-tailed t-test was significant ($P < 0.001$). Visualized is the boxplot with the dots representing the different patient cohorts and the 'x' representing the means per group.

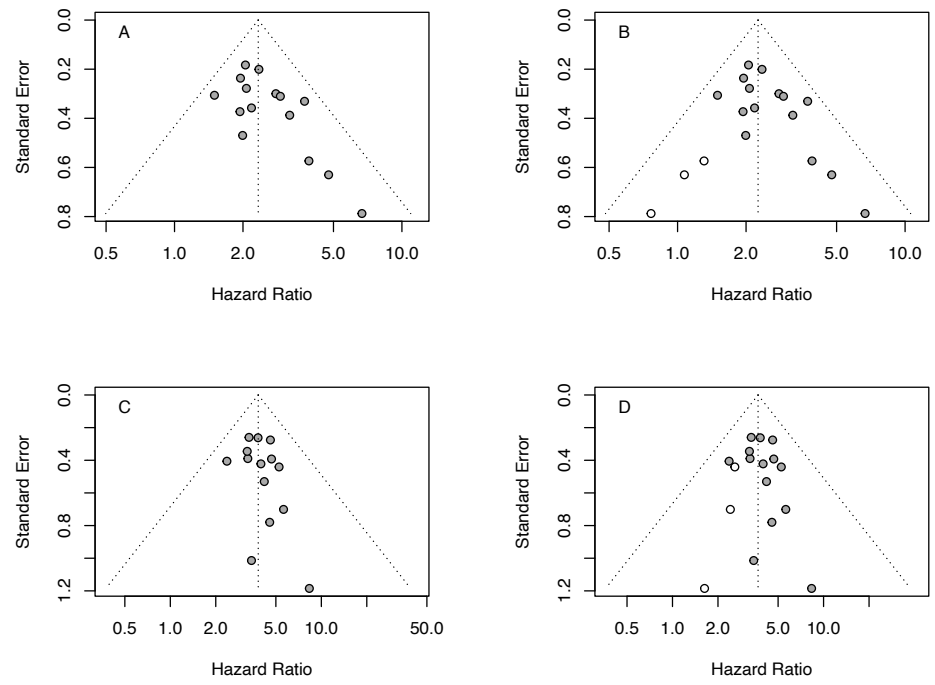

Supplementary Figure 2: The funnel plots and trimfill plots associated with the meta-analyses of the progression free survival (PFS) and overall survival (OS) achieved by androgen receptor signaling inhibitors (ARSIs) in patients with castration resistant prostate cancer (CRPC). (**A**) Funnel plot of the reported hazard ratio's between the PFS of *AR* gain and *AR* neutral patients. (**B**) Trimfill plot associated with Suppl. Figure 2A. (**C**) Funnel plot of the reported hazard ratio's between the OS of *AR* gain and *AR* neutral patients. (**D**) Trimfill plot associated with Suppl. Figure 2C.

Supplementary Table 1: The results of the different studies described in the meta-analyses.

Study	Patients	Treatment	Line	PFS*		OS*		PSA50
				***AR* gain vs *AR* neutral**		***AR* gain vs *AR* neutral**		***AR* gain vs *AR* neutral**
Author [ref]	*n*			HR [95% CI]	Median months	HR [95% CI]	Median months	Proportion PSA50 achieved
Annala [23]	201	Abi, Enza	First	2.05 [1.43-2.93]	5.0 vs 9.3	*4.60 [2.68-7.90]*	15.6 vs NR	0.67 vs 0.64
Azad [24]	39	Enza	Second-eighth	3.21 [1.5-6.85]	2.3 vs 7.0	-	-	0.21 vs 0.44
Buelens [20]	15	Abi	First-third	6.67 [1.52-33.33]	1.7 vs NR	8.33 [0.96-100]	7.0 vs 20.9	0.40 vs 0.60
	20	Enza	First-third	4.76 [1.41-16.67]	1.7 vs 10.8	4.55 [0.94-20]	6.1 vs 16.5	0.33 vs 0.55
	22	Doce	First-third	2.38 [0.84-6.67]	3.2 vs 6.5	3.43 [1.08-11.0]	3.9 vs NR	0.86 vs 0.91
Conteduca [26]	73	Abi, Enza	First	2.18 [1.08-4.39]	7.3 vs 9.2	3.98 [1.74-9.1]	12.4 vs NR	0.5 vs 0.84
	98	Abi, Enza	Second- third	1.95 [1.23-3.11]	5.0 vs 7.4	3.81 [2.28-6.37]	9.5 vs 21.8	0.15 vs 0.44
Conteduca [33]	115	Doce	First	*0.78 [0.52-1.19]*	8.7 vs 7.0	*1.25 [0.77-2.05]*	21.5 vs 22.5	-
	48	Doce	Second	*2.98 [1.53-5.81]*	4.8 vs 7.4	*3.58 [1.70-7.52]*	9.3 vs 21.8	-
Conteduca [25]	59	Abi, Enza	First-higher	*1.99 [0.79-5.01]*	4.6 vs NR	*4.19 [1.48-11.8]*	20.6 vs NR	0.45 vs 0.69
Conteduca [32]	155	Caba	Second-third	1.47 [1.05-2.07]	4.0 vs 5.0	1.44 [0.98-2.13]	10.5 vs 14.1	0.25 vs 0.36
	71	Caba	Second-third	*1.01 [0.61-1.67]*	6.3 vs 5.3	*1.02 [0.57-1.83]*	15.5 vs 18.1	-
De Laere [21]	168	Abi, Enza	First-third	2.35 [1.58-3.47]	3.9 vs 9.5	*3.32 [1.99-5.51]*	11.2 vs 29.7	0.37 vs 0.45
Hovelson [34]	16	Abi, Enza	Second-fifth	-	-	*3.45 [0.47-25.2]*	11.2 vs NR	0.00 vs 0.50
	13	Doce	First-fifth	-	-	*3.84 [0.83-17.7]*	4.5 vs 17.2	0.00 vs 0.44
Jayaram [27]	133	Abi	First	1.94 [0.897-3.87]	5.1 vs 16.3	2.37 [1.07-5.25]	21.5 vs 42.8	-
	94	Enza	First	3.9 [1.27-12.03]	-	5.62 [1.42-22.2]	-	-
Kohli [28]	70	Abi	First	*1.5 [0.82-2.73]*	7.1 vs 6.9	5.25 [2.21-12.5]	21.0 vs NR	-
Salvi [29]	53	Abi	Second-higher	3.73 [1.95-7.13]	2.8 vs 9.5	4.68 [2.17-10.1]	5.0 vs 21.9	0.31 vs 0.57
Salvi [30]	59	Enza	Second-higher	2.79 [1.55-5.02]	2.4 vs 4.0	3.23 [1.64-6.35]	6.1 vs 14.1	0.19 vs 0.37
Sumiyoshi [46]	24	Enza	Second-higher	-	-	-	-	0.55 vs 0.69
Torquato [31]	62	Abi, Enza	First-second	2.07 [1.20-3.57]	3.7 vs 7.8	3.26 [1.52-7.00]	14.4 vs 33.3	0.47 vs 0.67
Wyatt [12]	65	Enza	Second-higher	2.92 [1.59-5.37]	2.2 vs 4.5	-	-	0.16 vs 0.48

*Hazard ratios in *italic* are manually calculated. HR = hazard ratio, CI = confidence interval, Abi = Abiraterone, Enza = Enzalutamide, Doce = Docetaxel, Caba = Cabazitaxel.

Supplementary Table 2: The study cohorts excluded from the meta-analysis.

Study	Year	Study design	Patient	Cohort identification	Treatment	Reason of exclusion
Author [ref]			*n*	Ethical, trial number or *collection period*		
Conteduca [47]	2017	RS	80	REC 2192/2013	Abi , Enza	Possible overlap with cohort described in [26]
Conteduca [26]	2017	SGA	94	NCT02288936	Enza	Longer follow-up described in [27]
Conteduca [33]	2018	RS	73	REC 04/Q0801/6	Abi , Enza	Possible overlap with cohort described in [26]
Conteduca [25]	2018	RS	197	REC 2192/2013	Abi , Enza	Possible overlap with cohort described in [26]
Romanel [35]	2015	PS	80	REC 04/Q0801/6, REC 2192/2013	Abi	Possible overlap with cohort described in [26]
Conteduca [32]	2019	RCT	84	NCT01308580	Caba	Cabazitaxel was given in a reduced dose
		RS	85	REC 2192/2013	Abi, Enza	Possible overlap with cohort described in [26]
Conteduca [48]	2019	RS	105	REC 2192/2013	Abi, Enza	Possible overlap with cohort described in [26]
Jayaram [27]	2019	RS	73	REC 04/Q0801/6, REC 2192/2013	Abi, Enza	Previously described in [26]
		RCT	201	NCT02125357	Abi, Enza	Previously described in [23]
Lolli [49]	2019	RS	128	Not described	Abi, Enza	Possible overlap with cohort described in [26]

PS = Prospective Study, RS = Retrospective Study, RCT = Randomized Controlled Trail, SGA = Single Group Assignment, Abi = Abiraterone, Enza = Enzalutamide, Caba = Cabazitaxel.

Chapter 3

Early on-treatment changes in circulating tumor DNA fraction and response to enzalutamide or abiraterone in metastatic castration-resistant prostate cancer

Sofie H. Tolmeijer
Emmy Boerrigter
Takayuki Sumiyoshi
Edmond M. Kwan
Sarah Ng
Matti Annala
Gráinne Donnellan
Cameron Herberts
Guillemette E. Benoist
Paul Hamberg
Diederik M. Somford
Inge M. van Oort
Jack A. Schalken
Niven Mehra
Nielka P. van Erp
Alexander W. Wyatt

Clinical Cancer Research 2023 Mar 30:CCR-22-2998. doi: 10.1158/1078-0432.CCR-22-2998.

Abstract

Purpose: Androgen receptor pathway inhibitors (ARPI) are standard of care for treatment-naive metastatic castration-resistant prostate cancer (mCRPC), but rapid resistance is common. Early identification of resistance will improve management strategies. We investigated whether changes in circulating tumor DNA (ctDNA) fraction during ARPI treatment are linked with mCRPC clinical outcomes.

Experimental Design: Plasma cell-free DNA was collected from 81 patients with mCRPC at baseline and after 4-weeks of first-line ARPI treatment during two prospective multicenter observational studies (NCT02426333;NCT02471469). CtDNA fraction was calculated from somatic mutations in targeted sequencing and genome copy number profiles. Samples were classified into detected *vs.* undetected ctDNA. Outcome measurements were progression-free survival (PFS) and overall survival (OS). Nondurable treatment response was defined as PFS ≤ 6 months.

Results: CtDNA was detected in 48/81 (59%) baseline and 29/81 (36%) 4-week samples. CtDNA fraction for samples with detected ctDNA was lower at 4-weeks *vs*. baseline (median 5.0% *vs*. 14.5%, *P*=0.017). PFS and OS was shortest for patients with persistent ctDNA at 4 weeks (univariate HR, 4.79; 95%CI, 2.62-8.77 and univariate HR, 5.49; 95%CI, 2.76-10.91, respectively), independent of clinical prognostic factors. For patients exhibiting change from detected to undetected ctDNA by 4-weeks, there was no significant PFS difference *versus* patients with baseline undetected ctDNA. CtDNA change had a positive predictive value of 88% and negative predictive value of 92% for identifying nondurable responses.

Conclusions: Early changes in ctDNA fraction are strongly linked to duration of first-line ARPI treatment benefit and survival in mCRPC and may inform early therapy switches or treatment intensification.

Introduction

Metastatic castration-resistant prostate cancer (mCRPC) is fatal, but widespread availability of androgen receptor pathway inhibitors (ARPI) have resulted in clinically-meaningful improvements in long-term patient outcomes [1,2]. Despite recent level 1 evidence supporting use of combination treatment with ARPI and androgen deprivation therapy in metastatic hormone-sensitive prostate cancer (mHSPC) [3–6], physician choices or barriers to access are reflected in real-world treatment patterns where most patients do not receive ARPI until first-line therapy for mCRPC [7–9]. However, 20-30% of mCRPC will exhibit primary or rapidly-acquired resistance to first-line ARPI and progress within six months of starting treatment [1,2]. Current biochemical or radiographic assessments of treatment response are not considered reliable before 12 weeks due to early fluctuations in serum prostate-specific antigen (PSA) and flares in imaging [10]. Therefore, to improve mCRPC management in an era with multiple life-prolonging treatment options including chemotherapy, poly(ADP-ribose)polymerase (PARP) inhibitors, and radionuclide therapy, we require earlier indicators of ARPI response.

Longitudinal testing of plasma circulating tumor DNA (ctDNA) is an emerging approach to monitor disease [11]. On-treatment changes in ctDNA fraction (the proportion of total plasma cell-free DNA that is tumor-derived) are associated with clinical outcomes in some advanced cancers [12,13]. However, prior prostate cancer studies were hampered by inconsistent plasma sampling, heterogeneous study populations across different treatment lines, and ctDNA detection methods with limited sensitivity or inability to filter variants related to clonal hematopoiesis [14–17]. Furthermore, since ctDNA fraction prior to treatment is a strong prognostic indicator in mCRPC [18–20], it is currently unknown if on-treatment ctDNA measurements will provide additional clinical utility. Here, we leverage a prospective multicenter study to test whether baseline and 4-week on-treatment ctDNA fraction measurements can identify patients with mCRPC that have nondurable responses to first-line ARPI.

Materials and methods

Patient cohort and study procedures

This study represents a pooled analysis of patients prospectively enrolled in two observational multicenter studies conducted in the Netherlands between July 2015 and October 2018: OPTIMUM (ClinicalTrials.gov identifier: NCT02426333) and ILUMINATE (NCT02471469). In both studies, patients with biochemically/radiographically-progressive mCRPC and asymptomatic or minimally-symptomatic disease were

eligible if they had a life expectancy of ≥6 months. Exclusion criteria included prior systemic therapy (ARPI or chemotherapy) for mCRPC, although docetaxel for mHSPC was permitted in accordance with established standard-of-care [21,22]. ARPI was not locally indicated for mHSPC while these studies were conducted. Consequently, no patient received ARPI in the mHSPC setting. Patients were excluded if they stopped treatment before the second study visit at 4 weeks. Eligible patients received either abiraterone acetate 1000mg daily plus prednisolone 10mg daily (OPTIMUM), or enzalutamide 160mg daily (ILUMINATE). The studies and correlative ctDNA analysis were approved by the medical ethics committee at the Radboud University Medical Center and the University of British Columbia Clinical Research Ethics Board. The studies were conducted in accordance with Good Clinical Practice guidelines and the Declaration of Helsinki. All participants provided written informed consent.

A key prespecified objective of both studies was to define blood-based biomarkers associated with durable treatment response. Therefore, peripheral blood (9mL) for plasma ctDNA analysis was collected in a single Streck Cell-Free DNA BCT tube at two set timepoints: i) study baseline prior to treatment initiation (not exceeding two weeks before commencing ARPI), and ii) 4 weeks after commencing study treatment. The protocol-specified 4-week timepoint was selected based on practical reasons since it represents the first hospital visit in standard clinical practice. Additionally, at 4 weeks the steady-state concentration of abiraterone and enzalutamide in the blood is reached [23]. Furthermore, 4 weeks is within the period where radiographic reimaging (i.e. for response evaluation) may be obfuscated by false positives due to flare phenomenon. An additional whole blood EDTA sample (6mL) was collected for resolving germline variants from putative somatic mutations and to exclude somatic mutations present in white blood cell DNA (including from clonal hematopoiesis). Plasma cell-free DNA and white blood cell DNA was subjected to deep targeted sequencing with a laboratory-developed panel covering coding regions and select introns of 73 prostate cancer related genes and a genome-wide grid capturing common heterozygous germline single nucleotide polymorphisms (SNPs). CtDNA fraction (ctDNA%) at baseline and 4-week timepoints were estimated using allele fractions of autosomal somatic mutations in non-amplified regions, or genome-wide copy number and heterozygous SNP allele imbalance in cases with no eligible somatic mutations. Methodology for plasma processing, targeted sequencing, bioinformatic ctDNA% estimation and justification of ctDNA% detection threshold is provided in Supplementary Methods.

In addition to pre-defined sampling timepoints, all outcome measurements were prespecified in the study protocol. Prior treatment history, Eastern Cooperative Oncology Group (ECOG) performance status and baseline laboratory tests (including hemoglobin, alkaline phosphatase (ALP) and lactate dehydrogenase (LDH)) were

obtained at study entry. Patients underwent clinical assessment prior to the start of therapy (defined as 'baseline') and at 4 weeks, 3 months, and 6 months after commencing protocol treatment. PSA measurements were taken at each scheduled review, and radiographic tumor assessment (computer tomography [CT] or whole body magnetic resonance imaging [MRI] combined with bone scan) was performed at baseline, 3 months and 6 months after commencing ARPI therapy. Radiographic progression was evaluated by local investigator assessment, with subsequent independent blinded central review using Prostate Cancer Working Group 2 (PCWG2) guidelines for bone disease and Response Evaluation Criteria in Solid Tumors (RECIST) version 1.1 for soft-tissue disease [24,25]. For 3 patients the independent blinded central review was not performed. Local investigator assessment was used for calculating radiographic progression-free survival (PFS), with clinical decisions taken on local imaging results. After six months of protocol treatment, the interval between clinical assessments, PSA testing and radiographic imaging was not mandated, but instead left to the discretion of site investigators as per local institutional practices.

Outcome measurements and statistical methods

Due to the exploratory nature of biomarker discovery in both studies, no formal sample size calculation was performed for this pooled analysis. Baseline and 4-week plasma samples were classified based on presence of ctDNA (detected *vs.* undetected; see Supplementary Methods for limits of detection). On-treatment ctDNA response was assessed by comparing baseline and 4-week ctDNA%, and categorizing into four scenarios: i) detected to detected, ii) detected to undetected, iii) undetected to undetected, and iv) undetected to detected. Kaplan-Meier survival estimates were used to assess the association between ctDNA% and clinical outcomes: i) PFS (prospectively assessed and defined as the time from baseline to prostate cancer-related clinical progression according to the treating physician; radiographic progression according to local assessment; or death due to prostate cancer), and ii) overall survival (OS), defined as the time from baseline to death from any cause. Exploratory outcome measurements included: i) time on treatment (baseline to therapy discontinuation), ii) biochemical PFS (bPFS; time from baseline to PSA increase ≥25% beyond 12 weeks and confirmed with a second PSA measurement), and iii) combined PFS, defined as time from baseline to first of prostate-related clinical progression, radiographic progression, PSA progression or death due to prostate cancer. The independent utility of ctDNA% change to predict PFS and OS was assessed using multivariable Cox proportional hazard models (covariates: ctDNA% at baseline, PSA > cohort median, LDH > upper limit of normal (ULN), and ALP > ULN) [18,26,27]. For comparison, an additional multivariable analysis was performed with LDH, ALP and log-transformed PSA as continuous variables and an exploratory multivariable analysis was performed with ctDNA% change at 4-weeks (detected *vs* undetected at baseline and 4-weeks), PSA change at 4-weeks (PSA decline

of 30% achieved *vs* not achieved) and LDH normalization at 4-weeks (LDH below *vs* above ULN). For PFS analyses, patients were censored at the therapy stop date in cases where no PFS was observed, or at last follow-up if patients remained on treatment. For OS analyses, patients were censored at the last follow-up date. Follow-up was calculated from the date of baseline blood draw to last patient contact.

The potential for ctDNA% changes to differentiate patients with and without durable response was evaluated using positive predictive value (PPV) and negative predictive value (NPV). Durable treatment response was defined as PFS >6 months according to the local assessment. The 6-month threshold was selected on the basis of the registration trial for enzalutamide in chemotherapy-naive mCRPC, in which the median radiographic PFS of the placebo arm was 5.4 months [28]. Patients that ceased therapy before 6 months without PFS were excluded from the PPV/NPV analysis. The PPV and NPV of ctDNA change was compared to the PPV and NPV of a PSA decrease of 30% from baseline to 4 weeks (PSA30), which has been described as an early marker for treatment response [29,30]. Statistical significance was defined as $P<0.05$ and all statistical tests were two-sided. Statistical analyses were carried out using R v.3.6.2 using the survival and survminer packages.

Results

Clinical outcomes

Of 97 patients enrolled, 81 patients were eligible for ctDNA analysis (51 received abiraterone acetate and 30 received enzalutamide; Figure 1A). Baseline patient characteristics are presented in Table 1 (see also Supplementary Table S1). At data cut-off (26 February 2021), the median follow-up was 27.4 months (inter quartile range (IQR) 17.7-34.9) with 52 deaths (64%) and 60 patients (74%) experiencing radiographic and/or clinical progression. The median PFS was 10.2 months and median OS was 20.6 months. In total, 27 (33%) patients experienced nondurable response (PFS ≤6 months) and 50 (62%) patients experienced a durable response; four patients could not be assessed due to treatment cessation for toxicity within 6 months.

On-treatment ctDNA fraction changes

CtDNA was detected in 48/81 (59%) patients at baseline and 29/81 (36%) patients at 4 weeks (Figure 1B, Supplementary Table S2). Patients with detected ctDNA at baseline were enriched for clinical prognostic markers of disease aggression, including higher baseline PSA (median 64 ng/mL vs 29 ng/mL, Mann-Whitney U, P = 0.02), five or more bone metastases (73% vs 36%, Fisher's Exact Test, P=0.001), elevated ALP (54% vs 15%, Fisher's Exact Test, P<0.001) and elevated LDH (43% vs 18%, Fisher's Exact Test, P=0.03).

Table 1: Baseline patient characteristics

Patient characteristics at baseline	Total (n=81)
Age at baseline (years)	73.2 (67.5-77.9)
Hb (mmol/L)[a]	8.0 (7.5-8.5)
LDH (U/L)[b,*]	230 (202-263)
ALP (U/L)[c,*]	86 (73-127)
Albumin (g/L)[d,]**	40 (37-43)
PSA (ng/mL)	45 (23-110)
PSA doubling time (months)	3.1 (2.0-5.8)
Gleason score at diagnosis	
≤7	24 (29.6)
≥8	53 (65.4)
Missing	4 (4.9)
Ethnicity	
White	78 (96.3)
Asian	1 (1.2)
Unknown	2 (2.5)
ECOG performance status	
0	56 (69.1)
1	21 (25.9)
2	3 (3.7)
Unknown	1 (1.2)
Pre-treatment docetaxel[e]	18 (22.2)
Prostatectomy	35 (43.2)
Radiation to the primary site	16 (19.8)
Spread of metastasis (at baseline)	
Lymph node only	11 (13.6)
Bone only	24 (29.6)
Both bone and lymph node	39 (48.1)
Visceral + lymph node and/or bone	9 (11.1)

Abbreviations: Hb, hemoglobin; LDH, lactate dehydrogenase; ALP, alkaline phosphatase; PSA, prostate-specific antigen.
Data are presented as median (Q1-Q3) for continuous data or N (%) for categorical data.
[a]: lower limit of normal was defined as 7.4 U/L
[b]: upper limit of normal was defined as 250 U/L
[c]: upper limit of normal was defined as 100 U/L
[d]: upper limit of normal was defined as 40 g/L
[e]: pre-treatment with docetaxel according to CHAARTED/STAMPEDE schedule
*: missing data for 2 patients
**: missing data for 4 patients

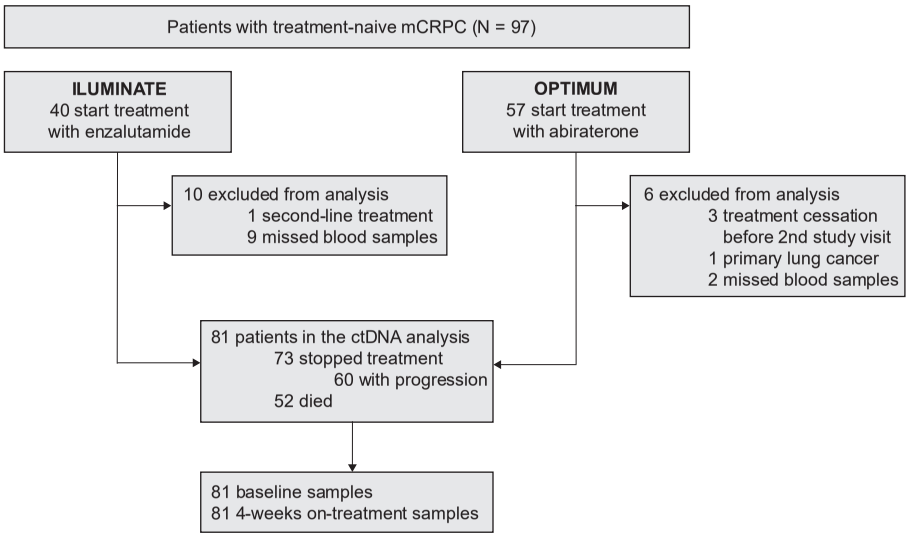

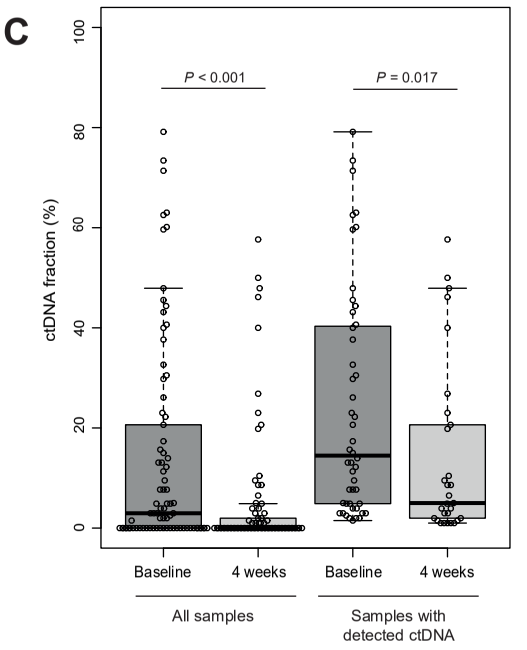

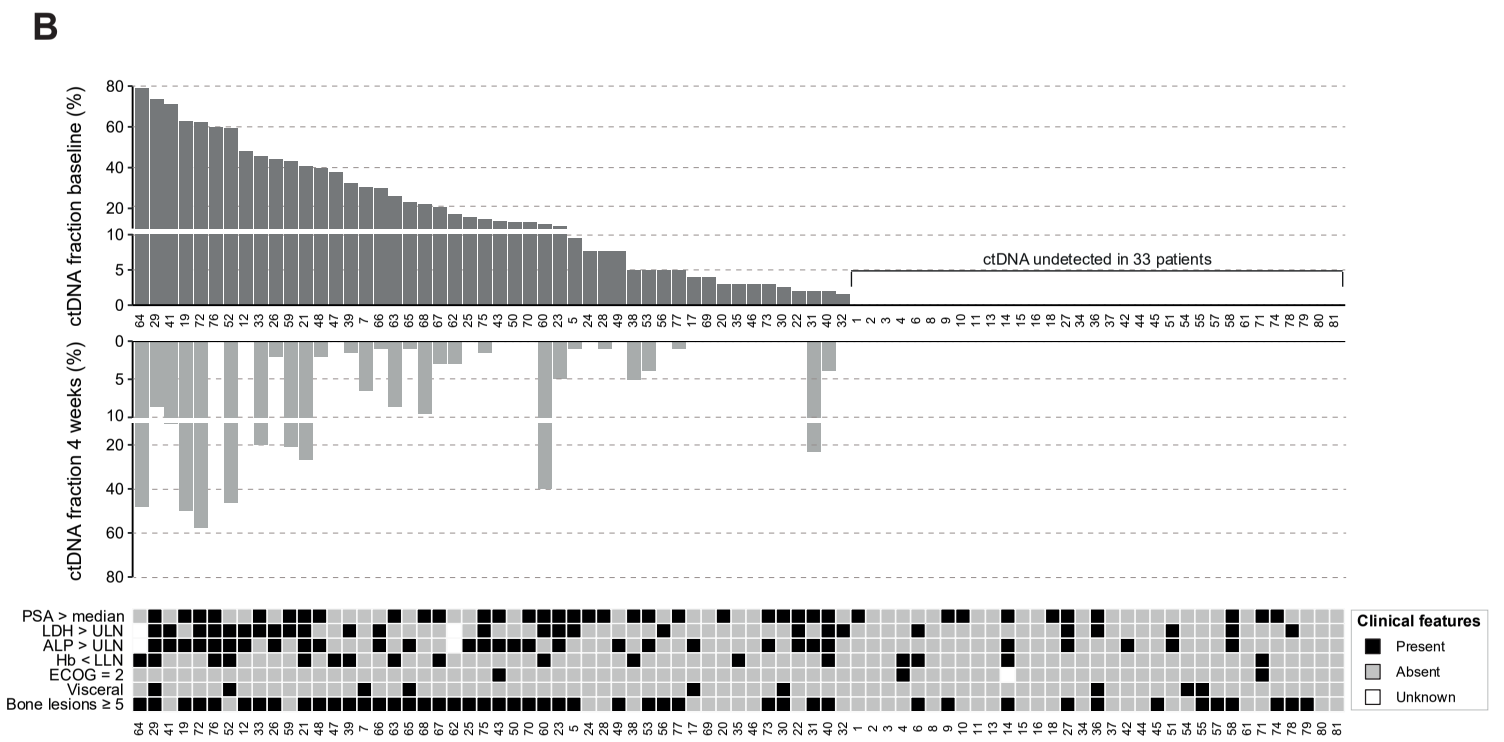

Figure 1: Cohort summary and circulating tumor DNA (ctDNA) fraction changes following 4 weeks of treatment. (A) CONSORT diagram illustrating the 81 patients eligible for ctDNA analysis. (B) CtDNA fraction at baseline and after 4 weeks of treatment per patient. Baseline patient clinical characteristics are provided in the lower matrix. (C) Box plot showing the difference in distribution of ctDNA fraction at baseline versus following 4 weeks of treatment.

Abbreviations: HB, hemoglobin; LDH, lactate dehydrogenase; ALP, alkaline phosphatase; PSA, prostate-specific antigen; ECOG, Eastern Cooperative Oncology Group performance status.

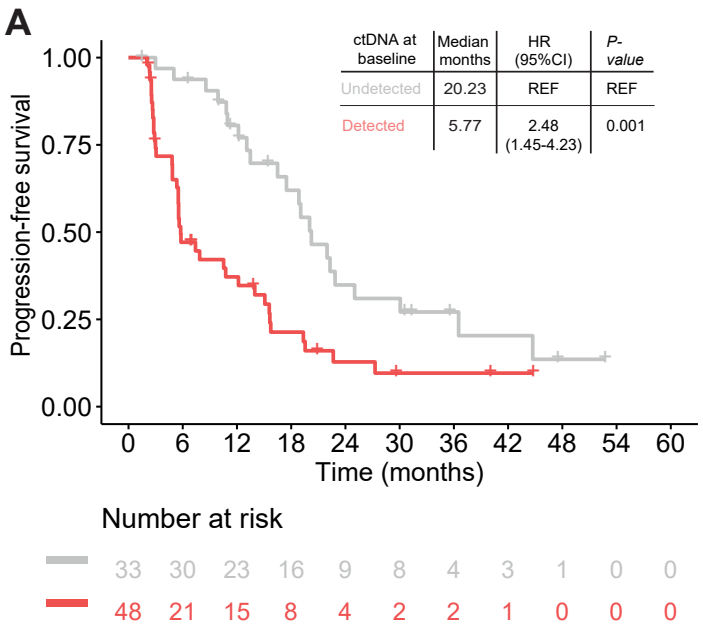

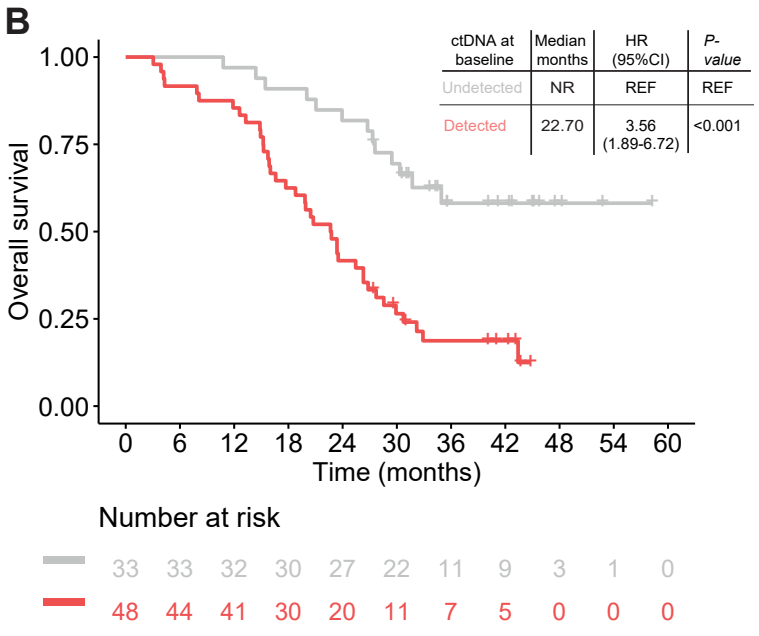

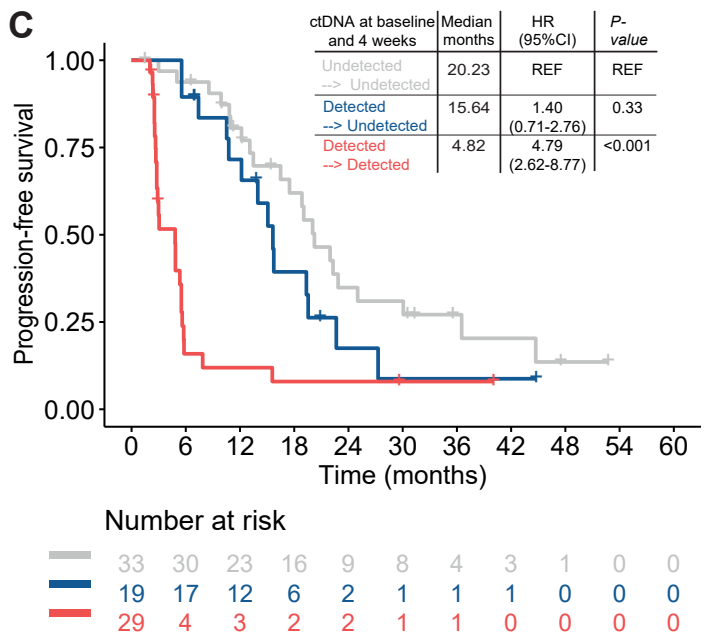

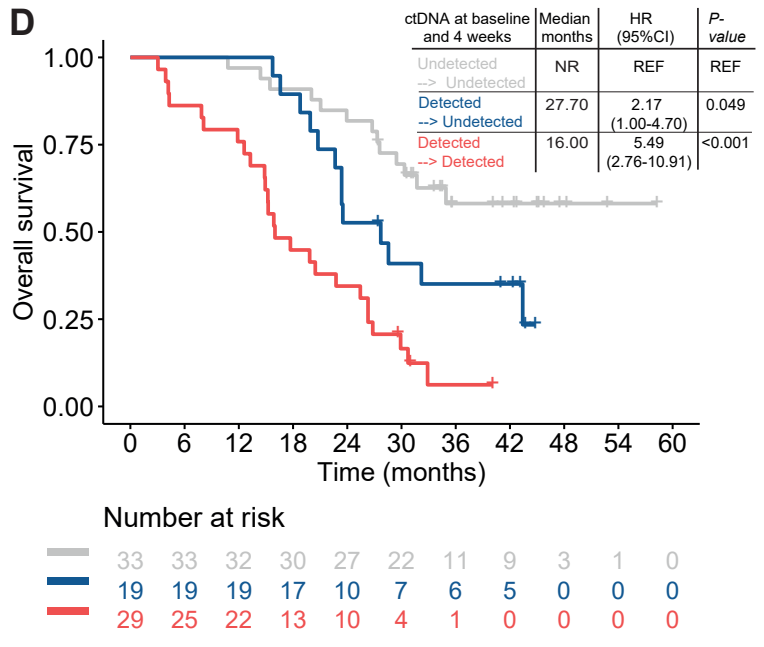

Figure 2: Relationship between on-treatment detection of circulating tumor DNA and progression-free survival or overall survival. Progression-free survival (PFS; A) and overall survival (OS; B) for patients with detected vs. undetected circulating tumor DNA (ctDNA) at baseline. PFS (C) and OS (D) according to change in ctDNA detection status after 4 weeks of treatment.

19 patients converted from detected ctDNA at baseline to undetected at 4 weeks; no patients converted from undetected to detected. Among patients with detected ctDNA at both timepoints, the median ctDNA% (as a proportion of total cell-free DNA) was lower at 4-weeks than at baseline (14.5% vs. 5.0%; P=0.017; Mann-Whitney U test; Figure 1C). The majority of patients showed a reduction in both ctDNA and PSA at 4 weeks of treatment, while LDH was mostly stable and below the upper limit of normal (Supplementary Figure S1, Supplementary Figure S2). Genomic alterations identified in ctDNA were consistent with previous cohorts of clinical mCRPC assessed by tissue or liquid biopsy (Supplementary Figure S3 and S4) [18,31–34].

Relationship between ctDNA fraction and treatment outcomes

Detected ctDNA at baseline was associated with shorter PFS and OS compared to undetected ctDNA (median PFS 5.77 vs. 20.23 months, hazard ratio (HR) = 2.48; 95% confidence interval (95%CI) 1.45-4.23, P=0.001, univariate; Figure 2A; median OS 22.70 months vs. not-reached (NR), HR=3.56; 95%CI 1.89-6.72, P<0.001, univariate; Figure 2B). Consistent with our prior work, very high baseline ctDNA% (>30%) was linked to particularly poor outcomes in comparison to patients with undetected ctDNA (median OS 15.80 months vs. NR, HR=8.12; 95%CI 3.75-17.61, P<0.001, univariate; Supplementary Figure S5) [18,20].

29 of 48 (60%) patients with detected ctDNA at baseline also had ctDNA detected in their 4 week blood collection. Compared to patients with undetected ctDNA at both timepoints, these patients experienced the shortest PFS and OS (median PFS 4.82 months, HR=4.79, 95%CI 2.62-8.77, P<0.001 and median OS 16.00 months, HR=5.49, 95%CI 2.76-10.91, P<0.001; Figure 2C-D). No significant PFS difference was observed between patients who converted from detected to undetected ctDNA by 4 weeks and patients with undetected ctDNA at baseline, although OS was shorter (Figure 2C-D; Table 2). Similar relationships were observed for other outcome measures including bPFS in isolation, and a combined PFS measure incorporating bPFS with radiographic and/or clinical progression (Supplementary Figure S6).

Clinical prognostic indicators of high tumor burden were enriched in patients with ctDNA detected at baseline and at 4 weeks (Supplementary Figure S7). Additionally, baseline ctDNA% (Supplementary Figure S8; two-sided t-test; P=0.002) and correspondingly the prevalence of detected baseline *AR* gain and *TP53* alterations was higher in this group compared to patients with undetected ctDNA at 4 weeks (Supplementary Figure S7; chi-square; P=0.021 and P=0.039, respectively). However, detection of ctDNA at 4 weeks remained independently associated with PFS and OS in a multivariable model incorporating ctDNA detection at baseline and clinical prognostic factors (multivariable HR 4.98 compared to patients with undetected

Table 2: Univariate and multivariable analyses for on-treatment circulating tumor DNA and progression-free survival or overall survival

			Progression-free survival					**Overall survival**				
Clinical marker	Subgroup	No. patients	Median (months)	Univariate analysis		Multivariable analysis		Median (months)	Univariate analysis		Multivariable analysis	
				HR (95% CI)	*P*-value	HR (95% CI)	*P*-value		HR (95% CI)	*P*-value	HR (95% CI)	*P*-value
ctDNA% change following 4 weeks	Undetected → Undetected	33	20.23	ref	ref	ref	ref	Not reached	ref	ref	ref	ref
	Detected → Undetected	19	15.64	1.40 (0.71-2.76)	0.325	1.16 (0.57-2.33)	0.681	27.70	2.17 (1.00-4.70)	0.049	1.82 (0.80-4.12)	0.15
	Detected → Detected	29	4.82	4.79 (2.62-8.77)	<0.001	4.98 (2.08-11.93)	<0.001	16.00	5.49 (2.76-10.91)	<0.001	3.69 (1.50-9.08)	0.005
ctDNA% at baseline		81	NA	1.04 (1.02-1.05)	<0.001	1.01 (0.99-1.03)	0.229	NA	1.03 (1.02-1.04)	<0.001	1.02 (1.00-1.04)	0.019
PSA (ng/mL)	≤ median	39	18.85	ref	ref	ref	ref	32.20	ref	ref	ref	ref
	> median	42	5.80	2.48 (1.48-4.15)	0.001	2.41 (1.38-4.22)	0.002	21.85	2.2 (1.26-3.82)	0.005	1.67 (0.92-3.03)	0.091
LDH (U/L)	≤ ULN	53	16.49	ref	ref	ref	ref	27.70	ref	ref	ref	ref
	> ULN	26	5.66	2.47 (1.45-4.21)	0.001	1.61 (0.90-2.89)	0.108	27.20	1.34 (0.76-2.36)	0.319	0.67 (0.36-1.27)	0.225
ALP (U/L)	≤ ULN	49	18.85	ref	ref	ref	ref	31.70	ref	ref	ref	ref
	> ULN	30	5.79	2.29 (1.34-3.89)	0.002	0.89 (0.47-1.66)	0.706	23.38	1.96 (1.12-3.43)	0.019	0.88 (0.43-1.81)	0.738

Abbreviations: PSA, prostate-specific antigen; LDH, lactate dehydrogenase; ALP, alkaline phosphatase; ctDNA%, circulating tumor DNA fraction; HR, Hazard ratio; 95% CI, 95% confidence interval; ULN, upper limit of normal; ref = reference group.

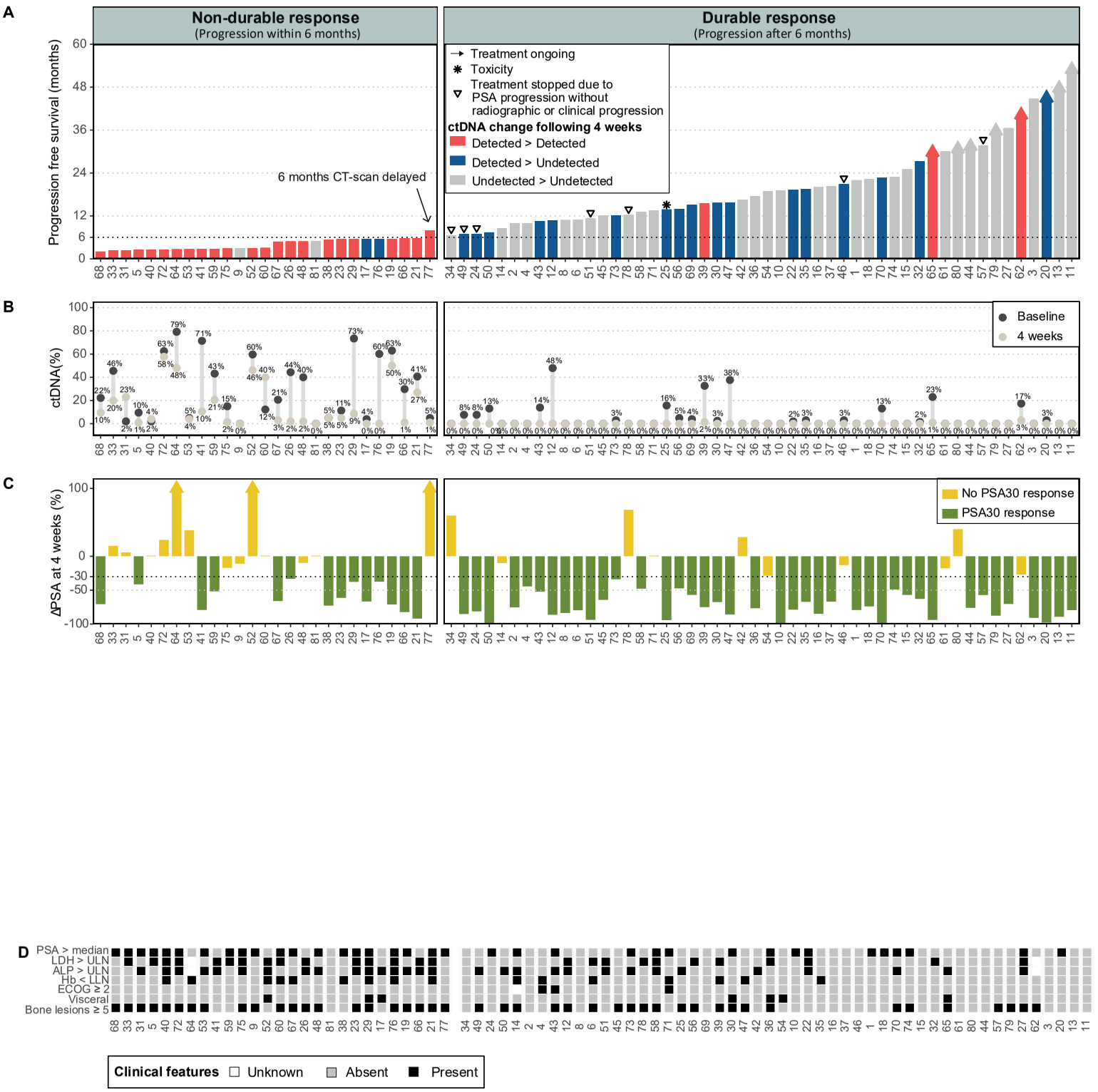

Figure 3: On-treatment circulating tumor DNA (ctDNA) fraction and durability of treatment response. (A) Swimmers plot showing per patient progression-free survival. Bar colors indicate the ctDNA change groups following 4 weeks of treatment. Arrows indicate patients still on treatment. (B) ctDNA fraction (ctDNA%) changes following 4 weeks of treatment. (C) The change in serum prostate specific antigen (PSA) following 4 weeks of treatment. Arrows indicate a PSA increase greater than 100%. Yellow bars indicate patients who did not achieve a PSA30 response at 4 weeks. Green bars indicate patients who did achieve a PSA30 response at 4 weeks. (D) Baseline patient clinical characteristics.

Abbreviations: HB, hemoglobin; LDH, lactate dehydrogenase; ALP, alkaline phosphatase; PSA, prostate-specific antigen; ECOG, Eastern Cooperative Oncology Group performance status; ctDNA, circulating tumor DNA; ΔPSA, prostate-specific antigen change; PSA30, 30% decline in prostate-specific antigen.

ctDNA at both timepoints, *P* <0.001 and HR 3.69, *P*=0.005 for PFS and OS respectively, Table 2, Supplementary Table S3).

Prediction of nondurable response to treatment

23 of 27 (85%) patients experiencing nondurable responses had ctDNA detected at both baseline and 4 weeks. Conversely, only 3 of 50 patients (6%) experiencing durable responses had ctDNA detected at both timepoints (Figure 3A-B). PPV and NPV for predicting nondurable responses with baseline and 4-week ctDNA detection was (23/26) 88%, 95%CI 72-96%, and (47/51) 92%, 95%CI 82-97%, respectively. 14 patients experienced progression by 12 weeks on-treatment, suggestive of primary resistance to ARPI. 13 of 14 patients had ctDNA detected at both timepoints.

Most patients converting from detected to undetected ctDNA at 4 weeks showed strong PSA responses at 4 and 12 weeks on-treatment (Supplementary Figure 7), while many patients with persistent ctDNA showed no PSA decrease (Supplementary Figure S9). However, the PPV and NPV of PSA30 at 4 weeks to identify nondurable responses was only (13/23) 57%, 95%CI 40-72%, and (40/54) 74%, 95%CI 66-81%, respectively (Figure 3C), suggesting considerably stronger performance for 4-week ctDNA measurements compared to PSA responses. The per patient changes in PSA levels and ctDNA fractions following 4 weeks of treatment in relation to the durability of response are visualized in Supplementary Figure S10. An exploratory multivariable analysis further emphasized that ctDNA measurements are independent of changes in conventional blood-based biomarkers at 4 weeks (PSA and LDH) (Supplementary Table S3).

Discussion

This study demonstrates that early on-treatment ctDNA% changes provide an accurate and independent indication of ARPI response in patients with mCRPC. Importantly, on-treatment blood draws for ctDNA analysis are practical to perform, and ctDNA% is increasingly reported by clinical test providers [35]. CtDNA% is a variable that can be measured with a range of different assays and does not strictly require the bespoke prostate cancer panel that we applied in our study [36]. Therefore we believe that early ctDNA% measurements represent a pragmatic near-term strategy to improve patient management.

Current clinical tools for mCRPC do not accurately predict impending disease progression before radiographic assessments at 3 and/or 6 months [10]. While 4-week PSA30 responses have been associated with PFS in mCRPC receiving ARPI [29,30], our data suggest suboptimal performance for identifying disease that will progress before 6 months of treatment. In line with our results, Petrylak *et al*. [37] reported that 4-week PSA30 failed the criteria for surrogacy to rapidly evaluate treatment response. In addition, the utility of PSA monitoring to reflect disease response is eroded with successive treatment exposure in mCRPC. It is estimated that up to 25% of patients with mCRPC experience progression on enzalutamide without rising PSA levels [38]. Consequently, the biomarker utility of 4-week PSA30 should be treated with caution.

Prior studies have indicated that baseline ctDNA% is associated with PFS and OS in mCRPC [18–20], independent of clinical prognostic factors. Here, 4-week on-treatment ctDNA% changes provided additional prognostic resolution versus baseline ctDNA% measurements alone, and was markedly superior to 4-week PSA30 measurements and 12-week PSA30/PSA50 measurements for identifying patients that will experience rapid disease progression during ARPI treatment. This result should not diminish the emerging value of baseline ctDNA testing, where prognosis and genomic alterations predictive of targeted therapy vulnerability can be identified prior to treatment selection. Both on-treatment and baseline ctDNA% were independently associated with OS in our study. In fact, the majority of patients with persistent ctDNA detected at 4 weeks had 1-30% ctDNA at baseline (rather than >30%, which was the baseline ctDNA% threshold associated with the poorest outcomes). Although we considered other measures of on-treatment ctDNA% decline, we choose to focus on ctDNA conversion (*i.e.* detected to not detected) on the basis of prior studies [16-20, 39, 40], the lack of a validated threshold for a meaningful ctDNA% decline and the inherent level of uncertainty surrounding ctDNA% estimates. Importantly, 15 of 27 (56%) patients with a nondurable response exhibited more than a 50% decline in ctDNA at 4 weeks, suggesting that this metric (which is described in literature for other cancer types [41,42]) is less informative than ctDNA conversion for understanding duration of response in mCRPC.

Several recent studies in other solid cancers have also linked on-treatment ctDNA clearance with improved PFS and/or OS [43–45], advocating for ctDNA as a potential pan-cancer biomarker. In prostate cancer, our findings are supported by a prior study investigating plasma ctDNA alterations in patients with mCRPC after one cycle of abiraterone acetate treatment [17]. In this published study, inability to detect baseline genomic alterations after one cycle of treatment was associated with good long-term outcomes. However, Jayaram *et al*. used a relatively small gene panel for mutation detection which may have hindered detection of ctDNA% between 1 and 10%. In our study, ctDNA% below 10% was still associated with poor treatment outcomes, suggesting that sensitivity for low ctDNA% will be important in any future clinical-grade tests. Furthermore, although we incorporated deep targeted sequencing of an

established broad gene panel [18, 20] together with genome-wide copy number and allelic imbalance profiling, some patients likely harbored ctDNA% below our detection threshold. Use of personalized mutation panels and/or methylation-based cell-free DNA profiling might boost sensitivity for very low ctDNA% (<1%) and potentially refine outcome predictions [44, 46]. However it is not always possible to profile relevant archival prostate cancer tissue in order to have ground truth for truncal patient-specific somatic mutations [47], and it is unknown whether very low on-treatment ctDNA levels are clinically-meaningful in patients with metastatic disease.

While ctDNA% at baseline and 4-weeks was prognostic in our study, early ctDNA% measurements could also be used to stratify randomized clinical trial interventions such as treatment changes or intensification. mCRPC likely to progress rapidly on ARPI may still respond to other therapeutic options such as taxane-based chemotherapy or radionuclides. Interestingly, several patients with rapid resistance had germline and/or somatic DNA homologous recombination repair or mismatch repair gene alterations, which are associated with benefit from PARP and immune checkpoint inhibitors, respectively [48]. Therefore, serial ctDNA profiling could serve a dual purpose of identifying inadequate disease control and indicating potential therapeutic vulnerabilities. Even if no further treatment options are available, early discontinuation of ineffective therapy on the basis of ctDNA measurements has potential to reduce patient exposure to unnecessary drug-related adverse effects and financial toxicity. Blood samples drawn at the end of cycle 1 would realistically provide ctDNA results within 2 weeks, meaning that decisions could be made before the end of cycle 2. Although ctDNA testing is not as cheap as PSA or other simple blood-based markers, ctDNA% may require a single on-treatment measurement, and more cost-effective techniques that could be implemented in molecular pathology laboratories are in development.

Our patient cohort was relatively small, and due to the exploratory design of our ctDNA analysis we did not perform formal sample size calculation. However, a key strength of our study above prior work was the mandated imaging at baseline, 3 months, and 6 months, together with the prospective assessment of radiographic and/or clinical progression. Although no imaging was mandated after 6 months, the strong relationships between ctDNA% and PFS were supported by OS data showing a 5.5 times shorter OS for patients with detected ctDNA at baseline and 4 weeks compared to patients with undetected ctDNA. Furthermore, the association of on-treatment ctDNA detection with both PFS and OS was independent of other prognostic clinical features (ctDNA% baseline, PSA, LDH, ALP), retaining high multivariable HR of 4.98 and 3.69, respectively. CtDNA measurements at 4 weeks also provided clear added value beyond PSA or LDH changes. In first-line mCRPC, most patients have LDH levels below

the upper limit of normal, making LDH changes around this threshold less suited for monitoring treatment response. PSA is a valuable biomarker in HSPC and in mCRPC exhibits reasonable sensitivity as a response biomarker after several measurements and a longer time on treatment (>12 weeks). However, ctDNA changes at 4 weeks appear to be more suitable for very early identification of patients with mCRPC who are expected to exhibit a short response to ARPI.

Our study was designed and accrued before several phase III clinical trials reported a survival benefit for use of ARPI upfront in mHSPC [3–6]. Therefore, our cohort of ARPI-naive mCRPC no longer represents all patients with newly-progressing mCRPC. However, real-world data demonstrates that although available only 3-46% of newly-diagnosed mHSPC patients in North America receive ADT with ARPIs despite reimbursement of therapy [8, 49–51], with even more limited use in other countries due to constraints from regulatory bodies, cost barriers, or disparities in access to care. As such, we believe that our results remain immediately relevant for a large subset of mCRPC. More importantly, it is plausible that early ctDNA% measurements can predict subsequent treatment response in the context of any line or class of systemic therapy for mCRPC. For example, Sumanasuriya *et al.* [39] reported that docetaxel or cabazitaxel responsive mCRPC had a median on-treatment ctDNA% of zero, while non-responding disease was associated with detected levels of ctDNA (measured by low-pass whole-genome sequencing). Similarly, in a retrospective analysis of patients with mCRPC, Tan *et al.* [52]showed a link between undetected on-treatment ctDNA% (after 3 or 4 cycles of chemotherapy) and a favorable 3-month PSA response. Finally, Goodall *et al.* [53] showed that a strong reduction in cfDNA (used as an indirect measurement of ctDNA%) after 8 weeks of PARP inhibitor treatment was associated with improved radiographic PFS and OS. Potential differences in depth and dynamics of on-treatment ctDNA% changes in the context of distinct therapy types should be further explored in future studies. These studies should also include additional blood collections (*e.g.* at 2 months), to determine if there is utility in repeat on-treatment testing.

In conclusion, detection of ctDNA at baseline and 4 weeks after treatment initiation is strongly linked to a nondurable response to first-line ARPI and a shorter overall survival in patients with mCRPC. Early ctDNA% measurements may have utility for informing early therapy changes or intensification in patients unlikely to experience durable treatment responses.

References

1. Ryan CJ, Smith MR, Fizazi K, et al. Abiraterone acetate plus prednisone versus placebo plus prednisone in chemotherapy-naive men with metastatic castration-resistant prostate cancer (COU-AA-302): final overall survival analysis of a randomised, double-blind, placebo-controlled phase 3 study. Lancet Oncol. 2015;16(2):152-160.
2. Armstrong AJ, Lin P, Tombal B, et al. Five-year Survival Prediction and Safety Outcomes with Enzalutamide in Men with Chemotherapy-naïve Metastatic Castration-resistant Prostate Cancer from the PREVAIL Trial. Eur Urol. 2020;78(3):347-357.
3. James ND, de Bono JS, Spears MR, et al. Abiraterone for Prostate Cancer Not Previously Treated with Hormone Therapy. N Engl J Med. 2017;377(4):338-351.
4. Fizazi K, Tran N, Fein L, et al. Abiraterone plus Prednisone in Metastatic, Castration-Sensitive Prostate Cancer. N Engl J Med. 2017;377(4):352-360.
5. Davis ID, Martin AJ, Stockler MR, et al. Enzalutamide with Standard First-Line Therapy in Metastatic Prostate Cancer. N Engl J Med. 2019;381(2):121-131.
6. Armstrong AJ, Szmulewitz RZ, Petrylak DP, et al. ARCHES: A Randomized, Phase III Study of Androgen Deprivation Therapy With Enzalutamide or Placebo in Men With Metastatic Hormone-Sensitive Prostate Cancer. J Clin Oncol. 2019;37(32):2974-2986.
7. Shayegan B, Wallis CJD, Malone S, et al. Real-world use of systemic therapies in men with metastatic castration resistant prostate cancer (mCRPC) in Canada. Urol Oncol. 2022;40(5):192.e1-e192.e9.
8. Swami U, Sinnott JA, Haaland B, et al. Treatment Pattern and Outcomes with Systemic Therapy in Men with Metastatic Prostate Cancer in the Real-World Patients in the United States. Cancers. 2021;13(19):4951.
9. Azad AA, Tran B, Davis ID, et al. Predictors of real-world utilisation of docetaxel combined with androgen deprivation therapy in metastatic hormone-sensitive prostate cancer. Intern Med J. 2021;52(8):1339-1346.
10. Scher HI, Morris MJ, Stadler WM, et al. Trial Design and Objectives for Castration-Resistant Prostate Cancer: Updated Recommendations From the Prostate Cancer Clinical Trials Working Group 3. J Clin Oncol. 2016;34(12):1402-1418.
11. Cescon DW, Bratman SV, Chan SM, Siu LL. Circulating tumor DNA and liquid biopsy in oncology. Nat Cancer. 2020;1(3):276-290.
12. Cindy Yang SY, Lien SC, Wang BX, et al. Pan-cancer analysis of longitudinal metastatic tumors reveals genomic alterations and immune landscape dynamics associated with pembrolizumab sensitivity. Nat Commun. 2021;12(1):5137.
13. Cullinane C, Fleming C, O'Leary DP, et al. Association of Circulating Tumor DNA With Disease-Free Survival in Breast Cancer: A Systematic Review and Meta-analysis. JAMA Netw Open. 2020;3(11):e2026921.
14. Conteduca V, Wetterskog D, Scarpi E, et al. Plasma tumour DNA as an early indicator of treatment response in metastatic castration-resistant prostate cancer. Br J Cancer. 2020;123(6):982-987.
15. Goodall J, Assaf ZJ, Shi Z, et al. Circulating tumor DNA (ctDNA) dynamics associate with treatment response and radiological progression-free survival (rPFS): Analyses from a randomized phase II trial in metastatic castration-resistant prostate cancer (mCRPC). Journal of Clinical Oncology. 2020;38(15_suppl):5508-5508.
16. Annala M, Taavitsainen S, Khalaf DJ, et al. Evolution of Castration-Resistant Prostate Cancer in ctDNA during Sequential Androgen Receptor Pathway Inhibition. Clin Cancer Res. 2021;27(16):4610-4623.
17. Jayaram A, Wingate A, Wetterskog D, et al. Plasma tumor gene conversions after one cycle abiraterone acetate for metastatic castration-resistant prostate cancer: a biomarker analysis of a multicenter international trial. Ann Oncol. 2021;32(6):726-735.
18. Annala M, Vandekerkhove G, Khalaf D, et al. Circulating Tumor DNA Genomics Correlate with Resistance to Abiraterone and Enzalutamide in Prostate Cancer. Cancer Discov. 2018;8(4):444-457.
19. Kohli M, Tan W, Zheng T, et al. Clinical and genomic insights into circulating tumor DNA-based alterations across the spectrum of metastatic hormone-sensitive and castrate-resistant prostate cancer. EBioMedicine. 2020;54:102728.
20. Annala M, Fu S, Bacon JVW, et al. Cabazitaxel versus abiraterone or enzalutamide in poor prognosis metastatic castration-resistant prostate cancer: a multicentre, randomised, open-label, phase II trial. Ann Oncol. 2021;32(7):896-905.
21. Sweeney CJ, Chen YH, Carducci M, et al. Chemohormonal Therapy in Metastatic Hormone-Sensitive Prostate Cancer. N Engl J Med. 2015;373(8):737-746.
22. James ND, Sydes MR, Clarke NW, et al. Addition of docetaxel, zoledronic acid, or both to first-line long-term hormone therapy in prostate cancer (STAMPEDE): survival results from an adaptive, multiarm, multistage, platform randomised controlled trial. Lancet. 2016;387(10024):1163-1177.
23. Benoist GE, Hendriks RJ, Mulders PFA, et al. Pharmacokinetic Aspects of the Two Novel Oral Drugs Used for Metastatic Castration-Resistant Prostate Cancer: Abiraterone Acetate and Enzalutamide. Clin Pharmacokinet. 2016;55(11):1369-1380.
24. Scher HI, Halabi S, Tannock I, et al. Design and end points of clinical trials for patients with progressive prostate cancer and castrate levels of testosterone: recommendations of the Prostate Cancer Clinical Trials Working Group. J Clin Oncol. 2008;26(7):1148-1159.
25. Eisenhauer EA, Therasse P, Bogaerts J, et al. New response evaluation criteria in solid tumours: revised RECIST guideline (version 1.1). Eur J Cancer. 2009;45(2):228-247.
26. Armstrong AJ, Lin P, Higano CS, et al. Development and validation of a prognostic model for overall survival in chemotherapy-naïve men with metastatic castration-resistant prostate cancer. Ann Oncol. 2018;29(11):2200-2207.

27. Ryan CJ, Kheoh T, Li J, et al. Prognostic Index Model for Progression-Free Survival in Chemotherapy-Naïve Metastatic Castration-Resistant Prostate Cancer Treated With Abiraterone Acetate Plus Prednisone. Clin Genitourin Cancer. 2017;25:S1558-7673(17):30211-30212.
28. Beer TM, Armstrong AJ, Rathkopf D, et al. Enzalutamide in Men with Chemotherapy-naïve Metastatic Castration-resistant Prostate Cancer: Extended Analysis of the Phase 3 PREVAIL Study. Eur Urol. 2017;71(2):151-154.
29. Rescigno P, Lorente D, Bianchini D, et al. Prostate-specific Antigen Decline After 4 Weeks of Treatment with Abiraterone Acetate and Overall Survival in Patients with Metastatic Castration-resistant Prostate Cancer. Eur Urol. 2016;70(5):724-731.
30. Rescigno P, Dolling D, Conteduca V, et al. Early Post-treatment Prostate-specific Antigen at 4 Weeks and Abiraterone and Enzalutamide Treatment for Advanced Prostate Cancer: An International Collaborative Analysis. Eur Urol Oncol. 2020;3(2):176-182.
31. Robinson D, Van Allen EM, Wu YM, et al. Integrative Clinical Genomics of Advanced Prostate Cancer. Cell. 2015;162(2):454.
32. Cancer Genome Atlas Research Network. The Molecular Taxonomy of Primary Prostate Cancer. Cell. 2015;163(4):1011-1025.
33. Abida W, Cyrta J, Heller G, et al. Genomic correlates of clinical outcome in advanced prostate cancer. Proc Natl Acad Sci U S A. 2019;116(23):11428-11436.
34. Stopsack KH, Nandakumar S, Wibmer AG, et al. Oncogenic Genomic Alterations, Clinical Phenotypes, and Outcomes in Metastatic Castration-Sensitive Prostate Cancer. Clin Cancer Res. 2020;26(13):3230-3238.
35. Antonarakis ES, Tierno M, Fisher V, et al. Clinical and pathological features associated with circulating tumor DNA content in real-world patients with metastatic prostate cancer. Prostate. 2022;82(7):867-875.
36. Herberts C, Wyatt AW. Technical and biological constraints on ctDNA-based genotyping. Trends Cancer Res. 2021;7(11):995-1009.
37. Petrylak DP, Ankerst DP, Jiang CS, et al. Evaluation of prostate-specific antigen declines for surrogacy in patients treated on SWOG 99-16. J Natl Cancer Inst. 2006;98(8):516-521.
38. Bryce AH, Alumkal JJ, Armstrong A, et al. Radiographic progression with nonrising PSA in metastatic castration-resistant prostate cancer: post hoc analysis of PREVAIL. Prostate Cancer Prostatic Dis. 2017;20(2):221-227.
39. Sumanasuriya S, Seed G, Parr H, et al. Elucidating Prostate Cancer Behaviour During Treatment via Low-pass Whole-genome Sequencing of Circulating Tumour DNA. Eur Urol. 2021;80(2):243-253.

40. Maurice-Dror C, Fonseca N, Herberts C, Fan W, Wyatt AW, Chi KN. Circulating tumor DNA fraction (ctDNA%) to independently predict for clinical outcomes in patients (pts) with metastatic castration-resistant prostate cancer (mCRPC). Journal of Clinical Oncology. 2021;39(15_suppl):5049-5049.
41. Zou W, Yaung SJ, Fuhlbrück F, et al. ctDNA Predicts Overall Survival in Patients With NSCLC Treated With PD-L1 Blockade or With Chemotherapy. JCO Precis Oncol. 2021;5:827-838.
42. Goldberg SB, Narayan A, Kole AJ, et al. Early Assessment of Lung Cancer Immunotherapy Response via Circulating Tumor DNA. Clin Cancer Res. 2018;24(8):1872-1880.
43. Darrigues L, Pierga JY, Bernard-Tessier A, et al. Circulating tumor DNA as a dynamic biomarker of response to palbociclib and fulvestrant in metastatic breast cancer patients. Breast Cancer Res. 2021;23(1):31.
44. Bratman SV, Cindy Yang SY, Iafolla MAJ, et al. Personalized circulating tumor DNA analysis as a predictive biomarker in solid tumor patients treated with pembrolizumab. Nature Cancer. 2020;1(9):873-881.
45. Malla M, Loree JM, Kasi PM, Parikh AR. Using Circulating Tumor DNA in Colorectal Cancer: Current and Evolving Practices. J Clin Oncol. 2022;40(24):2846-2857.
46. Liu MC, Oxnard GR, Klein EA, Swanton C, Seiden MV, CCGA Consortium. Sensitive and specific multi-cancer detection and localization using methylation signatures in cell-free DNA. Ann Oncol. 2020;31(6):745-759.
47. Gonzalez D, Mateo J, Stenzinger A, et al. Practical considerations for optimising homologous recombination repair mutation testing in patients with metastatic prostate cancer. J Pathol Clin Res. 2021;7(4):311-325.
48. Ku SY, Gleave ME, Beltran H. Towards precision oncology in advanced prostate cancer. Nat Rev Urol. 2019;16(11):645-654.
49. Freedland SJ, Sandin R, Sah J, et al. Treatment patterns and survival in metastatic castration-sensitive prostate cancer in the US Veterans Health Administration. Cancer Med. 2021;10(23):8570-8580.
50. Wallis CJD, Malone S, Cagiannos I, et al. Real-World Use of Androgen-Deprivation Therapy: Intensification Among Older Canadian Men With de Novo Metastatic Prostate Cancer. JNCI Cancer Spectr. 2021;5(6):kab082.
51. Ryan CJ, Ke X, Lafeuille MH, et al. Management of Patients with Metastatic Castration-Sensitive Prostate Cancer in the Real-World Setting in the United States. Journal of Urology. 2021;206(6):1420-1429.
52. Tan W, Zheng T, Wang A, et al. Dynamic changes in gene alterations during chemotherapy in metastatic castrate resistant prostate cancer. Sci Rep. 2022;12(1):4672.
53. Goodall J, Mateo J, Yuan W, et al. Circulating Cell-Free DNA to Guide Prostate Cancer Treatment with PARP Inhibition. Cancer Discov. 2017;7(9):1006-1017.

Supplementary methods

Blood processing and DNA isolation

Blood samples collected in Streck tubes were centrifuged at 300g for 20 minutes at room temperature and plasma was transferred to a new conical tube. Next, the plasma was centrifuged at 5000g for 10 minutes and transferred to 2 conical tubes, labeled and stored at -80℃. Total cell-free DNA (cfDNA) was extracted from plasma using the QIAamp Circulating Nucleic Acid Kit (Qiagen) according to the manufacturer's protocol and eluted in 45µL low-TE buffer. The DNA concentration was quantified using a HS dsDNA Qubit assay (Thermofisher) and samples with a high cfDNA concentration were checked for genomic contamination on a Fragment Analyzer (Agilent high sensitivity genomic DNA kit #DNF-488-0500). White blood cell (WBC) DNA was extracted from whole blood EDTA tubes using an automated nucleic acid isolation on a Chemagen-Hamilton robotic system. WBC DNA was eluted in chemagen Elution Buffer (CMG-1756) and diluted using low-TE buffer. The WBC DNA concentration was quantified using a BR dsDNA Qubit assay (Thermofisher).

Library preparation and sequencing

Sequencing libraries were prepared from 10-100 ng of DNA input per sample, depending on the overall yield from DNA extraction (Supplementary Table S2). WBC DNA libraries (all 100 ng) were prepared with the KAPA Hyper Plus Kit and underwent enzymatic fragmentation (15 minutes at 37℃) to ~180 bp. Plasma cfDNA libraries were prepared with the KAPA Hyper Prep Kit as per the manufacturer instructions. After end repair and A-tailing, IDT xGen CS UMI Adapters were ligated and subsequently PCR amplified with IDT xGen UDI Primer pairs. Library quantification was carried out via NanoDrop, and each library was run on an ethidium bromide gel to confirm success. Purified samples libraries were multiplexed to obtain single pools with a combined mass of 2 µg. Library pools were hybridized to a custom-designed KAPA HyperChoice probe set. This probe set captures coding regions of 73 prostate cancer relevant genes, and also introns and flanking regions of selected genes including *TP53*, *PTEN*, and *RB1* (these non-coding regions improve structural rearrangement detection and help inform loss of heterozygosity analysis). The probe set also includes a low-pass whole-genome backbone of regularly spaced probes capturing heterozygous germline SNPs at common frequencies across various ancestral backgrounds. The backbone aids in ctDNA purity estimation and improving chromosome arm copy number calls. The KAPA HyperCap Workflow protocol was followed for hybridization and subsequent wash, recovery, and amplification of the capture regions. Final libraries were purified with KAPA HyperPure Beads prior to quantification with the Quantus Fluorometer. Pools were diluted to 4 nM and were sequenced on Illumina machines.

Identification of mutations, structural rearrangements and copy number changes

First somatic mutations (single-nucleotide variants and indels) were identified in the targeted sequencing data according to the previously described and validated method [1,2]. In short, at least 8 supporting reads and a variant allele fraction (VAF) of at least 0.5% was required for independent mutation calling. The minimum of 8 supporting reads ensures false positive variant detection due to background error to be very low. As our assay aims for 1500x depth, 8 variant reads out of 1500 equates to a VAF of ~0.5%. This detection threshold is similar to most current commercial pan-cancer liquid biopsy platforms (e.g., FoundationOne Liquid CDx, Guardant360 CDx) [3,4]. Additionally, the observed VAF was required to be at least 20 times higher the average allele fraction from 83 WBC samples and 3 times higher compared to the patient-specific WBC sample again ensuring minimal false positive variant detection.. As all patients had two plasma samples available for ctDNA detection, additional dependent mutation calling was applied. For dependent calling, at least 3 supporting reads and a VAF of 0.5% were required to call a mutation in one plasma sample that was independently identified in the other same-patient plasma sample. A detailed description on structural rearrangement detection and copy number variant detection can be found in our previous reports [1,2].

ctDNA fraction estimation

The ctDNA fraction was estimated using 1) somatic autosomal mutations and 2) germline heterozygous SNPs according to published methodology [1,2], and is described below. The mutation-based ctDNA fraction was calculated using the variant allele fraction (VAF; corrected for statistical outliers and potential loss of heterozygosity; LOH) of autosomal somatic mutations in non-amplified genes (log-ratio <0.3) as detected by the 73-gene panel. Because mutant allele fractions are elevated when a mutation is concurrent with the loss of the other wildtype allele (i.e. LOH), and may be undetectable at low ctDNA fractions, we conservatively assumed that all somatic mutations may be associated with LOH. In regions of LOH, ctDNA fraction and VAF are related as ctDNA% = 2/(1/VAF + 1). To correct for outliers, we modeled the mutant read counts as arising from a binomial distribution, and conservatively calculated what the true VAF would be if the highest observed VAF was a 95% quantile outlier. A ctDNA fraction estimate was calculated for each somatic mutation, and the highest estimate was used as the overall estimate for the sample under the assumption that this mutation was the most likely to be truncal to the metastatic lineage. Germline variants, sequencing and alignment artifacts, and clonal-hematopoiesis of indeterminate potential (CHIP) can confound somatic mutation-based estimation of ctDNA fraction. These potential confounders are largely eliminated through our parallel sequencing of patient-matched WBC DNA.

We applied an orthogonal copy number-based ctDNA fraction estimation method using germline heterozygous SNPs with allele fractions that deviated from 50% heterozygosity in genes with evidence of LOH. Germline SNPs were identified from paired WBC DNA samples as any variant present in the ExAC or Kaviar databases with a minimum of 75x normal coverage. We filtered for heterozygous intragenic SNPs located on genes that had evidence for a single-copy deletion (log-ratio between -0.3 to -1.0) and contained at least 4 unique SNPs. We calculated the median major allele frequency (|0.5 - VAF| + 0.5) of SNPs within each eligible gene and used this value to estimate ctDNA% = 2 - VAF-1.

To validate our mutation- and copy number-based ctDNA fraction estimations, we leveraged the low-pass whole-genome backbone of heterozygous germline SNPs in our sequencing panel. Models testing various ctDNA fractions and diploid level log ratios were manually fitted to the genome-wide copy number levels and heterozygous SNP allele fractions [5]. Models that most closely adhered to the expected SNP allele fractions for each observed copy number were used to estimate ctDNA%. Samples with low ctDNA fraction (generally <20%) or highly complex copy number profiles due to aneuploidy or subclonality prevented confident ctDNA fraction estimation with this method and thus did not have models fit.

In the case that only an AR amplification was present in the ctDNA and was detected by both the genome-wide SNP backbone and intragenic copy number of the deep targeted sequencing, ctDNA estimation was conservatively estimated at 5%. Our threshold for the detection of mutations was a VAF of 0.5%. After correcting for sampling error and loss of heterozygosity this corresponds to a limit of detection of approximately 1% ctDNA. Therefore, we classified plasma samples into undetected (ctDNA < 1%) and detected (ctDNA ≥ 1%). Similar ctDNA estimate methods were used per patient at both timepoint to compare ctDNA% change.

Supplementary Data

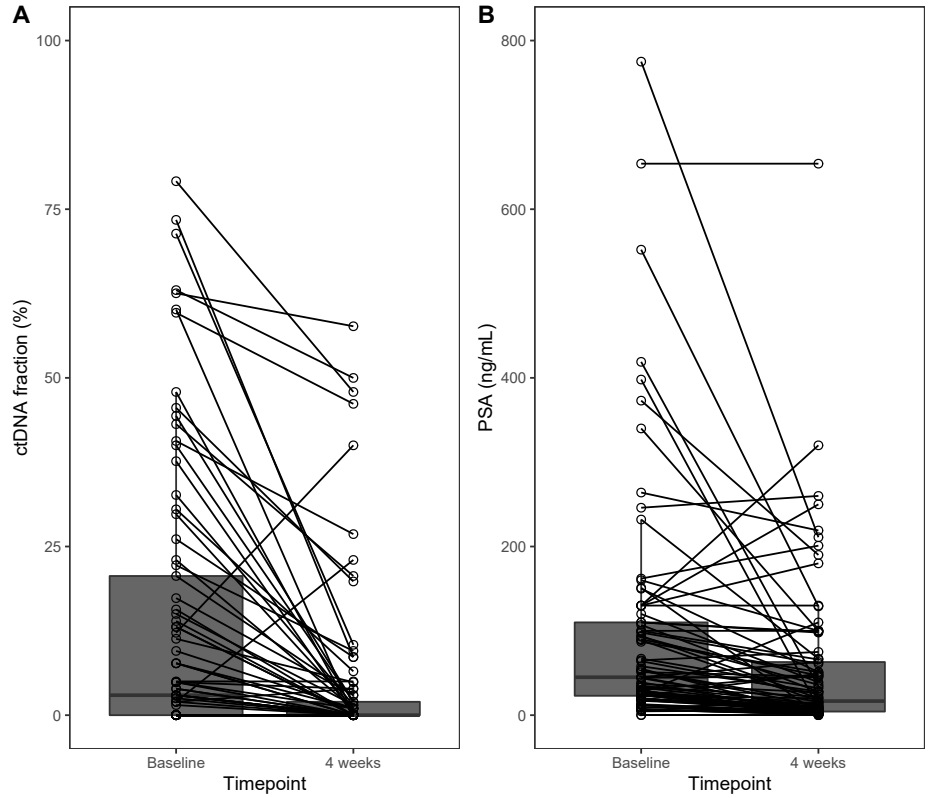

Supplementary Figure S1: Per patient (A) ctDNA fractions and (B) PSA levels at baseline and after 4 weeks of treatment.

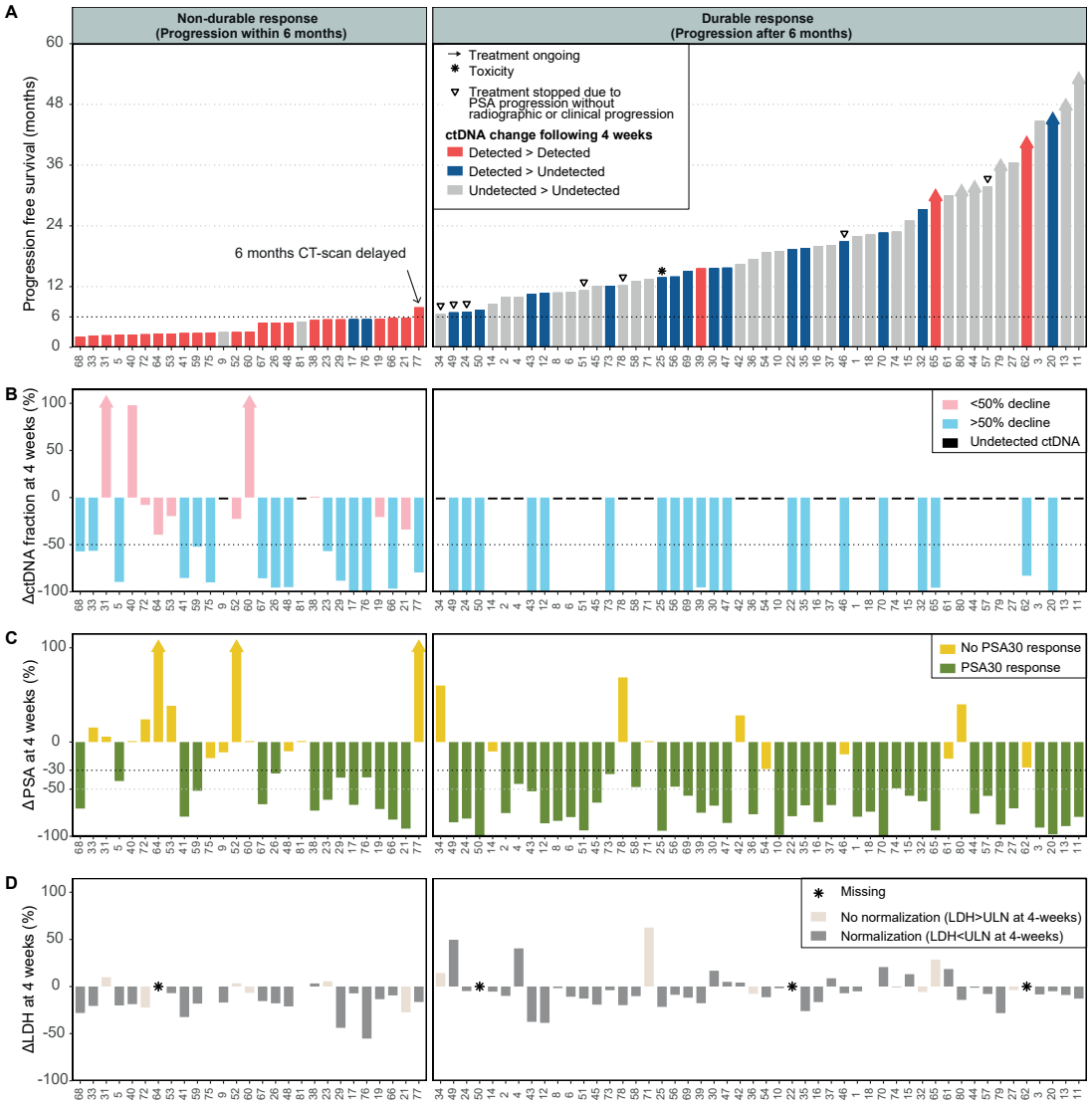

Supplementary Figure S2: On-treatment ctDNA fraction, PSA and LDH changes and durability of treatment response. (A) Swimmers plot showing per patient progression-free survival. Bar colors indicate the ctDNA conversion groups following 4 weeks of treatment. Arrows indicate patients still on treatment. (B) The change in ctDNA fraction following 4 weeks of treatment. Arrows indicate a ctDNA increase greater than 100%. Pink bars indicate patients who did not achieve a 50% decrease in ctDNA at 4 weeks. Patients with undetected ctDNA at baseline and 4-weeks were not evaluable. (C) The change in serum PSA following 4 weeks of treatment. Arrows indicate a PSA increase greater than 100%. Yellow bars indicate patients who did not achieve a PSA30 response at 4 weeks. (D) The change in LDH following 4 weeks of treatment. Dark-gray bars indicate patients with LDH normalization (LDH remaining or reducing to normal levels after 4 weeks of treatment). Off-white bars indicate patients without LDH normalization (LDH above the upper limit of normal at 4 weeks of treatment). Stars are indicated when LDH measurements were missing at baseline and/or 4-weeks.

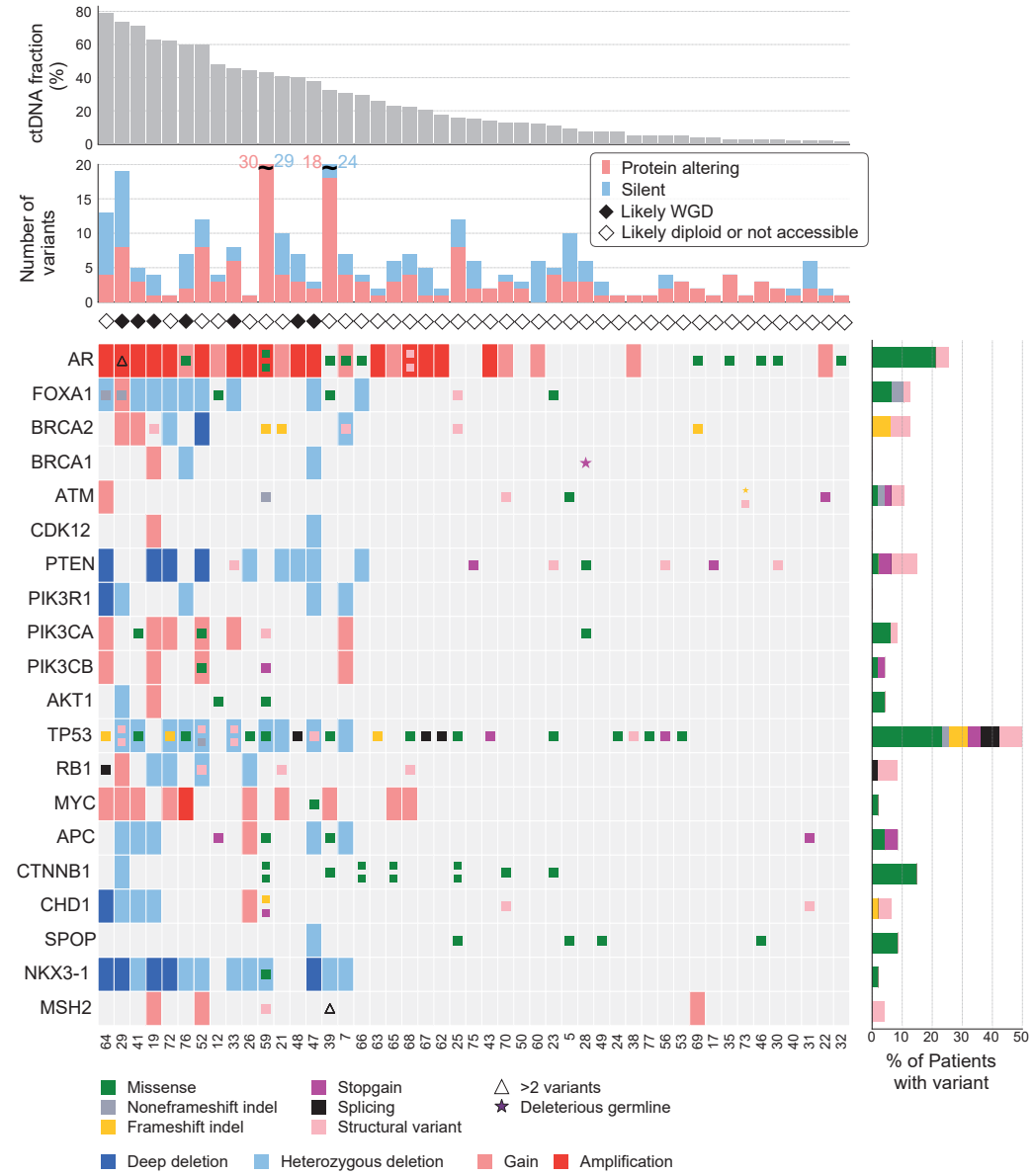

Supplementary Figure S3: Oncoprint showing the copy number alterations, structural variants and mutations per patient at baseline.

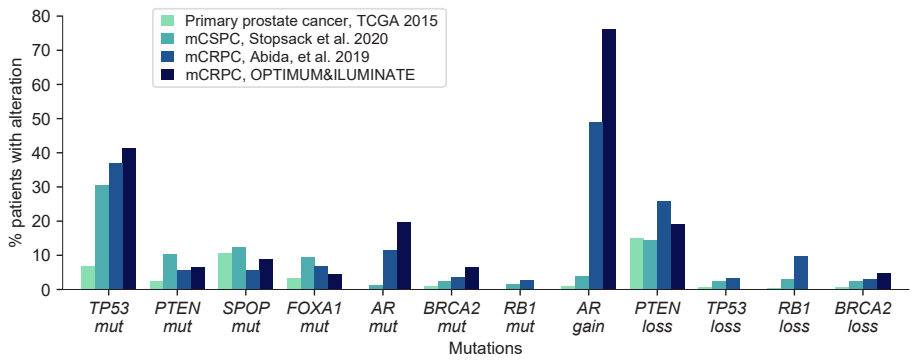

Supplementary Figure S4: Frequency of recurrent somatic alterations compared to published cohorts. Only ctDNA positive samples from the OPTIMUM and ILUMINATE were used for frequency assessment. The frequencies were compared to primary prostate cancer from The Cancer Genome Atlas (TCGA) [6], metastatic castration-sensitive prostate cancer (mCSPC) from Stopsack et al. 2020 [7] and metastatic castration-resistant prostate cancer (mCRPC) from Abida et al. 2019 [8]. Note that different sequencing platforms, materials and bioinformatic analysis were used in the different study populations, hampering direct comparison.

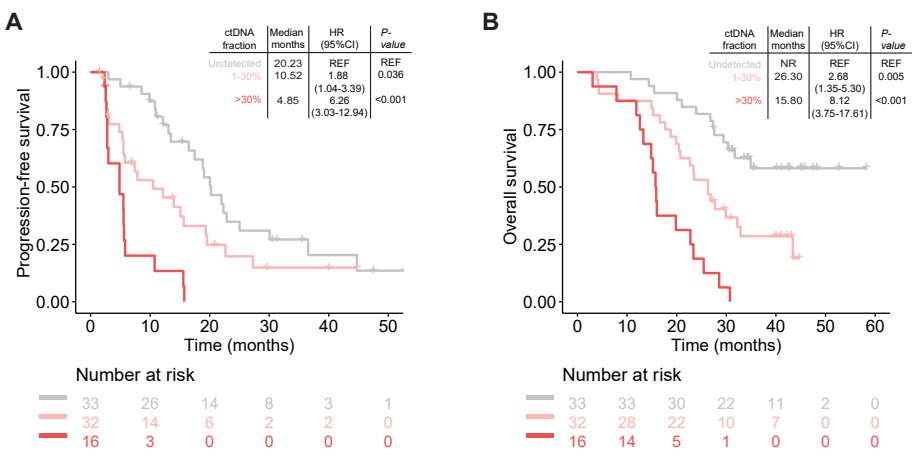

Supplementary Figure S5: Relationship between baseline circulating tumor DNA fraction and patient outcomes. Progression-free survival (PFS; A) and overall survival (OS; B) for patients with high (>30%), intermediate (1-30%) or low (undetected; <1%) circulating tumor DNA (ctDNA) at baseline.

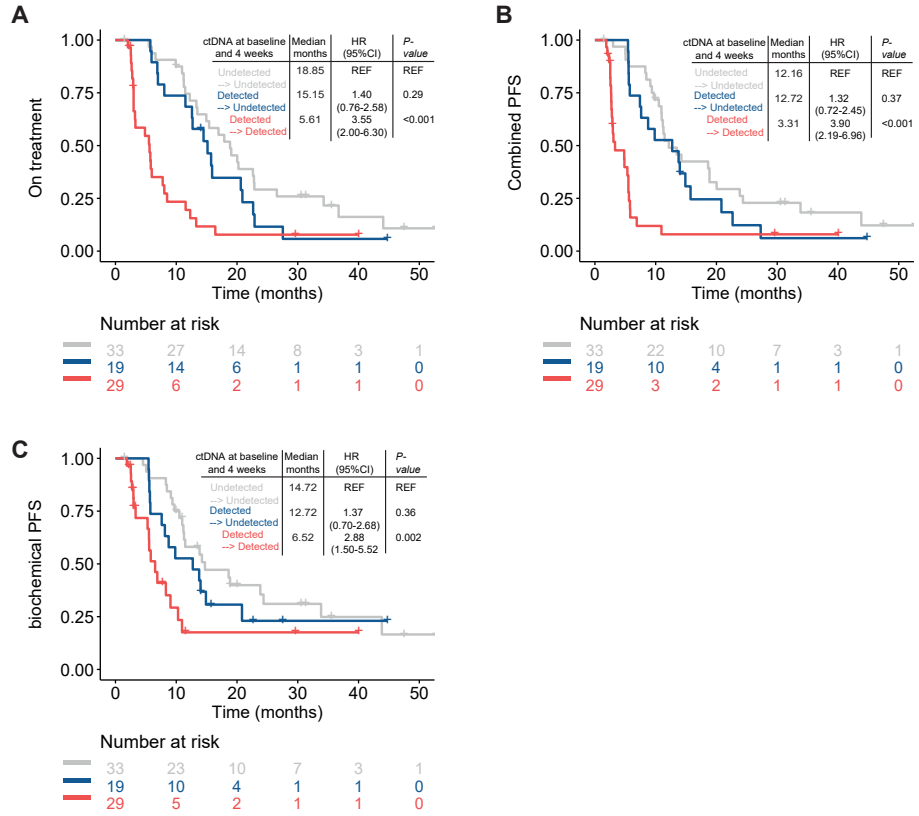

Supplementary Figure S6: Relationship between on-treatment detection of circulating tumor DNA patient outcomes. Time on treatment (A), combined progression-free survival (B) and biochemical progression-free survival (C) according to change in ctDNA detection status after 4 weeks of treatment.

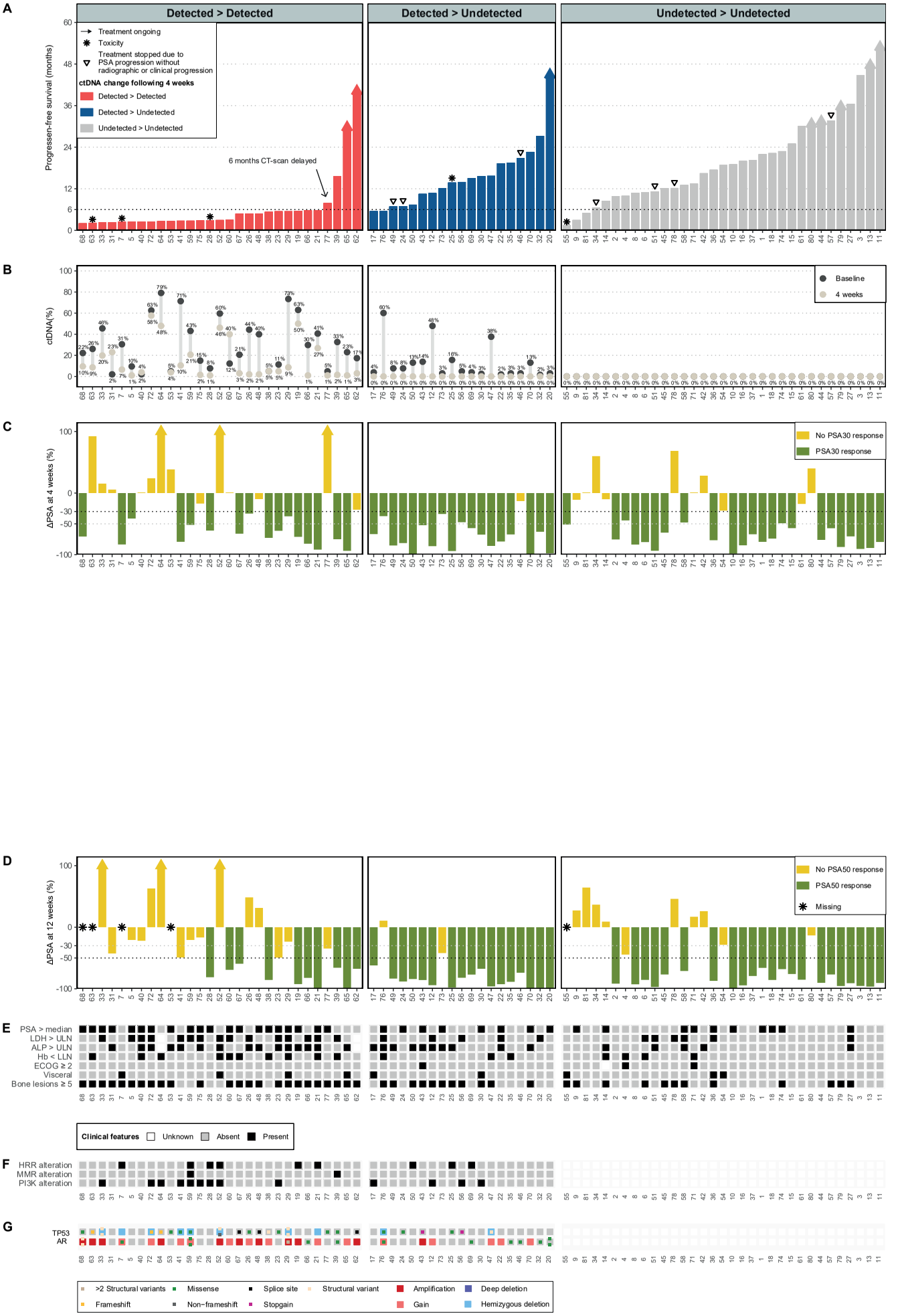

Supplementary Figure S7 (right page): On-treatment circulating tumor DNA (ctDNA) fraction, prostate specific antigen (PSA) responses and baseline genomic and clinical features. (A) Swimmers plot showing per patient progression-free survival. Bar colors indicate the ctDNA change groups following 4 weeks of treatment. Arrows indicate patients who are still on-treatment. (B) ctDNA fraction (ctDNA%) changes following 4 weeks of treatment. (C) The change in serum PSA following 4 weeks of treatment. Arrows indicate a PSA increase greater than 100%. Yellow bars indicate patients who did not achieve a PSA30 response at 4 weeks. (D) The change in serum PSA following 12 weeks of treatment. Arrows indicate a PSA increase greater than 100%. Yellow bars indicate patients who did not achieve a PSA50 response at 12 weeks. (E) Baseline patient clinical characteristics. (F) Potentially actionable alterations present in baseline ctDNA samples, within the homologous recombination repair (HRR) pathway, mismatch repair (MMR) pathway and phosphoinositide 3-kinase (PI3K) pathway. (G) Baseline TP53 and AR alterations.

Abbreviations: HB, hemoglobin; LDH, lactate dehydrogenase; ALP, alkaline phosphatase; PSA, prostate-specific antigen; ECOG, Eastern Cooperative Oncology Group performance status; ΔPSA, prostate-specific antigen change; PSA30, 30% decline in prostate-specific antigen; PSA50, 50% decline in prostate-specific antigen.

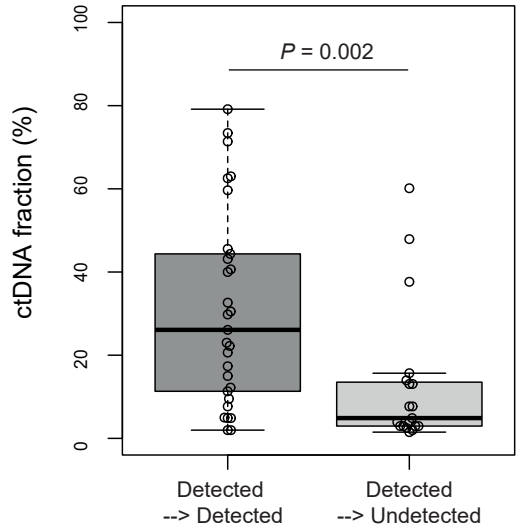

Supplementary Figure S8: Baseline circulating tumor DNA fraction according to detection status at 4 weeks. Box plot showing the difference in distribution of baseline ctDNA fraction in patients who have ctDNA detected at both baseline and 4 weeks compared to patients converting from detected to undetected ctDNA by 4 weeks.

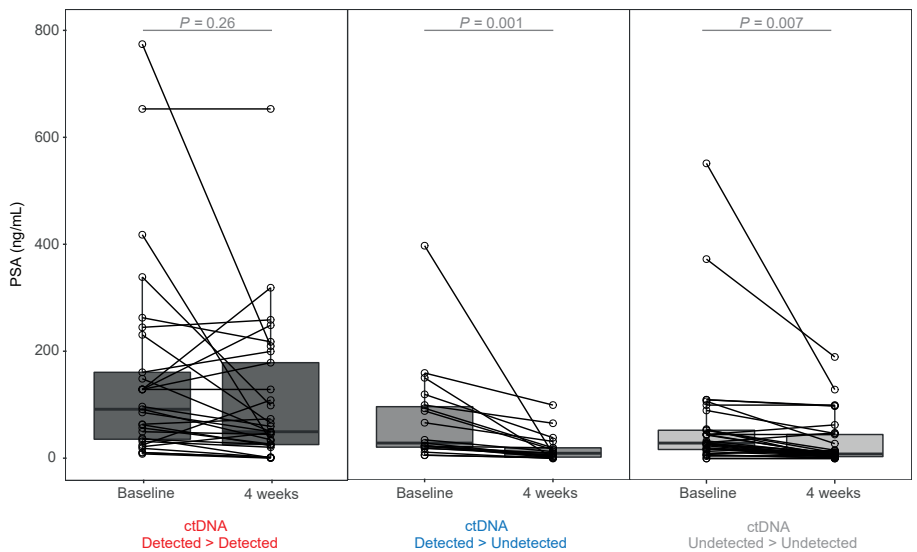

Supplementary Figure S9: Changes in PSA levels between baseline and 4 weeks on-treatment in the different ctDNA kinetics groups.

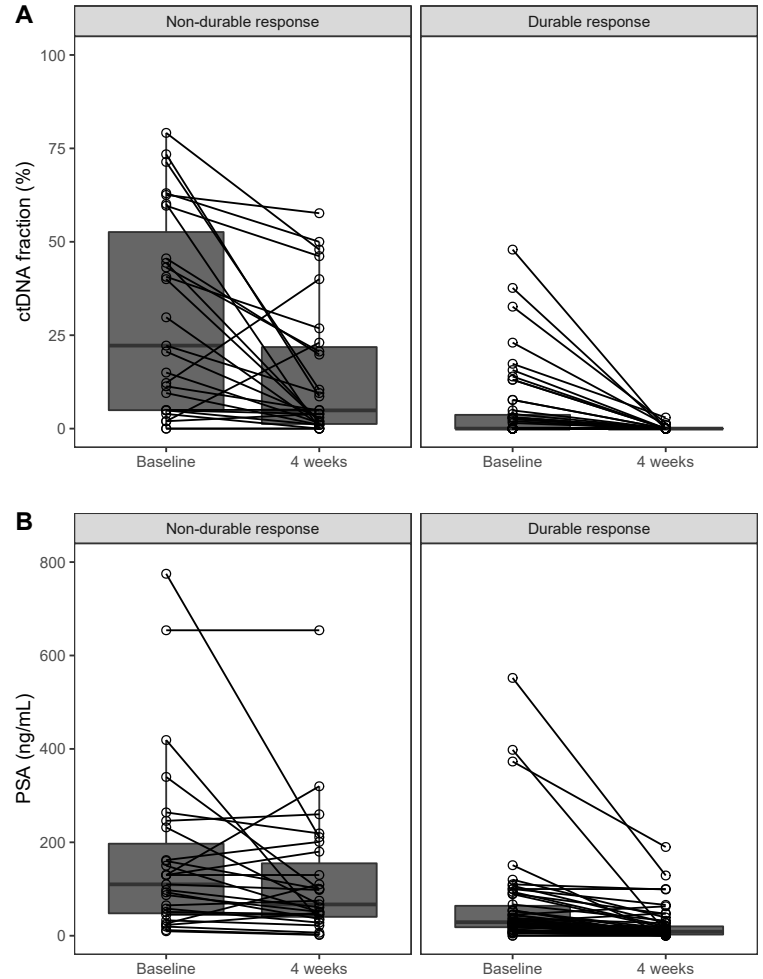

Supplementary Figure S10: Changes in (A) ctDNA fraction and (B) PSA levels between baseline and 4 weeks on-treatment in relation to the durability of response.

Supplementary Table S1: Representativeness of study participants

Cancer type(s)/subtype(s)/stage(s)/ condition	Metastatic castration resistant prostate cancer (mCRPC) prior to first-line therapy with Androgen-Receptor pathway inhibitors
Considerations related to:	
Sex	Prostate cancer only arises in people with prostates, i.e. biological males.
Age	The median age at mCRPC progression, and start of first-line mCRPC treatment is approximately 75 years old.
Race/ethnicity	In the USA from 2006 to 2010, the overall prostate cancer incidence was 136.6 cases per 100,000 among Black males, 146.6 cases per 100,000 among White males and 220.0 cases per 100,000 among Asian/Pasific Islander males [1]. In the Netherlands, the reported incidence on prostate cancer in 2020 is 147.3 per 100,000 among males [2]. Progression to mCRPC occurs in 5-15% of prostate cancer cases.
Geography	In the Netherlands, 113,656 new cases of prostate cancer were diagnosed in 2020 and 45,883 males died from prostate cancer that year.
Other considerations	n/a
Overall representativeness of this study	The age distribution of our study (median 73) is similar to the average age distribution of mCRPC in the literature. Our study included predominantly white males, broadly reflective of the Dutch population. However, ~5% of the Dutch population is from Turkish or Moroccan descent and ~5% from Indonesian descent, and these populations were underrepresented in our cohort.
[1] Edwards BK, et al. Annual Report to the Nation on the status of cancer, 1975-2010, featuring prevalence of comorbidity and impact on survival among persons with lung, colorectal, breast, or prostate cancer. Cancer. 2014 May 1;120(9):1290-314.	
[2] Dutch cancer registry (IKNL, 2011)	

Supplementary Table S2: Evidence for ctDNA estimates per patient per timepoint. This table shows the somatic alterations used for ctDNA fraction calculation.

Patient ID	Timepoint	Plasma volume	cfDNA yield (ng)	cfDNA ng/mL plasma	Input sequencer (ng)	Final ctDNA estimate	Final ctDNA estimate origin	Mutation-based ctDNA estimate	Mutation VAF	Mut ant reads	Chr	Position	Gene	Mutation type	Dependent call	Log ratio	SNP-based ctDNA estimate panel	SNP-based ctDNA estimate WGS
1	Baseline	3	25.6	8.5	10	0.00%		0.00%										NA
1	4 weeks	2.8	27.3	9.7	10	0.00%		0.00%										NA
2	Baseline	1.5	16.9	11.3	10	0.00%		0.00%										NA
2	4 weeks	1.6	11.9	7.5	10	0.00%		0.00%										NA
3	Baseline	3	29.3	9.8	10	0.00%		0.00%										NA
3	4 weeks	3.4	29.8	8.8	10	0.00%		0.00%										NA
4	Baseline	1.7	36.5	21.5	10	0.00%		0.00%										NA
4	4 weeks	2.6	64.8	24.9	25	0.00%		0.00%										NA
5	Baseline	3.1	37.8	12.2	10	9.52%	Mutation	9.52%	6.00%	47	chr3	37016272	MLH1	Intronic	0	0.023		NA
5	4 weeks	2.6	51.3	19.7	25	1.00%	Mutation	1.00%	0.50%	7	chr5	98921038	CHD1	Intronic	1	0.017		NA
6	Baseline	3	27.1	9.0	10	0.00%		0.00%										NA
6	4 weeks	2.7	47.7	17.7	10	0.00%		0.00%										NA
7	Baseline	3.1	63.5	20.5	25	30.51%	Mutation	30.51%	19.63%	305	chr3	71000947	FOXP1	Intronic	0	-0.016	55.91%	54%
7	4 weeks	3.5	32.1	9.2	10	6.50%	Mutation	6.50%	8.20%	44	chrX	67693123	AR	Intronic	0	0.028		NA
8	Baseline	2.9	31.6	10.9	10	0.00%		0.00%										NA
8	4 weeks	3.3	39.2	11.9	10	0.00%		0.00%										NA
9	Baseline	1	6.3	6.3	6	0.00%		0.00%										NA
9	4 weeks	1.3	11.6	8.9	10	0.00%		0.00%										NA
10	Baseline	3	10.0	3.3	10	0.00%		0.00%										NA
10	4 weeks	3	12.5	4.2	10	0.00%		0.00%										NA
11	Baseline	2.8	20.3	7.3	10	0.00%		0.00%										NA
11	4 weeks	3.1	64.8	20.9	25	0.00%		0.00%										NA
12	Baseline	3.2	85.1	26.6	10	47.91%	Mutation	47.91%	33.50%	328	chr14	104780214	AKT1	Missense	0	0.058	34.88%	27%
12	4 weeks	2.7	44.4	16.5	10	0.00%		0.00%										NA
13	Baseline	1.6	11.8	7.4	10	0.00%		0.00%										NA
13	4 weeks	1.3	14.0	10.7	10	0.00%		0.00%										NA
14	Baseline	2.7	34.2	12.7	10	0.00%		0.00%										NA
14	4 weeks	2.7	27.6	10.2	10	0.00%		0.00%										NA
15	Baseline	3	16.7	5.6	10	0.00%		0.00%										NA
15	4 weeks	3.1	24.9	8.0	10	0.00%		0.00%										NA
16	Baseline	3	31.6	10.5	10	0.00%		0.00%										NA
16	4 weeks	2.8	38.7	13.8	10	0.00%		0.00%										NA
17	Baseline	3	19.1	6.4	10	3.92%	Mutation	3.92%	2.50%	16	chr10	87925543	PTEN	Stopgain	0	-0.038		NA

Patient ID	Timepoint	Plasma volume	cfDNA yield (ng)	cfDNA ng/mL plasma	Input sequencer (ng)	Final ctDNA estimate	Final ctDNA estimate origin	Mutation-based ctDNA estimate	Mutation VAF	Mut ant reads	Chr	Position	Gene	Mutation type	Dependent call	Log ratio	SNP-based ctDNA estimate panel	SNP-based ctDNA estimate WGS
17	4 weeks	2.4	15.0	6.2	10	0.00%		0.00%										NA
18	Baseline	3.1	28.8	9.3	10	0.00%		0.00%										NA
18	4 weeks	2.9	33.0	11.4	10	0.00%		0.00%										NA
19	Baseline	1.3	37.3	28.7	10	63.01%	SNP-based	0.00%	Only mutations amplified/intergenic regions; but structural variant BRCA2								63.01%	60%
19	4 weeks	2.6	137.7	53.0	50	49.99%	SNP-based	0.00%	Only mutations amplified/intergenic regions; but structural variant BRCA2								49.99%	50%
20	Baseline	3.5	51.8	14.8	25	2.96%	Mutation	2.96%	1.50%	36	chr1	26771205	ARID1A	Synonymous	0	0.021		NA
20	4 weeks	3	77.9	26.0	25	0.00%		0.00%										NA
21	Baseline	2.8	135.9	48.5	25	40.64%	Mutation	40.64%	27.37%	240	chr13	32339699	BRCA2	Frameshift	0	-0.191	44.48%	47%
21	4 weeks	3	86.0	28.7	25	26.84%	Mutation	26.84%	17.60%	143	chr13	32339699	BRCA2	Frameshift	0	-0.079		30%
22	Baseline	2.7	24.8	9.2	10	1.98%	Mutation	1.98%	1.10%	10	chr11	108251953	ATM	Stopgain	0	-0.084		NA
22	4 weeks	2.6	7.7	2.9	8	0.00%		0.00%										NA
23	Baseline	2.9	33.2	11.4	10	11.32%	Mutation	11.32%	7.00%	72	chr17	7670700	TP53	Missense	0	-0.09		NA
23	4 weeks	2.9	25.1	8.7	10	4.88%	Mutation	4.88%	3.20%	37	chr17	7670700	TP53	Missense	0	-0.038		NA
24	Baseline	3.1	68.0	21.9	10	7.69%	Mutation	7.69%	4.90%	57	chr17	7674238	TP53	Missense	0	-0.041		NA
24	4 weeks	1.4	30.4	21.7	10	0.00%		0.00%										NA
25	Baseline	3.2	41.1	12.9	10	15.67%	Mutation	15.67%	9.50%	116	chr17	49619281	SPOP	Missense	0	0.108		NA
25	4 weeks	1.8	32.8	18.2	10	0.00%		0.00%										NA
26	Baseline	3	48.2	16.1	25	44.36%	Mutation	44.36%	29.90%	622	chr17	7675088	TP53	Missense	0	-0.184	33.18%	38%
26	4 weeks	2.4	38.6	16.1	10	1.98%	Mutation	1.98%	1.30%	18	chr17	7675088	TP53	Missense	1	0.007		NA
27	Baseline	3.2	33.7	10.5	10	0.00%		0.00%										NA
27	4 weeks	3.1	35.5	11.4	10	0.00%		0.00%										NA
28	Baseline	2.3	22.5	9.8	10	7.69%	Mutation	7.69%	4.30%	61	chr10	87933154	PTEN	Missense	0	-0.039		NA
28	4 weeks	3	17.5	5.8	10	1.00%	Mutation	1.00%	0.50%	5	chr8	70126763	NCOA2	Intronic	1	0.016		NA
29	Baseline	2.6	193.5	74.4	50	73.42%	Mutation	73.42%	59.39%	1316	chr12	49038958	KMT2D	Stopgain	0	0.179	78.86%	64%
29	4 weeks	2.5	13.1	5.2	10	8.61%	Mutation	8.61%	4.90%	76	chr12	49038958	KMT2D	Stopgain	0	0.029		NA
30	Baseline	2.4	13.0	5.4	10	2.50%	Mutation	2.50%	3.40%	20	chrX	67723743	AR	Missense	0	0		NA
30	4 weeks	2.7	16.0	5.9	10	0.00%		0.00%										NA
31	Baseline	2.9	35.8	12.3	10	1.98%	Mutation	1.98%	1.00%	10	chr5	112840155	APC	Stopgain	0	-0.027		NA
31	4 weeks	2.9	52.7	18.2	25	23.01%	Mutation	23.01%	14.20%	205	chr5	112840155	APC	Stopgain	0	-0.235		26%
32	Baseline	3	37.7	12.6	10	1.50%	Mutation	1.50%	1.80%	16	chrX	67717530	AR	Missense	0	-0.008		NA
32	4 weeks	3.1	42.2	13.6	25	0.00%		0.00%										NA
33	Baseline	3.2	59.0	18.4	25	45.56%	Mutation	45.56%	30.89%	530	chr7	140753345	BRAF	Missense	0	0.061	56.83%	60%
33	4 weeks	3.4	23.1	6.8	10	19.82%	Mutation	19.82%	12.20%	114	chr7	140753345	BRAF	Missense	0	0.085		NA
34	Baseline	3.2	30.4	9.5	10	0.00%		0.00%										NA
34	4 weeks	3.4	73.4	21.6	25	0.00%		0.00%										NA
35	Baseline	3.1	17.3	5.6	10	2.96%	Mutation	2.96%	1.90%	27	chr12	49033367	KMT2D	Missense	0	-0.007		NA

Patient ID	Timepoint	Plasma volume	cfDNA yield (ng)	cfDNA ng/mL plasma	Input sequencer (ng)	Final ctDNA estimate	Final ctDNA estimate origin	Mutation-based ctDNA estimate	Mutation VAF	Mut ant reads	Chr	Position	Gene	Mutation type	Dependent call	Log ratio	SNP-based ctDNA estimate panel	SNP-based ctDNA estimate WGS
35	4 weeks	3	14.5	4.8	10	0.00%		0.00%										NA
36	Baseline	2.6	28.7	11.0	10	0.00%		0.00%										NA
36	4 weeks	3.2	60.3	18.8	25	0.00%		0.00%										NA
37	Baseline	2.7	26.8	9.9	10	0.00%		0.00%										NA
37	4 weeks	3.3	32.8	9.9	10	0.00%		0.00%										NA
38	Baseline	2.7	87.8	32.5	25	5.00%	High AR gain	0.00%										NA
38	4 weeks	2.8	25.2	9.0	10	5.00%	High AR gain	0.00%										NA
39	Baseline	2.5	46.8	18.7	10	32.64%	Mutation	32.64%	21.20%	209	chr17	7675088	TP53	Missense	0	-0.226		30%
39	4 weeks	2.7	25.9	9.6	10	1.50%	Mutation	1.50%	1.90%	14	chrX	67695404	AR	3′-UTR	1	0.006		NA
40	Baseline	2.8	124.2	44.4	25	1.98%	Mutation	1.98%	1.00%	13	chr17	7673617	TP53	Intronic	1	-0.099		NA
40	4 weeks	3.1	44.9	14.5	25	3.92%	Mutation	3.92%	2.20%	28	chr17	7673617	TP53	Intronic	0	-0.083		NA
41	Baseline	2.6	151.7	58.3	50	71.38%	Mutation	71.38%	57.40%	868	chr17	7674220	TP53	Missense	0	-0.383	41.91%	72%
41	4 weeks	3.4	90.9	26.7	25	10.43%	Mutation	10.43%	6.10%	119	chr17	7674220	TP53	Missense	0	-0.044		NA
42	Baseline	2.9	21.8	7.5	10	0.00%		0.00%										NA
42	4 weeks	3.5	52.7	15.0	10	0.00%		0.00%										NA
43	Baseline	2.8	42.2	15.1	10	13.95%	Mutation	13.95%	8.60%	99	chr17	7674237	TP53	Stopgain	0	-0.05		NA
43	4 weeks	2.6	23.7	9.1	10	0.00%		0.00%										NA
44	Baseline	3.2	26.0	8.1	10	0.00%		0.00%										NA
44	4 weeks	2.5	19.8	7.9	10	0.00%		0.00%										NA
45	Baseline	2.7	12.2	4.5	10	0.00%		0.00%										NA
45	4 weeks	2.7	7.2	2.7	7	0.00%		0.00%										NA
46	Baseline	2.7	18.2	6.7	10	2.96%	Mutation	2.96%	1.60%	25	chr7	152181379	KMT2C	Stopgain	0	-0.002		NA
46	4 weeks	2.9	18.1	6.2	10	0.00%		0.00%										NA
47	Baseline	3.2	257.0	80.3	100	37.65%	SNP-based	2.96%	2.18%	25	chr8	127738607	MYC	Missense	0	0.297	37.65%	38%
47	4 weeks	2.6	31.3	12.0	10	0.00%		0.00%										NA
48	Baseline	2.5	78.8	31.5	25	40.00%	Mutation	40.00%	26.50%	409	chr17	7674858	TP53	Splice site	0	-0.207	37.39%	NA
48	4 weeks	3	30.0	10.0	10	1.98%	Mutation	1.98%	1.10%	14	chr17	7674858	TP53	Splice site	0	-0.04		NA
49	Baseline	2.5	25.7	10.3	10	7.69%	Mutation	7.69%	4.60%	33	chr17	49619198	SPOP	Intronic	0	0.045		NA
49	4 weeks	3.3	29.7	9.0	10	0.00%		0.00%										NA
50	Baseline	3.6	38.5	10.7	10	13.08%	Mutation	13.08%	7.80%	108	chr9	95114639	FANCC	Missense	0	0.028		NA
50	4 weeks	3.3	19.1	5.8	10	0.00%		0.00%										NA
51	Baseline	3.5	42.1	12.0	10	0.00%		0.00%										NA
51	4 weeks	3	34.0	11.3	10	0.00%		0.00%										NA
52	Baseline	3.3	117.5	35.6	10	59.65%	Mutation	59.65%	45.80%	290	chr7	140739789	BRAF	Intronic	0	0.208	52.89%	NA
52	4 weeks	3.1	73.4	23.7	25	46.15%	Mutation	46.15%	32.00%	329	chr7	140739789	BRAF	Intronic	0	0.205	38.42%	NA
53	Baseline	3.1	20.0	6.4	10	4.88%	Mutation	4.88%	3.30%	28	chr17	35116916	RAD51D	Missense	0	0.08		NA

Patient ID	Timepoint	Plasma volume	cfDNA yield (ng)	cfDNA ng/mL plasma	Input sequencer (ng)	Final ctDNA estimate	Final ctDNA estimate origin	Mutation-based ctDNA estimate	Mutation VAF	Mut ant reads	Chr	Position	Gene	Mutation type	Dependent call	Log ratio	SNP-based ctDNA estimate panel	SNP-based ctDNA estimate WGS
53	4 weeks	2.8	26.9	9.6	10	3.92%	Mutation	3.92%	2.30%	25	chr17	35116916	RAD51D	Missense	0	0.034		NA
54	Baseline	3.2	34.4	10.7	10	0.00%		0.00%										NA
54	4 weeks	2.7	24.8	9.2	10	0.00%		0.00%										NA
55	Baseline	2.9	37.9	13.1	10	0.00%		0.00%										NA
55	4 weeks	2.6	31.2	12.0	10	0.00%		0.00%										NA
56	Baseline	3.2	33.3	10.4	10	4.88%	Mutation	4.88%	2.90%	36	chr17	7675064	TP53	Stopgain	0	-0.028		NA
56	4 weeks	0.5	7.2	14.4	7	0.00%		0.00%										NA
57	Baseline	2.9	27.6	9.5	10	0.00%		0.00%										NA
57	4 weeks	2.7	19.9	7.4	10	0.00%		0.00%										NA
58	Baseline	2.8	45.5	16.2	10	0.00%		0.00%										NA
58	4 weeks	3.1	42.8	13.8	10	0.00%		0.00%										NA
59	Baseline	3	65.3	21.8	10	43.14%	Mutation	43.14%	29.50%	309	chr7	92725679	CDK6	Missense	0	0.158	41.15%	40%
59	4 weeks	2.4	27.1	11.3	10	20.63%	Mutation	20.63%	12.90%	113	chr7	92725679	CDK6	Missense	0	0.112		23%
60	Baseline	3.2	19.2	6.0	10	12.21%	Mutation	12.21%	7.90%	54	chr5	98861350	CHD1	Intronic	0	-0.024		NA
60	4 weeks	3.1	55.4	17.9	25	40.00%	Mutation	40.00%	26.80%	324	chr5	98861350	CHD1	Intronic	0	0.026		34%
61	Baseline	3.3	15.9	4.8	10	0.00%		0.00%										NA
61	4 weeks	3.3	63.9	19.4	25	0.00%		0.00%										NA
62	Baseline	3.4	22.0	6.5	10	17.35%	Mutation	17.35%	10.40%	134	chr17	7674858	TP53	Splice site	0	-0.04		NA
62	4 weeks	3.3	13.3	4.0	10	2.96%	Mutation	2.96%	1.50%	22	chr17	7674858	TP53	Splice site	0	0.013		NA
63	Baseline	3.3	702.0	212.7	100	26.09%	Mutation	26.09%	16.10%	273	chr17	7676026	TP53	Frameshift	0	-0.162		32%
63	4 weeks	2.4	284.0	118.3	100	8.61%	Mutation	8.61%	5.00%	93	chr17	7676026	TP53	Frameshift	0	-0.073		NA
64	Baseline	2.4	990.0	412.5	100	79.15%	Mutation	79.15%	67.80%	597	chr17	7675161	TP53	Frameshift	0	-0.095	72.85%	80%
64	4 weeks	3.4	87.8	25.8	25	47.91%	Mutation	47.91%	32.90%	722	chr7	152148678	KMT2C	Missense	0	0.197		30%
65	Baseline	2.9	29.8	10.3	10	23.01%	Mutation	23.01%	14.70%	141	chr14	37590389	FOXA1	3′-UTR	0	0.009		23%
65	4 weeks	2.8	34.6	12.3	10	1.00%	Mutation	1.00%	0.60%	9	chr3	41224613	CTNNB1	Missense	1	0.034		NA
66	Baseline	2.7	62.1	23.0	25	29.79%	Mutation	29.79%	19.20%	188	chr3	71493547	FOXP1	5′-UTR	0	-0.065	21.16%	30%
66	4 weeks	1.7	24.3	14.3	10	1.00%	Mutation	1.00%	0.70%	9	chr3	41224634	CTNNB1	Missense	0	-0.002		NA
67	Baseline	3	33.4	11.1	10	20.63%	Mutation	20.63%	13.20%	98	chr17	7687376	TP53	Splice site	0	-0.066		NA
67	4 weeks	2.4	29.0	12.1	10	2.96%	Mutation	2.96%	1.60%	14	chr17	7687376	TP53	Splice site	0	-0.04		NA
68	Baseline	3.1	64.4	20.8	25	22.22%	Mutation	22.22%	13.40%	202	chr17	7673803	TP53	Missense	0	-0.115		23%
68	4 weeks	3.3	63.9	19.4	25	9.52%	Mutation	9.52%	5.90%	97	chr17	7673803	TP53	Missense	0	-0.074		NA
69	Baseline	2.6	32.4	12.4	10	3.92%	Mutation	3.92%	2.40%	20	chr13	32333183	BRCA2	Frameshift	0	-0.018		NA
69	4 weeks	3.2	61.7	19.3	10	0.00%		0.00%										NA
70	Baseline	3	50.9	17.0	25	13.08%	Mutation	13.08%	7.80%	164	chr3	41224606	CTNNB1	Missense	0	-0.07		20%
70	4 weeks	3	45.9	15.3	10	0.00%		0.00%										NA
71	Baseline	3	51.8	17.3	25	0.00%		0.00%										NA

Patient ID	Timepoint	Plasma volume	cfDNA yield (ng)	cfDNA ng/mL plasma	Input sequencer (ng)	Final ctDNA estimate	Final ctDNA estimate origin	Mutation-based ctDNA estimate	Mutation VAF	Mut ant reads	Chr	Position	Gene	Mutation type	Dependent call	Log ratio	SNP-based ctDNA estimate panel	SNP-based ctDNA estimate WGS
71	4 weeks	2.8	67.1	23.9	25	0.00%		0.00%										NA
72	Baseline	1.2	66.2	55.1	10	62.54%	Mutation	62.54%	48.73%	287	chr17	7676209	TP53	Frameshift	0	-0.596	70.73%	70%
72	4 weeks	2.4	175.5	73.1	50	57.65%	Mutation	57.65%	42.66%	538	chr17	7676209	TP53	Frameshift	0	-0.479	65.86%	65%
73	Baseline	3.2	15.5	4.9	10	2.96%	Structural Variant	2.96%	1.57%	11	chr11		ATM	Structural variant	0	0.007		NA
73	4 weeks	3	18.3	6.1	10	0.00%		0.00%										NA
74	Baseline	3.3	51.8	15.7	25	0.00%		0.00%										NA
74	4 weeks	3.1	52.2	16.8	25	0.00%		0.00%										NA
75	Baseline	3.2	38.7	12.1	10	15.00%	Mutation	15.00%	17.40%	100	chrX	67712893	AR	Intronic	0	0.134		NA
75	4 weeks	3	25.6	8.5	10	1.50%	Mutation	1.50%	1.90%	10	chrX	67712893	AR	Intronic	1	0.014		NA
76	Baseline	3.6	320.4	89.0	100	60.14%	Mutation	60.14%	45.10%	467	chr17	7675131	TP53	Missense	0	-0.503	58.58%	60%
76	4 weeks	3.4	43.7	12.9	10	0.00%		0.00%										NA
77	Baseline	3	29.9	10.0	10	4.88%	Mutation	4.88%	2.80%	29	chr17	7673803	TP53	Missense	0	0		NA
77	4 weeks	3.2	94.5	29.5	10	1.00%	Mutation	1.00%	0.60%	3	chr17	7673803	TP53	Missense	1	-0.025		NA
78	Baseline	3.4	23.2	6.8	10	0.00%		0.00%										NA
78	4 weeks	3.3	40.2	12.2	10	0.00%		0.00%										NA
79	Baseline	2.7	32.6	12.1	10	0.00%		0.00%										NA
79	4 weeks	3.4	34.0	10.0	10	0.00%		0.00%										NA
80	Baseline	3	32.9	11.0	10	0.00%		0.00%										NA
80	4 weeks	3.3	24.4	7.4	10	0.00%		0.00%										NA
81	Baseline	2.9	22.7	7.8	10	0.00%		0.00%										NA
81	4 weeks	1.6	16.1	10.0	10	0.00%		0.00%										NA

Supplementary Table S3: Multivariable Cox proportional hazards models for time to progression and time to death. The table provides full results for on-treatment ctDNA fraction changes and prognostic clinical features studied in this manuscript.

Multivariable analysis with PSA, LDH and ALP as continues variables. Most patients with undetected ctDNA at baseline and/or 4 weeks had LDH levels below the upper limit of normal (ULN). Therefore, LDH results should be treated with caution.

			Progression-free survival					**Overall survival**				
Clinical marker	Subgroup	No. patients	Median (months)	Univariate analysis		Multivariable analysis		Median (months)	Univariate analysis		Multivariable analysis	
				HR (95% CI)	*P*-value	HR (95% CI)	*P*-value		HR (95% CI)	*P*-value	HR (95% CI)	*P*-value
ctDNA% change following 4 weeks	Undetected → Undetected	33	20.23	ref	ref	ref	ref	Not reached	ref	ref	ref	ref
	Detected → Undetected	19	15.64	1.4 (0.71-2.76)	0.325	1.20 (0.59-2.46)	0.61	27.7	2.17 (1-4.7)	**0.049**	1.49 (0.65-3.42)	0.34
	Detected → Detected	29	4.82	4.79 (2.62-8.77)	**<0.001**	4.55 (1.90-10.9)	**<0.001**	16	5.49 (2.76-10.91)	**<0.001**	3.12 (1.28-7.58)	**0.01**
Baseline ctDNA%		81	NA	1.04 (1.02-1.05)	**<0.001**	1.01 (0.99-1.03)	0.3	NA	1.03 (1.02-1.04)	**<0.001**	1.02 (1.01-1.04)	**0.01**
log10(PSA)		81	NA	1.68 (1.10-2.66)	**0.03**	1.43 (0.87-2.37)	0.16	NA	1.84 (1.10-3.07)	**0.02**	1.25 (0.72-2.19)	0.43
LDH (U/L)		79	NA	1.01 (1.00-1.01)	**0.005**	1.00 (1.00-1.01)	0.44	NA	1.00 (1.00-1.01)	0.56	0.99 (0.99-1.00)	**0.02**
ALP (U/L)		79	NA	1.00 (1.00-1.00)	**0.005**	1.00 (1.00-1.00)	0.94	NA	1.00 (1.00-1.01)	**0.001**	1.00 (1.00-1.00)	0.06

Multivariable analysis with on-treatment ctDNA groups and neutrophil-to-lymphocyte (NLR) ratio in subgroup of 48 patients with NLR data. NLR was not included in the main manuscript due to a high number of missing data for NLR (N = 32).

			Progression-free survival					**Overall survival**				
Clinical marker	Subgroup	No. patients	Median (months)	Univariate analysis		Multivariable analysis		Median (months)	Univariate analysis		Multivariable analysis	
				HR (95% CI)	*P*-value	HR (95% CI)	*P*-value		HR (95% CI)	*P*-value	HR (95% CI)	*P*-value
ctDNA% change following 4 weeks	Undetected → Undetected	21	20.23	ref	ref	ref	ref	Not reached	ref	ref	ref	ref
	Detected → Undetected	12	15.64	1.4 (0.71-2.76)	0.325	1.78 (0.77-4.15)	0.18	27.7	2.17 (1-4.7)	**0.049**	2.46 (0.96-6.3)	0.06
	Detected → Detected	15	4.82	4.79 (2.62-8.77)	**<0.001**	12.03 (4.73-30.57)	**<0.001**	16	5.49 (2.76-10.91)	**<0.001**	7.84 (3.14-19.61)	**<0.001**
NLR		48	NA	1.16 (0.97-1.38)	0.10	1.09 (0.92-1.28)	0.31	NA	1.23 (1.02-1.48)	**0.03**	1.24 (1.05-1.47)	**0.01**

Multivariable analysis with on-treatment ctDNA changes, LDH normalization and PSA30 response. For all variables the changes between baseline and 4-weeks were used. LDH normalization was defined as LDH remaining at normal levels or reducing to normal levels (<=250 U/L (upper limit of normal; ULN)) after 4-weeks of treatment. This included patients with either LDH>ULN or LDH<=ULN at baseline. Patients without LDH normalization had elevated LDH levels at 4-weeks (>ULN). Only 27/81 of patients had elevated LDH at start, with most patients showing only a limited elevation in LDH (250-285 U/L). At 4-weeks, only 13 patients had no LDH normalization, again with most patients only showing a limited elevation in LDH (250-282 U/L). Consequently, results on LDH changes should be treated with caution.

			Progression-free survival					**Overall survival**				
Clinical marker	Subgroup	No. patients	Median (months)	Univariate analysis		Multivariable analysis		Median (months)	Univariate analysis		Multivariable analysis	
				HR (95% CI)	*P*-value	HR (95% CI)	*P*-value		HR (95% CI)	*P*-value	HR (95% CI)	*P*-value
ctDNA% change following 4 weeks	Undetected → Undetected	33	20.23	ref	ref	ref	ref	Not reached	ref	ref	ref	ref
	Detected → Undetected	19	15.64	1.4 (0.71-2.76)	0.33	1.59 (0.77-3.27)	0.21	27.70	2.17 (1-4.7)	**0.049**	2.95 (1.33-6.55)	**0.01**
	Detected → Detected	29	4.82	4.79 (2.62-8.77)	**<0.001**	9.51 (4.61-19.62)	**<0.001**	16.00	5.49 (2.76-10.91)	**<0.001**	8.48 (3.92-18.36)	**<0.001**
LDH normalization following 4 weeks	with LDH normalization	64	15.57	ref	ref	ref	ref	29.44	ref	ref	ref	ref
	without LDH normalization	13	5.02	1.32 (0.68-2.56)	0.41	0.61 (0.29-1.28)	0.19	24.90	1.09 (0.53-2.25)	0.82	0.41 (0.18-0.93)	**0.03**
PSA30 following 4 weeks	PSA30 achieved	57	13.97	ref	ref	ref	ref	27.07	ref	ref	ref	ref
	PSA30 not achieved	24	5.80	1.59 (0.91-2.77)	0.10	2.12 (1.17-3.84)	**0.01**	30.33	1.5 (0.84-2.68)	0.17	1.57 (0.82-3.01)	0.17

Supplementary references

1. Annala M, Taavitsainen S, Khalaf DJ, et al. Evolution of Castration-Resistant Prostate Cancer in ctDNA during Sequential Androgen Receptor Pathway Inhibition. *Clin Cancer Res*. 2021;27(16):4610-4623.
2. Annala M, Vandekerkhove G, Khalaf D, et al. Circulating Tumour DNA Genomics Correlate with Resistance to Abiraterone and Enzalutamide in Prostate Cancer. *Cancer Discov*. 2018;8(4):444-457.
3. Woodhouse R, Li M, Hughes J, et al. Clinical and analytical validation of FoundationOne Liquid CDx, a novel 324-Gene cfDNA-based comprehensive genomic profiling assay for cancers of solid tumor origin. *PLoS One*. 2020;15(9):e0237802.Tukachinsky H, Madison RW, Chung JH, et al. Genomic Analysis of Circulating Tumor DNA in 3,334 Patients with Advanced Prostate Cancer Identifies Targetable BRCA Alterations and AR Resistance Mechanisms. *Clin Cancer Res*. 2021;27(11):3094-3105.Vandekerkhove G, Lavoie JM, Annala M, et al. Plasma ctDNA is a tumour tissue surrogate and enables clinical-genomic stratification of metastatic bladder cancer. *Nat Commun*. 2021;12(1):184.
4. Cancer Genome Atlas Research Network. The Molecular Taxonomy of Primary Prostate Cancer. Cell. 2015;163(4):1011-1025.
5. Stopsack KH, Nandakumar S, Wibmer AG, et al. Oncogenic Genomic Alterations, Clinical Phenotypes, and Outcomes in Metastatic Castration-Sensitive Prostate Cancer. *Clin Cancer Res*. 2020;26(13):3230-3238.
6. Abida W, Cyrta J, Heller G, et al. Genomic correlates of clinical outcome in advanced prostate cancer. *Proc Natl Acad Sci U S A*. 2019;116(23):11428-11436.

Chapter 4

Early on-treatment circulating tumor DNA measurements and response to immune checkpoint inhibitors in advanced urothelial cancer

Sofie H. Tolmeijer
Sandra van Wilpe
Maartje J. Geerlings
Daniel von Rhein
Tineke J. Smilde
Iris S.H. Kloots
Harm Westdorp
Mustafa Coskuntürk
Irma M. Oving
Jolique A. van Ipenburg
Antoine G. van der Heijden
Tom Hofste
Marjan M. Weiss
Jack A. Schalken
Winald R. Gerritsen
Marjolijn J.L. Ligtenberg
Niven Mehra

Adjusted version published in European Urology Oncology 2023 Sep; doi: 10.1016/j.euo.2023.08.009

Abstract

Background: Immune checkpoint inhibitors (ICI) can induce durable disease control in metastatic urothelial cancer (mUC), but only 20-25% of patients respond. Early identification of a nondurable response will improve management strategies.

Objective: To investigate whether on-treatment circulating tumor DNA (ctDNA) measurements can predict ICI responsiveness in mUC patients.

Design, setting, and participants: This study consists of a retrospective discovery cohort of 40 mUC patients and a prospective multicenter validation cohort of 16 mUC patients. Plasma cell-free DNA was collected at baseline and after 3- and 6-weeks on ICI. The ctDNA levels were calculated from targeted sequencing.

Outcome measurements and statistical analysis: Outcome measurements were progression-free survival (PFS), overall survival (OS), and nondurable response (PFS≤6 months). Relationships with ctDNA were assessed using Cox regression. Changes in ctDNA level at 3- and 6-weeks were categorized by an increase or decrease relative to baseline.

Results and limitations: In the discovery cohort, ctDNA was detected in 37/40 (93%) of patients at baseline. 12/15 (80%) and 10/12 (83%) patients with nondurable response showed an increase in ctDNA at 3-weeks and 6-weeks, respectively. 94% of patients with a durable response (PFS>6 months) showed a decrease. A ctDNA increase at 3-weeks was associated with a shorter PFS (HR 7.8, 95%CI 3.1-19.5) and OS (HR 8.0, 95%CI 3.0-21.0), independent of clinical prognostic variables. Similar results were observed at 6-weeks. 3-week associations with PFS were validated in a prospective cohort (HR 7.5, 95%CI 1.3-42.6). Limitations include the limited number of patients.

Conclusions: Early changes in ctDNA levels are strongly linked to duration of ICI benefit in mUC and may contribute to timely therapy modifications.

Patient summary: Benefit from immunotherapy can be predicted after only 3 weeks of treatment by investigating cancer DNA in blood. This could help timely therapy changes for urothelial cancer patients with limited benefit from immunotherapy.

Introduction

Approximately 25% of all patients with urothelial carcinoma (UC) are diagnosed at an advanced disease stage [1]. Palliative treatment options for locally advanced or metastatic disease include platinum-based chemotherapy and immune checkpoint inhibitors (ICI). ICI are used as first or second-line treatment or as maintenance therapy after chemotherapy [1, 2]. While ICI can induce durable disease control, the objective response rate for ICI in the first or second-line is only 20-25% [3-5]. With recent approval of enfortumab vedotin (an antibody-drug conjugate; ADC) in third-line and other therapeutic strategies (e.g. FGFR inhibitors) being investigated, there is an unmet need for (non-invasive) biomarkers to identify nondurable response to ICI. For ICI, predictive biomarkers of interest include PD-L1 expression, tumor mutational burden (TMB) and immune cell infiltrate, but no assay has been shown to be sufficiently sensitive and specific to be implemented in the clinic [6].

Besides predictive baseline biomarkers, early response biomarkers may also have clinical utility, facilitating an early switch to subsequent treatment lines. Previous studies have shown the utility of circulating tumor DNA (ctDNA) to characterize advanced UC [7-12] and the potential of serial ctDNA measurements to monitor therapy response [9, 12-14]. Utilizing a retrospective discovery cohort and a prospective validation cohort, this study aims to evaluate the use of early on-treatment ctDNA measurements (at 3 and 6 weeks) to identify nondurable response to ICI.

Patients and methods

Patients and samples

In both the discovery and validation cohort, patients with advanced UC were enrolled who started ICI (pembrolizumab or nivolumab) for the first time. Either 200mg pembrolizumab was given every 3 weeks intravenously or 240mg nivolumab was given every 2 weeks intravenously. The discovery cohort consisted of 40 patients initiating treatment between March 2017 and July 2020. Blood samples were collected in EDTA tubes at baseline and after 3 and 6 weeks of ICI. Sample processing was performed within 4 hours (Supplementary methods). Additionally, sequencing data of tumor tissue was available or generated for 36/40 patients, using different sequencing platforms (Supplementary methods). For the validation cohort, 16 patients with advanced UC were prospectively enrolled in a multicenter biomarker study in the Netherlands between November 2020 and August 2022. Blood samples were collected in cell-stabilizing collection tubes (Roche) at baseline and after 3 weeks of ICI and processed within 5 days (Supplementary methods).

The study was conducted in accordance with Good Clinical Practice guidelines and the Declaration of Helsinki and approved by the local medical ethical committee (dossier number NL60249.091.16 and local registration 2020-6778). Written consent was obtained from all patients.

CtDNA analysis

A median of 5.3 mL plasma (IQR 4.9-5.6 mL) was used for cell-free DNA (cfDNA) isolations. Afterwards, a median of 50ng cfDNA (IQR 30.6-50 ng) and 50ng sheared white blood cell DNA was used for the library preparation and targeted sequencing using an in-house developed and validated next-generation sequencing test [15]. Technical details on sequencing, the identification of somatic variants and copy number alterations, and the estimation of ctDNA levels are described in the Supplementary methods.

Outcome measurements and statistical analyses

On-treatment ctDNA response was assessed by comparing baseline ctDNA level (copies/mL plasma) with 3- and 6-weeks levels and categorizing the changes into three scenarios: (1) any increase after 3/6-weeks of treatment, (2) any decrease at 3/6-weeks of treatment or (3) undetected ctDNA at baseline and follow-up. We chose to evaluate ctDNA change by absolute ctDNA levels (ctDNA copies/mL plasma) rather than relative ctDNA fractions, as we expected total cfDNA to be influenced by ICI-induced T-cell activation or other immune-mediated inflammatory processes impacting ctDNA fractions. Kaplan-Meier survival estimates and Cox proportional hazard models were used to assess the association between changes in ctDNA quantity and clinical outcomes: (1) progression-free survival (PFS; defined as the time from commencing ICI to cancer-related clinical progression according to the treating physician; radiographic progression; or cancer related death), and (2) overall survival (OS; defined as the time from commencing ICI to death from any cause). The independent utility of ctDNA change to predict PFS and OS was assessed using a multivariable Cox proportional hazard model, which included prognostic variables significantly associated with PFS or OS in a univariate analysis. Nondurable response was defined as disease progression within 6 months of treatment [16]. Statistical significance was defined as $P<0.05$ and all statistical tests were two-sided. Statistical analyses were carried out using R v.4.1.3 using the survival and survminer packages. The sample size calculation of the validation cohort was performed using the powerSurvEpi package.

Results

Patient characteristics

In total, 40 patients were enrolled in the discovery cohort and 16 patients in the validation cohort. Baseline patient characteristics are presented in Table 1. At time of analysis, the median follow-up of the discovery cohort was 23.8 months (IQR 4.9-50.7 months) with 30 (75%) patients experiencing disease progression and 27 (68%) deaths. The median follow-up of the validation cohort was 7.9 months (IQR 5.2-11.6 months) with 10 (63%) patients experiencing progression and 6 (38%) deaths.

CtDNA profiling and quantification in the discovery cohort

In the discovery cohort, all patients had plasma available at baseline and 36 patients had tumor tissue available. Following initiation of ICI, 33 had plasma available at 3-weeks and 25 had plasma drawn at 6-weeks (Figure 1A). 37/40 (92%) patients had detected ctDNA at baseline with a median ctDNA fraction of 3.1% (IQR 0.7-19.4%). Across the 36 tissue samples, 130 somatic mutations were identified within the region of interest of the ctDNA panel. 111/130 (85%) were also detected in baseline plasma. The concordance between tissue and ctDNA was best for patients with a short sampling time between tissue and plasma (<6 months vs >6 months; 79% vs 48%, $P<0.001$, chi-square test, Supplementary Figure S1). Genomic alterations identified in ctDNA were consistent with previous cohorts of metastatic tissue biopsies of mUC patients (Supplementary Figure S2) [17].

No difference was observed among the median ctDNA fractions at baseline, 3- and 6-week on-treatment (3.1% vs 2.1% vs 2.5%; $P=0.3$; Kruskal Wallis test; Figure 1B, Supplementary Table S1). However, in comparison to baseline an increasing proportion of patients had undetected ctDNA at 3- and 6-weeks (8% vs 21% vs 40%; $P=0.001$, chi-square test). The three patients in whom ctDNA was undetected at baseline and during follow-up were excluded from further analyses as changes in ctDNA levels could not be assessed.

Table 1: Baseline patient characteristics discovery and validation cohort

Patient characteristics at baseline	Discovery cohort (n=40)	Validation cohort (n=16)
Age at baseline (median years; IQR)	69 (58-75)	62 (70-77)
Sex (n; %)		
Male	32 (80%)	13 (81%)
Female	8 (20%)	3 (19%)
Upper tract (n; %)		
Yes	7 (17.5%)	4 (25%)
No	29 (72.5%)	12 (75%)
Unknown	4 (10%)	0 (0%)
Initial histology (n; %)		
Pure urothelial	32 (80%)	16 (100%)
Urothelial dominant with variant	5 (12.5%)	0 (0%)
Unknown	3 (7.5%)	0 (0%)
Metastatic at diagnosis (n; %)	7 (17.5%)	4 (25%)
Immunotherapy (n; %)		
Pembrolizumab	33 (82.5%)	16 (100%)
Nivolumab	7 (17.5%)	0 (0%)
Systemic treatment before immunotherapy in mUC* (n; %)		
None	9 (22.5%)	6 (37.5%)
Gemcitabin/carboplatin	14 (35%)	5 (31%)
Gemcitabin/cisplatin	14 (35%)	3 (19%)
MVAC, dose dense	2 (5%)	1 (6%)
Other	1 (2.5%)	1 (6%)
ECOG performance status (n; %)		
0	5 (12.5%)	2 (12.5%)
1	25 (62.5%)	10 (62.5%)
2	10 (25%)	3 (19%)
Unknown	0 (0%)	1 (6%)
Spread of metastasis (at baseline) (n; %)		
Lymph node only	8 (20%)	3 (19%)
Lymph node and locally advanced	4 (10%)	5 (31%)
Bone ± locally advanced, lymph node	4 (10%)	2 (12.5%)
Soft tissue ± locally advanced, lymph node	4 (10%)	0 (0%)
Visceral (incl. liver) ± locally advanced, lymph node, bone	10 (25%)	4 (25%)
Visceral (excl. liver) ± locally advanced, lymph node, bone	8 (20%)	2 (12.5%)
Other sites**	2 (5%)	0 (0%)
Tumor mutational burden (non-synonymous mutations/Mb) (n; %)		
<10	21 (52.5%)	3 (19%)
>10	12 (30%)	0 (0%)
Unknown	7 (17.5%)	13 (81%)
PD-L1 positive tumor cells (%) (n; %)		
<10%	6 (15%)	7 (44%)
>10%	6 (15%)	5 (31%)
Unknown	28 (70%)	4 (25%)

*Two patients switched therapy type due to toxicity. Only the main received therapy is included in the table. **mesenteric and peritoneal metastasis.

Changes in on-treatment ctDNA level and response at 6 months

The main aim of this study was to evaluate the relationship between early on-treatment changes in ctDNA levels and nondurable response defined as PFS≤6months. 18/37 patients experienced disease progression within 6 months (Figure 2A). 15/18 patients had a sample at 3-weeks for which 12/15 (80%) showed an increase in ctDNA levels (Figure 2B). At 6-weeks, 12/18 patients had a plasma sample and 10/12 (83%) showed an increase in ctDNA levels (Figure 2C). Of the 18 patients with a durable response, 15 patients had a 3-week plasma sample and 12 patients a 6-week plasma sample. 94% of the 18 patients with a durable response to immunotherapy had a decrease in ctDNA (Figure 2B). The only patient with a rise in ctDNA had a 3-fold increase in total cfDNA after an infection and persistent fever for which the patient was hospitalized. At 6-weeks, the ctDNA level of this patients was reduced compared to the 3-week plasma sample (Figure 2B-C). The positive predictive value (PPV) of 3- and 6-weeks ctDNA change for identifying nondurable response was 92% and 91%, respectively. The negative predictive value (NPV) was 82% and 85%, respectively.

Changes in on-treatment ctDNA level and treatment outcomes

In total, 13 patients showed an increase in ctDNA level at 3-weeks and 18 patients a decrease. These groups showed no difference in median baseline ctDNA fractions (8.5% vs 10.9%, P=1, Wilcoxon rank test, Supplementary Figure S3). An increase in ctDNA level at 3-weeks was associated with a shorter PFS and OS compared to a decrease in ctDNA (median PFS 1.5 vs 34.1 months, HR 7.8, 95%CI 3.1-19.5, P<0.001, univariate; Figure 3A; median OS 2.6 vs 58.0 months, HR 8.0, 95%CI 3.0-21.0, P<0.001, univariate, Figure 3B). Similarly, an increase in ctDNA level at 6-weeks was associated with a shorter PFS and OS (median PFS 1.9 vs 25.7 months, HR 5.4, 95%CI 2.0-14.3, P<0.001, univariate; Figure 3C; median OS 5.3 vs 53.0 months, HR 4.5, 95%CI 1.7-12.2, P=0.003, univariate, Figure 3D).

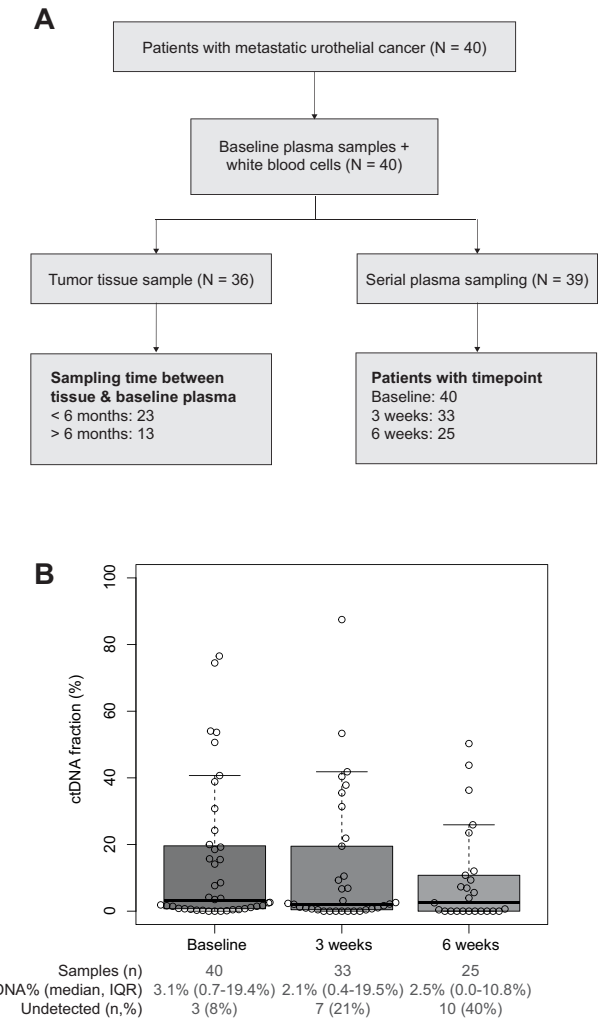

Figure 1: Discovery cohort sample summary and on-treatment circulating tumor DNA (ctDNA) fractions. (A) CONSORT diagram illustrating the available samples per patients for the ctDNA analysis. (B) Boxplot showing the ctDNA fractions at baseline, 3-weeks after immune checkpoint inhibitor (ICI) start and 6-weeks after ICI start. Abbreviations: IQR, inter quartile range.

No association was observed for baseline ctDNA fraction and PFS and OS in the discovery cohort (Supplementary Table S2, Supplementary Figure S4). Although patients with undetected ctDNA at baseline and follow-up samples were excluded from the main analysis, their outcomes are shown in Supplementary Figure S5. As most patients had a 3-week sample and this is the earliest available timepoint to evaluate response, we performed a multivariate analysis for 3-week on-treatment ctDNA change

and other clinical variables significantly associated with outcome in the univariate analysis, which were TMB status and the presence of liver metastasis (Supplementary Table S2). 3-week on-treatment ctDNA change was independently associated with both PFS and OS (Table 2).

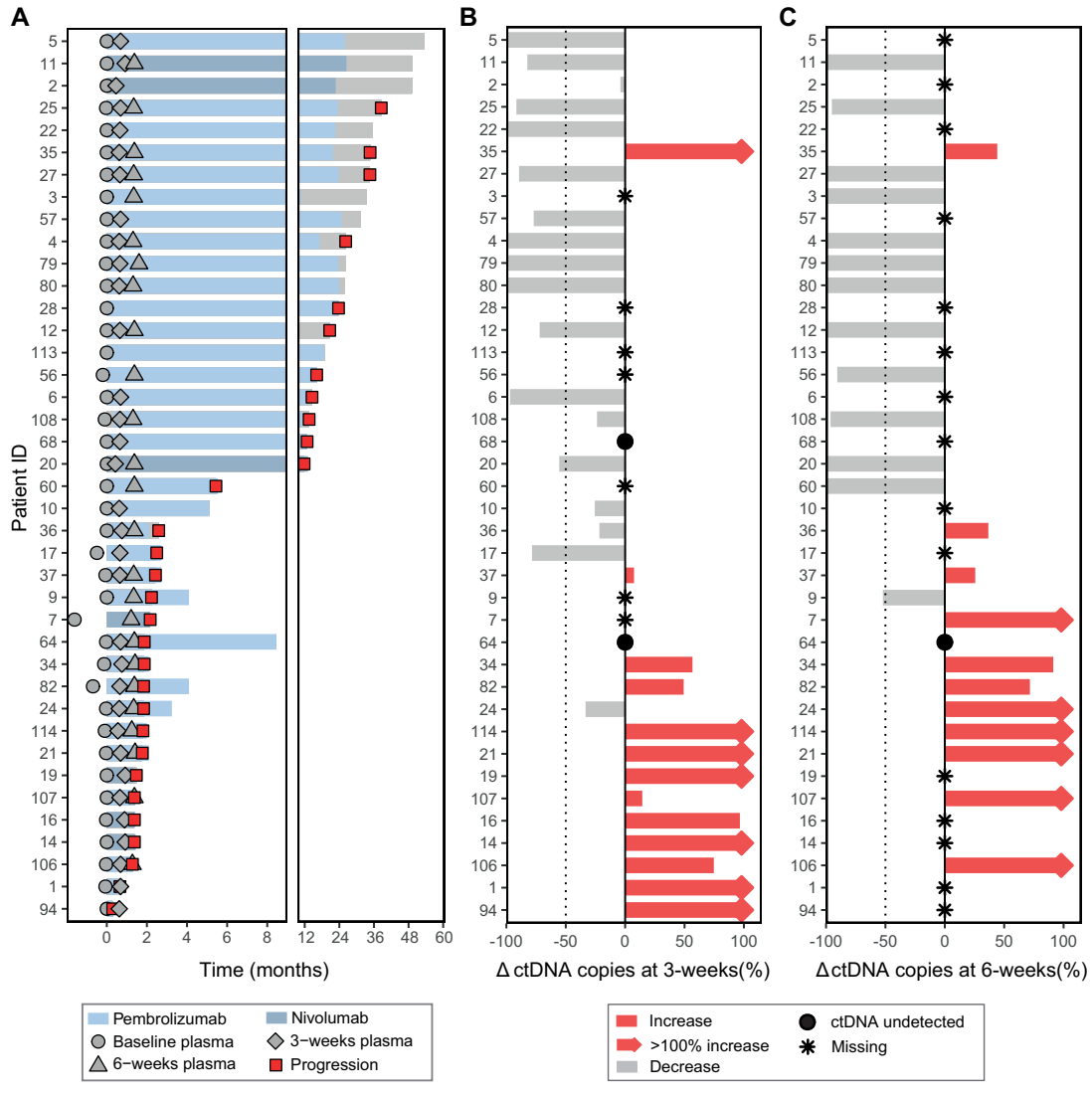

Figure 2: Change in on-treatment circulating tumor DNA (ctDNA) quantity and the durability of response to immune checkpoint inhibitor (ICI). (A) Swimmer plot illustrating the time on ICI and time to progression for the 40 patients in the discovery cohort. The change in the ctDNA level (copies/mL plasma) (B) from baseline to 3-weeks and (C) from baseline to 6-weeks on-treatment. Red bars indicate patients with an increase in ctDNA level. Arrows indicate ctDNA increase greater than 100%.

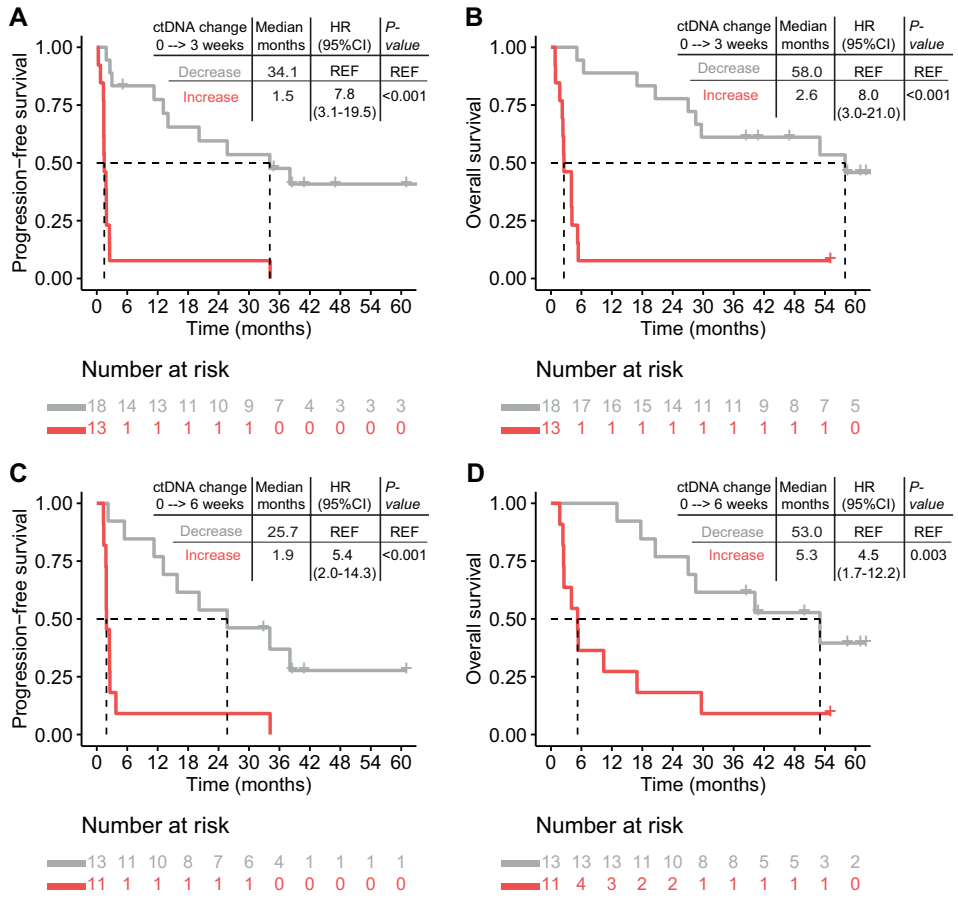

Figure 3: Relationship between change in on-treatment ctDNA level and progression-free survival (PFS) or overall survival (OS). (A) PFS and (B) OS for patients with an increase in ctDNA level from baseline to 3-weeks following initiation of immune checkpoint inhibitors (ICI) compared to patients with a decrease in ctDNA level at 3-weeks. (C) PFS and (D) OS for patients with an increase in ctDNA level from baseline to 6-weeks of ICI compared to patients with a decrease in ctDNA level at 6-weeks.

Table 2: Univariate and multivariate analysis for 3-week on-treatment circulating tumor DNA change and progression-free survival and overall-survival

			Progression-free survival					Overall survival				
				Univariate analysis		Multivariate analysis			Univariate analysis		Multivariate analysis	
Variable	Category	N	Median months	HR (95% CI)	*P*-value	HR (95% CI)	*P*-value	Median months	HR (95% CI)	*P*-value	HR (95% CI)	*P*-value
Liver metastasis	Absent	30	15.8	REF	REF	REF	REF	34.4	REF	REF	REF	REF
	Present	10	1.9	4.0 (1.8-8.8)	<0.001	1.1 (0.2-3.5)	0.9	4.8	3.0 (1.3-6.9)	0.008	0.5 (0.1-2.4)	0.4
TMB	High	12	34.2	REF	REF	REF	REF	NR	REF	REF	REF	REF
	Low	21	2.2	3.1 (1.2-7.8)	0.02	3.1 (0.9-10.4)	0.06	6.4	3.0 (1.1-8.1)	0.04	4.7 (1.2-19.3)	0.03
3-week ctDNA	Decrease	18	34.1	REF	REF	REF	REF	58.0	REF	REF	REF	REF
	Increase	13	1.5	7.8 (3.1-19.5)	<0.001	10.3 (2.2-47.4)	0.003	2.6	8.0 (3.0-21.0)	<0.001	16.2 (2.8-93.7)	0.002

On-treatment ctDNA changes in the validation cohort

To validate our results, a prospective multicenter validation cohort was recruited. As it appeared feasible to identify patients lacking benefit from immunotherapy as early as 3-weeks after treatment initiation, we focused on validating the clinical utility of 3-week on-treatment ctDNA changes compared to baseline. Assuming that 30% of patients would show an increase in ctDNA and 65% of patients would experience progression during follow-up, 14 patients were determined sufficient to provide 80% power at 5% significance level to detect a HR of 7.8 for PFS. In total, 16 patients were enrolled in the validation study of whom 14/16 (88%) had detected ctDNA at baseline. A high baseline ctDNA fraction was associated with a shorter PFS (Supplementary Figure S3). Nine patients developed progression before 6 months of ICI (Figure 4A), of whom four (44%) had an increase in ctDNA level at 3-weeks (Figure 4B). None of the patients with a response to immunotherapy beyond 6 months had an increase in ctDNA level at 3-weeks. The PPV and NPV of ctDNA change at 3-weeks for identifying nondurable response was 100% and 50%, respectively. Similar to the discovery cohort, an increase in ctDNA level at 3-weeks was associated with a shorter PFS (median PFS 2.0 vs 6.3, HR 7.5, 95%CI 1.3-42.6, P=0.02; univariate; Figure 4C). Associations with OS were not assessed due to the short follow-up.

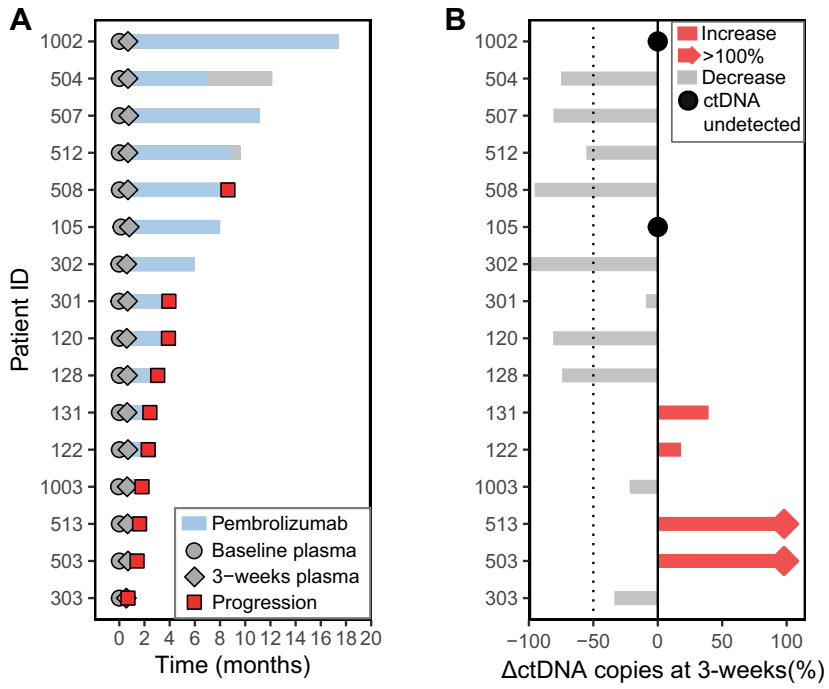

Figure 4 (left page): Relationship between change in on-treatment circulating tumor DNA (ctDNA) level and response to immune checkpoint inhibitors (ICI) in the validation cohort. (A) Swimmer plot illustrating the time on ICI and time to progression for the 16 patients in the validation cohort. (B) The change in the ctDNA level (copies/mL plasma) from baseline to 3-weeks. Red bars indicate patients with an increase in ctDNA level. Arrows indicate ctDNA increase greater than 100%. (C) Progression-free survival (PFS) for patients with an increase in ctDNA level from baseline to 3-weeks of ICI compared to patients with a decrease in ctDNA at 3-weeks.

Discussion

This study suggests that an early on-treatment increase in ctDNA level is a reliable indication of a nondurable response to immunotherapy in patients with advanced UC. Using a discovery and validation cohort, we show that an increase in ctDNA copies as early as 3 weeks on ICI is predictive of nondurable response and can be informative for timely therapy modifications. In contrast, a decrease in ctDNA level during ICI could indicate response and motivate treatment continuation in patients with equivocal clinical or inconclusive radiographic responses.

Current evaluation of ICI response in mUC is limited to radiographic imaging with a first assessment after 8-12 weeks of treatment and requiring confirmation of progression by additional imaging in the absence of unequivocal clinical progression [18]. In addition, RECIST1.1 non-measurable disease also hampers accurate response evaluation in mUC. Blood draws for ctDNA analysis are easy to perform and enable repetitive measurements. Like previous studies [7-11], we observe a high concordance between mutations in tumor tissue and ctDNA. In contrast to previous literature [7, 9, 10, 12], baseline ctDNA fractions were not associated with PFS and OS in our discovery cohort while an association with PFS was observed in the validation cohort. Interestingly, an increase in ctDNA level at 3-weeks was strongly associated with poor outcome in both cohorts indicating that early on-treatment changes in ctDNA level is a more robust marker for response compared to baseline ctDNA level alone. The prognostic value of undetected ctDNA throughout ICI could not be addressed in this study due to the limited number of patients (Discovery n=3, Validation n=2).

Comparable associations between on-treatment ctDNA changes and outcome were observed by Raja et al. [14] in a cohort of 28 mUC patients treated with ICI. Raja et al. [14] reported an increase in ctDNA fraction at 6-weeks in 7/28 (25%) patients. The median PFS for these patients was 1.6 months, which is similar to our results showing a median PFS of 1.5 months (discovery) and 2.0 months (validation) for patients with a 3-week ctDNA increase and 1.9 months for patients with a 6-week increase. In the adjuvant setting, Powles et al. [19] reported a worse OS for patients with resected UC showing a conversion from undetected to detected ctDNA or persistent

ctDNA detection during adjuvant ICI compared to patients with undetected ctDNA after 6-weeks of adjuvant treatment (HR 6.0). Importantly, an on-treatment ctDNA increase has also been associated with fast progression on other therapies for mUC (chemotherapy, FGFR inhibitors and ADC) [9, 12], suggesting that on-treatment ctDNA measurements can predict treatment response in the context of different disease stages and classes of systemic therapy.

To allow for ctDNA-based therapy modifications in patients with a nondurable response, a high PPV is necessary. In line with others [12, 14], we categorized on-treatment change by any increase or decrease in ctDNA level compared to baseline. Others used a threshold of 50% reduction in ctDNA level [20, 21]. In the discovery cohort the PPV for predicting nondurable response with less than 50% reduction of ctDNA level at 3-weeks was lower compared to the PPV for ctDNA increase (82% vs 92%). Therefore, ctDNA increase seems a more rigorous identifier for nondurable responses. Notably, only one patient with a durable response showed an increase in ctDNA level, which was most likely due to sepsis after replacement of a nephrostomy catheter associated with a large increase in cfDNA level [22]. Confirmation of ctDNA changes with a second measurement could improve the already high PPV and boost the NPV for identifying nondurable response, especially for patients with small changes in ctDNA level or circumstances potentially affecting ctDNA measurements.

Limitations of this study include the small cohort sizes, missing data, and the single center nature of the discovery cohort. Nevertheless, to our knowledge this is the largest study investigating early on-treatment ctDNA changes during immunotherapy in mUC, showing a strong relationship between 3- and 6-weeks on-treatment changes in ctDNA level and patient outcome. Key strengths of this study include the measurements of multiple on-treatment plasma samples, evaluations as early as 3-weeks and the validation of the retrospective results in a prospective multicenter study.

Conclusion

An increase in ctDNA after 3 and 6 weeks of immunotherapy is strongly associated with a lack in response to immunotherapy and shorter survival of patients with mUC. Early ctDNA monitoring may contribute to timely therapy modification in patients who are unlikely to respond durably to immunotherapy.

References

1. Kamat, A.M., et al., Bladder cancer. The Lancet, 2016. 388(10061): p. 2796-2810.
2. Cathomas, R., et al., The 2021 Updated European Association of Urology Guidelines on Metastatic Urothelial Carcinoma. Eur Urol, 2022. 81(1): p. 95-103.
3. Powles, T., et al., Atezolizumab versus chemotherapy in patients with platinum-treated locally advanced or metastatic urothelial carcinoma (IMvigor211): a multicentre, open-label, phase 3 randomised controlled trial. 2017(1474-547X (Electronic)).
4. Bellmunt, J., et al., Pembrolizumab as Second-Line Therapy for Advanced Urothelial Carcinoma. 2017(1533-4406 (Electronic)).
5. Balar, A.V., et al., First-line pembrolizumab in cisplatin-ineligible patients with locally advanced and unresectable or metastatic urothelial cancer (KEYNOTE-052): a multicentre, single-arm, phase 2 study. Lancet Oncol, 2017. 18(11): p. 1483-1492.
6. Aggen, D.H. and C.G. Drake, Biomarkers for immunotherapy in bladder cancer: a moving target. J Immunother Cancer, 2017. 5(1): p. 94.
7. Vandekerkhove, G., et al., Plasma ctDNA is a tumor tissue surrogate and enables clinical-genomic stratification of metastatic bladder cancer. Nat Commun, 2021. 12(1): p. 184.
8. Vandekerkhove, G., et al., Circulating Tumor DNA Reveals Clinically Actionable Somatic Genome of Metastatic Bladder Cancer. Clin Cancer Res, 2017. 23(21): p. 6487-6497.
9. Powles, T., et al., An adaptive, biomarker-directed platform study of durvalumab in combination with targeted therapies in advanced urothelial cancer. Nat Med, 2021. 27(5): p. 793-801.
10. Chalfin, H.J., et al., Circulating Tumor Cell and Circulating Tumor DNA Assays Reveal Complementary Information for Patients with Metastatic Urothelial Cancer. Eur Urol Oncol, 2021. 4(2): p. 310-314.
11. Agarwal, N., et al., Characterization of metastatic urothelial carcinoma via comprehensive genomic profiling of circulating tumor DNA. Cancer, 2018. 124(10): p. 2115-2124.
12. Shohdy, K.S., et al., Serial ctDNA analysis predicts clinical progression in patients with advanced urothelial carcinoma. Br J Cancer, 2022. 126(3): p. 430-439.
13. Sundahl, N., et al., Randomized Phase 1 Trial of Pembrolizumab with Sequential Versus Concomitant Stereotactic Body Radiotherapy in Metastatic Urothelial Carcinoma. Eur Urol, 2019. 75(5): p. 707-711.
14. Raja, R., et al., Early Reduction in ctDNA Predicts Survival in Patients with Lung and Bladder Cancer Treated with Durvalumab. Clin Cancer Res, 2018. 24(24): p. 6212-6222.
15. Radboudumc. Next-Generation sequencing voor ctDNA; Genenpanel ctDNA_NGSv1. 2022 3-3-2023; 31-8-2022:[Available from: https://www.palga.nl/datasheet/Radboudumc/ctDNA_NGSv1.pdf.

16. Kluger, H.M., et al., Defining tumor resistance to PD-1 pathway blockade: recommendations from the first meeting of the SITC Immunotherapy Resistance Taskforce. J Immunother Cancer, 2020. 8(1).
17. Clinton, T.N., et al., Genomic heterogeneity as a barrier to precision oncology in urothelial cancer. Cell Rep, 2022. 41(12): p. 111859.
18. Seymour, L., et al., iRECIST: guidelines for response criteria for use in trials testing immunotherapeutics. Lancet Oncol, 2017. 18(3): p. e143-e152.
19. Powles, T., et al., ctDNA guiding adjuvant immunotherapy in urothelial carcinoma. Nature, 2021. 595(7867): p. 432-437.
20. Zou, W., et al., ctDNA Predicts Overall Survival in Patients With NSCLC Treated With PD-L1 Blockade or With Chemotherapy. JCO Precis Oncol, 2021. 5: p. 827-838.
21. Goldberg, S.B., et al., Early Assessment of Lung Cancer Immunotherapy Response via Circulating Tumor DNA. Clin Cancer Res, 2018. 24(8): p. 1872-1880.
22. Jing, Q., C.H.C. Leung, and A.R. Wu, Cell-Free DNA as Biomarker for Sepsis by Integration of Microbial and Host Information. Clin Chem, 2022. 68(9): p. 1184-1195.

Supplementary Methods

Tumor tissue sequencing

Tumor tissue for molecular analysis was obtained from diagnostic biopsies in routine clinical practice. Sequencing data was readily available or generated utilizing different sequencing platforms: Whole Genome Sequencing at Hartwig Medical Foundation, TruSight Oncology 500 [1], Foundation Medicine T7 assay (CLIA: 22D2027531), single molecule Molecular Inversion Probe panel (PATHv3D) [2] and/or the ctDNA_NGSv1 targeted sequencing panel [3]. The latter panel was also used for circulating tumor DNA (ctDNA) measurements in this manuscript and further described below.

Blood collection

For the discovery cohort, blood was collected in EDTA tubes. Within 4 hours, the blood was centrifuged 20 min at 120g to separate plasma from blood cells. Afterwards, the plasma was centrifuged 20 min at 360g to remove platelets and 10 min at 14000g to remove cellular debris. The white blood cells (WBC) were separately stored. For the validation cohort, blood was collected in cell-stabilizing collection tubes (Roche). Within five days, samples were processed using two centrifugation steps; 10 min at 1600g to separate plasma from blood cells and 10 min at 16000g to remove cellular debris. The WBC from the buffycoat were separately stored. WBC were used to identify germline and clonal hematopoietic variants.

DNA isolation from plasma, white blood cells and tumor tissue

Cell-free DNA (cfDNA) was isolated from plasma using a QIAamp Circulating Nucleic Acid kit (Qiagen) according to the manufacturers protocol and DNA was eluted in 40µL low-TE buffer. DNA concentrations were measured using a Qubit High Sensitivity dsDNA kit (Thermo Fisher) and the quality was checked on a Fragment Analyzer (Agilent high sensitivity genomic DNA kit #DNF-488-0500). A median of 50ng cfDNA (IQR 30.6-50 ng) was used for the library preparation and targeted sequencing. For WBC samples, DNA was isolated using a QIAamp DNA Mini Kit (Qiagen) according to the manufacturers protocol. Tumor tissue DNA was isolated from formalin-fixed paraffin-embedded diagnostic biopsies using the Chelex-100 (Bio-Rad) method [4]. WBC and tumor tissue DNA concentrations were measured using a Qubit Broad Range dsDNA kit (Thermo Fisher) and DNA was mechanically fragmented on a Covaris (180 sec, duty 10, intensity 5, 200 cycles). 50ng of sheared WBC DNA or 100ng of sheared tissue DNA was used for library preparation and targeted sequencing.

Targeted sequencing

Plasma ctDNA analysis was performed using an in-house developed and validated (NEN-EN-ISO 15189+C11:2015) [3] NGS test as described by Hofste et al. [5]. In short, libraries were made using the Twist Library Preparation Kit (Twist Biosciences) in combination with xGen dual index unique molecular identifiers (UMI) adaptors (Integrated DNA Technologies) to enable correction for PCR errors and artifacts, and to assess the amount of sequenced template molecules, from which the minimal level of detection can be calculated. Hybrid-capture was executed with a customized probe set (Twist Biosciences) covering 117 kb [3]. Paired-end sequencing was performed on a NovaSeq 6000 (Illumina) using 2 × 150 cycles. Reads were aligned to hg19 and deduplicated using the read specific UMI information (Fgbio version 0.8.1). Unique reads based on one UMI read (singletons) were kept for copy number variant (CNV) detection but discarded for mutation detection to reduce background noise (except for TERT promoter region). The median unique sequencing depth excluding singletons per plasma sample was 4817x (IQR 3441-6430x) and per WBC sample 3128x (IQR 2867-3415).

Somatic mutation detection

Small somatic variants were identified in plasma using Genomic Analysis Toolkit (GATK) Mutect2 (version 4.1.5.0). Mutect2 filters included: 1) a population frequency <1% in the Radboud university medical center inhouse database of >5000 exomes, the ExAC (0.2) database [6], the Gnomad database [7] and the Dutch population database (GoNL) of >750 genomes [8], 2) exclusion of low confidence mutations based on the mutect2 quality filter, 3) exclusion of mutations with exclusively alternative reads on the forward or the reverse strand, and 4) exclusion of variants with <5 supporting alternative reads and a variant allele fraction (VAF) below 0.1%. The minimum of 5 supporting reads reduces false positive variant detection due to background error. As the median coverage for our assay was 4817x depth, 5 variant reads equate to a VAF of ~0.1%. Additionally, the VAF was required to be at least 20 times higher than the average VAF of 22 control cfDNA samples from healthy individuals and 3 times higher than the patient-specific WBC sample. As all patients had two or more plasma samples available, dependent calling was also applied. For dependent calling, at least 3 supporting reads and a VAF of 0.1% were required to call a previously independently detected mutation in a same-patient plasma sample. For tumor tissue samples, a minimum of 10 supporting reads and a VAF of >1% was required to further reduce background error induced by formalin fixation.

Copy-number variant detection

Copy-number variant detection was based on the recommendations described by Eijkelenboom et al. [9]. In short, per sample the mean coverage per probe was divided by the overall median coverage of the sample to obtain a normalized coverage per probe. This normalized coverage was compared to the median normalized coverage of a set of 22 healthy cfDNA samples to obtain the relative coverage per probe of every patient cfDNA sample. This relative coverage is expressed as the log2 ratio between the patient sample and the set of control samples. The median relative coverage was then calculated per gene. Additionally, heterozygous germline SNPs were identified in WBC samples and the corresponding allele fraction of these SNPs was investigated in the cfDNA samples. For each gene, the median allele fraction (MAF) divergence from heterozygosity was then calculated [10]. In line with previous literature [10], copy number loss was defined as relative coverage ≤ −0.3 regardless of MAF or relative coverage ≤ −0.1 and MAF ≥ 0.6. Copy number gain was defined as a relative coverage ≥ 0.3 regardless of MAF or ≥ 0.1 and MAF ≥ 0.6 (Supplementary Figure S6).

Estimation of ctDNA fractions and copies

Estimation of ctDNA fractions were estimated as described by Annala et al. [10]. In short, ctDNA fraction was estimated using (1) the somatic mutation with highest VAF in a non-amplified region corrected for loss of heterozygosity (LOH) and potential outliers using a binomial distribution or (2) using the MAF deviation from heterozygosity of germline SNPs in genes with a single-copy loss. For this last method, the ctDNA estimate could only be calculated when two or more genes had a single-copy loss and within those genes two or more independent SNPs were present to calculate the deviation from heterozygosity. The correlation between both ctDNA estimates, in samples in which both estimations were possible, is visualized in Supplementary Figure S7.

To compare ctDNA level over time, we converted ctDNA fractions (a relative measurement) to ctDNA copies per mL plasma (an absolute measurement). For this, the concentration-units of total cfDNA (ng per mL plasma) were multiplied with 303 under the assumption that a haploid genome is 3.3pg to determine the total cfDNA copies per mL plasma. Subsequently, the ctDNA copies per mL plasma could be calculated using the ctDNA fraction times the total cfDNA copies per mL plasma. Information on cfDNA concentrations and ctDNA estimates per sample are described in Supplementary Table S1.

Supplementary Data

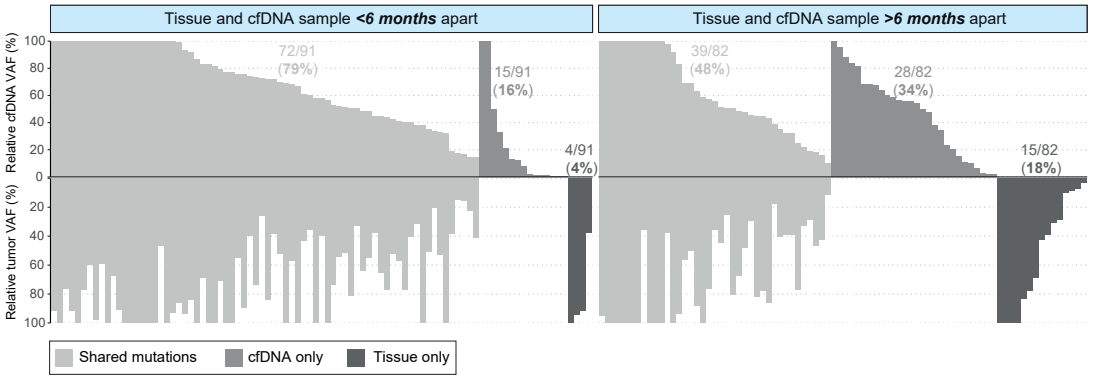

Supplementary Figure S1: Concordance of somatic mutations detected in ctDNA and patient-matched tumor tissue from 36 patients. The figure displays the relative variant allele fraction (VAF; VAF normalized to tumor fraction) per mutation in a baseline plasma sample and tissue.

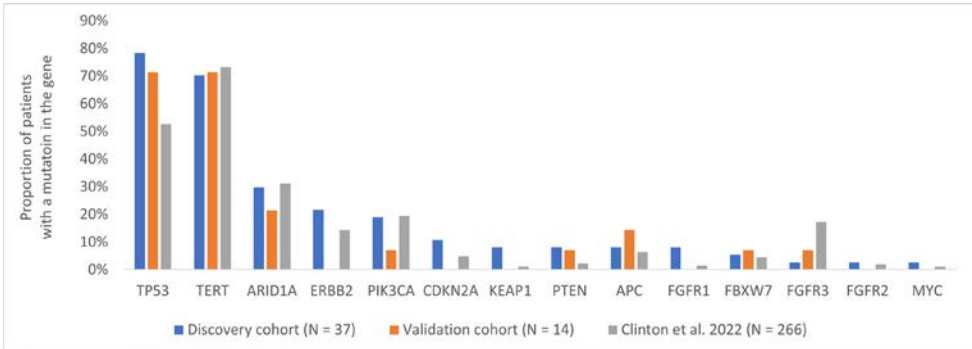

Supplementary Figure S2: Frequency of recurrent somatic alterations compared to published cohorts. Only ctDNA positive samples from the discovery and validation cohort were used for frequency assessment. The frequencies were compared to metastatic tissue samples of patients with urothelial carcinomas described in the cBioportal database [11] from the study of Clinton et al [12]. Only patients with 1 sample were considered to avoid duplicate counts.

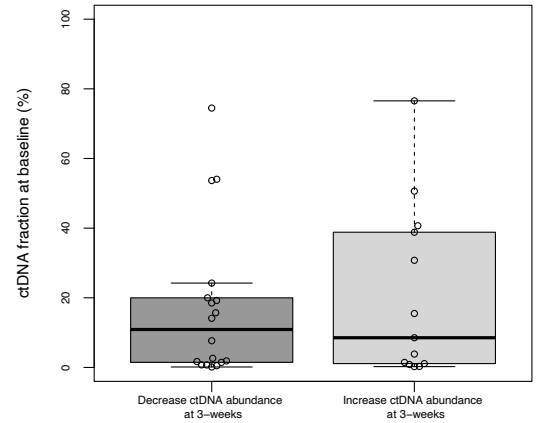

Supplementary Figure S3: Baseline ctDNA fraction in patients with a decrease in ctDNA level at 3-weeks (n = 18) or increase in ctDNA level at 3-weeks (n = 13).

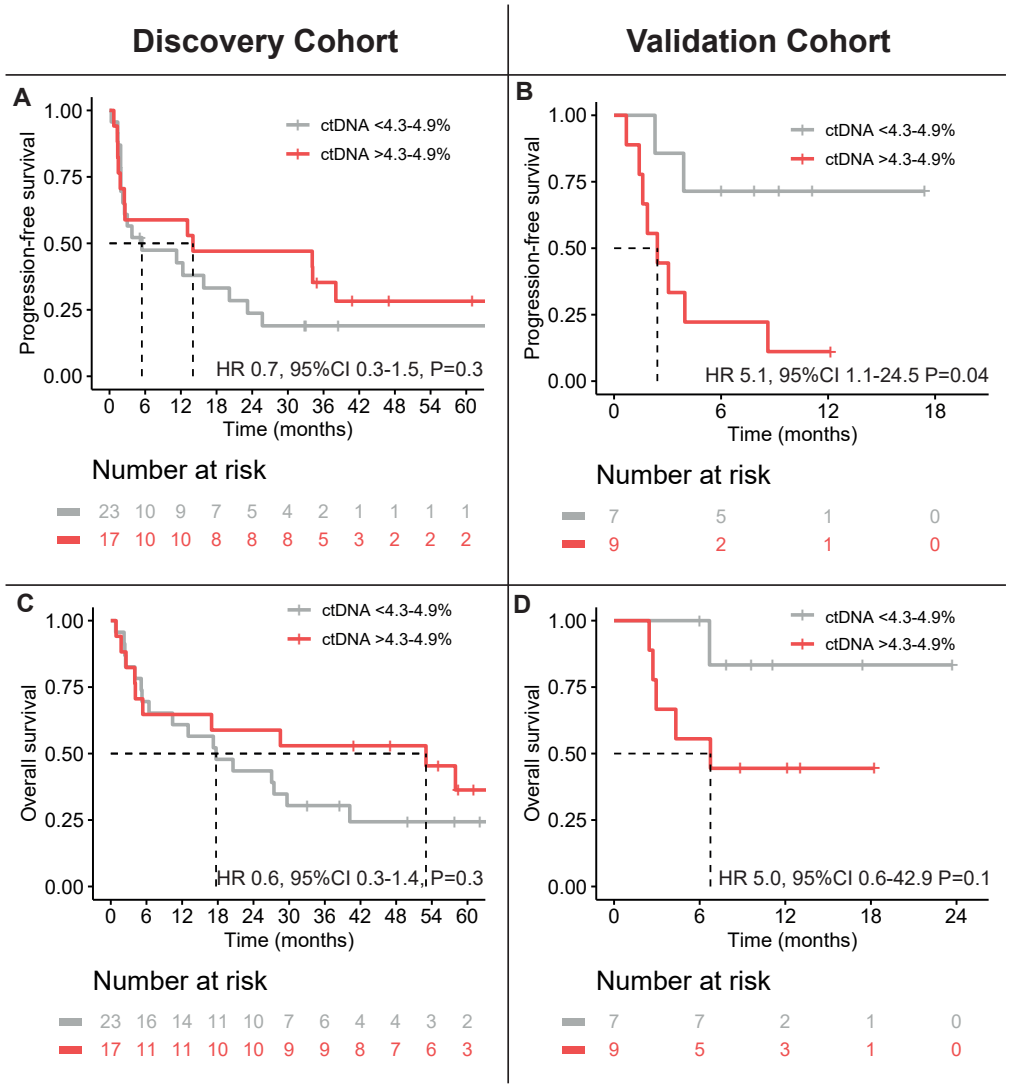

Supplementary Figure S4: Relationship between baseline ctDNA fraction and progression-free survival (PFS) or overall survival (OS). Cut-off of ctDNA was based on literature applying a cut-off of 4.3% and 4.9%, respectively [13, 14]. As no patients had ctDNA between 4.3% and 4.9%, the cut-offs were combined. (A) PFS and (C) OS for patients with ctDNA above or below the cut-off at baseline in the discovery cohort. (B) PFS and (D) OS for patients with ctDNA above or below the cut-off at baseline in the validation cohort. OS data is immature and should be treated with caution.

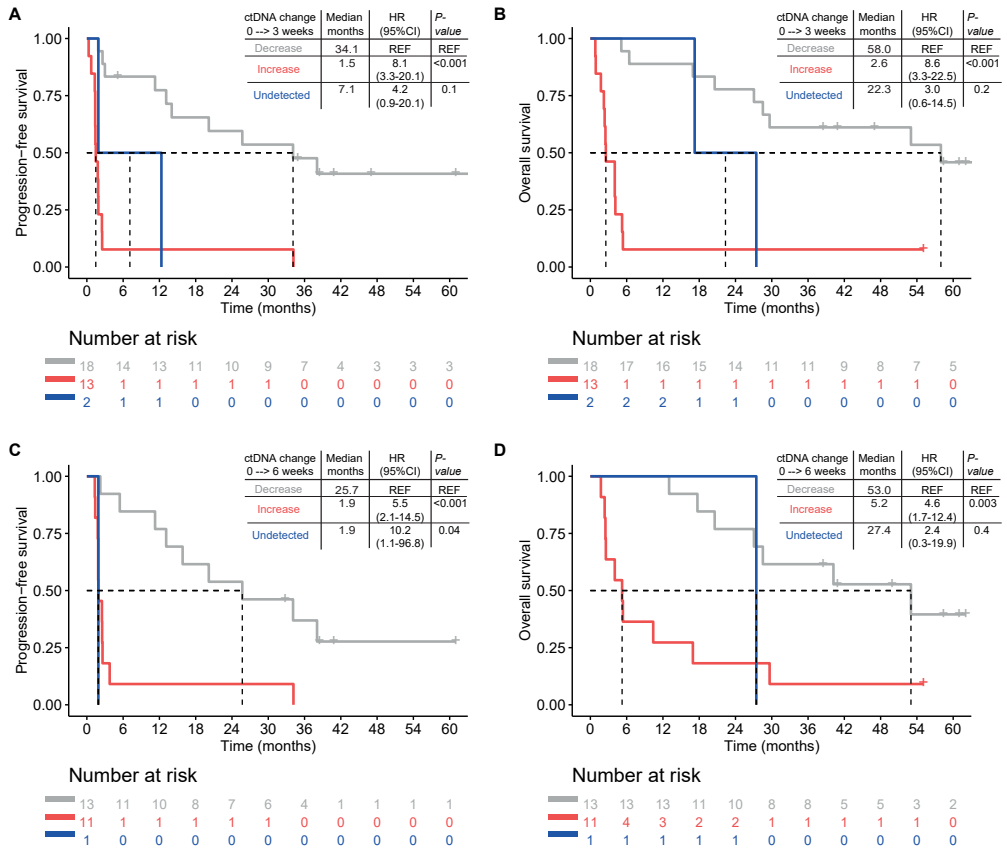

Supplementary Figure S5: Relationship between on-treatment ctDNA level and progression-free survival (PFS) or overall survival (OS). (A) PFS and (B) OS for patients with an increase in ctDNA level from baseline to 3-weeks of immune checkpoint inhibitors (ICIs) compared to patients with a decrease or undetected ctDNA at 3-weeks. (C) PFS and (D) OS for patients with an increase in ctDNA level from baseline to 6-weeks of ICIs compared to patients with a decrease or undetected ctDNA at 6-weeks.

Supplementary Figure S6: The threshold for calling gains and losses based on the relative coverage logratio and heterozygous SNP allele fraction. Scatter plot of observed relative gene coverage and heterozygous SNP allele fraction in patient with detected ctDNA (black), patients with undetected ctDNA (grey) and healthy control samples (green). Each dot represents one targeted gene within the panel in one of the cfDNA samples. The x-axis position indicates the relative coverage and the y-axis the heterozygous SNP allele fraction observed for that gene in that sample. The kernel density plot on the top summarizes the number of dots per coverage logratio and the kernel density plot on the right summarizes the number of dots per SNP allele fraction. Red and blue lines mark the thresholds for copy number loss or gain based on the results depicted in the figure. Consequently, each dot in the red square is classified as a copy number gain, each dot in the blue square is classified as a loss and the rest is classified as copy number neutral.

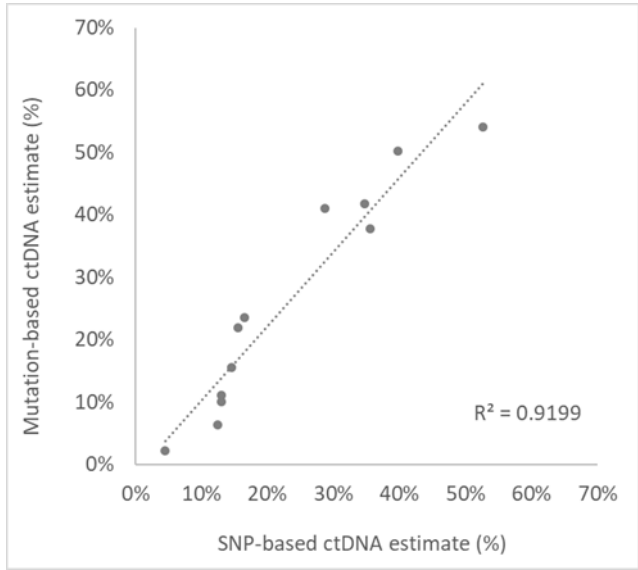

Supplementary Figure S7: Correlation between the mutation-based ctDNA estimate and the SNP-based ctDNA estimate. Every dot represents a patient sample in which both ctDNA estimates could be calculated.

Supplementary Table 1: Evidence for ctDNA estimates per patient per timepoint.

Patient ID	Cohort	Timepoint	Plasma volume for cfDNA isolation (mL)	cfDNA concentration (ng/uL)	cfDNA elution volume (uL)	cfDNA copies/mL plasma	Input for sequencing (ng)	Unique coverage	Limit of detection	ctDNA fraction estimate (%)	ctDNA copies/mL plasma	ctDNA estimate based-on	Mutation type	Alternative reads	Total reads	Variant allele fraction (%)
1	Discovery	T0	4.7	79.20	40	204255.3	50.0	9157	0.0%	76.54%	156346.7	TP53	missense_variant	7476	11918	62.73%
1	Discovery	T3	4.5	436	40	1174410.8	50.0	8376	0.0%	87.5%	1027503.6	SNP-based	NA	NA	NA	NA
2	Discovery	T0	4.4	2.79	40	7686.0	50.0	6127	0.0%	7.66%	589.0	ARID1A	missense_variant	309	7082	4.36%
2	Discovery	T3	5	3.49	40	8460.6	50.0	7710	0.0%	6.68%	565.4	ARID1A	missense_variant	373	9930	3.76%
3	Discovery	T0	5.2	1.26	40	2937.1	44.1	5407	0.1%	2.49%	73.3	ERBB2	missense_variant	105	7106	1.48%
3	Discovery	T6	4.6	9.71	40	25586.3	50.0	5569	0.1%	0.00%	0.0	NA	NA	0	0	0.0%
4	Discovery	T0	4.9	0.77	40	1899.8	26.9	4028	0.1%	0.74%	14.0	TP53	missense_variant	25	4923	0.51%
4	Discovery	T3	5.2	1.44	40	3356.6	50.4	5835	0.1%	0.00%	0.0	NA	NA	0	0	0.0%
4	Discovery	T6	5	1.46	40	3539.4	51.1	5847	0.1%	0.00%	0.0	NA	NA	0	0	0.0%
5	Discovery	T0	5.3	0.85	40	1937.1	29.6	3196	0.1%	0.13%	2.6	TP53	missense_variant	5	3866	0.13%
5	Discovery	T3	4.8	0.673	40	1699.5	23.6	3233	0.1%	0.00%	0.0	NA	NA	0	0	0.0%
6	Discovery	T0	5.5	3.11	40	6854.0	50.0	2622	0.1%	18.51%	1268.5	FGFR1	missense_variant	366	3311	11.05%
6	Discovery	T3	4.6	1.24	40	3267.5	43.4	4696	0.1%	1.22%	39.8	FGFR1	missense_variant	48	6209	0.77%
7	Discovery	T0	4.9	1.43	40	3537.4	50.1	6208	0.0%	1.62%	57.5	TP53	missense_variant	82	8374	0.98%
7	Discovery	T6	4.6	3.21	40	8458.5	50.0	6035	0.0%	25.91%	2191.7	TP53	missense_variant	1264	8139	15.53%
9	Discovery	T0	4.9	1.61	40	3982.7	50.0	5512	0.1%	3.49%	139.2	TERT	upstream_gene_variant	137	6713	2.04%
9	Discovery	T6	5.3	1.16	40	2652.9	40.6	5793	0.1%	2.51%	66.6	TERT	upstream_gene_variant	93	6193	1.50%
10	Discovery	T0	4.5	0.75	40	2014.8	26.2	3775	0.1%	2.62%	52.8	TP53	splice_acceptor_variant	49	2966	1.65%
10	Discovery	T3	4.8	0.668	40	1686.9	23.4	3803	0.1%	2.33%	39.3	TP53	splice_acceptor_variant	39	2564	1.52%
11	Discovery	T0	5.5	0.75	40	1644.1	26.1	1606	0.2%	14.12%	232.2	TP53	frameshift variant	152	1763	8.62%
11	Discovery	T3	5.2	0.822	40	1916.1	28.8	1874	0.2%	2.14%	41.0	TP53	frameshift variant	31	2159	1.44%
11	Discovery	T6	5.6	0.788	40	1705.6	27.6	1500	0.2%	0.00%	0.0	NA	NA	0	0	0.0%

Supplementary Table 1: Continued

Patient ID	Cohort	Timepoint	Plasma volume for cfDNA isolation (mL)	cfDNA concentration (ng/uL)	cfDNA elution volume (uL)	cfDNA copies/mL plasma	Input for sequencing (ng)	Unique coverage	Limit of detection	ctDNA fraction estimate (%)	ctDNA copies/mL plasma	ctDNA estimate based-on	Mutation type	Alternative reads	Total reads	Variant allele fraction (%)
12	Discovery	T0	4.6	0.61	40	1612.6	21.4	1612	0.2%	1.47%	23.7	PIK3CA	missense_variant	20	1907	1.05%
12	Discovery	T3	5.4	0.74	40	1661.1	25.9	2176	0.1%	0.40%	6.6	TP53	stop_gained	9	2709	0.33%
12	Discovery	T6	6	0.726	40	1466.7	25.4	1601	0.2%	0.00%	0.0	NA	NA	0	0	0.0%
14	Discovery	T0	7.3	0.64	40	1054.4	22.2	3189	0.1%	8.53%	89.9	TP53	missense_variant	176	3505	5.02%
14	Discovery	T3	9	2.97	40	4000.0	50.0	6737	0.0%	19.49%	779.8	TP53	missense_variant	841	7383	11.39%
16	Discovery	T0	5	1.94	40	4703.0	50.0	6611	0.0%	0.84%	39.3	ERBB2	missense_variant	40	7387	0.54%
16	Discovery	T3	5.3	4.74	40	10840.5	50.0	8253	0.0%	0.71%	77.3	ARID1A	frameshift variant	12	2147	0.56%
17	Discovery	T0	4.9	5.35	40	13234.4	50.0	7486	0.0%	1.87%	248.0	TP53	splice_acceptor_variant	107	9671	1.11%
17	Discovery	T3	4.9	1.04	40	2572.7	36.4	4691	0.1%	2.08%	53.5	TP53	splice_acceptor_variant	76	6013	1.26%
19	Discovery	T0	5.2	5.38	40	12540.8	50.0	6128	0.0%	50.63%	6349.7	TERT	upstream_gene_variant	3055	8798	34.72%
19	Discovery	T3	5.1	33.6	40	79857.4	50.0	6051	0.0%	53.34%	42594.4	TERT	upstream_gene_variant	2679	7183	37.30%
20	Discovery	T0	4.8	0.76	40	1926.8	26.7	3019	0.1%	0.49%	9.5	ERBB2	missense_variant	14	3755	0.37%
20	Discovery	T3	7.6	0.386	40	615.6	13.5	1985	0.2%	0.68%	4.2	TERT	upstream_gene_variant	9	1581	0.57%
20	Discovery	T6	6.6	1.06	40	1946.7	37.1	2819	0.1%	0.00%	0.0	NA	NA	0	0	0.0%
21	Discovery	T0	5.6	1.95	40	4220.8	50.0	7162	0.0%	30.77%	1298.5	TP53	stop_gained	1875	9967	18.81%
21	Discovery	T3	5.3	3.22	40	7364.2	50.0	7140	0.0%	35.50%	2614.0	TP53	stop_gained	2150	9657	22.26%
21	Discovery	T6	5.4	4.18	40	9382.7	50.0	5710	0.1%	43.79%	4108.9	TP53	stop_gained	2263	7840	28.86%
22	Discovery	T0	4.3	1.34	40	3777.3	46.9	4117	0.1%	24.23%	915.1	CDKN2A	missense_variant	793	5452	14.55%
22	Discovery	T3	4.7	1.3	40	3352.7	45.5	6984	0.0%	0.00%	0.0	NA	NA	0	0	0.0%
24	Discovery	T0	5.2	1.32	40	3076.9	46.2	5812	0.1%	1.69%	51.9	TP53	missense_variant	73	7104	1.03%
24	Discovery	T3	5.4	0.598	40	1342.3	20.9	2431	0.1%	2.58%	34.6	TP53	missense_variant	51	3120	1.63%

Supplementary Table 1: Continued

Patient ID	Cohort	Timepoint	Plasma volume for cfDNA isolation (mL)	cfDNA concentration (ng/uL)	cfDNA elution volume (uL)	cfDNA copies/mL plasma	Input for sequencing (ng)	Unique coverage	Limit of detection	ctDNA fraction estimate (%)	ctDNA copies/mL plasma	ctDNA estimate based-on	Mutation type	Alternative reads	Total reads	Variant allele fraction (%)
24	Discovery	T6	5.4	0.874	40	1961.8	30.6	3724	0.1%	5.58%	109.5	TP53	missense_variant	160	4911	3.26%
25	Discovery	T0	5.3	7.47	40	17084.0	50.0	14532	0.0%	53.66%	9166.9	TP53	missense_variant	2543	6759	37.62%
25	Discovery	T3	4.8	3.3	40	8333.3	50.0	7317	0.0%	9.31%	775.5	TP53	missense_variant	420	7962	5.28%
25	Discovery	T6	5.2	2.63	40	6130.5	50.0	8749	0.0%	7.31%	447.8	TP53	missense_variant	412	10042	4.10%
27	Discovery	T0	6	0.96	40	1939.4	33.6	4681	0.1%	19.99%	387.7	TP53	stop_gained	641	5431	11.80%
27	Discovery	T3	8	2.71	40	4106.1	50.0	6841	0.0%	1.01%	41.4	TP53	stop_gained	54	8551	0.63%
27	Discovery	T6	8.5	1.15	40	1639.9	40.3	3657	0.1%	0.00%	0.0	NA	NA	0	0	0.0%
28	Discovery	T0	5.1	0.25	40	601.3	8.9	1721	0.2%	0.00%	0.0	NA	NA	0	0	0.0%
34	Discovery	T0	5.2	2.11	40	4918.4	50.0	6661	0.0%	3.84%	188.9	KEAP1	missense_variant	157	7050	2.23%
34	Discovery	T3	5.1	1.81	40	4301.8	50.0	4508	0.1%	6.88%	296.0	KEAP1	missense_variant	189	4722	4.00%
34	Discovery	T6	4.8	1.19	40	3005.1	41.7	4738	0.1%	12.03%	361.4	KEAP1	missense_variant	360	5178	6.95%
35	Discovery	T0	5.5	1.08	40	2380.2	37.8	4817	0.1%	40.69%	968.5	TP53	missense_variant	1459	5505	26.50%
35	Discovery	T3	5.5	3.03	40	6677.7	50.0	6186	0.0%	41.82%	2792.9	TP53	missense_variant	2036	7464	27.28%
35	Discovery	T6	4.2	0.962	40	2776.3	33.7	4871	0.1%	50.29%	1396.2	TP53	missense_variant	1976	5709	34.61%
36	Discovery	T0	5	1.39	40	3369.7	48.7	7390	0.0%	15.71%	529.2	FBXW7	missense_variant	598	6642	9.00%
36	Discovery	T3	5.2	5.7	40	13286.7	50.0	5852	0.1%	3.12%	414.4	FBXW7	missense_variant	102	5493	1.86%
36	Discovery	T6	5.5	4.74	40	10446.3	50.0	5277	0.1%	6.92%	723.1	FBXW7	missense_variant	182	4510	4.04%
37	Discovery	T0	5.7	5.69	40	12099.9	50.0	5974	0.1%	15.49%	1874.2	TP53	frameshift variant	698	7836	8.91%
37	Discovery	T3	5.1	3.87	40	9197.9	50.0	4928	0.1%	21.90%	2014.4	TP53	frameshift variant	845	6519	12.96%
37	Discovery	T6	4.9	4.05	40	10018.6	50.0	4086	0.1%	23.50%	2354.3	TP53	frameshift variant	724	5139	14.09%
56	Discovery	T0	5.1	1.37	40	3256.1	48.0	5588	0.1%	4.15%	135.3	PIK3CA	missense_variant	162	6731	2.41%
56	Discovery	T6	4.9	0.789	40	1951.8	27.6	3941	0.1%	0.66%	12.8	TP53	missense_variant	22	4773	0.46%
57	Discovery	T0	5	3.35	40	8121.2	50.0	7004	0.0%	74.48%	6048.7	TP53	missense_variant	5689	9456	60.16%

Supplementary Table 1: Continued

Patient ID	Cohort	Timepoint	Plasma volume for cfDNA isolation (mL)	cfDNA concentration (ng/uL)	cfDNA elution volume (uL)	cfDNA copies/mL plasma	Input for sequencing (ng)	Unique coverage	Limit of detection	ctDNA fraction estimate (%)	ctDNA copies/mL plasma	ctDNA estimate based-on	Mutation type	Alternative reads	Total reads	Variant allele fraction (%)
57	Discovery	T3	5	1.83	40	4436.4	50.0	5069	0.1%	31.36%	1391.4	PIK3CA	missense_variant	1269	6546	19.39%
60	Discovery	T0	5.5	0.72	40	1578.0	25.1	3370	0.1%	0.43%	6.8	PARD3	missense_variant	12	3577	0.34%
60	Discovery	T6	5.7	0.781	40	1660.8	27.3	3149	0.1%	0.00%	0.0	NA	NA	0	0	0.0%
64	Discovery	T0	4.9	0.73	40	1800.9	25.5	4294	0.1%	0.00%	0.0	NA	NA	0	0	0.0%
64	Discovery	T3	5.5	2.06	40	4539.9	50.0	5335	0.1%	0.00%	0.0	NA	NA	0	0	0.0%
64	Discovery	T6	5.5	1.25	40	2754.8	43.8	5035	0.1%	0.00%	0.0	NA	NA	0	0	0.0%
68	Discovery	T0	5.6	1.09	40	2359.3	38.2	6242	0.0%	0.00%	0.0	NA	NA	0	0	0.0%
68	Discovery	T3	4.7	1.65	40	4255.3	50.0	6839	0.0%	0.00%	0.0	NA	NA	0	0	0.0%
79	Discovery	T0	6.9	0.70	40	1231.4	24.5	3072	0.1%	19.22%	236.7	TP53	missense_variant	409	3565	11.47%
79	Discovery	T3	5.4	5.95	40	13355.8	50.0	6977	0.0%	0.00%	0.0	NA	NA	0	0	0.0%
79	Discovery	T6	5.3	0.689	40	1575.8	24.1	3069	0.1%	0.00%	0.0	NA	NA	0	0	0.0%
80	Discovery	T0	5.5	0.96	40	2122.3	33.7	4955	0.1%	0.71%	15.1	PTEN	stop_gained	24	4853	0.49%
80	Discovery	T3	4.8	1.34	40	3383.8	46.9	5436	0.1%	0.00%	0.0	NA	NA	0	0	0.0%
80	Discovery	T6	4.6	0.842	40	2218.7	29.5	3415	0.1%	0.00%	0.0	NA	NA	0	0	0.0%
82	Discovery	T0	5.6	2.45	40	5303.0	50.0	6795	0.0%	0.29%	15.4	TERT	upstream_gene_variant	17	7991	0.21%
82	Discovery	T3	5.3	1.06	40	2424.2	37.1	4060	0.1%	0.95%	22.9	TP53	missense_variant	33	5263	0.63%
82	Discovery	T6	5.7	3.09	40	6571.0	50.0	5055	0.1%	0.40%	26.4	TERT	upstream_gene_variant	16	5386	0.30%
94	Discovery	T0	5.4	2.15	40	4826.0	50.0	6430	0.0%	0.24%	11.8	TERT	upstream_gene_variant	14	7536	0.19%
94	Discovery	T3	1.9	7.22	40	46060.6	50.0	7099	0.0%	0.42%	194.9	TP53	missense_variant	26	8985	0.29%
105	Validation	T0	8.5	4.74	40	6759.4	50	4412	0.1%	0.00%	0.0	NA	NA	0	0	0.00%
105	Validation	T3	8.2	2.41	40	3562.5	50	3664	0.1%	0.00%	0.0	NA	NA	0	0	0.00%
106	Discovery	T0	5.3	56.90	40	130131.5	50.0	6969	0.0%	38.83%	50530.8	SNP-based	missense_variant	NA	NA	NA
106	Discovery	T3	3.7	66.7	40	218509.4	50.0	9128	0.0%	40.4%	88260.4	SNP-based	missense_variant	NA	NA	NA
106	Discovery	T6	5	153	40	370909.1	50.0	8127	0.0%	36.3%	134661.5	SNP-based	missense_variant	NA	NA	NA
107	Discovery	T0	5.5	1.97	40	4341.6	50.0	6439	0.0%	1.45%	63.0	TP53	stop_gained	87	10006	0.87%

Supplementary Table 1: Continued

Patient ID	Cohort	Timepoint	Plasma volume for cfDNA isolation (mL)	cfDNA concentration (ng/uL)	cfDNA elution volume (uL)	cfDNA copies/mL plasma	Input for sequencing (ng)	Unique coverage	Limit of detection	ctDNA fraction estimate (%)	ctDNA copies/mL plasma	ctDNA estimate based-on	Mutation type	Alternative reads	Total reads	Variant allele fraction (%)
107	Discovery	T3	5.2	1.87	40	4359.0	50.0	7537	0.0%	1.65%	72.1	TP53	stop_ gained	110	11306	0.97%
107	Discovery	T6	5.6	2.89	40	6255.4	50.0	7442	0.0%	3.94%	246.6	TP53	stop_ gained	244	10941	2.23%
108	Discovery	T0	4.9	13.40	40	33147.8	50.0	7197	0.0%	54.04%	17913.1	TP53	splice_ acceptor_ variant	2615	6886	37.98%
108	Discovery	T3	5.5	16.4	40	36143.3	50.0	8493	0.0%	37.83%	13671.9	TP53	splice_ acceptor_ variant	1973	8190	24.09%
108	Discovery	T6	5.2	2.7	40	6293.7	50.0	5428	0.1%	10.77%	678.1	ERBB2	missense_ variant	493	8061	6.12%
113	Discovery	T0	5.3	1.26	40	2881.6	44.1	3553	0.1%	0.58%	16.8	TP53	missense_ variant	19	4529	0.42%
114	Discovery	T0	5.5	0.90	40	1990.1	31.6	4604	0.1%	1.11%	22.0	TP53	missense_ variant	38	5271	0.72%
114	Discovery	T3	5.3	1.03	40	2355.6	36.1	5686	0.1%	10.52%	247.8	TP53	missense_ variant	382	6345	6.02%
114	Discovery	T6	5.7	1.94	40	4125.5	50.0	8143	0.0%	9.35%	385.6	TP53	missense_ variant	485	9203	5.27%
120	Validation	T0	5.9	1.22	40	2506.4	42.7	4067	0.1%	1.02%	25.7	TP53	missense_ variant	33	4855	0.68%
120	Validation	T3	5.9	0.268	40	550.6	9.4	672	0.4%	0.88%	4.8	TP53	missense_ variant	6	747	0.80%
122	Validation	T0	5.3	1.31	40	2996.0	45.9	4232	0.1%	0.37%	11.0	KRAS	missense_ variant	11	3751	0.29%
122	Validation	T3	5.3	2.33	40	5328.8	50	6642	0.0%	0.24%	13.0	SERPINB8	missense_ variant	11	5666	0.19%
128	Validation	T0	4.8	2.27	40	5732.3	50	4063	0.1%	23.61%	1353.1	TERT	upstream_ gene_ variant	608	4272	14.23%
128	Validation	T3	5.3	0.763	40	1745.0	26.7	2481	0.1%	19.94%	348.0	TERT	upstream_ gene_ variant	298	2462	12.10%
131	Validation	T0	5.6	0.476	40	1030.3	16.7	2576	0.1%	7.09%	73.1	TP53	stop_ gained	145	3456	4.20%
131	Validation	T3	2.7	0.816	40	3663.3	28.6	2855	0.1%	2.78%	101.9	TP53	stop_ gained	67	3907	1.71%
301	Validation	T0	8.3	4.55	40	6644.8	50	3272	0.1%	48.37%	3213.9	APC	stop_ gained	918	2753	33.35%
301	Validation	T3	8.1	5.17	40	7736.6	50	4706	0.1%	37.77%	2922.1	APC	stop_ gained	999	4101	24.36%
302	Validation	T0	7.8	1.47	40	2284.4	50	2970	0.1%	2.82%	64.5	TP53	missense_ variant	63	3599	1.75%
302	Validation	T3	6.7	1.32	40	2388.1	46.2	2793	0.1%	0.00%	0.0	NA	NA	0	0	0.00%

Supplementary Table 1: Continued

Patient ID	Cohort	Timepoint	Plasma volume for cfDNA isolation (mL)	cfDNA concentration (ng/uL)	cfDNA elution volume (uL)	cfDNA copies/mL plasma	Input for sequencing (ng)	Unique coverage	Limit of detection	ctDNA fraction estimate (%)	ctDNA copies/mL plasma	ctDNA estimate based-on	Mutation type	Alternative reads	Total reads	Variant allele fraction (%)
303	Validation	T0	8.4	4.64	40	6695.5	50	3447	0.1%	7.32%	489.9	TP53	missense_variant	61	1313	4.65%
303	Validation	T3	7.4	2.85	40	4668.3	50	3728	0.1%	6.96%	325.0	TP53	missense_variant	61	1382	4.41%
503	Validation	T0	7.2	3.2	40	5387.2	50	3433	0.1%	16.82%	906.2	TP53	stop_gained	378	3800	9.95%
503	Validation	T3	8.7	4.91	40	6840.8	50	3823	0.1%	28.70%	1963.3	RHOA	missense_variant	953	5420	17.58%
504	Validation	T0	7.1	2.98	40	5087.5	50	2882	0.1%	7.44%	378.3	ARID1A	stop_gained	150	3411	4.40%
504	Validation	T3	8.6	3.34	40	4707.5	50	3486	0.1%	2.00%	94.2	ARID1A	stop_gained	52	4121	1.26%
507	Validation	T0	8.2	1.52	40	2246.9	50	3480	0.1%	2.55%	57.2	TERT	upstream_gene_variant	62	3924	1.58%
507	Validation	T3	8.4	1.59	40	2294.4	50	3441	0.1%	0.47%	10.9	TERT	upstream_gene_variant	14	3876	0.36%
508	Validation	T0	5.8	1.89	40	3949.8	50	4322	0.1%	6.31%	249.3	TP53	missense_variant	181	4932	3.67%
508	Validation	T3	5.8	1.7	40	3552.8	50	4738	0.1%	0.31%	11.0	FOXL2	missense_variant	4	1271	0.31%
512	Validation	T0	8.8	1.81	40	2493.1	50	4909	0.1%	2.93%	73.2	TP53	missense_variant	107	6152	1.74%
512	Validation	T3	6.5	1.69	40	3151.5	50	4094	0.1%	1.03%	32.6	TP53	missense_variant	37	5473	0.68%
513	Validation	T0	8	3.1	40	4697.0	50	4867	0.1%	29.26%	1374.3	TP53	stop_gained	1220	6822	17.88%
513	Validation	T3	7.5	6.66	40	10763.6	50	7049	0.0%	41.10%	4423.4	TP53	stop_gained	2351	8830	26.63%
1002	Validation	T0	5	0.983	40	2383.0	34.4	3165	0.1%	0.00%	0.0	NA	NA	0	0	0.00%
1002	Validation	T3	4.7	0.548	40	1413.3	19.2	2465	0.1%	0.00%	0.0	NA	NA	0	0	0.00%
1003	Validation	T0	4.1	0.455	40	1345.2	15.9	1269	0.2%	13.29%	178.7	TP53	frameshift variant	125	1528	8.18%
1003	Validation	T3	6.6	0.572	40	1050.5	20.0	1285	0.2%	13.30%	139.7	TP53	frameshift variant	156	1933	8.07%

Supplementary Table 2: Univariate analysis for the progression-free survival and overall survival.

			Progression-free survival			Overall survival		
Variable	Category	N	Median months	HR (95%CI)	P-value	Median months	HR (95%CI)	P-value
Liver metastasis	Absent	30	15.8	REF	REF	34.4	REF	REF
	Present	10	1.9	4.0 (1.8-8.8)	**<0.001**	4.8	3.0 (1.3-6.9)	**0.008**
TMB	High	12	34.2	REF	REF	Not-reached	REF	REF
	Low	21	2.2	3.1 (1.2-7.8)	**0.02**	6.4	3.0 (1.1-8.1)	**0.04**
ctDNA fraction at baseline		40	NA	1.3 (0.1-4.7)	0.8	NA	1.1 (0.1-6.4)	0.9
ECOG	0-1	30	11.3	REF	REF	27.2	REF	REF
	2	10	7.8	1.1 (0.5-2.6)	0.8	13	1.6 (0.7-3.8)	0.2
Age at baseline		40	NA	0.99 (0.96-1.0)	0.8	NA	1.0 (0.98-1.1)	0.3
mUC therapy line	First	9	13.1	REF	REF	28.5	REF	REF
	Second	31	5.4	1.5 (0.6-3.9)	0.4	20.6	0.87 (0.4-2.0)	0.8
PD-L1 positive cells	<10%	6	1.9	REF	REF	16.3	REF	REF
	>10%	6	19.4	0.6 (0.1-2.4)	0.4	28.5	0.4 (0.1-1.8)	0.2

Supplementary references

1. Radboudumc. TruSight Oncology 500 (TSO500). 2022 3-3-2023; 9-3-2022:[Available from: https://www.palga.nl/datasheet/Radboudumc/TSO500.pdf.
2. Radboudumc. Predictieve Analyse voor THerapie DNA genenpanel' (PATHv3D) (versie 3). 2022 3-3-2023; 31-8-2022:[Available from: https://www.palga.nl/datasheet/Radboudumc/PATHv3D.pdf.
3. Radboudumc. Next-Generation sequencing voor ctDNA; Genenpanel ctDNA_NGSv1. 2022 3-3-2023; 31-8-2022:[Available from: https://www.palga.nl/datasheet/Radboudumc/ctDNA_NGSv1.pdf.
4. Eijkelenboom, A., et al., Reliable Next-Generation Sequencing of Formalin-Fixed, Paraffin-Embedded Tissue Using Single Molecule Tags. J Mol Diagn, 2016. 18(6): p. 851-863.
5. Hofste, L.S.M., et al., Circulating Tumor DNA-Based Disease Monitoring of Patients with Locally Advanced Esophageal Cancer. Cancers (Basel), 2022. 14(18).
6. Karczewski, K.J., et al., The ExAC browser: displaying reference data information from over 60 000 exomes. Nucleic Acids Res, 2017. 45(D1): p. D840-D845.
7. Karczewski, K.J., et al., The mutational constraint spectrum quantified from variation in 141,456 humans. Nature, 2020. 581(7809): p. 434-443.
8. Genome of the Netherlands, C., Whole-genome sequence variation, population structure and demographic history of the Dutch population. Nat Genet, 2014. 46(8): p. 818-25.
9. Eijkelenboom, A., et al., Recommendations for the clinical interpretation and reporting of copy number gains using gene panel NGS analysis in routine diagnostics. Virchows Arch, 2019. 474(6): p. 673-680.
10. Annala, M., et al., Circulating Tumor DNA Genomics Correlate with Resistance to Abiraterone and Enzalutamide in Prostate Cancer. Cancer Discov, 2018. 8(4): p. 444-457.
11. Cerami, E., et al., The cBio cancer genomics portal: an open platform for exploring multidimensional cancer genomics data. Cancer Discov, 2012. 2(5): p. 401-4.
12. Clinton, T.N., et al., Genomic heterogeneity as a barrier to precision oncology in urothelial cancer. Cell Rep, 2022. 41(12): p. 111859.
13. Powles, T., et al., An adaptive, biomarker-directed platform study of durvalumab in combination with targeted therapies in advanced urothelial cancer. Nat Med, 2021. 27(5): p. 793-801.
14. Vandekerkhove, G., et al., Plasma ctDNA is a tumor tissue surrogate and enables clinical-genomic stratification of metastatic bladder cancer. Nat Commun, 2021. 12(1): p. 184.

Chapter 5

Plasma BRAF Mutation Detection for the Diagnostic and Monitoring Trajectory of Patients with LDH-High Stage IV Melanoma

Sofie H. Tolmeijer
Rutger H.T. Koornstra
Jan Willem B. de Groot
Maartje J. Geerlings
Dirk H. van Rens
Marye J. Boers-Sonderen
Jack A. Schalken
Winald R. Gerritsen
Marjolijn J.L. Ligtenberg
Niven Mehra

Cancers (Basel). 2021 Aug 3;13(15):3913. doi: 10.3390/cancers13153913.

Abstract

For patients with newly diagnosed metastatic melanoma, rapid BRAF mutation (mBRAF) assessment is vital to promptly initiate systemic therapy. Additionally, blood-based biomarkers are desired to monitor and predict treatment response. Circulating tumor DNA (ctDNA) has shown great promise for minimally invasive mBRAF assessment and treatment monitoring, but validation studies are needed. This prospective study utilized longitudinal plasma samples at regular timepoints (0, 6, 12, 18 weeks) to address the clinical validity of ctDNA measurements in stage IV melanoma patients with elevated serum lactate dehydrogenase (LDH > 250U/L) starting first-line systemic treatment. Using droplet digital PCR, the plasma mBRAF abundance was assessed in 53 patients with a BRAFV600 tissue mutation. Plasma mBRAF was detected in 50/51 patients at baseline (98% sensitivity; median fraction abundance of 19.5%) and 0/17 controls (100% specificity). Patients in whom plasma mBRAF became undetectable during the first 12–18 weeks of treatment had a longer progression-free survival (30.2 vs. 4.0 months; $P < 0.001$) and cancer-specific survival (not reached vs. 10.2 months; $P < 0.001$) compared to patients with detectable mBRAF. The ctDNA dynamics outperformed LDH and S100 dynamics. These results confirm the clinical validity of ctDNA measurements as a minimally invasive biomarker for the diagnostic and monitoring trajectory of patients with LDH-high stage IV melanoma.

Introduction

Metastatic melanoma is the most aggressive and lethal form of skin cancer [1–3]. Two therapeutic approaches have become standard of care for this disease: targeted therapy and immunotherapy. Targeted therapy (BRAF/MEK inhibitor) has a rapid anti-tumor effect and is of benefit to the majority of patients. However, this therapy is limited to those harboring a *BRAFV600* mutation (mBRAF) in their tumor, and resistance commonly occurs within 12 months [4,5]. Immunotherapy, on the other hand, can achieve long-term disease control and is independent of *BRAF* status. Still, immunotherapy does not demonstrate sufficient anti-tumor activity in 50–70% of patients and is associated with a higher incidence of grade 3–4 toxicity [6–9].

To determine the best treatment strategy per patient, it is essential to rapidly assess mBRAF status and closely monitor treatment response. In current practice, mBRAF status is determined from routinely performed tumor biopsies, but this remains an invasive and time-consuming method. Treatment response is monitored by radiographic imaging, which limits frequent measurements and has difficulties distinguishing pseudo-progression from true progression, particularly following checkpoint inhibitors [10,11]. Therefore, alternative strategies have been investigated to improve current practice, including the use of circulating tumor DNA (ctDNA). ctDNA is released into the bloodstream by apoptosis and necrosis of tumor cells [12], enabling the detection of mBRAF from blood. In addition, easily obtainable repetitive blood draws allow close monitoring of ctDNA dynamics in relation to treatment response.

Previous studies established ctDNA analysis as a highly specific tool for mBRAF detection, but ctDNA-based mBRAF detection can vary in sensitivity (56–90%) [13–19]. The varying sensitivity can be explained by the ctDNA quantity in patients, which is in turn dependent on the tumor burden and location of the tumor. For instance, in patients with M1c disease, it appeared 2–5 times more likely to detect ctDNA compared to M1a/b disease [20–22]. In addition, elevated lactate dehydrogenase (LDH), associated with tumor cells outgrowing their blood supply, is associated with 30–50 times higher ctDNA levels [14,23,24]. Consequently, the sensitivity of ctDNA-based mBRAF assessment can vary per patient, hampering the implementation of ctDNA-based mBRAF assessment in routine patient care.

Besides the diagnostic application of ctDNA for mBRAF assessment, the ctDNA burden is prognostic for patient outcome. Similar to LDH, the amount of ctDNA at the start of treatment appears prognostic for the progression-free survival (PFS) and overall survival (OS) of patients with metastatic melanoma [16,17,21,25,26]. Additionally,

changes in ctDNA were shown to be relevant for the monitoring of treatment response. For example, a conversion of ctDNA from detectable to undetectable levels during immunotherapy or targeted therapy was shown to reflect a 3–7 times longer PFS and 4-8 times longer OS [16,18,21,27]. Small and retrospective studies indicate that ctDNA outperforms the other blood-based biomarkers for melanoma, LDH and S100, in predicting patient outcome [15,28,29].

To validate the current applications for ctDNA, prospective clinical validation studies are needed using blood samples at regular time points and standardized blinded assessment of outcome parameters. Syeda and colleagues published the first large clinical validation study showing the potential of ctDNA as an independent biomarker for targeted therapy in patients with advanced melanoma [26]. Plasma mBRAF was detected in 93% (320/345) of all patients using droplet digital PCR (ddPCR) [26]. In patients with elevated LDH levels, the sensitivity was 98%, showing a great promise for ctDNA-based mBRAF assessment, particularly in LDH-high stage IV melanoma patients. As elevated LDH is associated with a 50% shorter OS compared to patients with normal LDH [30], prompt initiation of treatment and close treatment monitoring is essential for these patients. Interestingly, Syeda and colleagues observed a better predictive value of ctDNA dynamics for the PFS and OS in LDH-high patients compared to LDH-normal patients [26]. Unfortunately, longitudinal sampling beyond 4 weeks was missing in this study, and the ctDNA dynamics were not compared to other blood-based biomarkers.

The current study aimed to confirm and expand on the clinical validity of ctDNA measurements for diagnostic and monitoring trajectory of patients with LDH-high metastatic melanoma starting their first-line of systemic treatment. Utilizing longitudinal and prospectively collected plasma samples at fixed timepoints up to 18 weeks of treatment, accompanied by radiographic imaging and evaluation of other blood-based biomarkers, we aim to elaborate on the potential of ctDNA measurements for systemic treatment monitoring in LDH-high stage IV melanoma patients.

Materials and Methods

Patient Cohort and Study Design

Patients with stage IV metastatic melanoma were enrolled in the study between March 2017 and June 2020. All patients had a confirmed BRAFV600 mutation (mBRAF) in tissue based on routine diagnostic tests. All patients had elevated serum LDH (>250U/L) and were naïve for both immune checkpoint blockade agents and BRAF/MEK inhibitors. Written consent was obtained from all patients as approved by the local medical ethical committee (dossier number 2016–2769, December 2016). Patients underwent baseline characterization, including physical examination, blood marker evaluation, and radiographic tumor assessment. Patients started with either BRAF/MEK inhibitors or immune checkpoint blockade upon inclusion and underwent clinical evaluation every 6 weeks, which included blood collection and CT scans. CT results were assessed by RECIST 1.1 criteria [31], which distinguishes between complete response (CR), partial response (PR), stable disease (SD), or progressive disease (PD).

In order to confirm the specificity of ctDNA-based mBRAF detection, blood was also collected from three LDH-high melanoma patients without mBRAF in their tumor and 14 healthy controls.

Cell-Free DNA Isolation and ctDNA Quantification

Blood was collected at baseline and after 6, 12, and 18 weeks of treatment using EDTA tubes. Within 4 hours, the blood samples were first centrifuged at 120× *g* for 20 min to separate plasma from blood cells. Afterward, plasma was centrifuged at 360× *g* for 20 min to remove platelets. Finally, the plasma was centrifuged at 14,000× *g* for 10 min to remove cellular debris. Plasma was stored at –80°C until further processing.

Total cell-free circulating DNA was extracted from approximately 2 mL of plasma using the QIAamp Circulating Nucleic Acid Kit (Qiagen) according to the manufacturer's protocol and eluted in 30 µL low-TE buffer. The DNA concentration was quantified using Qubit (ThermoFisher), and the quality was checked on a Fragment Analyzer (Agilent high sensitivity genomic DNA kit #DNF-488-0500). Next, the presence of mBRAF ctDNA copies was assessed with the droplet digital PCR (ddPCR) BRAFV600 screening kit (#12001037, BioRad), which can detect BRAF p.V600E (c.1799T>A), p.V600R (c.1798_1799delinsAG), and p.V600K (c.1798_1799delinsAA) mutations. All samples were measured in duplicate. A binominal distribution was used to calculate the theoretical sensitivity of detecting mBRAF per sample based on the available input material (Figure S1). Samples with two or more mutant droplets were considered ctDNA positive.

To convert cell-free DNA concentration-units from ng per mL plasma to copies per mL plasma, we multiplied the concentrations by a factor of 303, assuming that the mass of a haploid genome is 3.3 pg. Subsequently, the ctDNA copies per mL plasma could be calculated based on the fractional abundance of mBRAF and the total cell-free DNA copies per mL plasma.

Statistical Analysis

The correlation between continuous variables was calculated using Spearman rank correlation statistics. Differences in ctDNA levels concerning the absence or presence of specific metastasis sites were calculated using an unpaired two samples Wilcoxon test. Time-to-event outcomes, including PFS and melanoma cancer-specific survival (CSS), were described via the Kaplan–Meier method. PFS and CSS were defined as the time from the start of therapy to the date of first reported PD for PFS and death as a consequence of melanoma for CSS. PFS and CSS curves were stratified according to patient characteristics and clinicopathologic features and compared using Cox-regression models. For the Cox-regression models, the baseline ctDNA copies were log-transformed for a normal distribution and assessed as a continuous variable. For assessment of ctDNA dynamics in longitudinal samples, ctDNA results were dichotomized as detectable (positive) or undetectable (negative) after 12–18 weeks of treatment. S100 and LDH dynamics were also dichotomized as below the upper limit of normal or above the upper limit of normal after 12–18 weeks. Due to missing data and a limited number of events for CSS (n = 16), a multivariable Cox-regression was only used to evaluate PFS. This multivariate Cox-regression analysis included all variables significantly associated with PFS in the univariate analysis ($p < 0.05$).

Results

Patient Characteristics

A total of 53 patients with LDH-high metastatic melanoma were included in this study (Table 1). Half of these patients were treated with combination immunotherapy (ipilimumab + nivolumab), while the other half was first treated with combination BRAF/MEK inhibitors before starting with immunotherapy. As this translational work is part of an ongoing clinical trial, we cannot disclose patient treatment specifics. The me-dian follow-up duration was 12.3 months (range 0–38.1 months). Fifty-eight percent of patients were alive at the time of analysis, and 42% had an ongoing treatment response.

ctDNA-Based mBRAF Assessment

In total, 153 blood samples were collected for ctDNA analysis (data available in Table S1). This included a baseline sample for 51/53 (96%) patients and longitudinal follow-up for 40/53 (75%) patients. Of all baseline plasma samples, mBRAF was detected in 50/51 (98%) with a median fractional abundance of 19.5% (range 0.2–66.5%). The one patient for whom mBRAF could not be detected had M1b disease and the smallest cumulative RE-CIST target lesions of the cohort.

Table 1: Baseline patient characteristics.

Total patients, n (%)	**53 (100%)**
Sex, n (%)	
Female	19 (36%)
Male	34 (64%)
Age, median years (range)	61 (28-78)
ECOG, n (%)	
0	34 (64%)
1	16 (30%)
2	3 (6%)
Initiated treatment, n (%)	
Immunotherapy	25 (53%)
BRAF/MEK inhibitor	25 (47%)
LDH (U/L), median (range)	357 (261-1560)
S100 (ng/mL), median (range)	1.43 (0.06-10.97)
Metastasis location, n (%)	
Skin	9 (17%)
Lymph node	34 (64%)
Lung	23 (43%)
Kidney	21 (40%)
Liver	19 (36%)
Follow-up, median months (range)	12.3 (0-38.1)

Figure 1A visualizes the baseline plasma mBRAF abundance in relation to other baseline characteristics, such as LDH levels and metastasis sites. mBRAF abundance moderately correlated with levels of LDH (Figure 1B, $\rho = 0.50$, $P < 0.001$), weakly correlated with S100 levels (Figure 1C, $\rho = 0.35$, $P = 0.03$), and strongly correlated with total cell-free circulating DNA (Figure 1D, $\rho = 0.83$, $P < 0.001$). No association was found between the mBRAF levels and the RECIST sum of the target lesion diameters (SLD) ($P = 0.74$), but higher mBRAF levels were observed in patients with liver metastasis (Figure 1E, $P = 0.05$).

To determine the specificity of ctDNA-based mBRAF detection, plasma of 17 controls was tested for the presence of mBRAF. Fourteen of these controls were healthy individuals, and three were patients with LDH-high metastatic melanoma but without mBRAF in their tumor. All the plasma samples tested negative for mBRAF (Table S1). Combined, this in-dicates that ctDNA-based mBRAF detection has a specificity of 100% and sensitivity of 98% in LDH-high stage IV melanoma patients.

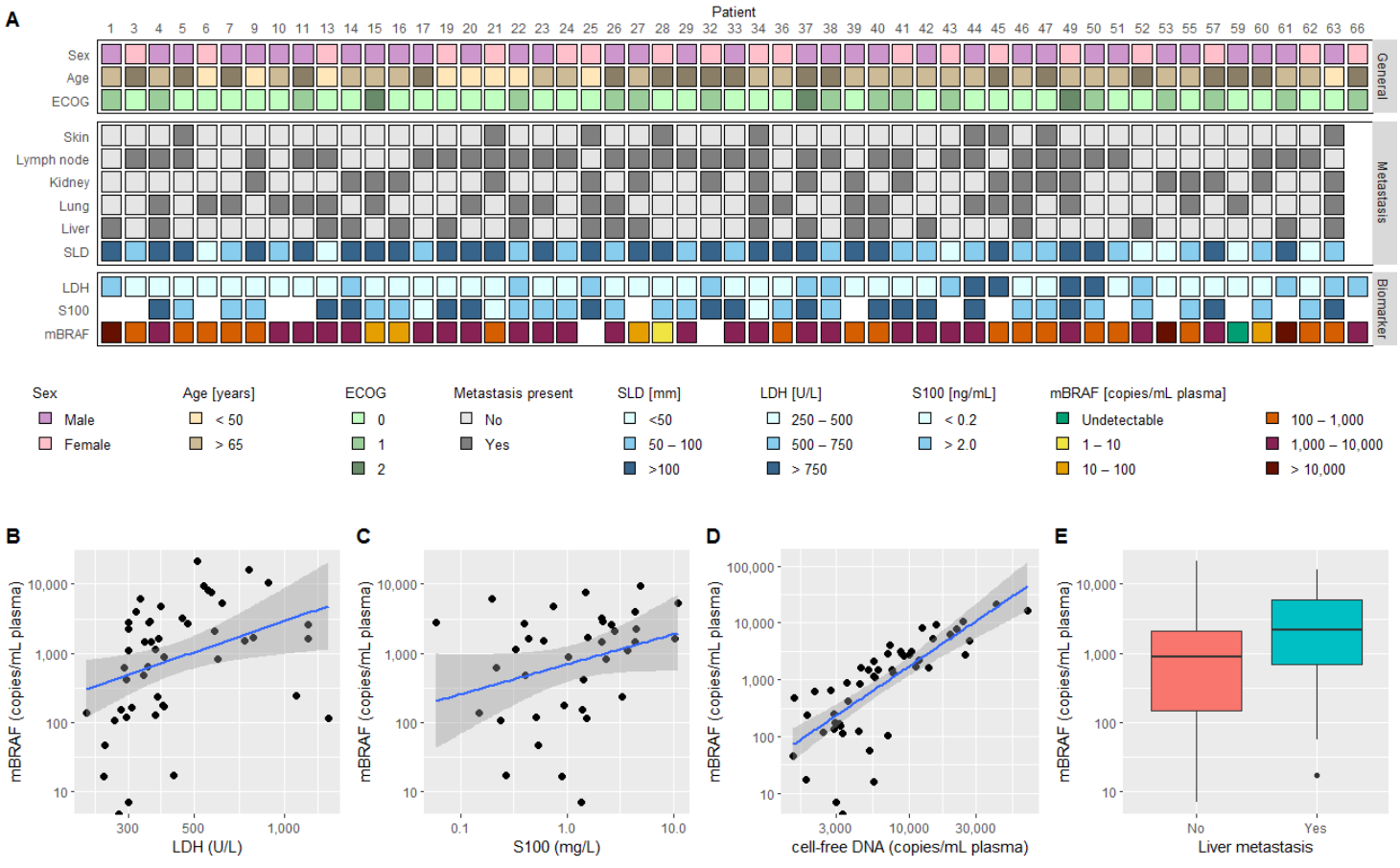

Figure 1 (left page): Baseline patient characteristics and clinicopathologic features in relation to baseline plasma mBRAF copies. (A) Schematic overview illustrating the patient characteristics (sex, age, ECOG), metastasis sites and blood-based biomarkers (LDH, S100) relative to the plasma mBRAF copies; (B) Correlation between plasma mBRAF copies and LDH levels ($\rho = 0.50$, $P < 0.001$); (C) Correlation between plasma mBRAF copies and S100 levels ($\rho = 0.35$, $P = 0.03$); (D) Correlation between plasma mBRAF copies and total cell free circulating DNA copies ($\rho = 0.83$, $P < 0.001$); (E) Association between plasma mBRAF copies and the presence of liver metastasis ($P = 0.05$).

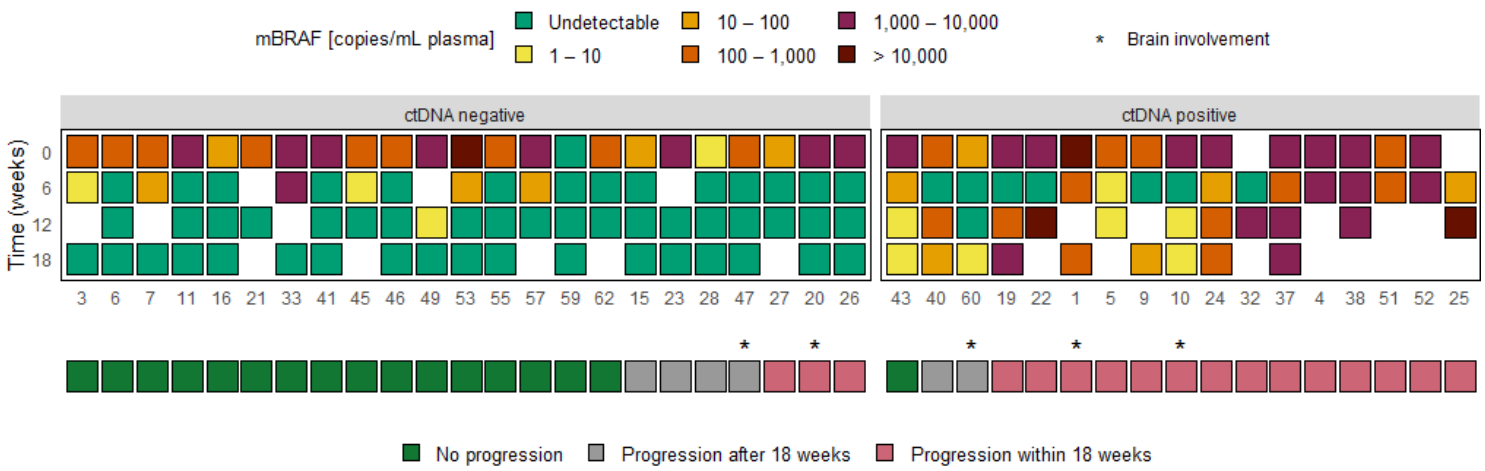

Figure 2: Overview of the ctDNA dynamics (mBRAF copies/mL plasma) related to treatment response within 18 weeks. Patients were stratified according to their ctDNA levels at 12–18 weeks, being either detectable (ctDNA positive) or undetectable (ctDNA negative).

ctDNA Dynamics and Treatment Response

After treatment initiation, we investigated ctDNA dynamics in relation to the treatment response. For 40 patients, follow-up plasma samples were available up to 12–18 weeks and/or at progression. An overview of the longitudinal blood-biomarker assessments available per patient is given in Table S3. The ctDNA dynamics of these patients could be divided into two groups: (1) 23 patients in whom plasma mBRAF became unde-tectable during the first 12–18 weeks of treatment, including the patient who was tested mBRAF-negative at baseline, and (2) 17 patients in whom plasma mBRAF remained de-tectable (or became detectable again) during the first 12–18 weeks of treatment. Figure 2 visualizes the ctDNA dynamics in both groups, referred to as (1) ctDNA negative and (2) ctDNA positive. Figure S2 includes the results on the S100 and LDH dynamics in the ctDNA dynamics groups.

In the ctDNA negative group, only three (13%) patients experienced disease progression within 18 weeks. All three patients had an ongoing response per RECIST1.1 of their target lesions but developed one or more new lesions. One of the three patients developed only one new lesion that was located in the brain. Four (17%) patients in the ctDNA nega-tive group had disease progression after 18 weeks, and 16 (70%) had an ongoing treatment response at the time of analysis. In the ctDNA positive group, 14 (82%) patients developed disease progression within 18 weeks and 2 (12%) after 18 weeks. Only one (6%) patient had a continuing treatment response. The ctDNA content of this patient was still declin-ing from baseline to the last measured timepoint.

ctDNA Dynamics Associates with the PFS and CSS

Next, we investigated the ctDNA dynamics in relation to PFS and CSS. Figure 3A demonstrates that patients with undetectable ctDNA after 12-18 weeks of treatment had a 7.4 times longer median PFS compared to patients with still detectable ctDNA (30.2 vs. 4.0 months; hazard ratio (HR) 12.6 (95% confidence interval [95% CI] 4.3–36.8)). A similar difference was observed for CSS (Figure 3B; not reached vs. 10.2 months; HR 14.6 (95% CI 3.3–64.6)).

Other parameters that were significantly associated with a shorter PFS in the univariable analysis included the presence of liver metastasis, the amount of mBRAF copies at baseline, and the S100 dynamics (being above or under the upper limit of normal after 12-18 weeks) (Table 2). Interestingly, only ctDNA dynamics remained significant in a multivariable model (Table 2). The univariable analysis for CSS revealed that similar variables associated with a shorter PFS were also associated with a shorter CSS (Table S2). Due to limited events in the CSS analysis and missing data (Table S3), we did not perform a multivariable analysis with all significantly associated variables for CSS. Still, ctDNA dynamics was the strongest prognostic variable in the univariate analysis for both PFS and CSS.

Table 2: Factors associated with the progression-free survival (PFS). HR = hazard ratio, 95% CI = 95% confidence interval, ULN = upper limit of normal.

		Progression-free survival					
		Univariable analysis			Multivariable analysis		
Variable		HR	95% CI	*P*-value	HR	95% CI	*P*-value
Liver metastasis	Present vs. absent	3.65	1.73–7.71	<0.001	1.38	0.36–5.3	0.643
ctDNA baseline	log10 (mBRAF per mL plasma)	1.68	1.07–2.64	0.02	1.26	0.67–2.4	0.473
S100 dynamics	Above vs. below ULN at 12-18 weeks	5.5	2.21–13.71	<0.001	0.95	0.23–4.0	0.94
ctDNA dynamics	Positive vs. negative at 12-18 weeks	12.57	4.30–36.76	<0.001	18.75	3.55–98.9	<0.001

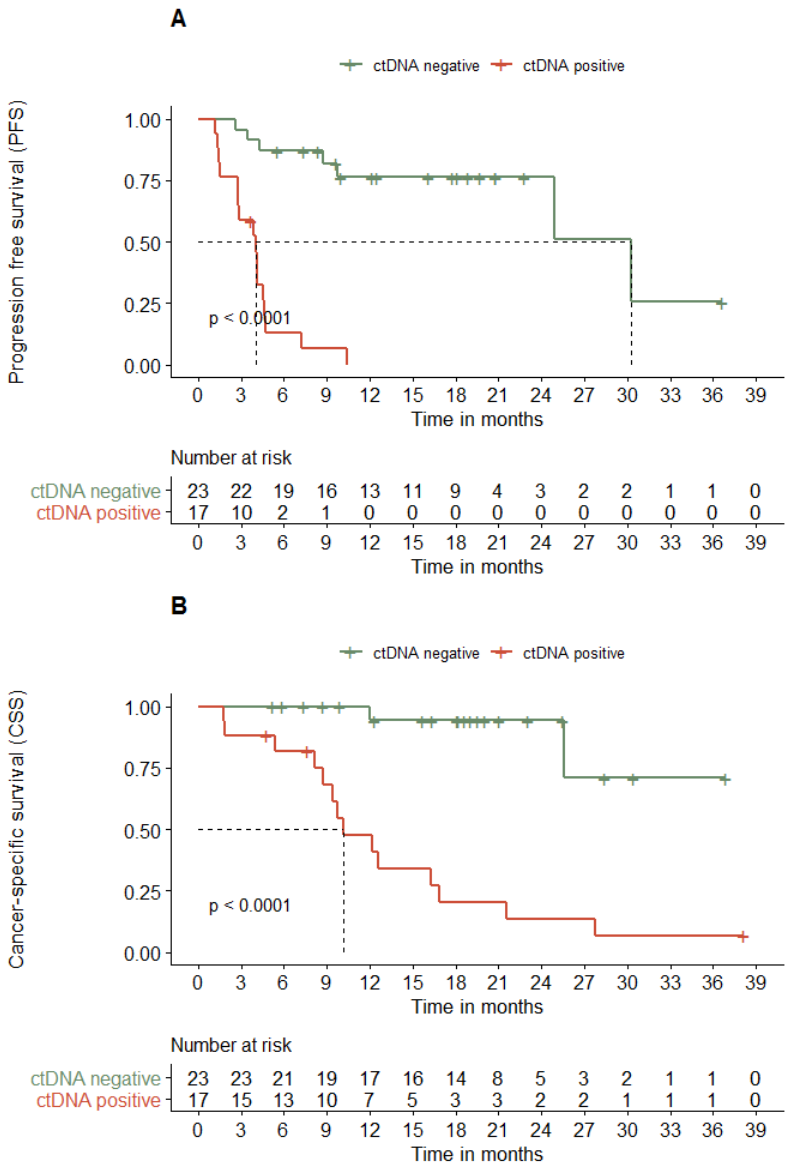

Figure 3: ctDNA dynamics related to (A) progression-free survival (PFS) and (B) cancer-specific survival (CSS). Patients were stratified according to their ctDNA levels at 12–18 weeks, being either detectable (ctDNA positive) or undetectable (ctDNA negative).

Discussion

The current study confirmed that ctDNA could be a valuable diagnostic and predictive tool in patients with LDH-high metastatic melanoma. Before treatment initiation, ctDNA-based mBRAF assessment was shown to be highly sensitive and specific for these patients. Using prospectively collected longitudinal data at fixed timepoints, it was shown that ctDNA dynamics can be used to monitor treatment response. The ctDNA dynamics defined favorable and unfavorable profiles that could be used as an independent predictor of long-term response and survival and may eventually be used to guide treatment adaptations.

To determine optimal therapeutic choices in metastatic melanoma, knowledge on the BRAF status is vital. Particularly in newly diagnosed, symptomatic, LDH-high metastatic melanoma, prompt treatment initiation with BRAF/MEK inhibition allows for a rapid tumor and clinical response in patients harboring mBRAF. At present, BRAF status is assessed using a tumor biopsy, but ctDNA-based mBRAF detection could become a new standard being a less-invasive and faster strategy for accurate BRAF assessment (within days instead of weeks). With the level of ctDNA in blood to a large extent dependent on tumor burden [4,20,21], we hypothesized that ctDNA-based mBRAF detection would be most reliable in patients with LDH-high metastatic disease. Elevated LDH is associated with tumors outgrowing their blood supply [32] and has clinical utility in melanoma. LDH is used as a classifier for the American joint committee on cancer staging [33] and is a strong prognostic biomarker for metastatic melanoma independent of treatment [34,35]. Moreover, previous studies revealed a clear correlation between LDH and ctDNA levels (R = 0.50–0.76) [14–16,23].

A moderate correlation between LDH and ctDNA was still observed in this study even though patients were preselected for elevated LDH levels (ρ = 0.50). More importantly, 50/51 patients positive for mBRAF by tumor tissue test also had detectable mBRAF in plasma resulting in a 98% sensitivity of the ctDNA-based assay. This is similar to the results of Syeda and colleagues, who also observed a 98% sensitivity among 125 patients with LDH-high advanced melanoma [26]. The sensitivity is higher compared to previous studies in which patients were not treatment-naïve or preselected for elevated LDH (56–90%) [13–19]. The sensitivity was independent of the assay threshold that was previously reported to affect sensitivity [18]. The specificity obtained in this study (100%) was comparable to other studies [13–19,36]. As approximately 40% of all metastatic melanoma patients have elevated serum LDH [4], ctDNA-based mBRAF detection can become a reliable alternative to tissue-based testing for a substantial number of patients to guide the initial choice of systemic therapy. The next step for the

implementation of ctDNA-based mBRAF testing in the clinic would be to offer ctDNA-based mBRAF testing in parallel to tissue testing and compare the turn-around time, sensitivity, and costs.

Besides the baseline ctDNA detection, the ctDNA changes in relation to treatment response were investigated in this study. Figure 2 illustrates that the majority of patients in whom ctDNA became undetectable during the first 12-18 weeks (ctDNA negative) had a favorable treatment response. Disease progression within 18 weeks was only observed in three patients. Interestingly, all these patients had responding RECIST target lesions but developed one or more new lesions. In patient 20, the new lesion was located in the brain, potentially explaining the absence of ctDNA in plasma [18,21,37]. Patient 26 was later diagnosed with myelofibrosis, which might explain the new lesions on the CT-scan without mBRAF detection in blood. This patient was switched to BRAF/MEK inhibitors after the new lesions were observed and had a complete response following the next 2.5 years, which is a remarkable duration of response to BRAF/MEK inhibitors. In contrast to the ctDNA negative group, most patients in the ctDNA positive group experienced disease progression within the first 18 weeks of treatment. Only one patient had a long-term treatment response beyond 18 weeks. This patient showed an ongoing decline in ctDNA copies from baseline in all measured timepoints and a longer ctDNA evaluation period may therefore have resulted in undetectable mBRAF level following the 18-week period. Altogether, the data suggest that longitudinal measurements of ctDNA during treatment could help monitor treatment response.

When translating the observations from Figure 2 to a survival analysis, a clear association was observed between ctDNA dynamics and time to progression or death. Patients with undetectable levels of ctDNA after 12–18 weeks of treatment had a 7.6 time longer median PFS compared to patients with detectable ctDNA (Figure 3A). Moreover, only two melanoma-related deaths were observed in this group following a median follow-up of 18.4 months and included the death of patient 20, who developed brain metastasis (Figure 3B). These observations are in line with previous literature, describing comparable hazard ratios for the ctDNA detectability at 3 to 12 weeks [18,21,27]. Similarly, around 50% of the patients with detectable ctDNA at the start of treatment convert to undetectable ctDNA after a few weeks of treatment [18,27].

Importantly, ctDNA dynamics improved discrimination between progressing and non-progressing patients within the observation period of 18 weeks when compared to S100 and LDH dynamics (Figure S2; Table S2; Table 2). This is in line with results from other small studies and retrospective studies [15,28,29]. Overall, the ctDNA dynamics resembled S100 dynamics despite a weak correlation between the variables at baseline. Nonetheless, S100 dynamics misclassified five patients that were correctly classified by ctDNA dynamics (Figure S2). LDH dynamics misclassified nine patients and was not significantly associated with PFS in the univariate analysis (Figure S2; Table S2). Only ctDNA dynamics remained significant in a multivariate Cox-regression model for PFS after correction for the significant baseline characteristics and S100 dynamics (Table 2). Therefore, ctDNA dynamics seems a very specific and valuable biomarker to distinguish long-term responders from patients who may benefit from an early switch to an alternative treatment strategy or possibly treatment intensification. Ongoing randomized trials are evaluating whether ctDNA-informed early treatment switch may improve outcome compared to standard of care; this includes a randomized phase II trial in patients with metastatic melanoma treated with dabrafenib and trametinib, where following a predefined ctDNA drop of ≥80%, patients are switched to nivolumab and ipilimumab (NCT03808441). In the adjuvant setting, a phase 3 randomized, blinded trial will investigate whether ctDNA-informed early treatment initiation with nivolumab has a superior outcome to the standard of care in patients following resection of stage IIB/C melanoma (NCT04901988).

To conclude, this study on prospectively collected material underlines the potential of ctDNA assessment as a diagnostic and predictive tool for patients with LDH-high metastatic melanoma. Limitations of this study included the small number of patients and a ctDNA follow-up that stopped at 18 weeks. Future studies will be needed to investigate the clinical utility of ctDNA-based mBRAF assessment in routine practice and help identify optimal use of longitudinal ctDNA follow-up. Nevertheless, this study supports the next steps in the implementation of ctDNA assessments in routine clinical care of metastatic melanoma patients.

Conclusion

In conclusion, the current study confirmed the clinical validity of ctDNA-based mBRAF detection as an alternative to tissue-based testing for patients with LDH-high metastatic melanoma. Using prospectively collected blood samples at regular timepoint, the study underlines the potential of ctDNA dynamics to monitor and independently predict treatment response.

References

1. Rigel, D.S.; Carucci, J.A., Malignant melanoma: Prevention, early detection, and treatment in the 21st century.CA Cancer J. Clin. 2000, 50, 215–236.
2. Guy, G.P., Jr.; Thomas, C.C.; Thompson, T.; Watson, M.; Massetti, G.M.; Richardson, L.C., Vital signs: melanoma incidence and mortality trends and projections - United States, 1982-2030.MMWR Morb. Mortal Wkly. Rep. 2015, 64, 591–596.
3. Siegel, R.L.; Miller, K.D.; Jemal, A., Cancer statistics, 2019.CA Cancer J. Clin. 2019, 69, 7–34.
4. Long, G.V.; Flaherty, K.T.; Stroyakovskiy, D.; Gogas, H.; Levchenko, E.; de Braud, F.; Larkin, J.; Garbe, C.; Jouary, T.; Hauschild, A.; et al. Dabrafenib plus trametinib versus dabrafenib monotherapy in patients with metastatic BRAF V600E/K-mutant melanoma: long-term survival and safety analysis of a phase 3 study.Ann. Oncol. 2017, 28, 1631–1639.
5. Larkin, J.; Ascierto, P.A.; Dreno, B.; Atkinson, V.; Liszkay, G.; Maio, M.; Mandala, M.; Demidov, L.; Stroyakovskiy, D.; Thomas, L.; et al. Combined vemurafenib and cobimetinib in BRAF-mutated melanoma.N. Engl. J. Med. 2014, 371, 1867–1876.
6. Topalian, S.L.; Sznol, M.; McDermott, D.F.; Kluger, H.M.; Carvajal, R.D.; Sharfman, W.H.; Brahmer, J.R.; Lawrence, D.P.; Atkins, M.B.; Powderly, J.D.; et al. Survival, durable tumor remission, and long-term safety in patients with advanced melanoma receiving nivolumab.J. Clin. Oncol. 2014, 32, 1020–1030.
7. Schadendorf, D.; Hodi, F.S.; Robert, C.; Weber, J.S.; Margolin, K.; Hamid, O.; Patt, D.; Chen, T.T.; Berman, D.M.; Wolchok, J.D., Pooled Analysis of Long-Term Survival Data From Phase II and Phase III Trials of Ipilimumab in Unresectable or Metastatic Melanoma.J. Clin. Oncol. 2015, 33, 1889–1894.
8. Weber, J.S.; Gibney, G.; Sullivan, R.J.; Sosman, J.A.; Slingluff, C.L., Jr.; Lawrence, D.P.; Logan, T.F.; Schuchter, L.M.; Nair, S.; Fecher, L.; et al. Sequential administration of nivolumab and ipilimumab with a planned switch in patients with advanced melanoma (CheckMate 064): an open-label, randomised, phase 2 trial.Lancet Oncol. 2016, 17, 943–955.
9. Hamid, O.; Puzanov, I.; Dummer, R.; Schachter, J.; Daud, A.; Schadendorf, D.; Blank, C.; Cranmer, L.D.; Robert, C.; Pavlick, A.C.; et al. Final analysis of a randomised trial comparing pembrolizumab versus investigator-choice chemotherapy for ipilimumab-refractory advanced melanoma.Eur. J. Cancer 2017, 86, 37–45.
10. Hodi, F.S.; Hwu, W.-J.; Kefford, R.; Weber, J.S.; Daud, A.; Hamid, O.; Patnaik, A.; Ribas, A.; Robert, C.; Gangadhar, T.C.; et al. Evaluation of Immune-Related Response Criteria and RECIST v1.1 in Patients With Advanced Melanoma Treated With Pembrolizumab.J. Clin. Oncol. 2016, 34, 1510–1517.
11. Seymour, L.; Bogaerts, J.; Perrone, A.; Ford, R.; Schwartz, L.H.; Mandrekar, S.; Lin, N.U.; Litière, S.; Dancey, J.; Chen, A.; et al. iRECIST: guidelines for response criteria for use in trials testing immunotherapeutics.The Lancet.Oncology 2017, 18, e143–e152.
12. Stroun, M.; Lyautey, J.; Lederrey, C.; Olson-Sand, A.; Anker, P., About the possible origin and mechanism of circulating DNA: Apoptosis and active DNA release.Clinica. Chimica. Acta. 2001, 313, 139–142.
13. Garlan, F.; Blanchet, B.; Kramkimel, N.; Puszkiel, A.; Golmard, J.L.; Noe, G.; Dupin, N.; Laurent-Puig, P.; Vidal, M.; Taly, V.; et al. Circulating Tumor DNA Measurement by Picoliter Droplet-Based Digital PCR and Vemurafenib Plasma Concentrations in Patients with Advanced BRAF-Mutated Melanoma.Target Oncol. 2017, 12, 365–371.
14. Kozak, K.; Kowalik, A.; Gos, A.; Wasag, B.; Lugowska, I.; Jurkowska, M.; Krawczynska, N.; Kosela-Paterczyk, H.; Switaj, T.; Teterycz, P.; et al. Cell-free DNA BRAF V600E measurements during BRAF inhibitor therapy of metastatic melanoma: long-term analysis.Tumori. 2020, 300891619900928.
15. Braune, J.; Keller, L.; Schiller, F.; Graf, E.; Rafei-Shamsabadi, D.; Wehrle, J.; Follo, M.; Philipp, U.; Hussung, S.; Pfeifer, D.; et al. Circulating Tumor DNA Allows Early Treatment Monitoring in BRAF- and NRAS-Mutant Malignant Melanoma.JCO Precis. Oncol. 2020, 4, 20–31.
16. Gray, E.S.; Rizos, H.; Reid, A.L.; Boyd, S.C.; Pereira, M.R.; Lo, J.; Tembe, V.; Freeman, J.; Lee, J.H.; Scolyer, R.A.; et al. Circulating tumor DNA to monitor treatment response and detect acquired resistance in patients with metastatic melanoma.Oncotarget. 2015, 6, 42008–42018.
17. Sanmamed, M.F.; Fernandez-Landazuri, S.; Rodriguez, C.; Zarate, R.; Lozano, M.D.; Zubiri, L.; Perez-Gracia, J.L.; Martin-Algarra, S.; Gonzalez, A., Quantitative cell-free circulating BRAFV600E mutation analysis by use of droplet digital PCR in the follow-up of patients with melanoma being treated with BRAF inhibitors.Clin. Chem. 2015, 61, 297–304.
18. Lee, J.H.; Long, G.V.; Boyd, S.; Lo, S.; Menzies, A.M.; Tembe, V.; Guminski, A.; Jakrot, V.; Scolyer, R.A.; Mann, G.J.; et al. Circulating tumour DNA predicts response to anti-PD1 antibodies in metastatic melanoma.Ann. Oncol. 2017, 28, 1130–1136.
19. Forthun, R.B.; Hovland, R.; Schuster, C.; Puntervoll, H.; Brodal, H.P.; Namlos, H.M.; Aasheim, L.B.; Meza-Zepeda, L.A.; Gjertsen, B.T.; Knappskog, S.; et al. ctDNA detected by ddPCR reveals changes in tumour load in metastatic malignant melanoma treated with bevacizumab.Sci. Rep. 2019, 9, 17471.
20. McEvoy, A.C.; Warburton, L.; Al-Ogaili, Z.; Celliers, L.; Calapre, L.; Pereira, M.R.; Khattak, M.A.; Meniawy, T.M.; Millward, M.; Ziman, M.; et al. Correlation between circulating tumour DNA and metabolic tumour burden in metastatic melanoma patients.Bmc Cancer 2018, 18, 726.
21. Seremet, T.; Jansen, Y.; Planken, S.; Njimi, H.; Delaunoy, M.; El Housni, H.; Awada, G.; Schwarze, J.K.; Keyaerts, M.; Everaert, H.; et al. Undetectable circulating tumor DNA (ctDNA) levels correlate with favorable outcome in metastatic melanoma patients treated with anti-PD1 therapy.J. Transl. Med. 2019, 17, 303.

22. Rowe, S.P.; Luber, B.; Makell, M.; Brothers, P.; Santmyer, J.; Schollenberger, M.D.; Quinn, H.; Edelstein, D.L.; Jones, F.S.; Bleich, K.B.; et al. From validity to clinical utility: the influence of circulating tumor DNA on melanoma patient management in a real-world setting.Mol. Oncol. 2018, 12, 1661–1672.
23. Santiago-Walker, A.; Gagnon, R.; Mazumdar, J.; Casey, M.; Long, G.V.; Schadendorf, D.; Flaherty, K.; Kefford, R.; Hauschild, A.; Hwu, P.; et al. Correlation of BRAF Mutation Status in Circulating-Free DNA and Tumor and Association with Clinical Outcome across Four BRAFi and MEKi Clinical Trials.Clin. Cancer Res. 2016, 22, 567–574.
24. Chang, G.A.; Tadepalli, J.S.; Shao, Y.; Zhang, Y.; Weiss, S.; Robinson, E.; Spittle, C.; Furtado, M.; Shelton, D.N.; Karlin-Neumann, G.; et al. Sensitivity of plasma BRAFmutant and NRASmutant cell-free DNA assays to detect metastatic melanoma in patients with low RECIST scores and non-RECIST disease progression.Mol. Oncol. 2016, 10, 157–165.
25. Ascierto, P.A.; Minor, D.; Ribas, A.; Lebbe, C.; O'Hagan, A.; Arya, N.; Guckert, M.; Schadendorf, D.; Kefford, R.F.; Grob, J.J.; et al. Phase II trial (BREAK-2) of the BRAF inhibitor dabrafenib (GSK2118436) in patients with metastatic melanoma.J. Clin. Oncol. 2013, 31, 3205–3211.
26. Syeda, M.M.; Wiggins, J.M.; Corless, B.C.; Long, G.V.; Flaherty, K.T.; Schadendorf, D.; Nathan, P.D.; Robert, C.; Ribas, A.; Davies, M.A.; et al. Circulating tumour DNA in patients with advanced melanoma treated with dabrafenib or dabrafenib plus trametinib: a clinical validation study.Lancet Oncol. 2021, 22, 370–380.
27. Gonzalez-Cao, M.; Mayo de Las Casas, C.; Jordana Ariza, N.; Manzano, J.L.; Molina-Vila, M.A.; Soriano, V.; Puertolas, T.; Balada, A.; Soria, A.; Majem, M.; et al. Early evolution of BRAFV600 status in the blood of melanoma patients correlates with clinical outcome and identifies patients refractory to therapy.Melanoma Res. 2018, 28, 195–203.
28. Varaljai, R.; Wistuba-Hamprecht, K.; Seremet, T.; Diaz, J.M.S.; Nsengimana, J.; Sucker, A.; Griewank, K.; Placke, J.M.; Horn, P.A.; von Neuhoff, N.; et al. Application of Circulating Cell-Free Tumor DNA Profiles for Therapeutic Monitoring and Outcome Prediction in Genetically Heterogeneous Metastatic Melanoma.JCO Precis. Oncol. 2019, 3, PO.18.00229.
29. Forschner, A.; Weißgraeber, S.; Hadaschik, D.; Schulze, M.; Kopp, M.; Kelkenberg, S.; Sinnberg, T.; Garbe, C.; Biskup, S.; Battke, F., Circulating Tumor DNA Correlates with Outcome in Metastatic Melanoma Treated by BRAF and MEK Inhibitors - Results of a Prospective Biomarker Study.Onco. Targets. Ther. 2020, 13, 5017–5032.
30. Balch, C.M.; Gershenwald, J.E.; Soong, S.-J.; Thompson, J.F.; Atkins, M.B.; Byrd, D.R.; Buzaid, A.C.; Cochran, A.J.; Coit, D.G.; Ding, S.; et al. Final version of 2009 AJCC melanoma staging and classification.J. Clin. Oncol. 2009, 27, 6199–6206.
31. Eisenhauer, E.A.; Therasse, P.; Bogaerts, J.; Schwartz, L.H.; Sargent, D.; Ford, R.; Dancey, J.; Arbuck, S.; Gwyther, S.; Mooney, M.; et al. New response evaluation criteria in solid tumours: revised RECIST guideline (version 1.1). Eur. J. Cancer 2009, 45, 228–47.
32. Van Wilpe, S.; Koornstra, R.; Den Brok, M.; De Groot, J.W.; Blank, C.; De Vries, J.; Gerritsen, W.; Mehra, N., Lactate dehydrogenase: a marker of diminished antitumor immunity.Oncoimmunology 2020, 9, 1731942–1731942.
33. Gershenwald, J.E.; Scolyer, R.A.; Hess, K.R.; Sondak, V.K.; Long, G.V.; Ross, M.I.; Lazar, A.J.; Faries, M.B.; Kirkwood, J.M.; McArthur, G.A.; et al. Melanoma staging: Evidence-based changes in the American Joint Committee on Cancer eighth edition cancer staging manual.CA Cancer J. Clin.2017, 67, 472–492.
34. Nosrati, A.; Tsai, K.K.; Goldinger, S.M.; Tumeh, P.; Grimes, B.; Loo, K.; Algazi, A.P.; Nguyen-Kim, T.D.L.; Levesque, M.; Dummer, R.; et al. Evaluation of clinicopathological factors in PD-1 response: derivation and validation of a prediction scale for response to PD-1 monotherapy.Br. J. Cancer 2017, 116, 1141–1147.
35. Bucheit, A.D.; Syklawer, E.; Jakob, J.A.; Bassett Jr, R.L.; Curry, J.L.; Gershenwald, J.E.; Kim, K.B.; Hwu, P.; Lazar, A.J.; Davies, M.A., Clinical characteristics and outcomes with specific BRAF and NRAS mutations in patients with metastatic melanoma.Cancer 2013, 119, 3821–3829.
36. Calbet-Llopart, N.; Potrony, M.; Tell-Marti, G.; Carrera, C.; Barreiro, A.; Aguilera, P.; Podlipnik, S.; Puig, S.; Malvehy, J.; Puig-Butille, J.A., Detection of cell-free circulating BRAF(V) (600E) by droplet digital polymerase chain reaction in patients with and without melanoma under dermatological surveillance.Br. J. Dermatol. 2020, 182, 382–389.
37. Wong, S.Q.; Raleigh, J.M.; Callahan, J.; Vergara, I.A.; Ftouni, S.; Hatzimihalis, A.; Colebatch, A.J.; Li, J.; Semple, T.; Doig, K.; et al. Circulating Tumor DNA Analysis and Functional Imaging Provide Complementary Approaches for Comprehensive Disease Monitoring in Metastatic Melanoma.JCO Precis. Oncol. 2017, 1.

Supplementary Data

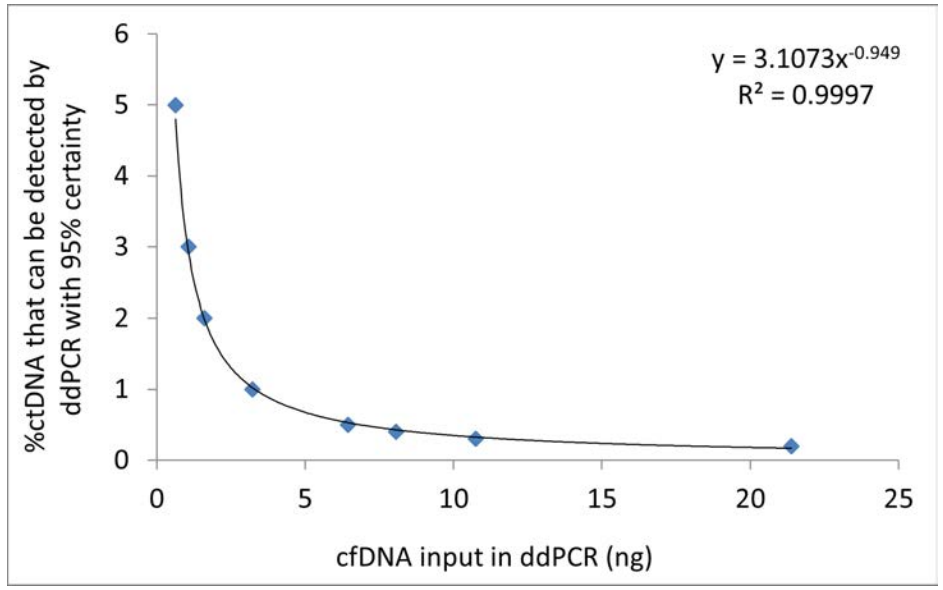

Figure S1: The theoretical sensitivity of the droplet digital PCR (ddPCR). In the graph the theoretical minimally detectable fractional abundance of mBRAF is visualized against the input DNA. The calculation is based on the binominal distribution with the assumption that a minimal of 2 mutant droplets should be detected by the ddPCR.

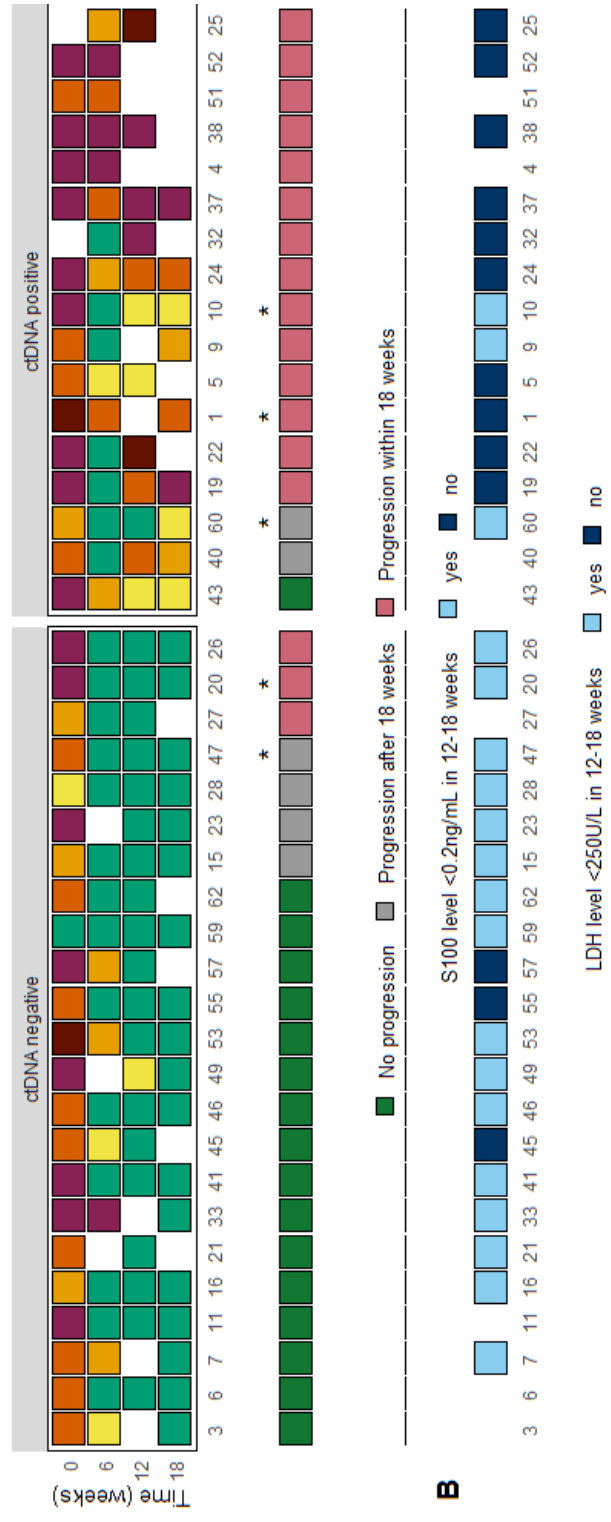

Figure S2: The ctDNA dynamics in relation to the S100 and LDH dynamics. (A) Overview of the ctDNA dynamics (mBRAF copies/mL plasma) related to treatment response within 18 weeks. Patients were stratified according to their ctDNA levels at 12–18 weeks, being either detectable (ctDNA positive) or undetectable (ctDNA negative). (B) The S100 and LDH dynamics of the patients visualized in Figure S2A. Patients in whom S100/LDH levels normalized within 12–18 weeks were marked by a light-blue box. If S100 or LDH levels remained elevated, patients were marked with a dark-blue box.

Table S1: All the droplet digital PCR data on the mBRAF assessment in all patient and control samples. Control samples included 14 plasma samples of healthy individuals and three of LDH-high melanoma patients without mBRAF in their tumor.

Patient ID[3]	Time category (Figure 2 + extra timepoints)	Exact weeks after start therapy	Plasma volume used (mL)	cell-free DNA ng/mL plasma	Total cell-free DNA input ddPCR	Minimal fractional abundance detectable in sample (%)	Mutant droplets ddPCR	mBRAF copies / mL plasma	Fractional abundance detected (%)	ctDNA dynamics category (Figure 2 and 3)
1	0 weeks	0	2.3	235.04	108.12	0.04	3148	16357	22.95	Positive
1	6 weeks	6	2.4	18.54	29.37	0.14	188	270	4.60	Positive
1	18 weeks	18	2	9.28	12.25	0.32	78	108	3.80	Positive
1	End of treatment	22	2.5	6.08	10.03	0.38	53	61	3.35	Positive
3	0 weeks	0	1.8	10.33	12.28	0.32	83	161	5.10	Negative
3	6 weeks	7	2.6	12.99	18.91	0.21	2	3	0.07	Negative
3	18 weeks	19	2.6	64.69	111.01	0.04	0	0	0.00	Negative
4	0 weeks	0	2.3	38.35	58.21	0.07	1473	2232	19.20	Positive
4	6 weeks	6	2.2	68.99	40.47	0.10	1240	3651	21.45	Positive
5	0 weeks	-1	2.4	11.91	18.87	0.21	302	415	11.55	Positive
5	6 weeks	6	2.4	14.31	22.66	0.18	2	2	0.05	Positive
5	12 weeks	14	2.1	11.85	22.23	0.18	3	3	0.08	Positive
5	Progression	28	2.5	44.99	74.24	0.06	173	181	1.32	Positive
6	0 weeks	0	2.5	14.28	23.56	0.17	98	125	2.90	Negative
6	6 weeks	6	2.7	8.51	15.17	0.26	0	0	0.00	Negative
6	12 weeks	12	2.4	10.31	16.34	0.24	0	0	0.00	Negative
6	Extra blood draw	16	2.5	7.01	11.57	0.33	0	0	0.00	Negative
6	18 weeks	18	2.5	6.03	9.95	0.39	0	0	0.00	Negative
7	0 weeks	0	2.3	23.16	35.15	0.12	82	104	1.48	Negative
7	6 weeks	6	2.6	37.95	32.89	0.12	12	27	0.24	Negative
7	18 weeks	18	2.6	44.30	76.01	0.06	0	0	0.00	Negative
9	0 weeks	0	2.4	4.87	7.71	0.49	371	482	32.70	Positive
9	6 weeks	6	1.9	73.36	37.17	0.11	0	0	0.00	Positive
9	Extra blood draw	16	2.6	12.15	20.85	0.19	3	3	0.09	Positive
9	18 weeks	19	2.6	8.83	15.14	0.26	47	59	2.20	Positive
9	End of treatment	20	2.4	7.64	12.10	0.32	316	365	15.75	Positive
10	0 weeks	0	2.7	29.29	52.20	0.08	2473	2827	31.85	Positive
10	6 weeks	6	2.4	11.92	18.88	0.21	0	0	0.00	Positive
10	12 weeks	12	2.7	5.91	10.53	0.37	3	3	0.18	Positive
10	18 weeks	17	2.5	6.76	11.16	0.35	9	9	0.46	Positive
11	0 weeks	0	2.8	25.28	46.73	0.09	1337	1317	17.20	Negative
11	6 weeks	6	2.6	9.77	16.77	0.23	0	0	0.00	Negative
11	12 weeks	12	2.4	14.39	22.80	0.18	0	0	0.00	Negative

Table S1: Continued

Patient ID[3]	Time category (Figure 2 + extra timepoints)	Exact weeks after start therapy	Plasma volume used (mL)	cell-free DNA ng/mL plasma	Total cell-free DNA input ddPCR	Minimal fractional abundance detectable in sample (%)	Mutant droplets ddPCR	mBRAF copies / mL plasma	Fractional abundance detected (%)	ctDNA dynamics category (Figure 2 and 3)
11	18 weeks	18	2.4	12.38	19.60	0.20	0	0	0.00	Negative
13	0 weeks	0	1.7	19.54	21.93	0.18	1072	1471	24.80	Baseline only
14	0 weeks	0	2.8	51.78	95.69	0.04	7855	9405	59.80	Baseline only
15	0 weeks	0	2.6	18.41	31.60	0.13	13	16	0.29	Negative
15	6 weeks	6	2.4	6.74	10.68	0.36	1	1	0.06	Negative
15	12 weeks	12	2.5	11.22	18.51	0.21	0	0	0.00	Negative
15	18 weeks	18	2.4	4.71	7.46	0.51	0	0	0.00	Negative
16	0 weeks	-1	1.2	6.01	4.76	0.78	8	17	1.50	Negative
16	6 weeks	6	1.8	10.42	12.38	0.31	0	0	0.00	Negative
16	12 weeks	12	1.4	2.73	2.53	1.42	1	2	0.30	Negative
16	18 weeks	19	1.7	16.11	18.08	0.22	0	0	0.00	Negative
17	0 weeks	0	2.1	32.96	45.68	0.09	2447	2781	28.00	Baseline only
19	0 weeks	0	1.5	28.72	28.43	0.14	1941	3169	35.20	Positive
19	6 weeks	6	2.4	3.06	4.85	0.76	0	0	0.00	Positive
19	12 weeks	12	2.8	6.50	12.01	0.32	193	165	7.70	Positive
19	18 weeks	18	2.4	12.39	19.63	0.20	1361	1422	36.80	Positive
20	0 weeks	0	2.4	23.28	36.88	0.11	2650	2861	40.55	Negative
20	6 weeks	6	2.2	11.30	16.41	0.24	0	0	0.00	Negative
20	12 weeks	12	2.7	7.44	13.25	0.29	0	0	0.00	Negative
20	18 weeks	15	2.6	13.16	22.58	0.18	0	0	0.00	Negative
21	0 weeks	0	2.5	9.42	15.55	0.25	110	136	4.75	Negative
21	12 weeks	13	2.2	5.81	8.43	0.45	0	0	0.00	Negative
22	0 weeks	0	2.4	71.69	34.41	0.12	1688	7746	35.55	Positive
22	6 weeks	6	3	9.87	19.54	0.20	1	1	0.03	Positive
22	12 weeks	12	2.7	113.97	71.80	0.06	5726	21057	60.90	Positive
23	0 weeks	0	2.3	14.81	22.48	0.18	1163	1604	35.75	Negative
23	12 weeks	12	2.9	1.63	3.13	1.15	0	0	0.00	Negative
23	18 weeks	18	2.6	3.36	5.77	0.65	0	0	0.00	Negative
24	0 weeks	0	2.6	89.47	31.01	0.13	797	4772	17.60	Positive
24	6 weeks	7	2.3	200.63	92.29	0.05	5	22	0.02	Positive
24	12 weeks	14	2.5	53.72	53.72	0.08	469	768	4.75	Positive
24	18 weeks	19	2.6	34.00	58.35	0.07	944	919	8.90	Positive
25	6 weeks	6	2.1	3.85	5.33	0.70	6	7	0.40	Positive
25	12 weeks	12	2.3	91.85	70.42	0.06	5531	12540	44.40	Positive
26	0 weeks	0	3.1	82.55	51.18	0.08	842	2697	10.80	Negative
26	6 weeks	6	2.4	56.83	36.37	0.11	0	0	0.00	Negative

Table S1: Continued

Patient ID[3]	Time category (Figure 2 + extra timepoints)	Exact weeks after start therapy	Plasma volume used (mL)	cell-free DNA ng/mL plasma	Total cell-free DNA input ddPCR	Minimal fractional abundance detectable in sample (%)	Mutant droplets ddPCR	mBRAF copies / mL plasma	Fractional abundance detected (%)	ctDNA dynamics category (Figure 2 and 3)
26	12 weeks	13	2.6	18.40	31.58	0.13	0	0	0.00	Negative
26	18 weeks	18	2.5	42.90	70.79	0.06	0	0	0.00	Negative
27	0 weeks	0	2.6	17.19	29.50	0.14	50	56	1.08	Negative
27	6 weeks	6	2.8	13.83	25.56	0.16	0	0	0.00	Negative
27	12 weeks	12	2.7	21.80	38.84	0.11	0	0	0.00	Negative
28	0 weeks	0	2.5	9.79	16.15	0.24	6	7	0.24	Negative
28	6 weeks	6	2.4	17.60	27.88	0.14	1	1	0.03	Negative
28	12 weeks	12	2.4	10.86	17.21	0.23	0	0	0.00	Negative
28	18 weeks	18	2.4	19.02	30.13	0.13	0	0	0.00	Negative
29	0 weeks	0	2.6	18.18	31.20	0.13	949	1124	20.45	Baseline only
32	6 weeks	6	2.7	15.61	27.81	0.15	1	1	0.02	Positive
32	12 weeks	12	2.5	21.10	34.81	0.12	2216	2233	34.95	Positive
33	0 weeks	0	2.4	23.93	37.90	0.11	3171	4000	55.10	Negative
33	6 weeks	6	2.6	15.94	27.36	0.15	1088	1126	23.25	Negative
33	18 weeks	17	2.5	12.10	19.97	0.20	1	1	0.03	Negative
34	0 weeks	0	2	64.36	42.91	0.10	2717	6237	32.00	Baseline only
36	0 weeks	0	2.6	11.76	20.18	0.20	680	885	24.80	Baseline only
37	0 weeks	0	2.5	18.35	30.27	0.13	1631	2107	38.00	Positive
37	6 weeks	6	2.4	14.03	22.22	0.18	596	738	17.40	Positive
37	12 weeks	12	3.1	13.52	27.67	0.15	1507	1345	32.90	Positive
37	18 weeks	18	2.7	18.04	32.15	0.13	1385	1456	26.65	Positive
38	0 weeks	0	2.6	36.77	38.25	0.11	912	1688	15.20	Positive
38	6 weeks	6	2.8	20.40	37.70	0.11	1028	1123	18.20	Positive
38	12 weeks	12	2.6	38.46	65.99	0.06	2651	2974	25.45	Positive
39	0 weeks	0	2.5	9.00	14.85	0.26	502	649	23.90	Baseline only
40	0 weeks	0	2.4	6.11	9.67	0.40	195	235	12.70	Positive
40	6 weeks	6	2.5	8.27	13.65	0.29	0	0	0.00	Positive
40	12 weeks	12	2.5	9.25	15.27	0.26	554	567	20.25	Positive
40	18 weeks	18	2.8	5.65	10.44	0.37	26	24	1.40	Positive
41	0 weeks	0	2.4	18.50	29.30	0.14	799	1089	19.45	Negative
41	6 weeks	6	2.6	5.97	10.24	0.38	0	0	0.00	Negative
41	12 weeks	12	2.6	6.64	11.40	0.34	0	0	0.00	Negative
41	18 weeks	19	2.5	4.37	7.22	0.52	0	0	0.00	Negative
42	0 weeks	0	2	48.38	45.16	0.09	2266	5351	36.50	Baseline only
43	0 weeks	0	2.3	40.65	61.71	0.07	5362	8188	66.45	Positive
43	6 weeks	7	2.6	2.97	5.10	0.73	25	24	2.80	Positive

Table S1: Continued

Patient ID[3]	Time category (Figure 2 + extra timepoints)	Exact weeks after start therapy	Plasma volume used (mL)	cell-free DNA ng/mL plasma	Total cell-free DNA input ddPCR	Minimal fractional abundance detectable in sample (%)	Mutant droplets ddPCR	mBRAF copies / mL plasma	Fractional abundance detected (%)	ctDNA dynamics category (Figure 2 and 3)
43	12 weeks	13	2.7	5.10	9.10	0.42	10	10	0.60	Positive
43	18 weeks	21	2.5	5.41	8.93	0.43	4	4	0.25	Positive
44	0 weeks	0	2.4	30.34	48.06	0.09	2036	2583	28.10	Baseline only
45	0 weeks	0	2.7	9.56	17.03	0.23	208	246	8.50	Negative
45	6 weeks	6	2.6	7.76	13.32	0.29	5	6	0.25	Negative
45	12 weeks	12	2.5	13.07	21.56	0.18	0	0	0.00	Negative
46	0 weeks	0	2.4	10.63	16.84	0.23	128	151	4.70	Negative
46	6 weeks	6	2.5	14.08	23.23	0.17	0	0	0.00	Negative
46	12 weeks	12	2.5	6.20	10.24	0.38	0	0	0.00	Negative
46	18 weeks	18	2.5	2.89	4.76	0.78	0	0	0.00	Negative
47	0 weeks	0	2.5	9.56	15.78	0.25	126	177	6.10	Negative
47	6 weeks	6	2.4	45.50	50.97	0.08	0	0	0.00	Negative
47	12 weeks	12	2.6	10.79	18.51	0.21	0	0	0.00	Negative
47	18 weeks	18	2.6	7.58	13.00	0.30	1	1	0.05	Negative
49	0 weeks	0	2.6	45.24	31.36	0.13	507	1650	12.00	Negative
49	12 weeks	12	2.6	5.85	10.03	0.38	4	4	0.21	Negative
49	18 weeks	18	2.9	4.06	7.77	0.49	1	1	0.08	Negative
50	0 weeks	0	2.6	10.86	18.64	0.21	100	113	3.40	Baseline only
51	0 weeks	0	2.8	10.39	19.20	0.21	151	171	5.45	Positive
51	6 weeks	6	2.6	7.80	13.39	0.29	138	172	7.35	Positive
52	0 weeks	0	2.5	16.77	27.68	0.15	1150	1496	29.50	Positive
52	6 weeks	7	2.5	23.33	38.50	0.11	1242	1391	19.65	Positive
53	0 weeks	0	2.5	140.12	70.06	0.06	4705	21472	50.55	Negative
53	6 weeks	6	2.9	11.61	22.23	0.18	57	48	1.35	Negative
53	12 weeks	12	2.5	125.17	62.59	0.07	1	3	0.01	Negative
53	18 weeks	17	2.4	6.80	10.77	0.36	0	0	0.00	Negative
55	0 weeks	0	2.3	6.91	10.49	0.37	481	623	29.75	Negative
55	6 weeks	6	2.5	10.12	16.70	0.24	0	0	0.00	Negative
55	12 weeks	12	1.7	47.62	53.43	0.08	0	0	0.00	Negative
55	18 weeks	18	2.5	11.97	19.75	0.20	0	0	0.00	Negative
57	0 weeks	0	2.5	24.93	41.13	0.10	1203	1473	19.50	Negative
57	6 weeks	6	2.8	17.83	32.95	0.12	54	46	0.87	Negative
57	12 weeks	12	2.8	6.40	11.83	0.33	0	0	0.00	Negative
57	End of treatment	25	2.3	3.02	4.59	0.80	0	0	0.00	Negative
59	0 weeks	0	2.7	11.00	19.60	0.20	0	0	0.00	Negative
59	6 weeks	6	2.6	18.78	32.23	0.13	0	0	0.00	Negative

Table S1: Continued

Patient ID[3]	Time category (Figure 2 + extra timepoints)	Exact weeks after start therapy	Plasma volume used (mL)	cell-free DNA ng/mL plasma	Total cell-free DNA input ddPCR	Minimal fractional abundance detectable in sample (%)	Mutant droplets ddPCR	mBRAF copies / mL plasma	Fractional abundance detected (%)	ctDNA dynamics category (Figure 2 and 3)
59	12 weeks	12	2.7	24.81	44.21	0.09	0	0	0.00	Negative
59	18 weeks	18	2.8	12.45	23.01	0.17	0	0	0.00	Negative
60	0 weeks	0	2.6	4.83	8.28	0.46	36	46	3.20	Positive
60	6 weeks	6	2.8	35.95	46.97	0.09	0	0	0.00	Positive
60	12 weeks	12	2.4	4.79	7.59	0.50	0	0	0.00	Positive
60	18 weeks	18	2.6	5.46	9.37	0.41	2	2	0.12	Positive
61	0 weeks	0	1.7	80.50	54.74	0.08	3316	10709	43.90	Baseline only
62	0 weeks	1	2.4	7.87	12.46	0.31	102	119	4.95	Negative
62	6 weeks	6	2.6	39.79	55.18	0.08	0	0	0.00	Negative
62	12 weeks	14	2.2	8.97	13.02	0.30	0	0	0.00	Negative
63	0 weeks	0	2.1	14.53	20.13	0.20	750	830	18.85	Baseline only
66	0 weeks	0	2.6	34.06	58.44	0.07	3315	3090	30.00	Baseline only
BRAF_WT_02	Patient control	0	3.4	5.03	11.29	0.34	0	0	0.00	Patient control
BRAF_WT_03	Patient control	0	3.4	13.24	29.70	0.14	0	0	0.00	Patient control
BRAF_WT_04	Patient control	0	3.1	11.73	18.00	0.22	0	0	0.00	Patient control
Healthy_1	Healthy control	0	7	6.26	17.35	0.23	0	0	0.00	Healthy control
Healthy_10	Healthy control	0	8	8.05	15.46	0.25	0	0	0.00	Healthy control
Healthy_11	Healthy control	0	10	4.53	17.93	0.22	0	0	0.00	Healthy control
Healthy_12	Healthy control	0	10	7.14	17.13	0.23	0	0	0.00	Healthy control
Healthy_13	Healthy control	0	10	4.44	17.57	0.22	0	0	0.00	Healthy control
Healthy_14	Healthy control	0	10	5.35	12.85	0.30	0	0	0.00	Healthy control
Healthy_2	Healthy control	0	8	6.05	19.17	0.21	0	0	0.00	Healthy control
Healthy_3	Healthy control	0	8	10.63	27.23	0.15	0	0	0.00	Healthy control
Healthy_4	Healthy control	0	9	4.79	17.06	0.23	0	0	0.00	Healthy control
Healthy_5	Healthy control	0	9	15.09	53.80	0.08	0	0	0.00	Healthy control
Healthy_6	Healthy control	0	9	10.65	37.97	0.11	0	0	0.00	Healthy control
Healthy_7	Healthy control	0	9	5.22	14.00	0.28	0	0	0.00	Healthy control
Healthy_8	Healthy control	0	9	10.76	23.25	0.17	0	0	0.00	Healthy control
Healthy_9	Healthy control	0	8	5.52	17.50	0.23	0	0	0.00	Healthy control

Table S2: Univariable Cox-regression analysis for the progression free survival and cancer-specific survival. HR = hazard ratio, 95% CI = 95% confidence interval.

			Progression free Survival			Cancer-specific survival		
Variable		**Patients (n)**	**HR**	**95% CI**	**p-value**	**HR**	**95% CI**	**p-value**
Baseline parameters								
Age	years	53	0.99	0.96-1.02	0.55	0.99	0.95-1.02	0.41
Sex	Female	19	Ref			Ref		
	Male	34	1.24	0.57-2.71	0.59	0.75	0.31-1.83	0.53
ECOG	Score continues	53	0.97	0.6-1.672	0.90	0.75	0.34-1.56	0.44
LDH baseline	log10[U/L]	53	1.96	0.33-11.84	0.46	1.38	0.13-14.68	0.79
S100 baseline	log10[ng/ml]	39	2.01	0.89-4.52	0.09	4.57	1.58-13.19	0.005
Skin metastasis	No	43	Ref			Ref		
	Yes	9	1.28	0.52-3.15	0.59	0.99	0.29-3.40	0.99
Lymph node metastasis	No	18	Ref			Ref		
	Yes	34	1.63	0.73-3.68	0.24	1.27	0.51-3.15	0.61
Lung metastasis	No	29	Ref			Ref		
	Yes	23	0.92	0.45-1.91	0.83	0.88	0.37-2.11	0.78
Liver metastasis	No	33	Ref			Ref		
	Yes	19	3.65	1.73-7.71	0.00069	2.49	1.05-5.89	0.0381
Kidney metastasis	No	31	Ref			Ref		
	Yes	21	0.69	0.33-1.43	0.32	0.57	0.22-1.49	0.25
Sum target lesion diameters (SLD)	log10[mm]	52	2.07	0.56-7.68	0.28	1.47	0.30-7.18	0.64
Baseline circulating cell-free DNA	log10[copies per mL plasma]	51	2.15	0.88-5.22	0.09	1.08	0.38-3.04	0.88
ctDNA baseline	log10[mBRAF per mL plasma]	51	1.68	1.07-2.64	0.0248	1.53	0.90-2.62	0.12
Longitudinal measurements								
LDH dynamics	LDH<250 U/L in 12-18 weeks	26	Ref			Ref		
	LDH>250 U/L in 12-18 weeks	24	1.93	0.92-4.03	0.08	3.1	1.24-7.76	0.016
S100 dynamics	S100<0.2ng/mL in 12-18 weeks	23	Ref			Ref		
	S100>0.2ng/mL in 12-18 weeks	16	5.5	2.21-13.71	0.00025	5.35	1.84-15.56	0.0021
ctDNA dynamics	ctDNA negative	23	Ref			Ref		
	ctDNA positive	17	12.57	4.30-36.76	0.0000038	14.6	3.30-64.62	0.000413

Table S3: An overview of the blood-based biomarkers assessed per patient at baseline and during treatment.

Patient ID	mBRAF [copies/mL plasma] at baseline	ctDNA dynamics at 12-18 weeks	S100 [ng/mL] at baseline	S100 dynamics at 12-18 weeks	LDH [U/L] at baseline	LDH dynamics at 12-18 weeks
1	16357	Positive		>ULN	589	<ULN
3	161	Negative			282	
4	2232	Positive	4.4		290	>ULN
5	415	Positive	1.43	>ULN	357	<ULN
6	125	Negative			347	<ULN
7	104	Negative	0.24	<ULN	271	>ULN
9	482	Positive	0.41	<ULN	339	<ULN
10	2827	Positive		<ULN	354	<ULN
11	1317	Negative			362	<ULN
13	1471		2.13	>ULN	357	>ULN
14	9405		4.88	<ULN	538	<ULN
15	16	Negative	0.89	<ULN	291	<ULN
16	17	Negative	0.27	<ULN	426	>ULN
17	2781		0.06	<ULN	280	<ULN
19	3169	Positive	2.09	>ULN	355	>ULN
20	2861	Negative	2.14	<ULN	354	<ULN
21	136	Negative	0.15	<ULN	288	<ULN
22	7746	Positive	1.5	>ULN	561	>ULN
23	1604	Negative	0.44	<ULN	378	<ULN
24	4772	Positive	0.74	>ULN	387	>ULN
25	Unknown	Positive	3.76	>ULN	593	>ULN
26	2697	Negative	0.4	<ULN	474	>ULN
27	56	Negative			270	>ULN
28	7	Negative	1.36	<ULN	302	<ULN
29	1124		0.33		356	>ULN
32	Unknown	Positive	2.76	>ULN	563	>ULN
33	4000	Negative	4.36	<ULN	319	<ULN
34	6237		0.2	>ULN	328	<ULN
36	885		1.02	>ULN	328	>ULN
37	2107	Positive	2.8	>ULN	584	>ULN
38	1688	Positive	1.57	>ULN	536	>ULN
39	649				335	<ULN
40	235	Positive	3.25		467	>ULN
41	1089	Negative	3.69	<ULN	412	<ULN

Table S3: Continued

Patient ID	mBRAF [copies/mL plasma] at baseline	ctDNA dynamics at 12-18 weeks	S100 [ng/mL] at baseline	S100 dynamics at 12-18 weeks	LDH [U/L] at baseline	LDH dynamics at 12-18 weeks
42	5351		10.97		419	>ULN
43	8188	Positive			590	<ULN
44	2583		2.58		1201	
45	246	Negative		>ULN	1065	<ULN
46	151	Negative	1.4	<ULN	270	>ULN
47	177	Negative	0.94	<ULN	335	<ULN
49	1650	Negative	10.2	<ULN	1013	<ULN
50	113		1.54	<ULN	1560	>ULN
51	171	Positive			368	>ULN
52	1496	Positive	0.61	>ULN	594	>ULN
53	21472	Negative		<ULN	309	<ULN
55	623	Negative	0.22	>ULN	292	>ULN
57	1473	Negative	4.3	>ULN	359	<ULN
59	0	Negative		<ULN	280	<ULN
60	46	Positive	0.54	<ULN	261	<ULN
61	10709				743	<ULN
62	119	Negative	0.51	<ULN	296	>ULN
63	830		2.3	<ULN	646	>ULN
66	3090				650	

Table S3: Continued

Chapter 6

Serial circulating tumor DNA measurements during adjuvant treatment in patients with resected stage III/IV melanoma

Sofie H. Tolmeijer
Nydia de Kock
Maartje J. Geerlings
Dirk H. van Rens
Marye J. Boers-Sonderen
Sandra van Wilpe
Winald R. Gerritsen
Avital Amir
Niven Mehra
Kalijn F. Bol
Marjolijn J.L. Ligtenberg

Preliminary analysis

Abstract

Background: Patients with resected stage III/IV melanoma can develop distant metastases despite adjuvant therapy, while other patients are cured by surgery alone. The aim of this study is to investigate whether circulating tumor DNA (ctDNA) measurements can be used to monitor molecular response to adjuvant therapy and predict relapse in patients with resected melanoma.

Patients and methods: This interim analysis includes 53 patients with resected stage III or IV BRAF or NRAS mutated melanoma, all starting adjuvant therapy. Plasma samples were collected at start of adjuvant treatment and after 1, 3, 6, 9, and 12 months of therapy. Droplet digital PCR for either BRAF V600 or NRAS Q61 was carried out to quantify ctDNA in plasma. As this study is part of an ongoing study, only descriptive statistics were used to describe ctDNA associates with clinical outcomes.

Results: CtDNA was detectable in 6/53 (11.3%) patients at the start of adjuvant treatment. In three of the patients with detectable ctDNA at baseline, ctDNA increased after 1 month of therapy and disease recurrence was observed at their first radiographic evaluation at 3 months. In the other three patients, ctDNA decreased during adjuvant treatment and no disease recurrence was observed during follow-up (range 8.0-18.1 months). CtDNA was detectable during follow-up in most patients who developed distant metastases (7/9), including 7/8 patients with visceral metastases and specifically in patients who developed liver metastases (6/6), with a median lead time of 2.5 months compared to radiographic imaging. Local recurrences were often missed by ctDNA (3/5). CtDNA remained undetectable or converted from detectable to undetectable during follow-up in 95% (37/39) of patients without a recurrence to date.

Conclusion: Preliminary analyses of this ongoing study suggest that ctDNA measurements can be utilized to evaluate early molecular response or relapse to adjuvant treatment in resected stage III/IV melanoma patients with minimal-residual disease and can aid in the early detection of distant metastases.

Introduction

Melanoma is the most aggressive form of skin cancer and its incidence increased over the past decades [1]. Until 2015, no adjuvant treatment options were available for resected advanced melanoma and approximately 40% and 60% of patients developed disease recurrence within 1 and 3 years, respectively [2-4]. The introduction of adjuvant therapy with immune checkpoint inhibitors (ICI) and BRAF/MEK inhibitors (BRAF/MEKi) has significantly improved the recurrence-free survival (RFS) of resected advanced melanoma patients [3-5]. Nevertheless, adjuvant treatment is associated with significant costs and toxicity, including grade 3-4 toxicity in 14-41% of patients [3-5]. This highlights the need for biomarkers that can be used to reduce overtreatment of patients that have already been cured by surgery and to monitor adjuvant treatment response in patients who do require additional treatment.

Circulating tumor DNA (ctDNA), the fraction of cell-free DNA that is tumor derived, is an emerging biomarker for unresectable metastatic (stage IV) melanoma. In stage IV melanoma, ctDNA reflects the tumor burden [6-12] and can be used to monitor treatment response [8, 9, 12-14]. In early-stage cancer of different tumor types, ctDNA measurements show utility to detect minimal residual disease (MRD) post-surgery [15-18]. Importantly, two large clinical trials in stage II/III colorectal cancer showed that only patients with detectable ctDNA after surgery have benefit from adjuvant treatment [15, 16]. For resected melanoma, detectable ctDNA after surgery was observed in 11.8-23.5% of patients, which was associated with a 3-10-fold higher risk of recurrence compared to patients with undetectable ctDNA if no adjuvant treatment was given [19, 20]. The effect of adjuvant therapy in resected melanoma patients with detectable versus undetectable ctDNA is still unknown. This study aims to investigate the association between detectable ctDNA at start of adjuvant treatment and clinical outcome. Additionally, using serial ctDNA measurements during adjuvant treatment, we aim to investigate if ctDNA measurements can be used to monitor molecular response to adjuvant treatment and predict recurrence.

Methods

Study design

Patients with resected stage III or IV melanoma starting standard of care adjuvant treatment were enrolled in the study between October 2019 and September 2022. Adjuvant treatment consisted of ICI directed against PD-1 (nivolumab or pembrolizumab) or BRAF/MEKi (dabrafenib plus trametinib) and was started within 12 weeks after surgery. The fast majority of patients received ICI. Patients with a BRAF

V600 or NRAS Q61 mutation in their tumor, determined by routine tissue testing, were selected for further analysis. Plasma samples for ctDNA evaluation were obtained at the start of adjuvant treatment (baseline) and 1, 3, 6, 9, and 12 months after commencing treatment. For all patients, the baseline sample and the first available follow-up sample were analyzed to determine how many patients had ctDNA-based MRD before the start of adjuvant therapy and to study if early changes in ctDNA fraction could inform on molecular treatment response. For patients with detectable baseline ctDNA and/or a recurrence additional plasma samples up to the time of recurrence were tested. As a control, for some patients without a recurrence all follow-up sample were tested. Data cut-off for clinical follow-up was at the 22nd of November 2022. The study was approved by the local medical ethical committee (dossier number 2019-5350, October 2019) and conducted in accordance with Good Clinical Practice guidelines and the Declaration of Helsinki. Written consent was obtained from all patients.

Analysis of ctDNA

Blood was collected in cell-stabilization tubes (Roche). Within five days, plasma was processed using two centrifugation steps; 10 min at 1,600g to separate plasma from blood cells applying a soft centrifuge brake and 10 min at 16,000g to remove cellular debris. To obtain maximum sensitivity, 3 blood tubes were used for total cell-free DNA (cfDNA) isolation equating a median of 12mL (inter quartile range (IQR) 11-13mL) plasma per sampling timepoint. Total cfDNA was isolated with a QIAamp Circulating Nucleic Acid kit (Qiagen) according to the manufactures protocol and DNA was eluted in 35uL low-TE buffer. DNA concentrations were measured using a Qubit High Sensitivity dsDNA kit (Thermo Fisher). Next, the presence of the BRAF V600 or NRAS Q61 mutations in plasma was measured using a droplet digital PCR BRAF V600 screening kit (#12001037, BioRad) [12] or NRAS Q61 screening kit (#12001006, RioRad). The median cfDNA input used for droplet digital PCR was 42ng (IQR 32-59ng). The limit of detection (LOD) was defined as the minimal fractional abundance which should be detectable with 95% confidence based on a binominal distribution with the total number of filled droplets. The median LOD across timepoints was 0.1% (IQR 0.07-0.13%). To ensure optimal sensitivity, while reducing false positive signals, samples with ≥1 single positive droplet and/or ≥3 double positive droplets were considered as samples with detectable ctDNA.

Statistical analysis

For patients with ctDNA-based MRD, the ctDNA response on adjuvant therapy was assessed by comparing baseline and the first on-treatment ctDNA fraction. On-treatment ctDNA was categorized into 2 scenarios: (1) ctDNA was detectable at baseline and ctDNA fraction increased during treatment or (2) ctDNA was detectable at baseline and ctDNA fraction decreased during treatment. The main outcome measure was the RFS defined as the time from commencing adjuvant treatment to local or distant recurrence evaluated by radiographic imaging and/or clinical examination. Radiographic imaging was performed every 3 months. The association between RFS and ctDNA response (ctDNA decrease vs increase) in patients with ctDNA-based MRD was described using a Kaplan-meier curve. To study the association between RFS and baseline ctDNA (undetectable vs detectable) in all patients, another Kaplan-meier curve was generated. For all patients, both with detectable and undetectable ctDNA at baseline, ctDNA measurements during follow-up were related to the development of recurrence within the study period of 12 months. For this, both the type and time of recurrence was assessed in relation to ctDNA detection. As this study represents an preliminary analysis of an ongoing study, only descriptive statistics are used to describe ctDNA associations.

Results

Patient characteristics and baseline ctDNA

In this preliminary analysis, 53 patients with resected stage III/IV melanoma were included. Patient demographics are presented in Table 1. At time of analysis, the median follow-up was 10.3 months (range 1.8-24.4 months) with 14 (26%) patients experiencing disease recurrence within the study period of 12 months. In total, 6/53 (11.3%) patients had detectable ctDNA at baseline (ctDNA-based MRD). 5/6 (83%) patients with detectable ctDNA had macroscopic regional lymph node metastasis prior to surgery. CtDNA was undetectable at baseline in all 8 stage IIIA (AJCC7) melanoma patients.

CtDNA changes during adjuvant treatment

Patients with ctDNA-based MRD showed a shorter RFS compared to patients without MRD (median 2.4 vs 24.1 months, Figure 1A). Of the patients with ctDNA-based MRD, three patients showed an increase in ctDNA after 1 month of therapy, which was associated with a fast disease recurrence (all within 3 months) and three patients showed a decrease in ctDNA in their next follow-up sample of whom none developed recurrence to-date (follow-up range 8.0-18.1 months, Figure 1B and Figure 2).

Table 1: Demographics of patients with and without detectable ctDNA at baseline

Characteristic	Total (N = 53)	Detectable ctDNA at baseline (N = 6)	Undetectable ctDNA at baseline (N = 47)
Age (years) – median (IQR)	62 (53-71)	57 (48-71)	62 (53-71)
Sex – N (%)			
Female	30 (57%)	4 (67%)	26 (55%)
Male	23 (43%)	2 (33%)	21 (45%)
Adjuvant treatment – N (%)			
Nivolumab	44 (83%)	6 (100%)	38 (81%)
Pembrolizumab	7 (13%)	0 (0%)	7 (15%)
Dabrafenib+Trametinib	2 (4%)	0 (0%)	2 (4%)
Mutation status – N (%)			
BRAF V600E/K/R	36 (68%)	5 (83%)	31 (66%)
NRAS Q61K/L/R	17 (32%)	1 (17%)	16 (34%)
Breslow (mm) – median (IQR)*	2.6 (1.7-3.9)	1.8 (0.7-5.1)	2.8 (1.8-3.8)
Ulceration – N (%)			
Yes	15 (28%)	2 (33%)	13 (28%)
No	31 (58%)	3 (50%)	28 (60%)
Unknown	7 13%)	1 (17%)	6 13%)
Tumor positive lymph nodes – N (%)			
Only in-transit or microsatellite	4 (8%)	0 (0%)	4 (9%)
1	26 (49%)	3 (50%)	23 (49%)
2-3	17 (32%)	2 (33%)	15 (32%)
≥4	6 (11%)	1 (17%)	5 (11%)
Type of lymph node involvement – N (%)			
Macro-metastasis	30 (57%)	5 (83%)	25 (53%)
Micro-metastasis	19 (36%)	1 (17%)	18 (38%)
In-transit only	3 (6%)	0 (0%)	3 (6%)
Microsatellite only	1 (2%)	0 (0%)	1 (2%)
Disease stage at baseline (AJCC7) – N (%)			
IIIA	8 (15%)	0 (0%)	8 (17%)
IIIB	29 (55%)	4 (67%)	25 (53%)
IIIC	14 (26%)	2 (33%)	12 (26%)
IV	1 (2%)	0 (0%)	1 (2%)
Disease stage at baseline (AJCC8) – N (%)			
IIIA	1 (2%)	0 (0%)	1 (2%)
IIIB	26 (49%)	4 (67%)	24 (51%)
IIIC	25 (47%)	2 (33%)	21 (45%)
IIID	0 (0%)	0 (0%)	0 (0%)
IV	1 (2%)	0 (0%)	1 (2%)

* Unknown for 4 patients.

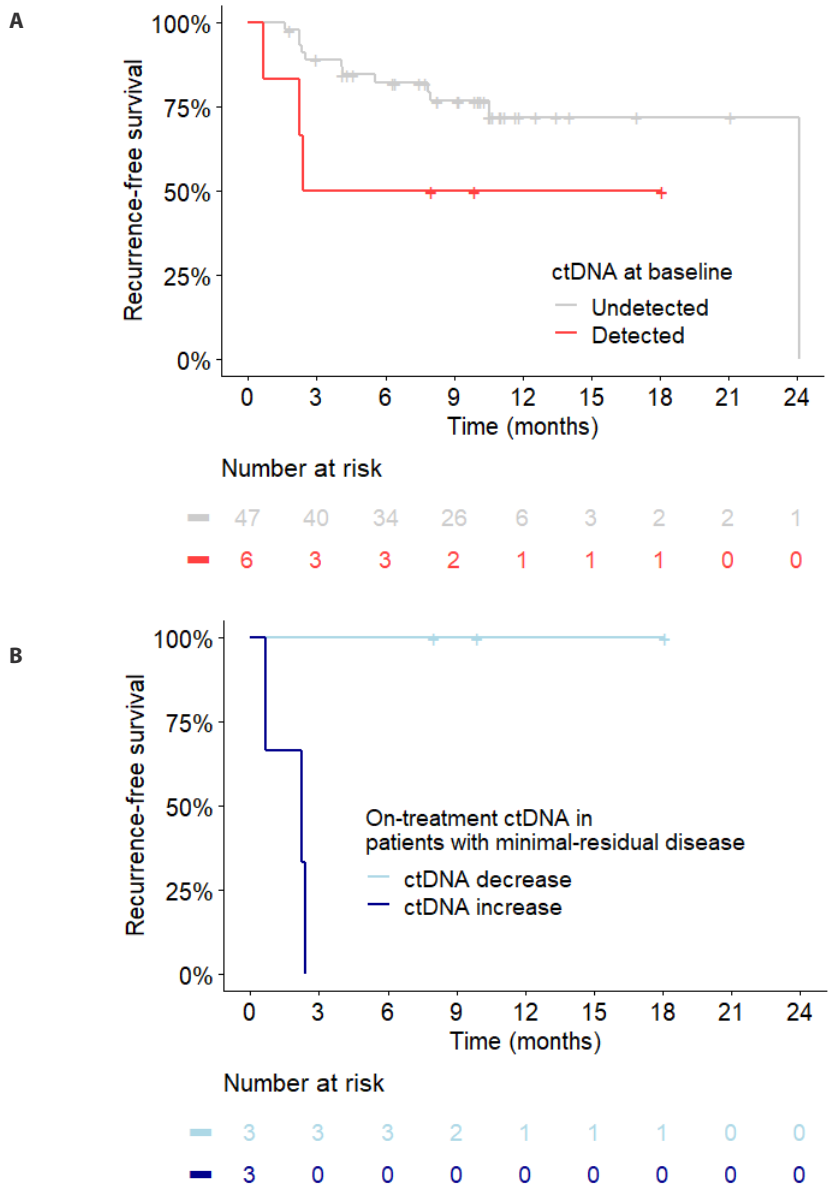

Figure 1: The association between the recurrence-free survival and the (**A**) detectability of ctDNA at baseline and (**B**) first on-treatment ctDNA fraction change. For the on-treatment ctDNA changes only patients with detected ctDNA at baseline are shown.

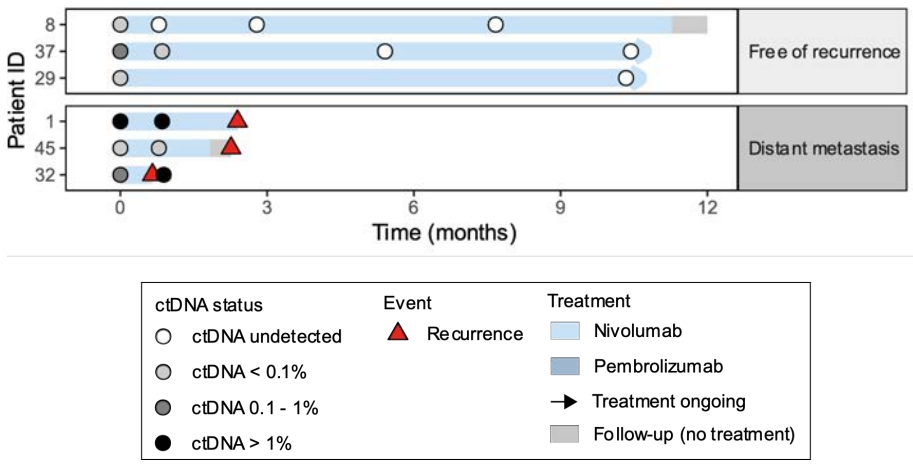

Figure 2: Swimmer plot showing the results of the serial ctDNA measurements in patients with detected ctDNA at baseline. Bar colors represent the treatment received. Bars with an arrow represent patients who are still on-treatment. Triangles represent the time of recurrence. Dots indicate the plasma sampling timepoints, with the color indicating the ctDNA fraction.

Presence of ctDNA to predict recurrence

In total, 14 patients had detectable ctDNA at baseline and/or follow-up (Figure 3A), while ctDNA remained undetectable in 39 patients (Figure 3B). Most patients who did not develop disease recurrence showed undetectable ctDNA at all timepoints (34/39) or showed a decrease in ctDNA from baseline (3/39). Only two patients without a recurrence had detectable ctDNA at 1 month, but not at baseline (Figure 3A). One of these patients had an infusion-related reaction to pembrolizumab and switched to nivolumab after 1 month of treatment after which ctDNA became undetectable again. This patient is still free of recurrence after 10.6 months follow-up. The other patient developed polyarthritis and stopped treatment. No disease recurrence was observed during 6 months follow-up and no additional ctDNA follow-up was available.

Thus far, 14 patients developed recurrence within the study period of 12 months (Figure 3A-B). Although some patients missed a ctDNA measurement at time of recurrence, distant recurrences were detected by ctDNA in 7/9 (78%) patients. CtDNA was undetectable in one patient with a brain metastasis and one patient with a solitary lung metastasis of 10mm. All patients who developed liver metastases had detectable ctDNA at or before the time of recurrence (6/6), with a median lead time of 2.5 months compared to radiographic imaging. Interestingly, one patient with undetectable ctDNA had a suspicious liver lesion on radiographic imaging that remained unchanged during follow-up scans and is therefore considered no tumor lesion.

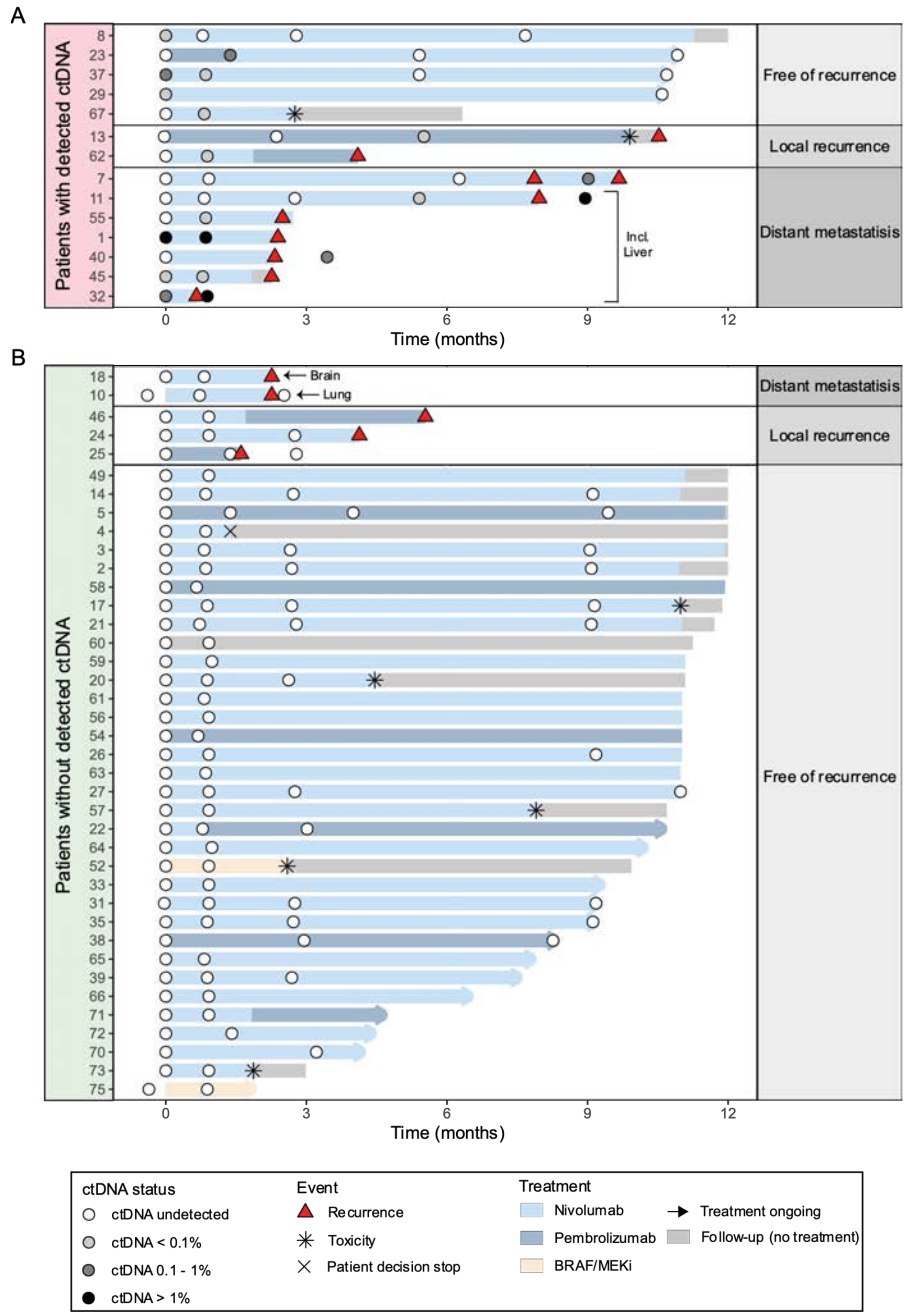

Figure 3: Swimmer plot showing the serial ctDNA detection in patients (A) with detected ctDNA at baseline or during follow-up and (B) without detected ctDNA at baseline and during follow-up. Bar colors represent the treatment received. Bars with an arrow represent patients who are still on-treatment. Triangles represent the time of recurrence. Dots indicate the plasma sampling timepoints, with the color indicating the ctDNA fraction.

For patients with a local recurrence, recurrences were detected by physical examination at timepoints not corresponding with ctDNA collection timepoints. Sometimes, samples at the time of recurrence were missed (Figure 3). Two patients showed detectable ctDNA >3 months before showing clinical local recurrence. The ctDNA fractions were below 0.1% and no second plasma sample was available to confirm ctDNA detection.

Discussion

The development of disease recurrence in stage III/IV melanoma is approximately 30% despite surgery with curative intent and adjuvant treatment. This preliminary analysis shows the potential of on-treatment ctDNA detection to monitor the molecular response to adjuvant therapy in patients with residual disease detected by ctDNA. Moreover, ctDNA analysis may indicate the presence of distant recurrence before this is possible with radiographic imaging and may be used as an alternative for pathological confirmation, requiring tissue biopsies, to confirm disease recurrence suggested by imaging.

In line with two large melanoma studies [19, 20], we detected ctDNA before the start of adjuvant treatment in 11.3% of patients. Compared to our study and the study of Lee et al. [19] (11.8%), Tan et al. [20] described a higher proportion of patients with detectable ctDNA post-surgery (23.5%). Nevertheless, more patients in the study of Tan et al. [20] had stage IIIC/D disease which is associated with higher probability of MRD [21]. Gouda et al. [22] reported an even higher proportion of melanoma patients with detectable ctDNA post-surgery using sampling timepoints a few hours after surgery and a different ctDNA quantification method applying a pre-amplification step favoring mutant alleles before ddPCR analysis. Consequently, the detection rate of MRD after melanoma resection seems dependent on the clinical characteristics of patients and technical characteristics of used assays should be carefully investigated to ensure optimal MRD detection.

Post-surgery MRD by ctDNA detection is significantly associated with a high probability of melanoma recurrence if no adjuvant treatment is given [19, 20]. In this study, we show that patients with ctDNA-based MRD have a shorter RFS compared to patients without detectable MRD despite adjuvant treatment. Additionally, early on-treatment ctDNA measurements seemed informative for the response to adjuvant treatment in patients with ctDNA-based MRD. Only patients who converted from detectable to undetectable ctDNA during treatment remained free of recurrent disease, while all patients with an increase in ctDNA as early as 1 month after treatment initiation developed rapid disease recurrences. Although limited data on ctDNA monitoring during adjuvant treatment in melanoma is available, these findings are supported by Tan et al. [20] who describe conversion from detectable to undetectable ctDNA during adjuvant ICI in two melanoma patients without disease recurrence after at least 7 months follow-up. Therefore, ctDNA could be a valuable biomarker for early adjuvant therapy monitoring in patients with detectable MRD and might be used to timely change or intensify treatment in patients with persistent ctDNA during adjuvant treatment.

Besides the identification of patients at high risk of recurrence and monitoring of adjuvant treatment response in patients with ctDNA-based MRD, we show that serial ctDNA analysis during treatment might help identify patients with recurrent disease. Especially patients who developed liver metastasis had early detectable ctDNA with a median lead time of 2.5 months compared to radiographic imaging. Interestingly, we previously showed a particularly high ctDNA abundance in stage IV melanoma patients with liver metastasis [12]. One patient with a non-progressing, and therefore a putatively benign liver lesion on radiographic imaging, had undetectable ctDNA. Consequently, ctDNA detection seems a reliable tool to detect or rule out liver metastasis and may possibly prevent invasive liver biopsies in patients with suspicious liver lesions. This could be relevant for patients with cutaneous melanoma, with the liver as one of the most common sites of distant relapse [23], and patients with uveal melanoma with >90% of patients presenting with liver metastases although recurrent hotspot mutations in other genes should be considered for ctDNA detection (e.g. GNA11, GNAQ) [24].

For the detection of local recurrences, ctDNA proves to be less suited with only 2/5 patients with a local recurrence having detectable ctDNA. In both cases, the ctDNA fraction was below 0.1% and no second sample was available to confirm the presence of ctDNA making it difficult to draw conclusions for the utility of ctDNA in patients with a local recurrence. As local recurrences are usually detected clinically, without imaging, extra diagnostic tools are unnecessary.

The vast majority of patients without disease recurrence (95%) had undetectable ctDNA at baseline and follow-up or converted from detectable to undetectable ctDNA during treatment. The negative predictive value of ctDNA detection was therefore strong, although two patients without a recurrence had detectable ctDNA after 1 month of adjuvant treatment. As ctDNA was only detected in an early plasma sample and the follow-up is still limited, these results could be false positive or a response to adjuvant treatment. Optimal sampling timepoints and the necessity of confirmatory plasma samples to ensure reliable recurrence detection should be explored in future analyses.

Although results from the larger patient cohort should be awaited, these preliminary results underline a potential of ctDNA measurements for molecular response monitoring to adjuvant treatment in patients with ctDNA-based MRD and predict the development of distant (visceral) metastases. In resected colorectal cancer, the GALAXY and DYNAMIC trial show promise for ctDNA-guided therapy after surgery, with only patients with detectable post-surgery ctDNA significantly benefitting from adjuvant treatment [15, 16]. Similar trials are now conducted for resected stage IIB/C melanoma investigating the added value of adjuvant treatment in patients with detectable ctDNA post-surgery (NCT04901988). Ultimately, the results of this preliminary analysis, validated in a larger cohort, could pave the way for new clinical trial designs investigating the added value of ctDNA testing before and during adjuvant treatment in resected stage III/IV melanoma. In these trials, ctDNA-guided adjuvant therapy administration and on-treatment ctDNA changes for adjuvant therapy modifications should be considered.

References

1. Troiani, T., et al., How we treat locoregional melanoma. ESMO Open, 2021. 6(3): p. 100136.
2. Eggermont, A.M., et al., Adjuvant ipilimumab versus placebo after complete resection of high-risk stage III melanoma (EORTC 18071): a randomised, double-blind, phase 3 trial. Lancet Oncol, 2015. 16(5): p. 522-30.
3. Long, G.V., et al., Adjuvant Dabrafenib plus Trametinib in Stage III BRAF-Mutated Melanoma. N Engl J Med, 2017. 377(19): p. 1813-1823.
4. Eggermont, A.M.M., et al., Adjuvant Pembrolizumab versus Placebo in Resected Stage III Melanoma. N Engl J Med, 2018. 378(19): p. 1789-1801.
5. Ascierto, P.A., et al., Adjuvant nivolumab versus ipilimumab in resected stage IIIB-C and stage IV melanoma (CheckMate 238): 4-year results from a multicentre, double-blind, randomised, controlled, phase 3 trial. Lancet Oncol, 2020. 21(11): p. 1465-1477.
6. Ascierto, P.A., et al., Phase II trial (BREAK-2) of the BRAF inhibitor dabrafenib (GSK2118436) in patients with metastatic melanoma. J Clin Oncol, 2013. 31(26): p. 3205-11.
7. Sanmamed, M.F., et al., Quantitative cell-free circulating BRAFV600E mutation analysis by use of droplet digital PCR in the follow-up of patients with melanoma being treated with BRAF inhibitors. Clin Chem, 2015. 61(1): p. 297-304.
8. Gray, E.S., et al., Circulating tumor DNA to monitor treatment response and detect acquired resistance in patients with metastatic melanoma. Oncotarget, 2015. 6(39): p. 42008-18.
9. Seremet, T., et al., Undetectable circulating tumor DNA (ctDNA) levels correlate with favorable outcome in metastatic melanoma patients treated with anti-PD1 therapy. J Transl Med, 2019. 17(1): p. 303.
10. Syeda, M.M., et al., Circulating tumor DNA in patients with advanced melanoma treated with dabrafenib or dabrafenib plus trametinib: a clinical validation study. Lancet Oncol, 2021. 22(3): p. 370-380.
11. Bando, H., et al., Effects of Metastatic Sites on Circulating Tumor DNA in Patients With Metastatic Colorectal Cancer. JCO Precis Oncol, 2022. 6: p. e2100535.
12. Tolmeijer, S.H., et al., Plasma BRAF Mutation Detection for the Diagnostic and Monitoring Trajectory of Patients with LDH-High Stage IV Melanoma. Cancers (Basel), 2021. 13(15).
13. Lee, J.H., et al., Circulating tumor DNA predicts response to anti-PD1 antibodies in metastatic melanoma. Annals of Oncology, 2017. 28(5): p. 1130-1136.
14. Gonzalez-Cao, M., et al., Early evolution of BRAFV600 status in the blood of melanoma patients correlates with clinical outcome and identifies patients refractory to therapy. Melanoma Res, 2018. 28(3): p. 195-203.

15. Kotani, D., et al., Molecular residual disease and efficacy of adjuvant chemotherapy in patients with colorectal cancer. Nat Med, 2023. 29(1): p. 127-134.
16. Tie, J., et al., Circulating Tumor DNA Analysis Guiding Adjuvant Therapy in Stage II Colon Cancer. N Engl J Med, 2022. 386(24): p. 2261-2272.
17. Garcia-Murillas, I., et al., Mutation tracking in circulating tumor DNA predicts relapse in early breast cancer. Sci Transl Med, 2015. 7(302): p. 302ra133.
18. Vessies, D.C.L., et al., Combining variant detection and fragment length analysis improves detection of minimal residual disease in postsurgery circulating tumor DNA of stage II-IIIA NSCLC patients. Mol Oncol, 2022. 16(14): p. 2719-2732.
19. Lee, R.J., et al., Circulating tumor DNA predicts survival in patients with resected high-risk stage II/III melanoma. Ann Oncol, 2018. 29(2): p. 490-496.
20. Tan, L., et al., Prediction and monitoring of relapse in stage III melanoma using circulating tumor DNA. Ann Oncol, 2019. 30(5): p. 804-814.
21. Gershenwald, J.E., et al., Melanoma staging: Evidence-based changes in the American Joint Committee on Cancer eighth edition cancer staging manual. CA Cancer J Clin, 2017. 67(6): p. 472-492.
22. Gouda, M.A., et al., Ultrasensitive detection of BRAF mutations in circulating tumor DNA of non-metastatic melanoma. ESMO Open, 2022. 7(1): p. 100357.
23. Romano, E., et al., Site and timing of first relapse in stage III melanoma patients: implications for follow-up guidelines. J Clin Oncol, 2010. 28(18): p. 3042-7.
24. Carvajal, R.D., et al., Metastatic disease from uveal melanoma: treatment options and future prospects. Br J Ophthalmol, 2017. 101(1): p. 38-44.

Chapter 7

Summary, general discussion and future perspectives

Summary

Cancer is one of the leading causes of death worldwide. As more and more treatment strategies become available for cancer patients, personalized medicine has become a new paradigm in healthcare. The aim of personalized medicine is to select the most optimal treatment strategy per patient to improve overall survival, and reduce unnecessary side effects, exposure to ineffective treatment and costs. To allow for personalized treatment strategies biomarkers are needed for therapy guidance. In **Chapter 1**, the potential of circulating tumor DNA (ctDNA) measurements as a promising biomarker for therapy guidance and disease monitoring both in early and late-stage cancers is introduced.

One of the key promises of ctDNA measurements is their use for molecular analyses. The molecular characteristics of the tumor can be used to select targeted therapy options or detect resistance mechanisms to treatment. A prominent and well described resistance mechanism in metastatic castration resistant prostate cancer (mCRPC) is the presence of androgen receptor (AR) alterations. The AR pathway is essential for prostate cancer growth and standard of care treatment for mCRPC include AR pathway inhibitors (ARPI). Using a systematic literature evaluation and meta-analysis, **Chapter 2** shows that the presence of an *AR* copy number gain, detected in cell-free DNA (cfDNA), is associated with an impaired response to ARPI in mCRPC patients. This impaired response was observed throughout different types of ARPI and different therapy lines. Importantly, our data suggest that patients with a cfDNA-based *AR* gain might benefit more from alternative treatment strategies such as taxane chemotherapy. This implies that ctDNA might have utility for therapy guidance in mCRPC patients.

Besides the molecular analysis of ctDNA, the quantity of ctDNA in plasma is related to tumor burden and could therefore be used for disease monitoring. In **Chapter 3** we investigated whether early changes in ctDNA fraction during ARPI treatment are predictive of mCRPC clinical outcomes. For this, ctDNA was quantified at the start of ARPI and after 4 weeks of treatment using a deep targeted sequencing approach. CtDNA was detected in 48/81 (59%) baseline and 29/81 (36%) 4-week samples. Patients with persistent ctDNA above 1% had the worst progression-free survival (PFS) and overall survival (OS). Importantly, 85% of patients experiencing non-durable responses to ARPI could be identified by detected ctDNA (>1%) at both baseline and 4 weeks, while 94% of patients with a durable response had undetected ctDNA (<1%) at 4 weeks. Consequently, the positive predictive value (PPV) and negative predictive value (NPV) for the identification of patients with a non-durable response by early on-treatment ctDNA detection was high and 4-week ctDNA fraction changes may guide early therapy switches or treatment intensification.

In **Chapter 4** we investigated early ctDNA changes in metastatic urothelial cancer (mUC) in relation to immunotherapy response. The majority of mUC patients has limited to no benefit from immunotherapy in the first or second line. Early identification of non-response will improve tumor management strategies. Utilizing a retrospective discovery cohort and a prospective validation cohort, we show that early increases in ctDNA levels (copies per mL plasma) after 3 weeks or 6 weeks of immunotherapy is highly predictive of a short PFS and OS. In the discovery cohort, ctDNA increase at 3-weeks had a PPV and NPV for identification of non-durable responses to immunotherapy of 92% and 82%, respectively. Similar results were observed for 6-week ctDNA increase. In the validation cohort, the PPV was 100% for 3-week ctDNA increase, indicating that ctDNA increase can reliably detect patients who are unlikely to have durable response to immunotherapy and might benefit from early therapy modifications.

In **Chapter 5**, serial ctDNA measurements were investigated in metastatic melanoma. All 53 patients in this study had a *BRAF*V600 mutation in their tumor. In 98% of the patients, this *BRAF*V600 mutation could also be detected in plasma using a droplet digital PCR assay. In none of the 17 control plasma samples *BRAF*V600 mutated molecules were detected, resulting in a 100% specificity for BRAF mutation detection in plasma. Consequently, plasma-based *BRAF*V600 mutation detection is a reliable and less invasive alternative to a tissue-based *BRAF* status assessment in most patients. Importantly, again we observed that patients with persistent ctDNA detection after 12-18 weeks of treatment have a shorter PFS and OS compared to patients with a reduction in ctDNA to undetectable levels (median limit of detection (LOD) of 0.2%). Changes in ctDNA levels from detected to undetected levels outperformed other blood-based biomarkers commonly used in melanoma diagnostics (LDH and S100) for outcome prediction.

Besides the utility of ctDNA measurements in late-stage metastatic diseases, ctDNA detection may also have utility for minimal residual disease (MRD) detection and prediction of disease recurrence in melanoma patients who underwent curative surgery. **Chapter 6** demonstrated that 6/53 (11.3%) of patients with resected stage III/IV melanoma still had detectable ctDNA post-surgery (median LOD of 0.1%). All patients in this study were treated with adjuvant therapy. Of all patients with ctDNA-based MRD, 3 showed an increase in ctDNA and had disease recurrence within 3 months. The other 3 patients with MRD showed a decrease in ctDNA and none showed a recurrence during follow-up. Serial ctDNA measurements during follow-up could detect most non-brain distant metastases (7/8), with a median lead time of 2.5 months for the detection of liver metastasis. Consequently, ctDNA measurements show promise for adjuvant therapy monitoring and recurrence prediction in curatively resected cancers.

General discussion

The aim of the studies described in this thesis was to investigate if ctDNA measurements can help refine therapy guidance for patients with cancer. The results of this thesis cover the applications of ctDNA in multiple cancer types, different disease stages and a variety of therapeutic strategies. Figure 1 visualizes the different ctDNA applications described in this thesis, which are discussed in more detail below.

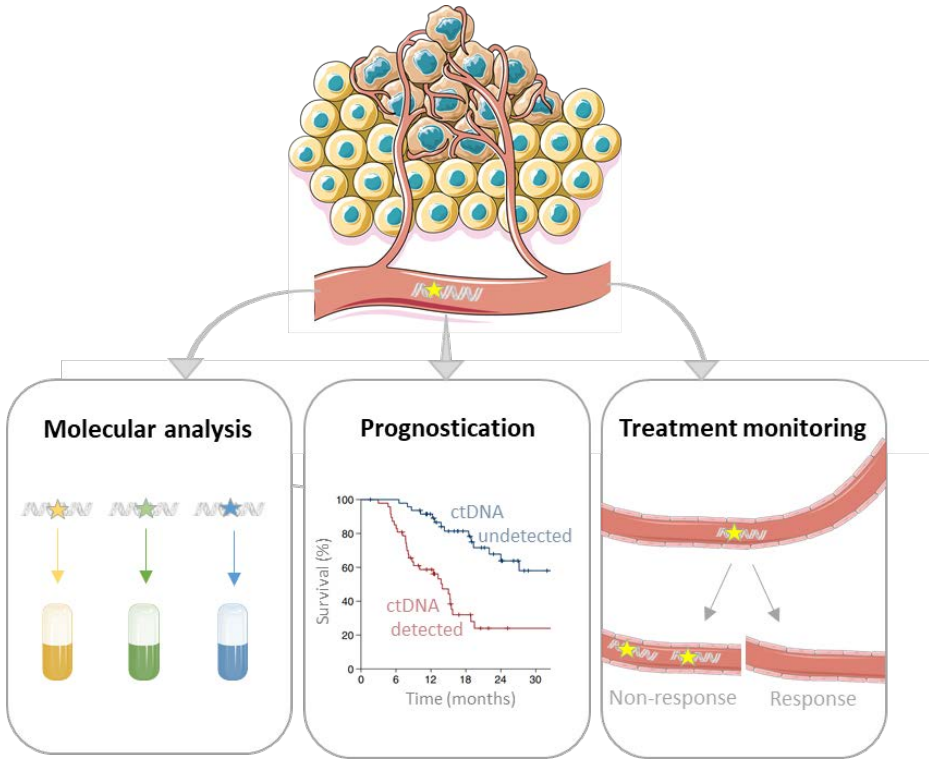

Figure 1: Applications of circulating tumor DNA

CtDNA for molecular analyses

One of the promises for ctDNA is its use for molecular diagnostics. Molecular diagnostics has become more and more important in cancer care as increasing numbers of targeted therapeutic agents have become available for cancer treatment. Examples relevant for this thesis include the detection of *BRCA1/2* alterations for PARP inhibition in prostate cancer, *FGFR* alterations in urothelial cancer for FGFR inhibitors, and *BRAF* mutations in melanoma for BRAF/MEK inhibition. In **Chapter 4**, we observed that 85% of the identified tumor tissue variants could be detected in the plasma of metastatic urothelial cancer (mUC) patients. Importantly, a higher concordance was observed between tumor tissue and plasma when the sampling time between both materials was shorter. This is in line with previous studies comparing tumor tissue results and plasma results in bladder cancer [1], lung cancer [2] and colorectal cancer [3]. Discordance between tissue and plasma is common in case of low ctDNA levels in blood, tumor evolution or tumor heterogeneity [4]. Therefore, the concordance is best for clonal mutations in patients with high ctDNA content. In line with this, we observed 98% concordance between tissue and plasma for driver mutations in BRAF in patients with LDH-high stage IV melanoma, a patient population with high ctDNA (**Chapter 5**).

The importance of plasma-based liquid biopsy testing as an alternative to tissue biopsy testing is underlined by recent clinical trials investigating PARP inhibitors in prostate cancer, such as the PROpel, TRITON2 and GALAHAD, in which liquid biopsy testing was used in combination with tissue testing or as alternative to tissue testing when tissue testing failed [5-8]. Results of the PROpel study showed that tumor tissue testing failed in 23% (186/796) of patients and molecular testing had to rely on liquid biopsy evaluation [8]. A large pan-cancer study also reported a 23% (343/1528) failure rate for next-generation sequencing (NGS) tests on tumor tissue samples with site and type of biopsy highly impacting success rates [9]. For instance, bone lesions are difficult to biopsy and are associated with high failure rates due to insufficient amount of tumor cells or insufficient quality of DNA to perform next-generation sequencing tests [9]. In patients with predominantly bone disease, such as in metastatic prostate cancer, urothelial cancer, breast cancer or lung cancer [10], ctDNA can be a valuable alternative source for molecular testing. Additionally, ctDNA testing is valuable in patients for which taking a biopsy of the tumor is highly invasive or impossible to perform. For example, lung and liver biopsies are associated with discomfort and pain in most patients plus a low but important risk on (severe) bleeding or hemorrhage [11]. Interestingly, results from this thesis demonstrated that the presence of liver metastasis is associated with a high ctDNA fraction in multiple cancer types indicating that liquid biopsies could be a reliable alternative for liver biopsies. Other prognostic clinical features, such as lactate dehydrogenase (LDH) levels, are also associated with the levels of ctDNA (**chapter 3 and 5**). Consequently, the use of ctDNA-based molecular testing could be refined based on the patient characteristics, tumor location and associated success rates of both tissue and ctDNA testing.

A great advantage of ctDNA testing over tissue testing is the minimally invasive character of obtaining blood, which allows sampling outside of (academic) hospitals, for example at general practitioner's office, and enables repetitive measurements over the course of treatment. This is particularly important when resistance mechanisms to therapy are investigated. In **Chapter 2**, we describe the prognostic and potentially

predictive value of cfDNA-based *AR* copy number gains as a resistance mechanism to treatment in mCRPC. Our meta-analysis shows a fixed effect of *AR* gain on the PFS and OS of mCRPC patients treated with ARPI, independent of the line and type of ARPI. Interestingly, the proportion of patients with a cfDNA-based *AR* gain increases with consecutive lines of treatment (**Chapter 2**). Annala et al. [12] describe not only evolution by copy number alterations in *AR*, but also structural rearrangements and mutations. Novel third-generation ARPI seem particularly effective in patients with *AR* alterations, such as activating mutations, necessitating use of ctDNA for patient selection [13]. Like the selective pressure on the AR pathway during AR pathway inhibition, others have shown occurrence of reversion mutations in *BRCA1/2* after PARP inhibition in the majority of mCRPC patients [14-17]. All these studies utilized liquid biopsies when repetitive tissue biopsies are not feasible.

Challenges of the use of liquid biopsies in cancer molecular diagnostics include the low fraction of ctDNA in a proportion of patients, which is associated with increased sequencing costs to ensure detection of low variant allele frequencies and hampers detection of copy number variations (CNVs) and structural variants. For example, tumor specific bi-allelic deletions in *BRCA1/2* were only detected in the plasma of 8/30 (27%) mCRPC patients with a bi-allelic deletion detected in their tumor, mostly due to low ctDNA content [18]. Additionally, false positive results can arise due to technical errors, such as PCR errors, or the presence of clonal hematopoiesis [19-21]. Luckily, novel approaches, such as the use of unique molecular identifiers and the sequencing of patient-matched white blood cells, can reduce false positive results in liquid biopsy testing [20, 21].

In summary, ctDNA is a valuable tool for real-time molecular cancer diagnostics but should be carefully evaluated in different technical and clinical contexts to ensure cost-effectiveness and reliability. A recent study by Kramer et al. [22] generated a micro-costing framework for ctDNA testing in Dutch clinical practice showing the wide variability of ctDNA costs in different case studies. They demonstrate that besides the impact of the technique used and the materials necessary to perform the ctDNA analyses (e.g. blood collection tubes, PCR primers, etc.), also the number of samples per run highly impacts the price per sample with lower costs associated with bulk testing. As a consequence, not only the technical and clinical context should be considered for ctDNA testing, but also the framework in which ctDNA testing is performed can potentially reduce costs. An example for such a framework is centralized testing, which is also implemented in the non-invasive prenatal testing program [23].

CtDNA quantification and prognostication

Besides the use of ctDNA for molecular profiling, the quantity of ctDNA is associated with the tumor burden of patients and seems prognostic for patient survival. In **Chapter 3 and 5**, we demonstrate that the levels of tumor markers, such as prostate specific antigen (PSA) for prostate cancer or S100 for melanoma, are correlated with the levels of ctDNA. Both the location of the tumor and the tumor volume impacts total ctDNA levels [24-27]. Despite the association between ctDNA levels and other clinical prognostic variables, multiple groups have shown the independent prognostic value of ctDNA quantity for the survival of cancer patients irrespective of treatment, making ctDNA quantity a strong prognostic marker [28-30].

Especially patients with low or undetected ctDNA tend to have a longer overall survival compared to patients with detected ctDNA, both in early-stage disease as measure for minimal residual disease (MRD) and late-stage disease [31-37]. As a results, ctDNA quantification could inform treatment strategies by advising additional treatment for patients with ctDNA-based MRD in early disease stages or treatment intensification in ctDNA-high patients with late-stage disease. The reason for high and low levels of ctDNA in patients can be related to the tumor burden, but also to the tumor biology. For example, chromosomal instable tumor have been shown to shed more ctDNA via micronuclei [38] and are often considered as more aggressive tumors [39]. Still, how detected and undetected (or high vs low levels) ctDNA is defined depends on the technique used for ctDNA detection, the LOD of the technique, the type of alterations present in the tumor and the input of total cfDNA analyzed. First, the technique used for ctDNA detection should match the alterations present in the tumor to avoid false negative ctDNA results. While tumors with a high number of CNVs may benefit from genome wide ctDNA detection approaches, tumors with only point mutations do not and require a more targeted approach. Additionally, CNV detection is limited to samples with a higher ctDNA content (>3% ctDNA [31, 40]) compared to point mutations and small insertions/deletions (<0.1% ctDNA) [41].

Furthermore, the more unique cfDNA molecules are analyzed, the lower the ctDNA fraction that can be detected [42]. In turn, the amount of cfDNA per mL of plasma is dependent on the disease type and disease stage. Figure 2 illustrates the different levels of total cfDNA and the fraction of ctDNA detected in different disease types and stages described in the thesis. While mCRPC and mUC show similar levels of cfDNA (median 11ng/mL plasma) and ctDNA (median 3%), which is also described by Husain et al. [41], LDH-high metastatic melanoma patients showed very high levels of cfDNA (median 18ng/mL plasma) and ctDNA (median 19%). Like we demonstrated in **Chapter 6** others also showed that ctDNA fraction below 0.1% can still be relevant for MRD detection and for the prediction of recurrence [33-36]. Consequently, ctDNA detection

is impacted by various clinical, biological and technical factors and the prognostic value of different cut-off levels for detected vs undetected ctDNA (or high vs low ctDNA levels) can differ per disease type and setting.

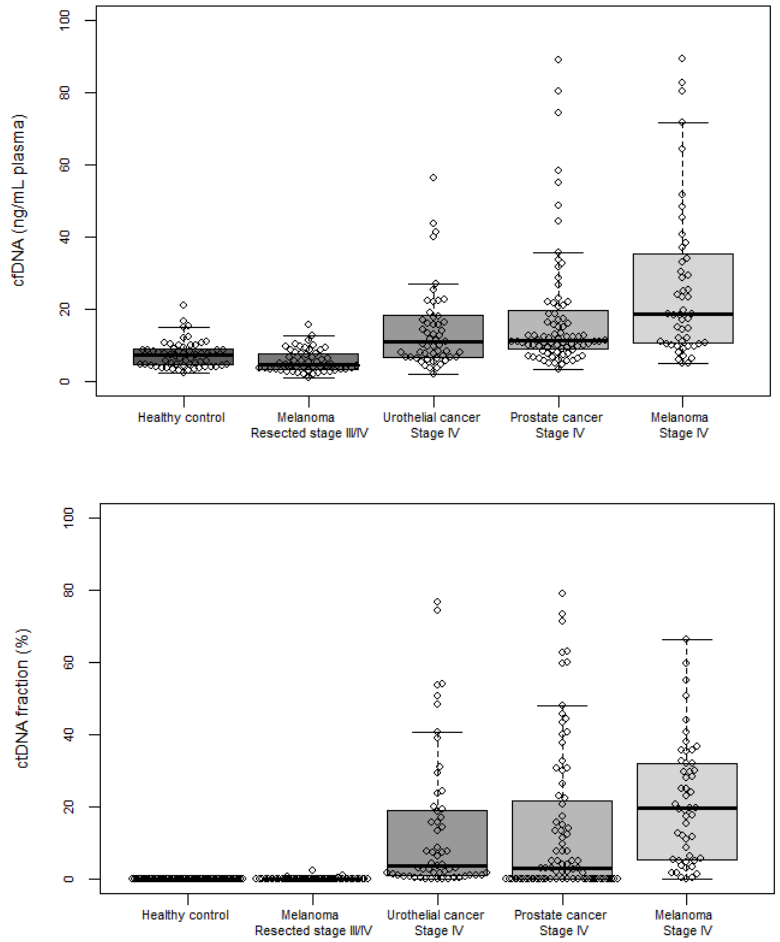

Figure 2: Plasma cell-free DNA (cfDNA) concentrations and circulation tumor DNA (ctDNA) fractions in different tumor types and stages described in this thesis.

To ensure optimal detection of low ctDNA fractions, especially for MRD detection, the amount of plasma needed for ctDNA analysis should be adjusted per disease setting. For example, for the detection of a 0.1% ctDNA fraction with 95% certainty, a cfDNA input of at least 33ng is required to have sufficient template molecules [42]. Although the conversion rate from genomic DNA to evaluable DNA molecules depends on the technique, 33ng DNA correlates to approximately 10,000 template molecules which

allows for the detection of 10 mutant molecules if 0.1% ctDNA fraction is expected. To guarantee this for most patients with resected stage III/IV melanoma >10mL plasma is needed for cfDNA isolation, while only 3mL is needed for unresected stage IV melanoma. This information is crucial for the design of robust diagnostic workflows and new clinical trials in which ctDNA evaluation is incorporated.

Finally, sensitivity of ctDNA detection can be boosted by the interrogation of other ctDNA characteristics. For example, Wan et al. [43] used machine learning on cfDNA samples from healthy individuals and individuals with stage I-IV cancer to find mutational signatures associated with the presence of ctDNA. Although this tool was not validated in an independent patient-control cohort, cross-validation revealed high accuracy of distinguishing healthy individuals from patients with stage I-IV cancer (area under the curve of 0.96). The identification of mutational signatures or point mutation detection could be combined with the identification of fragmentation patterns [43-46]. Overall, ctDNA fragments seem shorter compared to non-tumor derived cfDNA fragments [47-49]. As many tumor-derived fragments do not carry a mutation, exploiting cfDNA fragment size could provide independent information on ctDNA levels and improve sensitivity. This was also demonstrated by Cristiano et al. [44] who detected ctDNA by mutation analysis with deep targeted sequencing in 66% of stage I-IV cancer patients, but in 91% of patients when data on whole genome fragmentation was added. Importantly, whole genome fragmentation patterns detected 80% of cases with mutation-based ctDNA levels below 1%. Finally, ctDNA detection can be boosted by the analysis of tissue- and cancer-specific methylation patterns. Although this was previously hampered by technical challenges of traditional bisulfite sequencing, novel enrichment strategies have shown potential to detect the low ctDNA content that is associated with early-stage tumors [50].

Applications of sensitive ctDNA detection techniques are broad and include the use for MRD detection and cancer screening. However, sensitive ctDNA detection could also be relevant in late-stage cancers. For example, utilizing a lower limit of detection (LOD) in **Chapter 4** compared to **Chapter 3** (0.1% vs 1%, respectively), we observed more patients with detected ctDNA in mUC patients (93%, **Chapter 4**) compared to mCRPC patients (59%, **Chapter 3**) despite similar median ctDNA fractions in both cohorts. Additionally, it is not possible to investigate changes in ctDNA quantity below the LOD while these changes might still be informative for therapy monitoring. As a result, sensitivity boosting with novel techniques could potentially improve treatment monitoring for patients with undetected ctDNA by current detection strategies. The use of ctDNA testing for therapy monitoring is further discussed below.

CtDNA measurements for treatment monitoring

Thus far, the clinical utility of ctDNA measurements for molecular diagnostics and prognostication are described, including some of the technical promises and pitfalls. Given that the ctDNA burden is related to the tumor burden, ctDNA measurements during treatment can also be used to evaluate treatment responses. Advantages of ctDNA measurements compared to standard-practice radiographic evaluations of treatment response include the easy sampling of ctDNA and the possibility of early on-treatment measurements. For some cancers, no blood-based biomarkers are available to-date or biomarkers are unreliable for treatment monitoring, stressing the need for alternatives. **Chapter 3-6** all describe serial ctDNA measurements during cancer treatment for therapy and disease monitoring, but in different disease and treatment contexts.

Both **Chapter 3** and **Chapter 4** demonstrate the utility of early on-treatment ctDNA changes to predict the durability of response and the survival of metastatic cancer patients. Results suggested that ctDNA changes as early as 3-4 weeks on-treatment can identify 80-85% of patients who are likely to have no response or a non-durable response to treatment. Importantly, on-treatment detection of ctDNA was highly specific for the identification of non-durable responses in both studies, which is also reported by others in various cancer types [51-53]. Still some patients can experience a durable response to treatment despite initial unfavorable on-treatment ctDNA results. Although the reason for this is yet to be uncovered, delayed responses to therapy could play a role. Results of **Chapter 4** suggest that confirmatory ctDNA measurements at an extra timepoint during treatment might help improve both the positive predictive value (PPV) and the negative predictive value (NPV) of ctDNA changes. This is also supported by data of Parikh et al. [51] showing that especially metastatic gastrointestinal cancer patients with ctDNA reductions at multiple timepoints during systemic therapy respond well to therapy. **Chapter 5** illustrates that in case therapy is switched before disease progression, ctDNA levels change according to the response on the different therapies given. For example, fast ctDNA reductions were observed in most patients after 6 weeks of BRAF/MEKi, while fast ctDNA increases were observed in patients who switched to ICI at 6-weeks and experienced a fast disease progression thereafter. In this context, a longer follow-up might be required to identify durable responders to sequential therapies. Finally, for the detection of disease recurrence after surgery, early sampling might identify early relapse in patients with MRD (detectable ctDNA post-surgery), but a continuous ctDNA follow-up is required for timely detection of late recurrences especially in patients without MRD immediately after surgery (**Chapter 6**).

Besides the quantity and timing of ctDNA measurements to answer the specific clinical question, also the practical implementation of ctDNA measurements in the routine clinical procedures should be considered when selecting on-treatment ctDNA sampling timepoints. For example, while mCRPC patients visit the hospital every 4 weeks after the start of ARPI, mUC patients visit the hospital every 3 or 6 weeks for intravenous immunotherapy at which blood can be drawn for ctDNA testing. Consequently, practical logistics have dictated the timing of the earliest on-treatment timepoint for ctDNA evaluations in this thesis and differed per treatment setting due to differences in clinical practice. Additionally, the type of treatment will impact ctDNA dynamics. Different drugs have different steady state concentrations in blood and a different time to treatment effect can be expected regardless of the exposure-efficacy relationship. For example, the steady state concentration of ipilimumab, an immune checkpoint inhibitor (ICI), is reached after 9 weeks [54], while the steady state of dabrafenib, a BRAF inhibitor, is reached after only 2 weeks [55]. Moreover, antitumor effects of dabrafenib can mostly be observed within 6 weeks of treatment, while ICI can take months to induce an objective response by radiographic imaging [56-58]. As a result, the magnitude of ctDNA changes can be expected to differ per treatment type at different timepoints. Fundamental evidence for this is shown in this thesis. Namely, in **Chapter 3** we observed that 17/20 (85%) mCRPC patients with a durable response to ARPI (a targeted therapy) and detected ctDNA at baseline converted to undetected ctDNA after 4 weeks of treatment. In contrast, **Chapter 4** shows that only 6/17 (35%) of mUC patients with a durable response to immunotherapy and detected ctDNA at baseline converted to undetected ctDNA after 3 weeks of ICI. Although this proportion further expanded to 8/12 (57%) at 6 weeks, the overall ctDNA reduction associated with treatment response seems slower for immunotherapy compared to targeted therapy in the first few weeks of treatment. A more direct comparison between the effect of immunotherapy and targeted therapy on ctDNA dynamics can be made based on **Chapter 5**, in which metastatic melanoma patients were treated with immunotherapy alone or started BRAF/MEK inhibition for 6 weeks after which patients switched to immunotherapy. All patients with a PFS beyond 6 months cleared ctDNA after 6 weeks of BRAF/MEK inhibition (n=8), while only 5/14 (36%) patients cleared ctDNA after 6 weeks of immunotherapy. Still prominent reductions in ctDNA fractions were observed in all patients and all but 1 patient cleared ctDNA after 12-18 weeks. Combined, these results suggest that the time and magnitude of ctDNA reductions associated with a durable response to treatment can differ per treatment type.

Importantly, also the most optimal metric for ctDNA changes can differ per disease and treatment setting. While **Chapter 4** focuses on absolute changes in ctDNA levels (ctDNA copies per mL plasma), **Chapter 3, 5 and 6** focus on the detectability of ctDNA and ctDNA clearance. The advantages of dichotomizing ctDNA detection

during treatment in undetected vs detected, includes an easily understandable biomarker, even though the lower limit of detection is of importance to define detected vs undetected. Other advantages are not having to use debatable thresholds for ctDNA decline which may not be properly validated in relation to outcome (e.g. 30%, 50% or 90% reductions) and the inherent level of uncertainty surrounding ctDNA fraction estimates due to sampling bias and variability in technical execution of the ctDNA measurements. However, as described above, the ctDNA declines during treatment can vary per treatment type and disease setting and dichotomized ctDNA measurements with a specific LOD might insufficiently identify responders in particular disease settings (at early timepoints). While dichotomized ctDNA measurements are insufficiently predictive of response, reduction of ctDNA levels should be considered as metric for response prediction. Absolute ctDNA levels would be preferred over relative ctDNA fraction changes, as the ctDNA levels reflect the tumor burden more accurately compared to ctDNA fractions [27, 59-61] and ctDNA fractions are impacted by non-tumor related changes in total cfDNA such as exercise or an infection [63, 64]. Consequently, the changes in absolute rather than relative ctDNA levels might better represent the changes in actual tumor volume. At the same time, ctDNA levels are sensitive to analytical factors, such as the cfDNA isolation efficiency and molecular coverage with sequencing [61]. Combined these results suggest that the optimal and most reliable metric for on-treatment ctDNA changes can vary per disease setting and should utilize standardized ctDNA workflows to ensure reproducible results.

Besides the technical aspects affecting accuracy of on-treatment ctDNA changes to predict durability of treatment response (e.g. sampling timepoints, ctDNA detection techniques and metric used for ctDNA changes), also disease characteristics can influence predictions. For example, none of the patients described in **Chapter 5 and 6** who developed brain metastasis had detectable ctDNA. This is in line with literature [37, 65, 66], limiting the utility of blood-based ctDNA assessments for the detection of brain metastasis. Nevertheless, ctDNA measurements could also provide additional information to standard-practice radiographic imaging. For example, ctDNA reductions have been observed in patients with bone flares or pseudo-progression [67, 68], indicating that on-treatment ctDNA could help distinguish true progression from false positive radiographic imaging results. Furthermore, ctDNA measurements may also help discriminate between patients who do or don't experience a durable treatment effect while initial radiographic imaging is suggestive for stable disease. Studies in lung cancer and melanoma showed a remarkable longer disease control for patients with initial stable disease by radiographic imaging and clearance of ctDNA compared to patients with initial stable disease by radiographic imaging but without clearance of ctDNA [69-71]. In summary, the clinical applications of on-treatment ctDNA are broad and evidence for the added value of ctDNA measurements in the routine clinical practice are abundant. Still, technical and analytical factors should be carefully addressed when conducting ctDNA measurements in different disease settings.

Future perspectives

The number of studies on ctDNA measurements has greatly increased in the past decades. With more affordable sequencing techniques, optimalization of ctDNA detection and standardized (FDA approved) ctDNA assays becoming available it is now time to take the next step for implementing ctDNA measurements into the clinic. The question remains how and when to implement ctDNA measurements?

Firstly, for molecular profiling ctDNA measurements have shown great promise as alternative to tissue analysis. Clinical trials investigating ctDNA and/or tumor tissue samples for molecular profiling reported a median time from patient enrolment to ctDNA results of 10-17 days, while tissue results were obtained with a median of 33 days [72-74]. Importantly, the turnaround time for ctDNA testing was reported to improve over time with optimized lab workflows and standardization of ctDNA reporting [72]. Consequently, ctDNA testing for genomic profiling seems feasible to implement in clinical trial settings and clinical practice. Both we and others have shown high concordance between genetic aberrations detected in ctDNA and tumor tissue, with great advantages of ctDNA testing for patients with no tumor tissue material available or with (high) medical risk associated with taking a tissue biopsy. Trials such as the Prostate Cancer Biomarker Enrichment and Treatment Selections umbrella trial (NCT03385655), will give clarity on ctDNA-based treatment decision making compared to standard of care for improving the overall survival of cancer patients utilizing molecular based treatment strategies. Also, studies testing liquid biopsies and tissue biopsies in parallel should give insight in which clinical scenarios liquid biopsy testing could potentially replace tissue testing. Prediction tools for assessment of ctDNA fractions based on clinical parameters, such as ctDNA.org for mCRPC patients, might also help to select patients for liquid biopsy testing.

Secondly, ctDNA detection and quantification can be used for treatment decision making. Especially for the detection of MRD, ctDNA analysis has shown great success for the selection of patients in need of adjuvant treatment after surgery with curative-intend. For resected colorectal cancer results from the GALAXY and DYNAMIC trial demonstrated that only patients with ctDNA-based MRD benefit from adjuvant treatment [35, 36]. Although results from other trials in different solid tumors are still on the way (e.g. NCT04901988; NCT04089631), the results underline the promise for ctDNA-guided therapy, reducing cost and potential side effects of ineffective

treatment. Additionally, in advanced cancer stages ctDNA quantity can be used for treatment selection. An example is the PROTRACT trial in which mCRPC patients with a high ctDNA burden (>2%) receive chemotherapy and patients with a low ctDNA burden (<2%) receive ARPI (NCT04015622). A post-hoc analysis from the GETUG15 and CHAARTED trial indicated that patients with metastatic hormone sensitive prostate cancer (mHSPC) and a high tumor burden benefit more from early treatment intensification with docetaxel compared to those with low tumor burden [75]. Consequently, trials investigating double or triple therapy could also include ctDNA quantification to investigate whether patients with a high ctDNA burden benefit more from aggressive treatment strategies compared to patients with low ctDNA burden.

Lastly, ctDNA-based therapy modifications by on-treatment ctDNA measurements can have promise for minimally invasive disease monitoring in early and late-stage cancers. Although we and others have shown the potential of on-treatment ctDNA measurements to predict durability of treatment response or relapse, to the best of our knowledge no clinical trials studying ctDNA-informed therapeutic interventions have reported their results thus far. Nevertheless, results of many clinical trials studying the potential of on-treatment ctDNA testing to inform early therapeutic interventions in patients with unfavorable ctDNA dynamics in advanced solid tumors are now on the way (e.g. NCT04093167; NCT04966676; NCT05635630). Also in earlier cancer stages, the utility of longitudinal ctDNA measurements after surgery are tested to inform early therapeutic interventions in patients with detectable ctDNA during follow-up (e.g. NCT04966663; NCT04089631; NCT04866680). Important discussion points for the utility of ctDNA-based treatment adaptations include the required positive predictive value and negative predictive value for therapy intensification or therapy switch, the timepoints needed for ctDNA testing and the cost-effectiveness. Hopefully, the results of these clinical trials will pave the way to ctDNA implementations in routine care.

In order to make ctDNA available as standard of care for all these different clinical applications, standardization of ctDNA testing and reporting are crucial to provide consistency across hospitals. Projects such as the COIN project (ctDNA on the road to implementation in the Netherlands) help to standardize ctDNA testing across research groups. The COIN project has the goals to implement controlled, cost-effective and validated liquid biopsy testing in clinical practice in the Netherlands. By joining forces of all relevant disciplines in the field of ctDNA testing, COIN facilitate efficient implementation of ctDNA testing in routine clinical practice. This includes the development of standard operating procedures and standardization on reporting. These procedures include quality control measurements to ensure that sensitivity and specificity criteria are met, and reliable and reproducible results are reported.

With further development of improved and cost-effective detection techniques, and standardization of ctDNA testing, I believe that ctDNA testing will become standard of care in cancer management and will prove its utility in improving patient outcomes.

References

1. Vandekerkhove, G., et al., Plasma ctDNA is a tumor tissue surrogate and enables clinical-genomic stratification of metastatic bladder cancer. Nat Commun, 2021. 12(1): p. 184.
2. Thompson, J.C., et al., Detection of Therapeutically Targetable Driver and Resistance Mutations in Lung Cancer Patients by Next-Generation Sequencing of Cell-Free Circulating Tumor DNA. Clin Cancer Res, 2016. 22(23): p. 5772-5782.
3. Kagawa, Y., et al., Combined Analysis of Concordance between Liquid and Tumor Tissue Biopsies for RAS Mutations in Colorectal Cancer with a Single Metastasis Site: The METABEAM Study. Clin Cancer Res, 2021. 27(9): p. 2515-2522.
4. Merker, J.D., et al., Circulating Tumor DNA Analysis in Patients With Cancer: American Society of Clinical Oncology and College of American Pathologists Joint Review. J Clin Oncol, 2018. 36(16): p. 1631-1641.
5. Abida, W., et al., Rucaparib in Men With Metastatic Castration-Resistant Prostate Cancer Harboring a BRCA1 or BRCA2 Gene Alteration. J Clin Oncol, 2020. 38(32): p. 3763-3772.
6. Abida, W., et al., Non-BRCA DNA Damage Repair Gene Alterations and Response to the PARP Inhibitor Rucaparib in Metastatic Castration-Resistant Prostate Cancer: Analysis From the Phase II TRITON2 StudyRucaparib in mCRPC with a Non-BRCA DDR Gene Alteration. Clinical Cancer Research, 2020. 26(11): p. 2487-2496.
7. Smith, M.R., et al., Niraparib in patients with metastatic castration-resistant prostate cancer and DNA repair gene defects (GALAHAD): a multicentre, open-label, phase 2 trial. The Lancet Oncology, 2022. 23(3): p. 362-373.
8. Clarke, N.W., et al., Abiraterone and Olaparib for Metastatic Castration-Resistant Prostate Cancer. NEJM Evidence, 2022: p. EVIDoa2200043.
9. Al-Kateb, H., et al., Identification of major factors associated with failed clinical molecular oncology testing performed by next generation sequencing (NGS). Mol Oncol, 2015. 9(9): p. 1737-43.
10. Coleman, R.E., Metastatic bone disease: clinical features, pathophysiology and treatment strategies. Cancer Treat Rev, 2001. 27(3): p. 165-76.
11. Di Tommaso, L., et al., Role of liver biopsy in hepatocellular carcinoma. World J Gastroenterol, 2019. 25(40): p. 6041-6052.
12. Annala, M., et al., Evolution of Castration-Resistant Prostate Cancer in ctDNA during Sequential Androgen Receptor Pathway Inhibition. Clin Cancer Res, 2021. 27(16): p. 4610-4623.
13. Fizazi, K., et al., Phase 1 results of the ODM-208 first-in-human phase 1-2 trial in patients with metastatic castration-resistant prostate cancer (CYPIDES). Journal of Clinical Oncology, 2022. 40(6_suppl): p. 18-18.
14. Loehr, A., et al., Emergence of BRCA Reversion Mutations in Patients with Metastatic Castration-resistant Prostate Cancer After Treatment with Rucaparib. European Urology, 2022.
15. Urtishak, K., et al., High prevalence and heterogeneity of emergence of BRCA reversion mutations at progression on niraparib treatment in BRCA-mutant metastatic castration-resistant prostate cancer (mCRPC) patients. Cancer Research, 2022. 82(12_ Supplement): p. 4133-4133.
16. Warner, E., et al., BRCA2, ATM, and CDK12 Defects Differentially Shape Prostate Tumor Driver Genomics and Clinical Aggression. Clin Cancer Res, 2021. 27(6): p. 1650-1662.
17. Goodall, J., et al., Circulating Cell-Free DNA to Guide Prostate Cancer Treatment with PARP Inhibition. Cancer Discov, 2017. 7(9): p. 1006-1017.
18. Chi, K.N., et al., Detection of BRCA1, BRCA2, and ATM Alterations in Matched Tumor Tissue and Circulating Tumor DNA in Patients with Prostate Cancer Screened in PROfound. Clin Cancer Res, 2023. 29(1): p. 81-91.
19. Jensen, K., et al., Association of Clonal Hematopoiesis in DNA Repair Genes With Prostate Cancer Plasma Cell-free DNA Testing Interference. JAMA Oncol, 2021. 7(1): p. 107-110.
20. Sena, J.A., et al., Unique Molecular Identifiers reveal a novel sequencing artefact with implications for RNA-Seq based gene expression analysis. Sci Rep, 2018. 8(1): p. 13121.
21. Abbosh, C., C. Swanton, and N.J. Birkbak, Clonal haematopoiesis: a source of biological noise in cell-free DNA analyses. Ann Oncol, 2019. 30(3): p. 358-359.
22. Kramer, A., et al., A Micro-Costing Framework for Circulating Tumor DNA Testing in Dutch Clinical Practice. J Mol Diagn, 2023. 25(1): p. 36-45.
23. van der Meij, K.R.M., L. Henneman, and E.A. Sistermans, Non-invasive prenatal testing for everybody or contingent screening? Prenat Diagn, 2022.
24. Bando, H., et al., Effects of Metastatic Sites on Circulating Tumor DNA in Patients With Metastatic Colorectal Cancer. JCO Precis Oncol, 2022. 6: p. e2100535.
25. Zhang, E.W., et al., Association between circulating tumor DNA burden and disease burden in patients with ALK-positive lung cancer. Cancer, 2020. 126(20): p. 4473-4484.
26. Kirchweger, P., et al., Circulating tumor DNA correlates with tumor burden and predicts outcome in pancreatic cancer irrespective of tumor stage. Eur J Surg Oncol, 2022. 48(5): p. 1046-1053.
27. McEvoy, A.C., et al., Correlation between circulating tumor DNA and metabolic tumor burden in metastatic melanoma patients. BMC Cancer, 2018. 18(1): p. 726.
28. Reichert, Z.R., et al., Prognostic value of plasma circulating tumor DNA fraction across four common cancer types: a real-world outcomes study. Ann Oncol, 2023. 34(1): p. 111-120.
29. Annala, M., et al., Cabazitaxel versus abiraterone or enzalutamide in poor prognosis metastatic castration-resistant prostate cancer: a multicentre, randomised, open-label, phase II trial. Ann Oncol, 2021. 32(7): p. 896-905.

30. Syeda, M.M., et al., Circulating tumor DNA in patients with advanced melanoma treated with dabrafenib or dabrafenib plus trametinib: a clinical validation study. Lancet Oncol, 2021. 22(3): p. 370-380.
31. Annala, M., et al., Circulating Tumor DNA Genomics Correlate with Resistance to Abiraterone and Enzalutamide in Prostate Cancer. Cancer Discov, 2018. 8(4): p. 444-457.
32. Powles, T., et al., ctDNA guiding adjuvant immunotherapy in urothelial carcinoma. Nature, 2021. 595(7867): p. 432-437.
33. Tan, L., et al., Prediction and monitoring of relapse in stage III melanoma using circulating tumor DNA. Ann Oncol, 2019. 30(5): p. 804-814.
34. Lee, R.J., et al., Circulating tumor DNA predicts survival in patients with resected high-risk stage II/III melanoma. Ann Oncol, 2018. 29(2): p. 490-496.
35. Kotani, D., et al., Molecular residual disease and efficacy of adjuvant chemotherapy in patients with colorectal cancer. Nat Med, 2023. 29(1): p. 127-134.
36. Tie, J., et al., Circulating Tumor DNA Analysis Guiding Adjuvant Therapy in Stage II Colon Cancer. N Engl J Med, 2022. 386(24): p. 2261-2272.
37. Seremet, T., et al., Undetectable circulating tumor DNA (ctDNA) levels correlate with favorable outcome in metastatic melanoma patients treated with anti-PD1 therapy. J Transl Med, 2019. 17(1): p. 303.
38. Stejskal, P., et al., Circulating tumor nucleic acids: biology, release mechanisms, and clinical relevance. Mol Cancer, 2023. 22(1): p. 15.
39. Bakhoum, S.F. and L.C. Cantley, The Multifaceted Role of Chromosomal Instability in Cancer and Its Microenvironment. Cell, 2018. 174(6): p. 1347-1360.
40. Norgaard, M., et al., Prognostic Value of Low-Pass Whole Genome Sequencing of Circulating Tumor DNA in Metastatic Castration-Resistant Prostate Cancer. Clin Chem, 2023.
41. Husain, H., et al., Tumor Fraction Correlates With Detection of Actionable Variants Across > 23,000 Circulating Tumor DNA Samples. JCO Precis Oncol, 2022. 6: p. e2200261.
42. Heitzer, E., et al., Current and future perspectives of liquid biopsies in genomics-driven oncology. Nat Rev Genet, 2019. 20(2): p. 71-88.
43. Wan, J.C.M., et al., Genome-wide mutational signatures in low-coverage whole genome sequencing of cell-free DNA. Nat Commun, 2022. 13(1): p. 4953.
44. Cristiano, S., et al., Genome-wide cell-free DNA fragmentation in patients with cancer. Nature, 2019. 570(7761): p. 385-389.
45. Vessies, D.C.L., et al., Combining variant detection and fragment length analysis improves detection of minimal residual disease in postsurgery circulating tumor DNA of stage II-IIIA NSCLC patients. Mol Oncol, 2022. 16(14): p. 2719-2732.
46. Renaud, G., et al., Unsupervised detection of fragment length signatures of circulating tumor DNA using non-negative matrix factorization. Elife, 2022. 11.
47. Mouliere, F., et al., Enhanced detection of circulating tumor DNA by fragment size analysis. Sci Transl Med, 2018. 10(466).
48. Chabon, J.J., et al., Integrating genomic features for non-invasive early lung cancer detection. Nature, 2020. 580(7802): p. 245-251.
49. Marass, F., et al., Fragment Size Analysis May Distinguish Clonal Hematopoiesis from Tumor-Derived Mutations in Cell-Free DNA. Clin Chem, 2020. 66(4): p. 616-618.
50. Shen, S.Y., et al., Sensitive tumor detection and classification using plasma cell-free DNA methylomes. Nature, 2018. 563(7732): p. 579-583.
51. Parikh, A.R., et al., Serial ctDNA Monitoring to Predict Response to Systemic Therapy in Metastatic Gastrointestinal Cancers. Clin Cancer Res, 2020. 26(8): p. 1877-1885.
52. Kruger, S., et al., Repeated mutKRAS ctDNA measurements represent a novel and promising tool for early response prediction and therapy monitoring in advanced pancreatic cancer. Ann Oncol, 2018. 29(12): p. 2348-2355.
53. Olsson, E., et al., Serial monitoring of circulating tumor DNA in patients with primary breast cancer for detection of occult metastatic disease. EMBO Mol Med, 2015. 7(8): p. 1034-47.
54. Feng, Y., et al., Model-based clinical pharmacology profiling of ipilimumab in patients with advanced melanoma. Br J Clin Pharmacol, 2014. 78(1): p. 106-17.
55. Ouellet, D., et al., Population pharmacokinetics of dabrafenib, a BRAF inhibitor: effect of dose, time, covariates, and relationship with its metabolites. J Clin Pharmacol, 2014. 54(6): p. 696-706.
56. Bowyer, S., et al., Dabrafenib and its use in the treatment of metastatic melanoma. Melanoma Manag, 2015. 2(3): p. 199-208.
57. Robert, C., et al., Pembrolizumab versus ipilimumab in advanced melanoma (KEYNOTE-006): post-hoc 5-year results from an open-label, multicentre, randomised, controlled, phase 3 study. Lancet Oncol, 2019. 20(9): p. 1239-1251.
58. Le, D.T., et al., Phase II Open-Label Study of Pembrolizumab in Treatment-Refractory, Microsatellite Instability-High/Mismatch Repair-Deficient Metastatic Colorectal Cancer: KEYNOTE-164. J Clin Oncol, 2020. 38(1): p. 11-19.
59. Smith, J.T., et al., Circulating Tumor DNA as a Biomarker of Radiographic Tumor Burden in SCLC. JTO Clin Res Rep, 2021. 2(3): p. 100110.
60. Strijker, M., et al., Circulating tumor DNA quantity is related to tumor volume and both predict survival in metastatic pancreatic ductal adenocarcinoma. Int J Cancer, 2020. 146(5): p. 1445-1456.
61. Bos, M.K., et al., Comparison of variant allele frequency and number of mutant molecules as units of measurement for circulating tumor DNA. Mol Oncol, 2021. 15(1): p. 57-66.
62. Viller Tuxen, I., et al., Plasma total cell-free DNA is a prognostic biomarker of overall survival in metastatic solid tumor patients. Br J Cancer, 2019. 121(2): p. 125-130.

63. Jing, Q., C.H.C. Leung, and A.R. Wu, Cell-Free DNA as Biomarker for Sepsis by Integration of Microbial and Host Information. Clin Chem, 2022. 68(9): p. 1184-1195.
64. Haller, N., et al., Circulating, cell-free DNA as a marker for exercise load in intermittent sports. PLoS One, 2018. 13(1): p. e0191915.
65. Lee, J.H., et al., Circulating tumor DNA predicts response to anti-PD1 antibodies in metastatic melanoma. Annals of Oncology, 2017. 28(5): p. 1130-1136.
66. Wong, S.Q., et al., Circulating Tumor DNA Analysis and Functional Imaging Provide Complementary Approaches for Comprehensive Disease Monitoring in Metastatic Melanoma. Jco Precision Oncology, 2017. 1.
67. Lee, J.H., et al., Association Between Circulating Tumor DNA and Pseudoprogression in Patients With Metastatic Melanoma Treated With Anti-Programmed Cell Death 1 Antibodies. JAMA Oncol, 2018. 4(5): p. 717-721.
68. Conteduca, V., et al., Flare phenomenon in prostate cancer: recent evidence on new drugs and next generation imaging. Ther Adv Med Oncol, 2021. 13: p. 1758835920987654.
69. Anagnostou, V., et al., Dynamics of Tumor and Immune Responses during Immune Checkpoint Blockade in Non-Small Cell Lung Cancer. Cancer Res, 2019. 79(6): p. 1214-1225.
70. Goldberg, S.B., et al., Early Assessment of Lung Cancer Immunotherapy Response via Circulating Tumor DNA. Clin Cancer Res, 2018. 24(8): p. 1872-1880.
71. Warburton, L., et al., Circulating Tumor DNA in Advanced Melanoma Patients Ceasing PD1 Inhibition in the Absence of Disease Progression. Cancers (Basel), 2020. 12(11).
72. Kwan, E.M., et al., Prospective ctDNA genotyping for treatment selection in metastatic castration-resistant prostate cancer (mCRPC): The Canadian Cancer Trials Group phase II PC-BETS umbrella study. Journal of Clinical Oncology, 2023. 41(6_suppl): p. 218-218.
73. Turner, N.C., et al., Circulating tumor DNA analysis to direct therapy in advanced breast cancer (plasmaMATCH): a multicentre, multicohort, phase 2a, platform trial. Lancet Oncol, 2020. 21(10): p. 1296-1308.
74. Nakamura, Y., et al., Clinical utility of circulating tumor DNA sequencing in advanced gastrointestinal cancer: SCRUM-Japan GI-SCREEN and GOZILA studies. Nat Med, 2020. 26(12): p. 1859-1864.
75. Gravis, G., et al., Burden of Metastatic Castrate Naive Prostate Cancer Patients, to Identify Men More Likely to Benefit from Early Docetaxel: Further Analyses of CHAARTED and GETUG-AFU15 Studies. Eur Urol, 2018. 73(6): p. 847-855.

Chapter 8

Nederlandse samenvatting

De behandelmogelijkheden voor patiënten met kanker worden steeds uitgebreider. Dit geldt zowel voor chirurgische en radiotherapeutische strategieën als voor systemische therapieën, die steeds vaker gericht zijn op tumoren met specifieke moleculaire kenmerken. Hierdoor is er meer aandacht gekomen voor gepersonaliseerde zorg. Het doel van gepersonaliseerde zorg is het selecteren van het meest optimale behandelplan per patiënt. Betrouwbare biomarkers kunnen helpen bij het selecteren of monitoren van een behandeling. In **hoofdstuk 1** wordt de potentie van circulerend tumor DNA (ctDNA), de fractie cel-vrij DNA in het bloed dat afkomstig is van de tumor, als een veelbelovende biomarker voor het selecteren en monitoren van de behandeling van kankerpatiënten beschreven.

Eén van de mogelijkheden is het gebruik van ctDNA om de moleculaire karakteristieken van tumoren in kaart te brengen. Dit is met name van belang indien weefsel van de tumor(en) zelf niet of moeilijk verkregen kan worden. Met een moleculaire karakterisatie kan er gekeken worden welke behandelopties aansluiten op de moleculaire kenmerken van de tumor en welke resistentiemechanismes aanwezig zijn. In **hoofdstuk 2** wordt ingegaan op een veelvoorkomend resistentiemechanisme in castratieresistente prostaatkanker: een toename van androgeenreceptor (AR) kopieën. Met een systematische review is de betekenis van een toename in AR kopieën, gemeten in cel-vrij DNA uit bloedplasma, onderzocht. Dit bleek geassocieerd te zijn met een slechtere respons op AR remmers. Mogelijk hebben patiënten met een toename in AR kopieën in hun cel-vrij DNA meer baat bij een alternatieve behandeling, zoals chemotherapie. Dit zal verder prospectief moeten worden uitgezocht voor het in de klinische praktijk kan worden toegepast.

Naast het gebruik van ctDNA bij de moleculaire karakterisatie van de tumor, kunnen veranderingen in de hoeveelheid ctDNA tijdens een behandeling informatie geven over het effect van de behandeling. De hoeveelheid ctDNA in het bloed is namelijk gerelateerd aan het tumorvolume. In **hoofdstuk 3** beschrijven wij de voorspellende waarden van een afname in ctDNA tot ondetecteerbare niveaus (<1%) voor het bepalen van de effectiviteit van de behandeling van castratieresistent prostaatkanker. Hiervoor werd ctDNA in 81 patiënten voor de start van de behandeling en na 4 weken gemeten. De patiënten met detecteerbaar ctDNA op beide tijdspunten hadden de slechtste progressievrije en totale overleving. De ctDNA metingen hadden een goede voorspellende waarde voor het identificeren van patiënten met weinig baat van de behandeling en zouden mogelijk kunnen worden gebruikt bij het vroegtijdig aanpassen van het behandelplan.

In **hoofdstuk 4** onderzochten wij veranderingen in de hoeveelheid ctDNA tijdens immunotherapie bij patiënten met uitgezaaid urotheelcelcarcinoom. Hierbij zagen wij dat een toename in ctDNA tijdens de eerste 3 tot 6 weken van de behandeling sterk voorspellend was voor een snelle progressie en korte overleving. Deze observatie werd bevestigd in een validatiecohort. CtDNA metingen tijdens de eerste weken immunotherapie zouden daarom kunnen helpen bij het identificeren van patiënten die mogelijk baat hebben van een alternatief behandelplan.

In **hoofdstuk 5** werden ctDNA metingen onderzocht voor zowel de moleculaire analyse als het monitoren van de behandeling van patiënten met een uitgezaaid melanoom. In 98% van de patiënten met een *BRAF* mutatie in de tumor kon de mutatie ook gedetecteerd worden in bloed. Hieruit blijkt dat ctDNA een betrouwbaar en minimaal invasief alternatief voor de moleculaire diagnostiek op melanoomweefsel kan zijn. Verder was een afname in ctDNA tot ondetecteerbare niveaus (<0.2%) tijdens de eerste 12-18 weken van de behandeling gerelateerd aan een langdurige respons op systemische therapie. CtDNA metingen waren hierbij sterker voorspellend dan biomarkers die nu regulier in bloed worden gemeten.

In **hoofdstuk 6** werd ctDNA gebruikt als biomarker voor residuale ziekte na de operatie van een melanoom met regionale lymfklier metastase. In 6/53 patiënten kon ctDNA gedetecteerd worden na de operatie. Patiënten met een toename in ctDNA tijdens adjuvante behandeling hadden een snelle terugkeer van de ziekte, terwijl patiënten met een afname in ctDNA tijdens adjuvante behandeling geen terugkeer van de ziekte lieten zien. Patiënten die viscerale metastases kregen, ontwikkelden veelal detecteerbaar ctDNA tijdens hun follow-up. Met name bij patiënten met levermetastase werd een toename in ctDNA vaak al gedetecteerd voordat de metastase zichtbaar was met beeldvorming.

Hoofdstuk 7 biedt een algemene discussie over de bevindingen die zijn beschreven in dit proefschrift. De beloftes en uitdagingen van ctDNA analyses voor de moleculaire karakterisatie van de tumor, het gebruik van ctDNA niveaus voor het stellen van een prognose van patiënten en het gebruik van ctDNA bij het monitoren van systemische behandelingen worden belicht. Verder wordt gespeculeerd over de klinische implementatie van cfDNA analyses.

Appendices

PhD portfolio

Research data management

List of publications

Curriculum vitae

Dankwoord

PhD portfolio of Sofie H. Tolmeijer

Department: **Medical Oncology**
PhD period: **01/01/2019 – 31/03/2023**
PhD Supervisor(s): **Dr. N. Mehra, Prof. Dr. M.J.L. Ligtenberg, Prof. Dr. W.R. Gerritsen**
PhD Co-supervisor(s): **Dr. M.J. Geerlings-Wagemaker**

Training activities	Hours
Courses	
RIMLS - Introduction course "In the lead of my PhD" (2019)	15.00
RIMLS PhD course (2019)	21.00
Literature Review for your PhD (2019)	14.00
Meet the expert Illustrator (2019)	2.80
EBROK (2019)	42.00
Statistiek voor promovendi met SPSS (opfriscursus) (2019)	56.00
RU - Scientific Writing for PhD candidates (2020)	84.00
Radboudumc - Scientific integrity (2020)	20.00
IMM - Scientific Integrity (2020)	16.00
RU - Mindfulness Based Stress Reduction (2020)	28.00
RU - Grant Writing and Presenting for Funding Committees (2022)	18.00
The next step in my career (2022)	24.00
Seminars	
Webinar: Clinical Application of Circulating Tumour DNA in Melanoma (2019)	1.00
	1.00
Webinar Life Sciences: A complete workflow for analysis of cfDNA from plasma to variant (2020)	1.00
Robust Detection of Translocations in FFPE Biopsies with TLA-based NGS Application (2020)	1.00
GenomeWebinars: Adoption of Broad NGS Profiling for HRR Deficiency:	6.00
Looking Beyond BRCA, SNPs, and Indels (2020)	6.00
Illumina Virtual Benchtop Day (Benelux) (2021)	
Radboud Research Rounds 2019-2022 (2023)	
Conferences	
Speaker tour Prof. Dr. Fizazi (2019)	5.60
Symposium Da Vinci Challenge (2019)	2.80
PhD retreat 2019 (2019)	16.00
Human Genetics Infrastructure day (2019)	7.00
Mini Symposium Somatic Variant Analysis (2019)	2.80
Derde Nederlandse cfDNA themaday 2019 (2019)	14.00
Prostate Cancer Acedemy 2019 (2019)	14.00
Seminar Dr. Alexander Wyatt (incl. oral presentation) (2019)	14.00
ENABLE - Radboud Frontiers (incl. poster presentation) (2019)	42.00
ASCO Virtual Meeting 2020 (2020)	24.00
ESHG Congress 2020 (Vitual) (2020)	24.00
5th LBx Summit: Liquid Biopsy for precision Oncology Summit (2021)	15.00
Radboudumc Prostaatkanker Patienten Symposium 2021 (incl. oral presentation) (2021)	10.00
	21.00
PhD retreat (incl. poster presentation) (2021)	24.00
Radboud New Frontiers (incl. poster presentation) (2021)	56.00
ASCO meeting Chicago 2022 (incl. poster presentation) (2022)	8.00
Nederlandse cfDNA dag 2022 (2022)	28.00
Radboudumc Cancer Research Retreat 2022 (incl. oral presentation) (2022)	28.00
PhD retreat 2022 (incl. oral presentation) (2022)	12.00
Prostate Cancer Academy (incl. oral presentation) (2022)	
Other	
Introduction day Radboudumc (2019)	14.00
Workshop: Interpretation of variants from whole exome sequencing data (2019)	14.00
Workshop Personal Grant Writing (2021)	2.00
Participation Theme Discussion department of Human Genetics (2022)	120.00
Teaching activities	
Lecturing	
Grant Proposal Supervision + Participation in Workshops (2020)	66.00
Supervision of internships / other	
Bachelor Student Supervision (2022)	60.00
Total	**1,001.00**

Research data management

All human studies included in this thesis were conducted in accordance with the principles of the Declaration of Helsinki. The studies meet the criteria for proper use of human samples of the Netherlands. The medical and ethical review board 'Committee on Research Involving Human Subjects Region Arnhem Nijmegen, Nijmegen, the Netherlands' has given approval to conduct these studies. The research data obtained during this PhD trajectory is archived according to the Findable, Accessible, Interoperable and Reusable (FAIR) principles. All laboratory experiments performed in this thesis were documented in Labguru, a digital lab book client which is centrally stored and daily backed-up on the local Radboudumc server. All sequencing data generated for **chapter 3** are stored on the Tambio server in the Vancouver Prostate Centre and are available at the European Genome-phenome Archive (accession code EGAS00001006856) under standard controlled release. All sequencing data generated for **chapter 4** are stored on a local server for bulk data of the Medical Oncology department of the Radboudumc. All ddPCR data generated for **chapter 5 and 6** are stored digitally on a local server of the Medical Oncology department of the Radboudumc ("H:\Niven Mehra\Sofie Tolmeijer\Projecten\ Melanoma - COWBOY studie\ddPCR data" and "H:\Niven Mehra\Sofie Tolmeijer\Projecten\Melanoma - BAM studie\ddPCR data", respectively). Additionally, de-identified clinical data used in chapter 3-6 have been documented in the electronic data capture (EDC) system Castor. All data will be stored for 15 years after termination of the studies. Most data collected during this PhD trajectory are included in the chapters of this thesis and are part of published articles. Additional data is available from the corresponding author upon reasonable request.

List of publications

Tolmeijer SH, van Wilpe S, Geerlings MJ, von Rhein D, Smilde TJ, Kloots ISH, Westdorp H, Coskuntürk M, Oving IM, van Ipenburg JA, van der Heijden AG, Hofste T, Weiss MM, Schalken JA, Gerritsen WR, Ligtenberg MJL, Mehra N. Early On-treatment Circulating Tumor DNA Measurements and Response to Immune Checkpoint Inhibitors in Advanced Urothelial Cancer. European Urology Oncology. 2023 Sept; doi: 10.1016/j.euo.2023.08.009

Tolmeijer SH, Boerrigter E, Sumiyoshi T, Kwan EM, Ng S, Annala M, Donnellan G, Herberts C, Benoist GE, Hamberg P, Somford DM, van Oort IM, Schalken JA, Mehra N, van Erp NP, Wyatt AW. Early on-treatment changes in circulating tumor DNA fraction and response to enzalutamide or abiraterone in metastatic castration-resistant prostate cancer. Clin Cancer Res. 2023 Mar 30:CCR-22-2998. doi: 10.1158/1078-0432.CCR-22-2998. PMID: 36996325.

Tolmeijer SH, Koornstra RHT, de Groot JWB, Geerlings MJ, van Rens DH, Boers-Sonderen MJ, Schalken JA, Gerritsen WR, Ligtenberg MJL, Mehra N. Plasma BRAF Mutation Detection for the Diagnostic and Monitoring Trajectory of Patients with LDH-High Stage IV Melanoma. Cancers (Basel). 2021 Aug 3;13(15):3913. doi: 10.3390/cancers13153913. PMID: 34359813; PMCID: PMC8345527.

Tolmeijer SH, Boerrigter E, Schalken JA, Geerlings MJ, van Oort IM, van Erp NP, Gerritsen WR, Ligtenberg MJL, Mehra N. A Systematic Review and Meta-Analysis on the Predictive Value of Cell-Free DNA-Based Androgen Receptor Copy Number Gain in Patients With Castration-Resistant Prostate Cancer. JCO Precis Oncol. 2020 Nov;4:714-729. doi: 10.1200/PO.20.00084. PMID: 35050750.

van Wilpe S, **Tolmeijer SH**, Koornstra RHT, de Vries IJM, Gerritsen WR, Ligtenberg M, Mehra N. Homologous Recombination Repair Deficiency and Implications for Tumor Immunogenicity. Cancers (Basel). 2021 May 7;13(9):2249. doi: 10.3390/cancers13092249. PMID: 34067105; PMCID: PMC8124836.

van Wilpe S, **Tolmeijer SH**, de Vries IJM, Koornstra RHT, Mehra N. LDH Isotyping for Checkpoint Inhibitor Response Prediction in Patients with Metastatic Melanoma. Immuno. 2021; 1(2):67-77. https://doi.org/10.3390/immuno1020005

Xie Y, **Tolmeijer SH**, Oskam JM, Tonkens T, Meijer AH, Schaaf MJM. Glucocorticoids inhibit macrophage differentiation towards a pro-inflammatory phenotype upon wounding without affecting their migration. Dis Model Mech. 2019 May 30;12(5):dmm037887. doi: 10.1242/dmm.037887. PMID: 31072958; PMCID: PMC6550045.

Geerlings MJ, Hofste LSM, Kamping EJ, Abdi Z, **Tolmeijer SH**, Garms LM, Klarenbeek BR, Ligtenberg MJL. Effect of Pneumatic Tube System Transport on Cell-Free DNA. Clin Chem. 2021 Jan 30;67(2):434-435. doi: 10.1093/clinchem/hvaa285. PMID: 33280007.

Hofste LSM, Geerlings MJ, von Rhein D, **Tolmeijer SH**, Weiss MM, Gilissen C, Hofste T, Garms LM, Janssen MJR, Rütten H, Rosman C, van der Post RS, Klarenbeek BR, Ligtenberg MJL. Circulating Tumor DNA-Based Disease Monitoring of Patients with Locally Advanced Esophageal Cancer. Cancers (Basel). 2022 Sep 11;14(18):4417. doi: 10.3390/cancers14184417. PMID: 36139577; PMCID: PMC9497103.

Marijt KA, Sluijter M, Blijleven L, **Tolmeijer SH**, Scheeren FA, van der Burg SH, van Hall T. Metabolic stress in cancer cells induces immune escape through a PI3K-dependent blockade of IFNγ receptor signaling. J Immunother Cancer. 2019 Jun 13;7(1):152. doi: 10.1186/s40425-019-0627-8. PMID: 31196219; PMCID: PMC6567539.

Curriculum vitae

Sofie Tolmeijer was born on the 15th of October 1995 in ‘s-Hertogenbosch. After obtaining her Gymnasium degree in 2013 at Stedelijk Gymnasium ‘s-Hertogenbosch, she started the bachelor Biology at Leiden University. Afterwards, she obtained her Master Biomedical Sciences at the Leiden University Medical Centre (LUMC). During her Master study, she did an internship at the Medical Oncology department of the LUMC during which she studied the effect of metabolic stress on the immune escape of cancer cells. Additionally, she did an internship abroad at the Department of Medicine of Cambridge University (United Kingdom) and studied the RNA-sequencing signatures of immune cell populations in patients with autoimmune disorders. Fascinated by the field of oncology and with a passion for translational research she continued with a PhD at the Medical Oncology department of the Radboudumc in 2019. Under supervision of Dr. Niven Mehra (department of Medical Oncology), Prof. Dr. Marjolijn Ligtenberg (department of Human Genetics and department of Pathology), Prof. Dr. Winald Gerritsen (department of Medical Oncology) and Dr. Maartje Geerlings (department of Human Genetics) she investigated the potential of circulating tumor DNA measurements to refine cancer treatment. The results obtained during this PhD project are described in this thesis and were presented at various national and international conferences. Sofie continues her research on circulating tumor DNA as a postdoctoral fellow at the Vancouver Prostate Centre (University of British Columbia, Canada).

Dankwoord

Ook al was mijn promotietraject soms uitdagend, ik heb het ook met veel plezier gedaan. Niet alleen door het mooie onderwerp waarover deze thesis gaat, maar vooral door de mensen om mij heen die hebben geholpen deze thesis tot stand te brengen. Het is mij daarom een genoegen deze mensen hier te kunnen bedanken.

Allereerst wil ik **alle patiënten** bedanken die hebben bijgedragen aan dit onderzoek. Zonder jullie was dit onderzoek nooit gelukt. Daarnaast wil ik de **Paul Speth Stichting** bedanken voor de financiële bijdrage aan dit onderzoek waardoor dit onderzoek tot stand heeft kunnen komen.

Dan natuurlijk mijn promotieteam: **Niven Mehra, Marjolijn Ligtenberg, Winald Gerritsen** en **Maartje Geerlings-Wagemaker**. Wat wil ik jullie ontzettend bedanken dat jullie met mij deze weg hebben bewandeld en me daarbij zo veel kansen hebben gegeven. Het was een waar genoegen met jullie samen te werken!

Niven, ten eerste wil ik jou bedanken voor je onuitputtelijke enthousiasme voor de wetenschap. Ik heb ontzettend genoten van het samen sparren, nieuwe projecten vormgeven en theorieën bedenken. Ook wil ik je bedanken voor alle kansen die je mij hebt gegeven en je onvoorwaardelijk steun. Samen vormden wij naar mijn mening geen slecht team ;)

Marjolijn, bedankt voor je wijze lessen, oog voor detail, het delen van jouw grote hoeveelheid kennis op het gebied van moleculaire pathologie en genetica, en je grote betrokkenheid. Deze betrokkenheid heb ik niet alleen gevoeld bij alle projecten maar ook voor mij als persoon en dat zal ik altijd waarderen.

Winald, voor mij was jij degene die het grotere plaatje in acht bleef houden, kritisch maar rechtvaardig was op de uitvoering van het onderzoek/klinische toepasbaarheid, en een optimistische kijk wist te houden op ingewikkelde materie. Dit heb ik altijd zeer gewaardeerd.

Maartje, bedankt voor het warme bad waarin ik terecht kwam toen ik begon, al je geduld bij het inwerken, het spacen over sequencen en natuurlijk je grote persoonlijke steun om de PhD te doorstaan. Je wist me altijd aan te moedigen om stappen te nemen die ik zelf spannend vond. Bedankt dat je er altijd was.

Geachte leden van de manuscriptcommissie, **prof. dr. Fred Witjes, prof. dr. Michel van den Heuvel** en **dr. ir. Wendy de Leng**, hartelijk dank voor de positieve beoordeling van mijn proefschrift.

Naast mijn promotieteam zijn mijn paranimfen toch wel de rotsen in de branding geweest tijdens deze PhD. **Lisa** en **Madeleine**, dankjewel voor het delen van dit avontuur samen. Ik weet niet hoe ik dit zonder jullie had kunnen doen. Jullie hebben mij altijd geholpen, opgevrolijkt en vooral zo veel plezier met deze PhD gegeven. Daarvoor ben ik jullie voor altijd dankbaar. Hopelijk maken we nog veel nieuwe avonturen mee, dit keer misschien met wat minder publicatie stress ;)

De themakamer; **Jitske, Maartje, Lisa** en **Madeleine**, jullie vormde toch wel de veilige haven van het radboudumc waar ik heb geleerd dat alles een aanleiding is tot een feestje, taart of versiering! Bedankt voor de warme herinneringen. Ook **Tessa** en **Rayan**, jullie zijn wat later bij de kamer aangesloten, maar het was me een genoegen met jullie de laatste maanden van mijn PhD door te brengen.

De Liquid babes; **Eveline, Maartje, Lisa**, wat was het leuk met jullie een team te zijn, samen naar genetica uitjes te gaan en natuurlijk lekker uiteten. Ik zal het rennen achter de buizenpost, samen op het lab, en UMI discussies nooit vergeten. Ook wil ik de rest van het **liquid biopsy team** natuurlijk bedanken voor al jullie kennis en enthousiasme, met in het specifiek **Hicham, Janneke, Daniel** en **Nydia** voor al jullie hulp.

Dan zijn er een paar belangrijke vrouwen die ik wil bedanken voor de fijne samenwerking. **Emmy**, mijn maatje bij internationale avonturen. Het was een genoegen met jou samen te werken, want alles ging makkelijker samen met jou. Bedankt voor al onze spar sessies, het delen van telkens nieuwe hypotheses en onze buitenland avonturen – wat was Chicogo leuk samen! **Sandra**, jij was een super fijne samenwerkingspartner, had altijd alles al klaar voor ik er naar hoefde te vragen en jij hebt mij met zo veel projecten en aanvragen geholpen. **Iris**, niet alleen ben jij mijn work-wife die altijd klaar stond voor mijn (klinische) vragen, maar jij zorgde ook voor een introductie bij de medische onco na Corona, veel gelach tijdens congressen en koffie pauzes op de juiste momenten. Dankjewel voor je onvoorwaardelijke support. **Samhita**, we started together and I am grateful to have shared this adventure with you. We went through ups and downs, but I am convinced we came out stronger.

Verder wil ik alle coauteurs bedankten voor jullie inzet bij het tot stand komen van de hoofdstukken. Hierbij wil ik een speciale dank geven aan **Kalijn, Nielka** en **Jack**. Met jullie hebt ik veel productieve en leuke meetings mogen hebben en ik heb jullie betrokkenheid en adviezen ontzettend gewaardeerd.

Graag wil ik alle collega's van de **genetica**, **pathologie** en **oncologie** bedanken voor alle hulp en de fijne tijd met en tussen alle afdelingen. Met extra dank aan alle mede PhD studenten die naast werk ook zorgde voor de leuke tijd bij afdelingsuitjes, borrels en PhD retreats! Ook een grote dank aan **Elze** en **Marion** voor het verwerken van zo veel samples die ik heb kunnen gebruiken uit de biobank, en het **bioptenteam** voor de hulp bij het verzamelen van al het materiaal.

Alex and **Vancouver team**, thank you for the warm welcome into your group, keeping me involved with nine hours' time difference and all the knowledge you shared with me. You taught me so much on cfDNA, can't wait for our future work together!

Lieve vrienden en vriendinnen, dankjewel voor jullie support, het aanhoren van oneindige praat over promoveren en alle leuke jaren samen. In het specifiek wil ik **Lisa, Jet, Eva, Julia** nog even noemen, gewoon omdat jullie altijd voor mij klaar staan. Ontladen en weer opladen!

Lieve familie; **Mama, Jeroen, Eef, Jan, Gioi** en **Suus**. Met jullie kon ik alle PhD struggles delen en relativeren. Maar inhoudelijk zijn jullie ook goede hulp geweest (mama you are truely a super woman). Dank jullie wel voor het altijd samen blijven lachen en genieten.

Lieve **Robin**, dankjewel voor je liefde, je zorg en je oneindige vertrouwen. Overal waar ik liep, liep je naast me. En soms heb je me zelf even gedragen. Daarvoor altijd mijn dankbaarheid. Kan niet wachten op ons volgende avontuur!

Radboudumc
university medical center

IN DEI NOMINE FELICITER

Radboud University